USAAVLABS TECHNICAL REPORT 65-37

HEAT REGENERATIVE SYSTEM FOR T53 SHAFT TURBINE ENGINES

July 1965

U. S. ARMY AVIATION MATERIEL LABORATORIES
FORT EUSTIS, VIRGINIA

CONTRACT DA 44-177-TC-824
LYCOMING DIVISION
AVCO CORPORATION

DISCLAIMER NOTICE

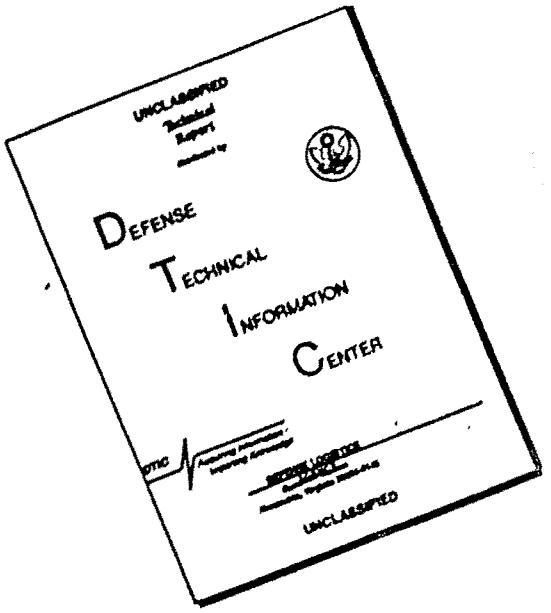

THIS DOCUMENT IS BEST QUALITY AVAILABLE. THE COPY FURNISHED TO DTIC CONTAINED A SIGNIFICANT NUMBER OF PAGES WHICH DO NOT REPRODUCE LEGIBLY.

DDC AVAILABILITY NOTICE

Qualified r questers may obtain copies of this report from DDC.

This report has been furnished to the Department of Commerce for sale to the public.

* * *

DISCLAIMER

The findings in this report are not to be construed as an official Department of the Army position, unless so designated by other authorized documents.

When Government drawings, specifications, or other data are used for any purpose other than in connection with a definitely related Government procurement operation, the United States Government thereby incurs no responsibility nor any obligation whatsoever; and the fact that the Government may have formulated, furnished, or in any way supplied the said drawings, specifications, or other data is not to be regarded by implication or otherwise as in any manner licensing the holder or any other person or corporation, or conveying any rights or permission, to manufacture, use or sell any patented invention that may in any way be related thereto.

Trade names cited in this report do not constitute an official indorsement or approval of the use of such commercial hardware or software.

* * *

DISPOSITION INSTRUCTIONS

Destroy this report when it is no longer needed. Do not return it to the originator.

DEPARTMENT OF THE ARMY
U. S. ARMY AVIATION MATERIEL LABORATORIES
FORT EUSTIS, VIRGINIA 23604

Appropriate technical personnel have reviewed the subject report and concur with the conclusions contained herein. This report is published for dissemination of regenerative engine data.

Task 1M121401D14409
Contract DA 44-177-TC-824
USAAVLABS Technical Report 65-37
July 1965

HEAT REGENERATIVE SYSTEM FOR T53 SHAFT TURBINE ENGINES

REPORT 2012.3

Prepared by
LYCOMING DIVISION
AVCO CORPORATION
STRATFORD, CONNECTICUT

for
U.S. ARMY AVIATION MATERIEL LABORATORIES
FORT EUSTIS, VIRGINIA

ABSTRACT

A heat regenerator has been designed to demonstrate the feasibility of regeneration for the T53 shaft turbine engine. Parameters of the initial design, a multiwave plate type, were optimized to provide a 27-percent fuel savings at 75 percent normal rated power. Test core modules leaked beyond the 0.25-percent flow-rate limit. Consequently, effort was directed toward a conventional tube-type regenerator, which was designed to provide a 24-percent fuel savings at 75 percent normal rated power. The tube-type regenerator and the interface hardware have been fabricated and integrated with the engine, and the system is ready for testing.

FOREWORD

This report describes the work conducted under Contract DA 44-177-TC-824 with the U. S. Army Aviation Materiel Laboratories. The work was performed in two phases.

Phase I covers the multiwave plate regenerator effort with regard to analytical studies, experimental core evaluation, and recommendations for the completion of the subject contract.

Phase II covers the tube-type regenerator effort with regard to analytical studies, design and fabrication, preparation of the engine-regenerator system for test, and recommendations for future effort.

TABLE OF CONTENTS

Appendixes

LIST OF ILLUSTRATIONS

LIST OF TABLES

LIST OF SYMBOLS

English Letters

A	-	Exchanger heat transfer surface area on one side, ft^2
A_c	-	Exchanger cross-sectional flow area, ft^2
A_{ci}	-	Individual passage cross-sectional flow area, ft^2
A_{fr}	-	Exchanger total frontal area, ft^2
C	-	Flow stream capacity rate (W_{cp}), Btu/hr-^oF
c_p	-	Specific heat at constant pressure, Btu/lb-^oF
D_H	-	Hydraulic Diameter ($4 A_{ci}/W.P.$), ft
D_t	-	Tube diameter, in.
f	-	Friction factor (viscosity)
G	-	Exchanger flow stream mass velocity (W/A_c), lb/hr-ft^2
g	-	Acceleration due to gravity, ft/sec^2
h	-	Unit conductance for thermal convection heat transfer. Btu/hr-ft^2-^oF
K	-	Loss coefficient, $\Delta P_t/q$
k	-	Unit thermal conductivity, Btu-^oF/hr-ft^3
l	-	Exchanger flow length, ft
P	-	Pressure, lb/ft^2
q	-	Dynamic pressure, lb/ft^2
T	-	Temperature, ^oF, ^oC, ^oR
U	-	Unit overall thermal conductance, Btu/hr-^oF-ft^2

V - Exchanger volume, ft^3

W - Mass flow rate, lb/hr

W.P. - Individual passage wetted perimeter

Greek Letters

$\propto$ - Proportional to

Δ - Denotes difference

ϵ - Exchanger effectiveness

μ - Viscosity, lb/hr-ft

Dimensionless Parameters

N_R - Reynolds number, $D_H G/\mu$

N_{st} - Stanton number, h/Gc_p

N_{pr} - Prandtl number, $\mu c_p/k$

$N_{st}N_{pr}^{2/3}$ - Colburn factor or generalized heat transfer grouping

NTU - Number of heat transfer units of exchanger (AU/C_{min})

C_{min}/C_{max} Flow stream capacity rate ratio

Subscripts

a - Air side

g - Gas side

s - Static value

t - Total (stagnation) value

max - Maximum

min - Minimum

Symbols Peculiar to Instrumentation

● - Pressure probe location

X - Temperature probe location

(0.0) - Engine station location

X:XX - Circumferential location ("o'clock" orientation)

a. . . z - Position relative to supporting wall, where:

a - Position nearest wall

z - Position farthest from wall

SECTION ONE. SUMMARY

Increasing demands made upon gas turbine-powered aircraft for longer flight-time capability have motivated efforts to reduce engine specific fuel consumption. Of the several possibilities available to the attainment of this end, heat regeneration appears to offer the greatest potentiality.

Heat regenerator performance is defined by effectiveness and pressure drop parameters. The theoretical limit of fuel savings can be determined from an engine temperature-entropy diagram, and is measured by the temperature difference between exhaust discharge gas and compressor discharge air. Assuming a regenerative T53-L-9 gas turbine engine with ideal (100 percent) effectiveness, the theoretical maximum fuel savings is approximately 50 percent. A practical-sized regenerator based upon optimization of weight, mission profile, etc., would have an effectiveness of 60 to 90 percent of ideal and a corresponding fuel savings diminished by pressure-loss effects. The particular effectiveness for a fixed regenerative engine design is a function of power setting and altitude.

Several regenerator core types were studied with regard to achieving an optimized engine application within a reasonable time. Selection of a multiwave plate-type regenerator core for the T53 engine was based in part upon the ability to form a multitude of very small fluid passages by the relatively straightforward process of joining a pair of stamped multiwave plates and joining the plate pairs to form a core module.

Sizing of the regenerator proceeded from a determination of the air-side to gas-side passage size and shape relationship and from a study of the interrelationships resulting from variations in hydraulic diameter, flow length, and frontal area parameters. Optimization was accomplished by selecting an arbitrary 4- to 5-hour mission at 75 percent normal rated power at sea level, then minimizing the hydraulic diameter and flow length and increasing the frontal area until the greatest fuel savings was attained. Off-design operation at high altitude and high power causes excessive gas-side pressure losses resulting in reduced power. Since these pressure losses vary directly with the weight flow through the regenerator, exhaust gas bypassing is normally used under these operating conditions to restore power.

Evaluation of the heat regenerator concept evolving with the foregoing analytical studies began with the establishment of design criteria for the fabrication of regenerator hardware. The regenerator is a stationary type with counterflow passages and 100 percent primary heat transfer

surfaces. Multiwave plate construction was selected as the means of achieving a compact, lightweight, efficient regenerator. Matched plates are joined in pairs by welding together corresponding crests to impart rigidity. Crest-on-crest wave forms were studied for heat transfer characteristics, as were crest-on-flat wave forms for the contingency of misalignment problems. The crest joints are not critical from the viewpoint of leakage and heat transfer; critical areas exist at the plate flanges joining the plate pairs. Joined pairs are stacked and brazed to form the core modules, which are arranged concentrically about the exhaust gas bypass area. The number of modules was determined by the required heat transfer properties, and the length of the cores was determined from the number of cores and the required gas flow area. The latter parameter also determined the necessary external diameter of the regenerator, which completed the dimensional packaging. An alternate regenerator design consists of replacing the wave plate flanges with metal spacers, which shows promise of producing a leak-proof core. This design also contributes to a weight reduction by providing a rigidity which eliminates the need for a secondary support structure.

Fabrication of test cores was initiated with the evaluation of wave plate and joining materials. Following the selection of appropriate materials, stamped wave plates of test size were studied for proper convolution formation, accurate alignment of pairs and stacks, and flange sizing to control pair dimensions and produce a brazeable fit-up. Manufacturing procedures were established to define surface preparation and plating techniques. Pairs of plates were fixtured and joined, then clamped and brazed. Problems of alignment and dimensioning were corrected to a great extent, whereas leakage problems were more persistent.

Of the several cores fabricated, three were earmarked for the performance evaluation of effectiveness and pressure loss. A limited amount of reliable test data was obtained. Reasonably accurate gas-side pressure drop information was derived from the first two cores, whereas the most complete and reliable information was derived from the third core. The effectiveness of the third core was close to design value, but the pressure drop was 2 percent high.

Because of core leakage, it was decided to continue with the Phase II goal to manufacture a regenerator by using a more conventional heat transfer surface. The objectives of this Phase II regenerator program, to manufacture and assemble an experimental T53 engine-regenerative system using a conventional tube-type stationary heat regenerator, have been successfully completed. A practical-size, lightweight regenerative system has been designed and fabricated to provide a fuel savings of approximately 24 percent at an engine power rating of 75 percent.

Analytical studies preparatory to regenerator design made use of the significant performance criteria of fuel savings and power penalty, which resulted in the selection of a two-pass, cross-counterflow tube-type regenerator. With this arrangement, compressed engine air makes two passes through the regenerator tubes, and the turbine exhaust gas makes one pass outside of and perpendicular to these tubes.

Requirements for optimum regenerator effectiveness, pressure loss, length, weight, tube size, and spacing were investigated, and the findings were applied to design considerations.

Techniques were established for manufacturing and fabricating hardware for both the regenerator and the engine interface. Knowledge and practical experience in the fabrication of the toroidal shell, in tube bending and brazing methods, and in material characteristics were important benefits derived from this program.

Final engine-regenerator assembly was successfully completed without significant difficulties. Instrumentation was incorporated for determining system overall performance, pressure losses, and regenerator effectiveness. The vehicle has been mounted in a special three-point-mount test stand and is ready for test. Follow-on test of components and regenerative engine is being considered under the continuing Government-sponsored Contributing Engineering Program.

SECTION TWO. CONCLUSIONS AND RECOMMENDATIONS

PHASE I

1) Physical limitations encountered with regard to the fabrication of the leak-tight cores for this multiwave plate-type core application have suggested the desirability for additional work in the area of core sealing prior to the fabrication and test of the full-size core module.

2) It was recommended that the remaining work under the subject contract be expedited by the use of an AiResearch tube-type regenerator core in order to determine the feasibility of a regenerative system on the T53 engine.

3) It was further recommended that solution of the fabrication problem for the multiwave plate-type core be pursued under Lycoming's Contributing Engineering Program. (This recommendation has since been implemented.)

PHASE II

1) A small tube-type regenerator has been successfully incorporated on a Lycoming T53 engine, thereby demonstrating the practicability of adapting regeneration to this engine.

2) The final, fully assembled engine-regenerator system weight, excluding special instrumentation provisions, is 810 pounds. Breakdown of the weight distribution is as follows:

	Weight (lb)
Basic Engine (T53-L-11)	487
Interface Hardware *	99
Regenerator	224
Total	810

(The use of exotic materials with modified heat transfer areas could have reduced the overall regenerator weight and size.)

* Interface hardware is defined as modified engine hardware and additional engine hardware necessary to adapt and mount the regenerator. No standard engine hardware is included. All interface hardware is itemized in Appendix III.

3) It is recommended that component and vehicle testing be undertaken immediately to determine performance and operational characteristics of the engine-regenerative system.

4) It is recommended that an investigation be conducted into a bypass valve system, infrared shielding, an atomizing combustor, and possible flight evaluation.

SECTION THREE. INTRODUCTION

In attempting to find ways to reduce gas turbine engine specific fuel consumption, studies both at Lycoming and elsewhere indicate that modification to the brayton cycle to include regeneration shows the most promise for immediate benefit. Recent technological advancements in lightweight, compact heat regenerators and the particular physical characteristics of the Lycoming aircraft gas turbine engines encouraged Lycoming to undertake a three-part research program in 1962 to investigate regeneration in detail for aircraft application. This program consisted of:

Phase I - Analytical Studies and Experimental Evaluation

Phase II - Manufacture of Prototype.

Phase III - Prototype Testing

Phase I was completed in the fourth quarter of 1963. As a direct result of the conclusions of Phase I, Phase II was redefined, and Phase III was made the subject of future effort.

The Phase II goal prior to redefinition was to manufacture and component-test a prototype regenerator of a totally new multiwave plate surface heat regenerator configuration which was representative of a practical unit. Toward the conclusion of Phase I, fabrication experience indicated that additional manufacturing development would be required before a successful prototype could be produced to this configuration. It was decided to continue with the Phase II goal to manufacture a prototype regenerator utilizing a more conventional tube-type regenerator surface, and to defer all testing, including component checkout, to a follow-on test program.

The objective of the redefined Phase II effort was to produce a practical prototype engine-regenerator system completely ready for a follow-on evaluation test program. The design goal for the engine-regenerator system was for fuel savings over the basic engine of 24 percent at 75 percent normal rated power with an overall weight increase to the basic engine of 260 pounds.

This engine-regenerator system consists of:

1. A tube-type regenerator designed to provide at 75 percent normal rated power an effectiveness of 0.66, a total core pressure loss of 3.9 percent, an air-side/gas-side core pressure drop proportion of 45:55, and a total system pressure loss of 9 percent.

2. A standard government-furnished T53 engine incorporating necessary modifications to accommodate the above regenerator.

3. Suitable instrumentation for determining system pressure losses and effectiveness during follow-on testing.

The following text describes in detail the analysis of data required to establish the design criteria, the hardware design, the hardware fabrication, instrumentation design and procurement, and vehicle assembly.

SECTION FOUR. ANALYTICAL STUDIES

4.1 INTRODUCTION

Demands made of the gas turbine-powered aircraft in recent years have emphasized longer flight missions. With this requirement, low specific fuel consumption becomes the prime concern. For long flight missions, the fuel load is of such a magnitude that any savings in fuel rate may show an attractive overall (fuel plus engine) weight reduction despite the fact that fuel savings necessitates an increase in the fixed weight of the engine.

The gas turbine designer has the following alternatives for reducing the engine's specific fuel consumption:

1) Increase component efficiencies
2) Operate at greater cycle temperature and pressures
3) Modify the brayton cycle with intercooling, reheat, or regeneration
4) Use variable area turbine geometry under off-design operating conditions.

Of these possibilities, regeneration shows the most promise for immediate benefit due to the recent advances made in the art of fabricating compace heat exchanger surfaces. Accordingly, Lycoming undertook a research program to investigate the regenerative approach in detail. The analytical studies which initiated the program are discussed in the following sections:

4.2 Effect of Regeneration on the Basic Thermodynamic Cycle of the Engine
4.3 Selection of Regenerator Type
4.4 Multiwave Plate Regenerator Design Optimization Study
4.5 Evaluation of Regenerator Off-Design and Bypass Performance
4.6 Specification Summary of Finalized Multiwave Plate Regenerator.

These divisions outline, in respective order, the manner in which the regenerator study was undertaken. The investigation terminates in a detailed specification of the finalized multiwave plate regenerator design selected. Approximately 25 percent of the work performed in Sections 4.2 and 4.4, and all the work performed in Section 4.3, was accomplished under Contributing Engineering programs of CY 1961 and 1962.

4.2 EFFECT OF REGENERATION ON THE BASIC THERMODYNAMIC CYCLE OF THE ENGINE

A heat exchanger, when used with a gas turbine engine to transfer heat from the exhaust gases to the compressor discharge air, serves to function as a regenerator. From the performance standpoint, there are only two parameters which define the regenerator; effectiveness and pressure drop. It is the "air side" effectiveness and the accumulated gas- and air-side pressure losses that determine the fuel savings realized by the engine.

Air-side temperature effectiveness of the regenerator is defined as:

$$\epsilon = \frac{T_{air\ out} - T_{air\ in}}{T_{gas\ in} - T_{air\ in}}$$

Thus, effectiveness is a measure of the actual change in temperature of the compressed air in this case as compared to the maximum thermodynamically limited air temperature change which could occur with idealized conditions. Air-side enthalpy effectiveness may be obtained by using air and gas enthalpy values in the above equation in place of the corresponding temperatures. Due to varying specific heats, enthalpy effectiveness will differ slightly from temperature effectiveness. Temperature effectiveness is used in the following text for purposes of simplicity.

Gas-side temperature effectiveness is likewise the measure of the actual change in the exhaust gas temperature compared to the maximum thermodynamically limited gas temperature change under idealized conditions. The ratio of air-side to gas-side effectiveness is always inversely proportional to the ratio of the respective flow stream capacity rates.

The potential fuel saving of any gas turbine engine can be determined from the engine thermodynamic cycle as shown on a temperature-entropy diagram. For the purpose of this study, the Lycoming T53-L-9 gas turbine engine was considered. Figure 1 shows this engine's T-S diagram at the arbitrarily chosen 75 percent cruise power point. It is the temperature difference between the exhaust gas discharge and compressor air discharge (points 9 and 3, respectively, of Figure 1) that presents the potential for transferring heat energy, which would otherwise be dumped or wasted, from the gas to the cooler compressor discharge air. If ideal regenerator performance were achieved (100 percent effectiveness), it can be seen in the T-S diagram that the compressor discharge air would be heated to point 3', a distance covering approximately 50 percent of the temperature rise required between points 3 and 5. This temperature rise

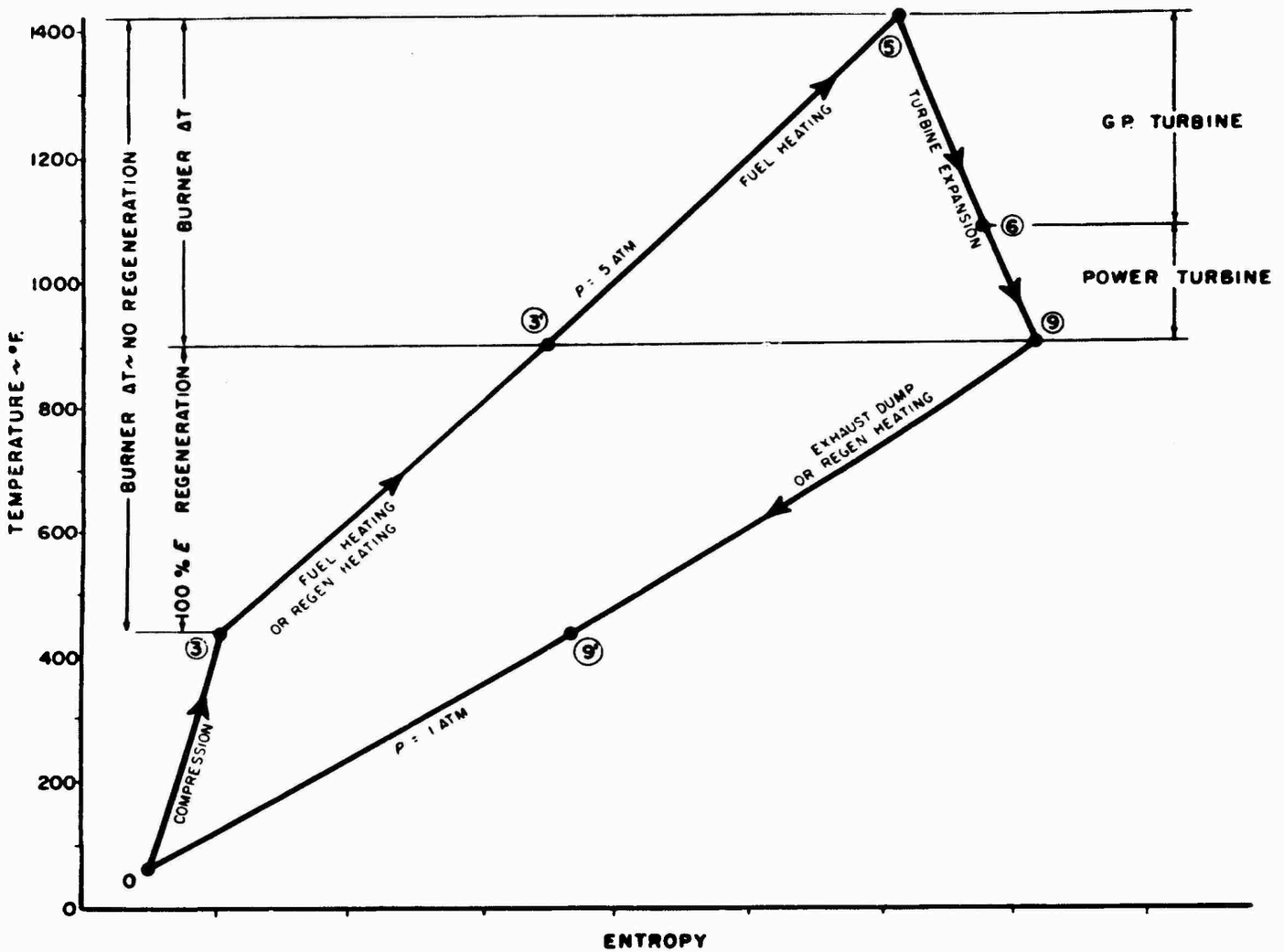

Figure 1. Basic Engine Cycle T-S Diagrams. (With and without ideal regeneration.)

is normally achieved with the burning of fuel in the engine combustor. Any portion then of the temperature rise handled by the regenerator results in a like proportion of fuel savings.

The effect of engine cycle pressure ratio on potential regenerative fuel savings is depicted on the T-S diagram in Figure 2. Here, compared with the previous T53 engine cycle, is a higher cycle pressure H (8 atmospheres), and a lower cycle pressure L (3 atmospheres), all at the same burner temperature level. If the same points, exhaust gas discharge and compressor air discharge temperatures, are compared for each cycle, it is seen that the higher pressure ratio cycles have less temperature difference at current temperature levels, and thus less margin for potential fuel savings. This temperature differential is reduced because the compressor discharge temperature increases as a function of the pressure ratio. In addition, at the fixed maximum temperature of the cycle, the availability of a greater pressure ratio for the turbine results in reduced exhaust gas discharge temperatures. It is, in fact, possible to go to extreme cycle pressure ratios where the exhaust gas is cooler than the compressor discharge, whereupon the regenerator would then cool the air, showing a negative fuel savings. A point of clarification to be made is that all of the foregoing statements concern the potential fuel saving available to the existing cycle.

It must be remembered that within reason the higher pressure ratio cycles provide more efficient specific fuel consumption initially. The decision as to whether to regenerate with a higher or lower cycle pressure engine involves many other trade-offs between engine weight, size, turbine inlet temperature, mission profile, etc.

The cycles investigated to this point have all been shown with 100 percent (ideal) effectiveness. Since such performance could be achieved only with an infinitely large regenerator, practicality requires something less than ideal regeneration. In general, a practical-sized regenerator, and again the actual size will depend upon an optimization study of weights, mission profile, etc., would have an effectiveness in the order of 60 to 90 percent and incur some pressure losses to the engine cycle. This means the actual fuel savings would be 60 to 90 percent of the ideal minus the additional reduction due to the pressure losses. Figure 3 shows (in solid line) the ideal T-S plot of Figure 1, plus a plot with air-side pressure losses and air-side plus gas-side pressure losses. In the cycle presented, if the compressor discharge air suffered a 4.8-psi pressure loss (6.5 percent), the pressure ratio available to expansion through the turbine and thus turbine power would be reduced a like amount. Since a fixed amount of the total turbine power (approximately 60 percent) must be extracted for the compressor work, all the power deficit would be extracted from

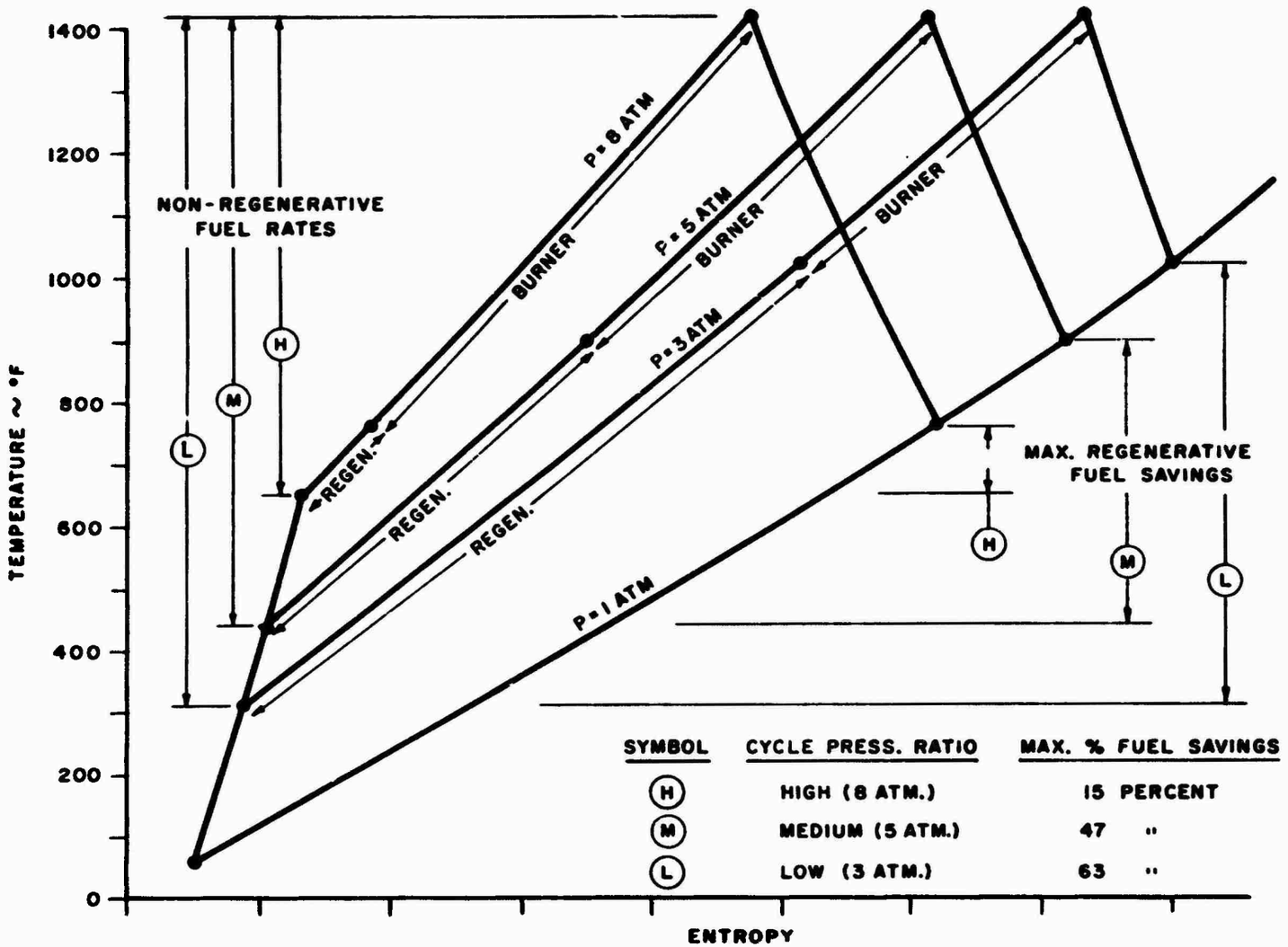

Figure 2. Basic Engine Cycle T-S Diagrams. (Effect of ideal regeneration at various cycle pressure ratios.)

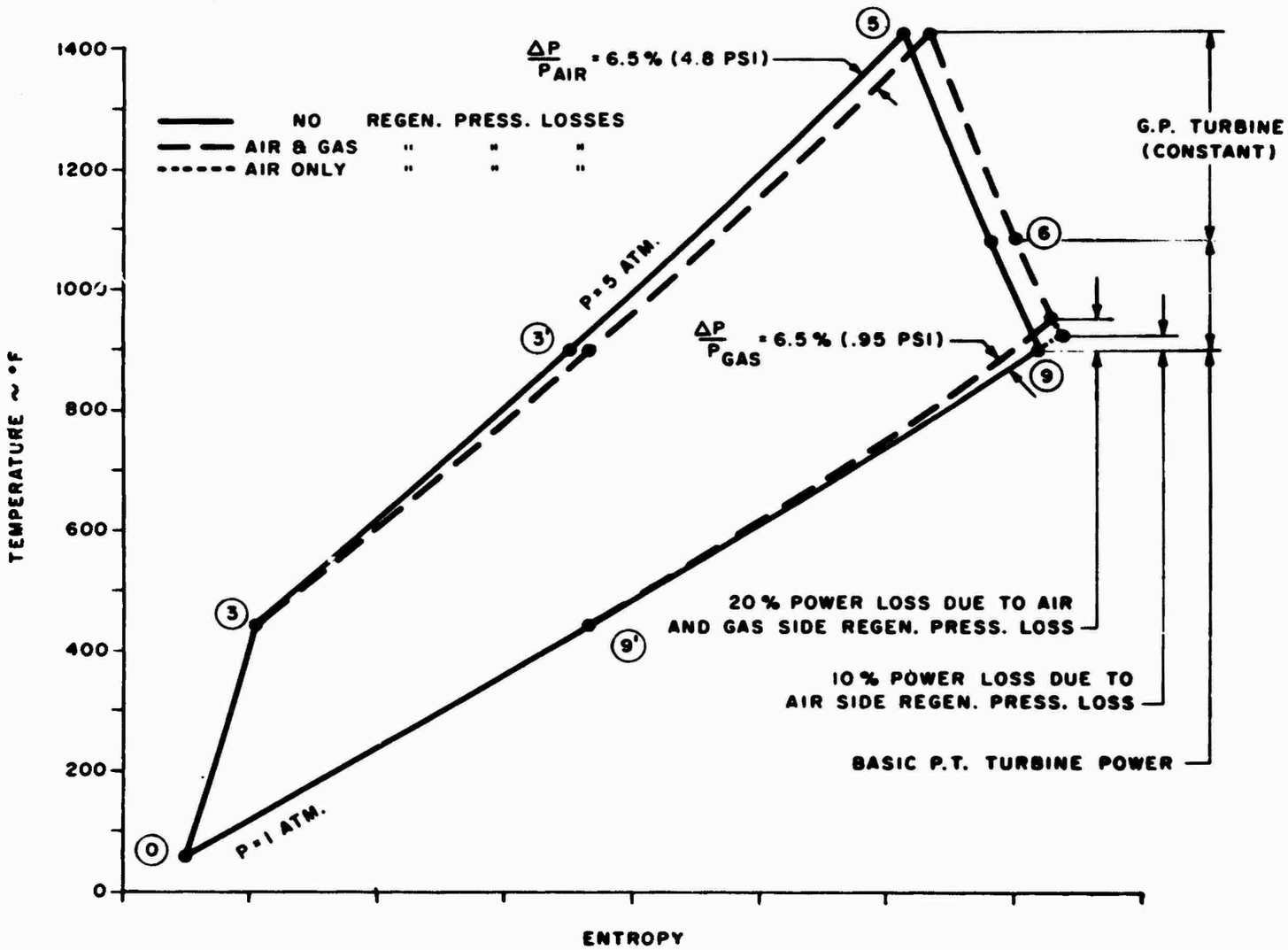

Figure 3. Basic Engine Cycle T-S Diagrams. (Effect of air and gas side regenerator pressure loss on power.)

the output turbine. The net result in this particular case is a 10 percent reduction in useful shaft output power if the maximum burner temperature was maintained. The net increase in fuel rate due to the 6.5 percent air-side pressure loss at fixed power setting is only 4 percent. Because of the lesser turbine expansion, the exhaust gases, having done 10 percent less work, discharge at a somewhat high temperature. This means a more favorable temperature difference between air and gas exists for heat transfer through the regenerator. Thus a portion of the energy, lost by the turbine due to pressure drops caused by the regenerator, is again recovered by the regenerator.

A similar loss in power and fuel savings will occur with gas-side pressure loss. It is noteworthy that the fuel savings and power losses are functions of the percent pressure drop on either the air or gas side and not of the absolute value of pressure loss. This is because turbine work at a given inlet temperature is a function of the pressure ratio through which the turbine gases expand. The percent pressure losses, air and gas sides, are then additive for overall loss effect determination.

In order to optimize a regenerator design for a specified engine, it is essential that fuel savings for the engine be accurately known for a range of regenerator effectiveness and pressure losses at various engine power settings and altitudes. This information was calculated for the T53-L-9 engine with the use of an IBM turbine engine performance program. The engine operating points covered were 35 percent normal rated, 75 percent normal rated, and military powers at sea level and 15,000-foot altitudes. The results of this investigation are presented in Figures 4 through 9. In comparing all six of these curves, it is evident that a given set of effectiveness and pressure loss values will show roughly the same percent fuel savings regardless of the power setting or altitude. The reason is that at various powers and altitudes examined, the burner temperature, compressed air discharge temperature, and exhaust gas temperatures vary more or less in proportion. As shown in Figure 3, the variation in potential fuel savings comes only from dissimilar relations among these three temperatures.

The foregoing statement of relatively constant fuel savings at different powers and altitudes was based on the assumption of fixed effectiveness and pressure loss values of the regenerator. In actual operation, the regenerator effectiveness and pressure loss do vary with power and altitude due to the thermodynamic state changes. Such regenerator off-design performance is covered in Section 4.5.

From the preceeding calculations, some incremental relationships between regenerator and engine performance have been established.

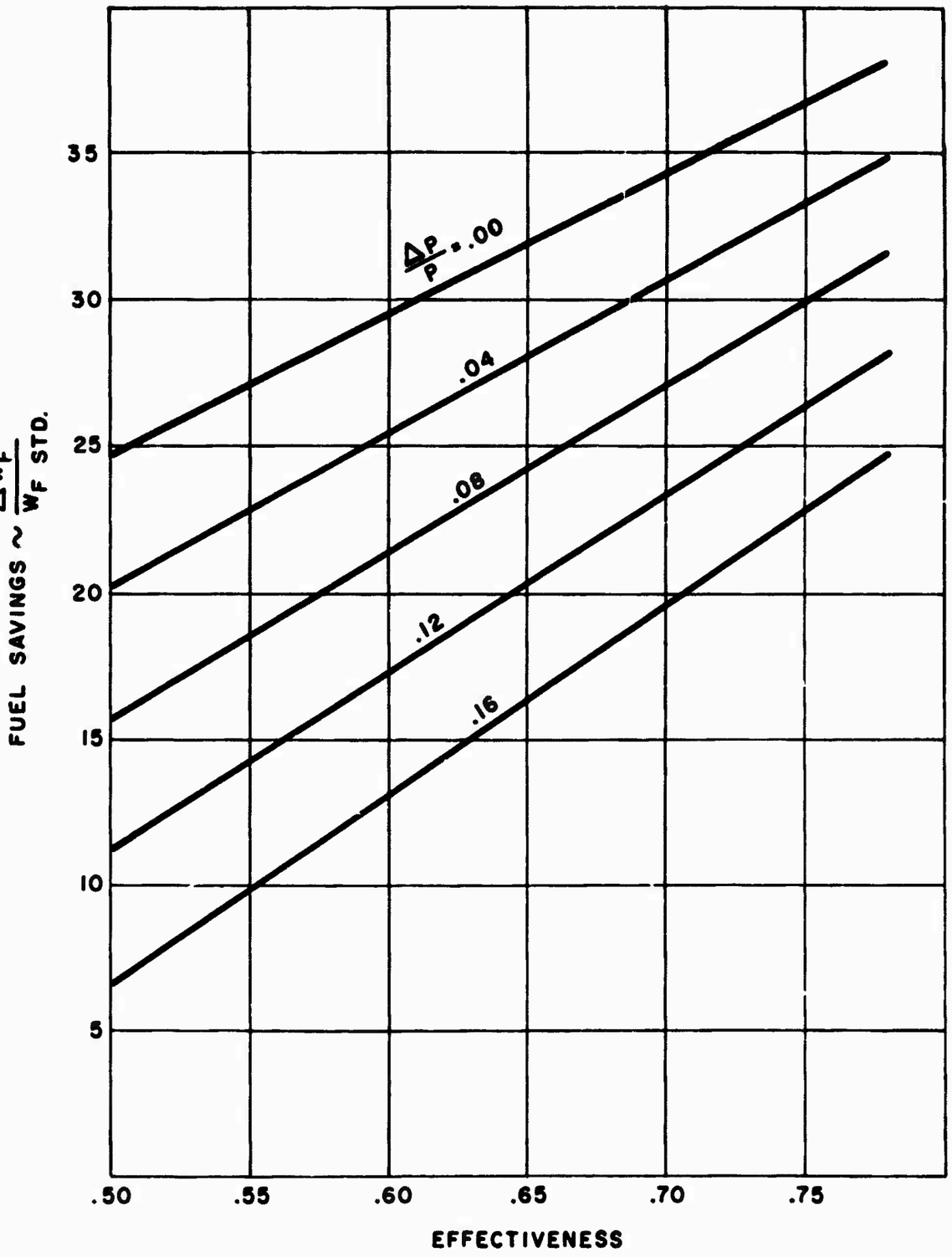

Figure 4. T53-L-9 Engine Regenerator Fuel Savings Benefit. (35% normal rated power at sea level.)

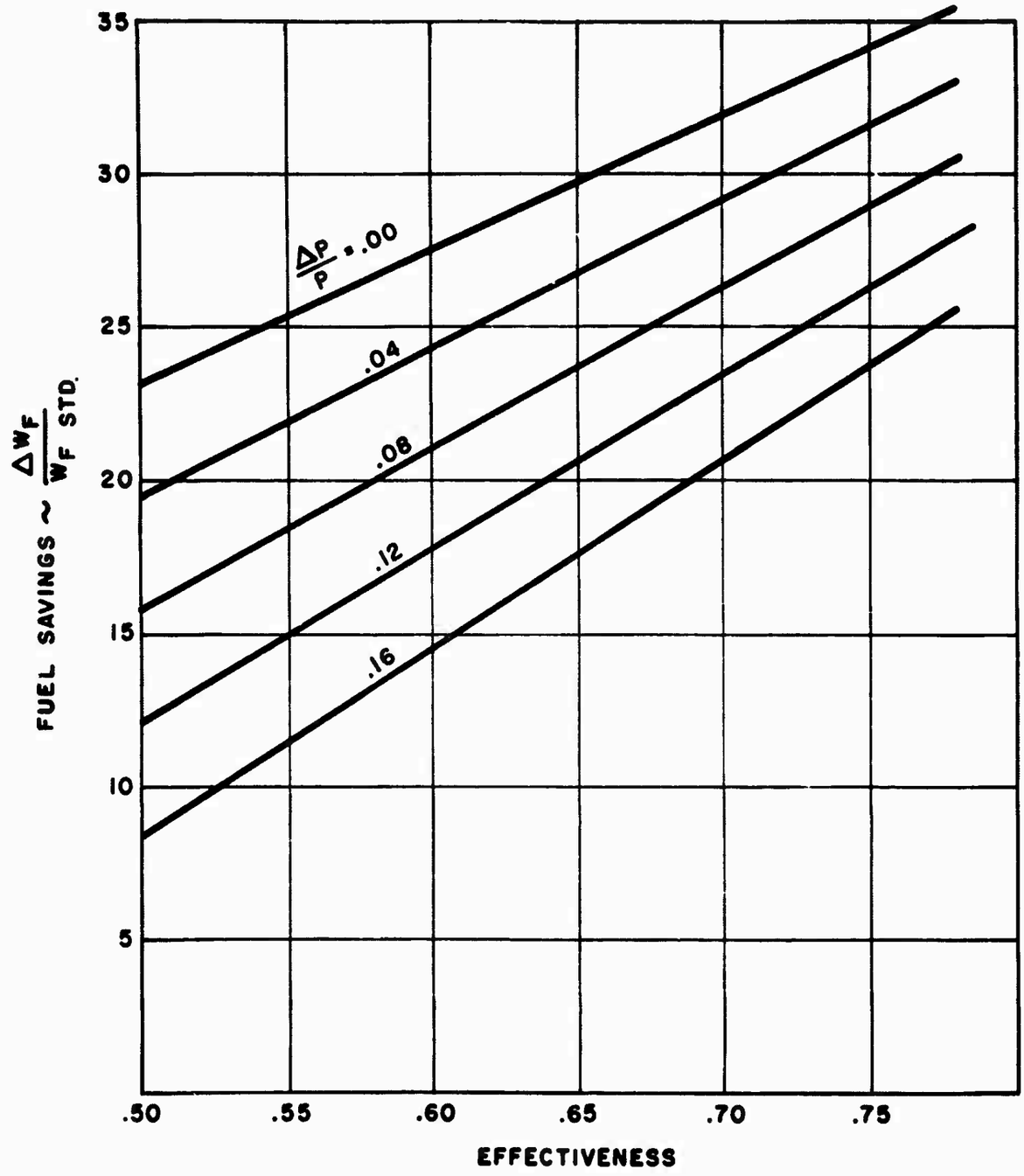

Figure 5. T53-L-9 Engine Regenerator Fuel Savings Benefit. (75% normal rated power at sea level.)

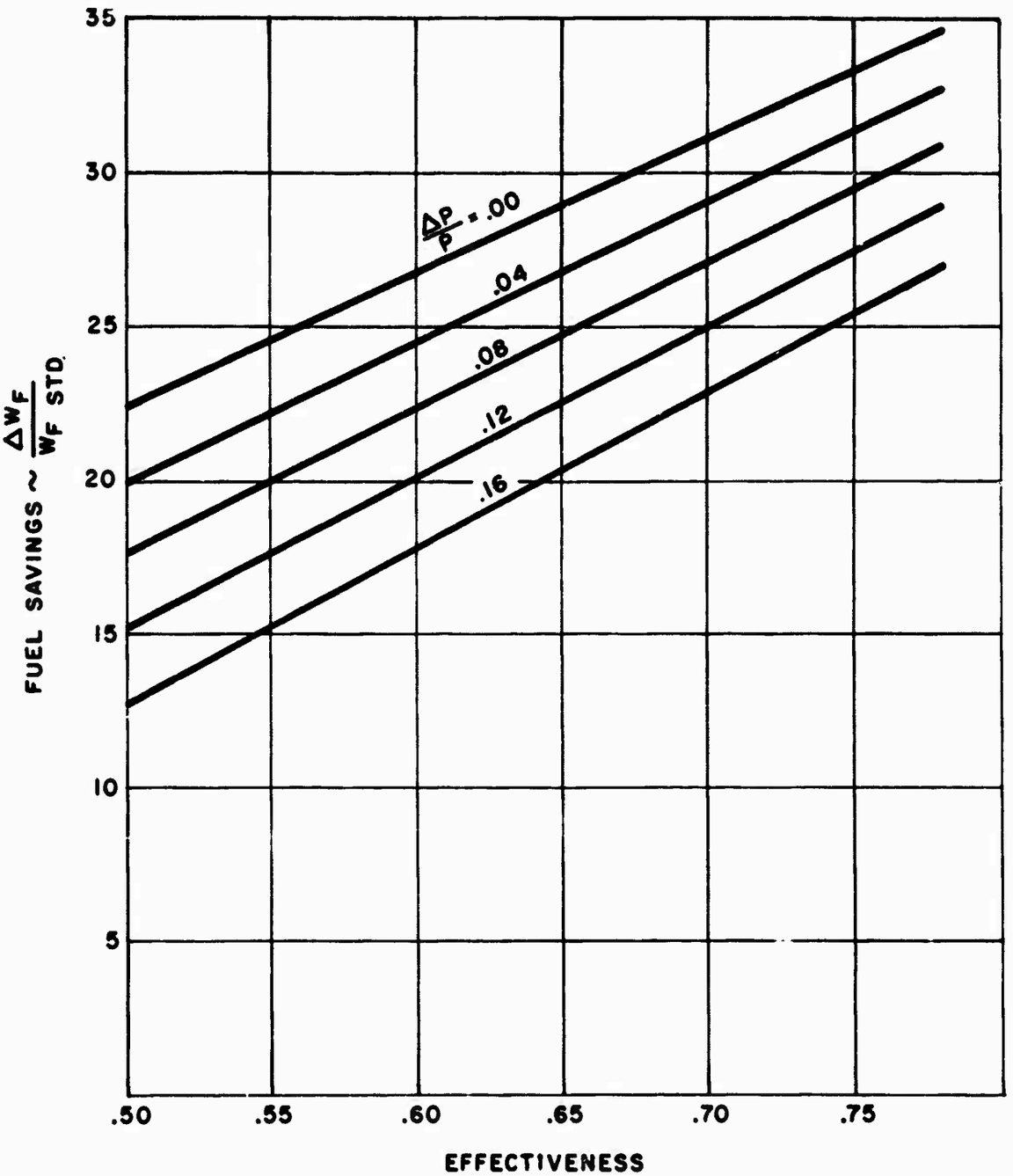

Figure 6. T53-L-9 Engine Regenerator Fuel Savings Benefit. (Military rated power at sea level.)

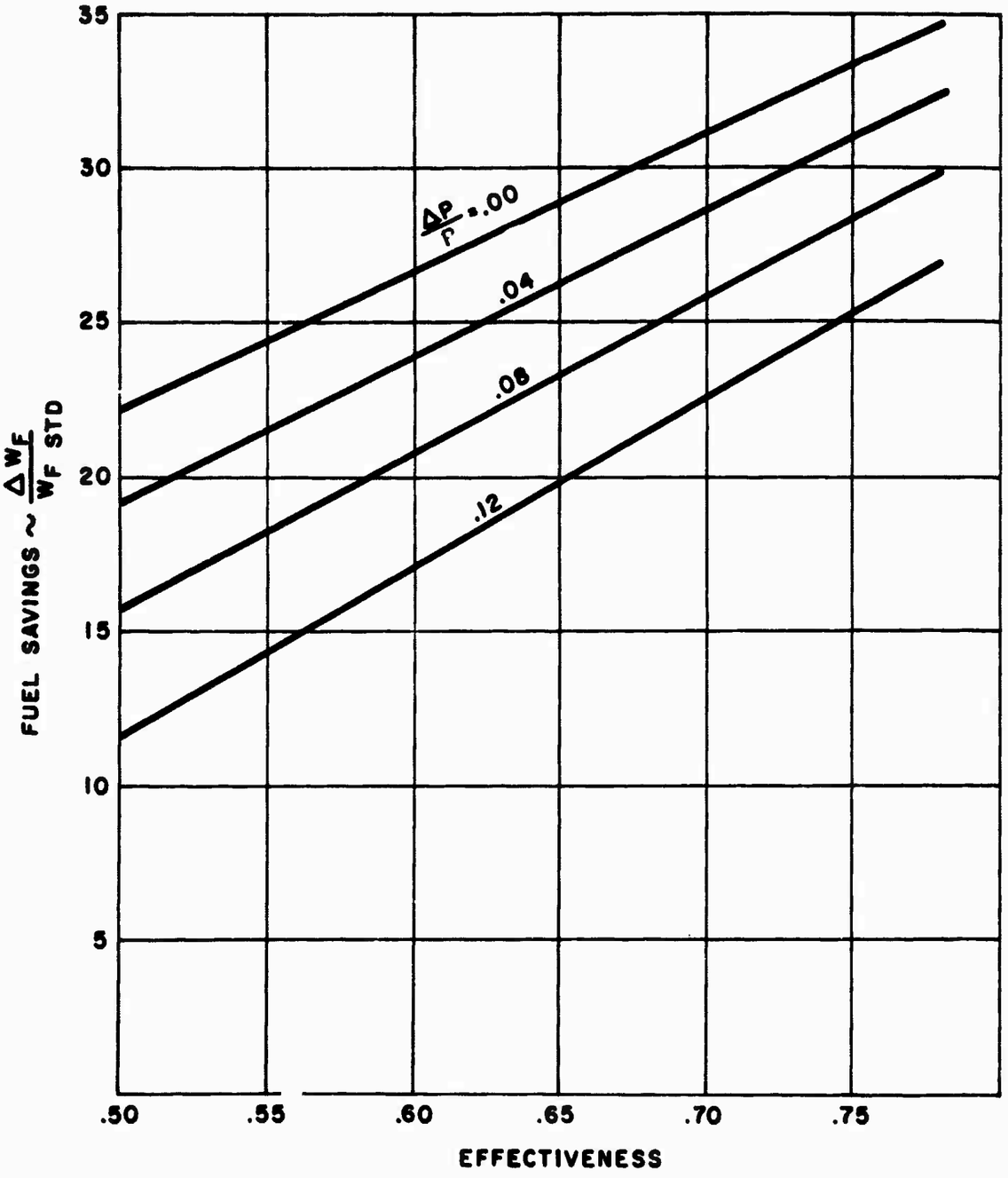

Figure 7. T53-L-9 Engine Regenerator Fuel Savings Benefit. (35% normal rated power at 15,000-foot altitude.)

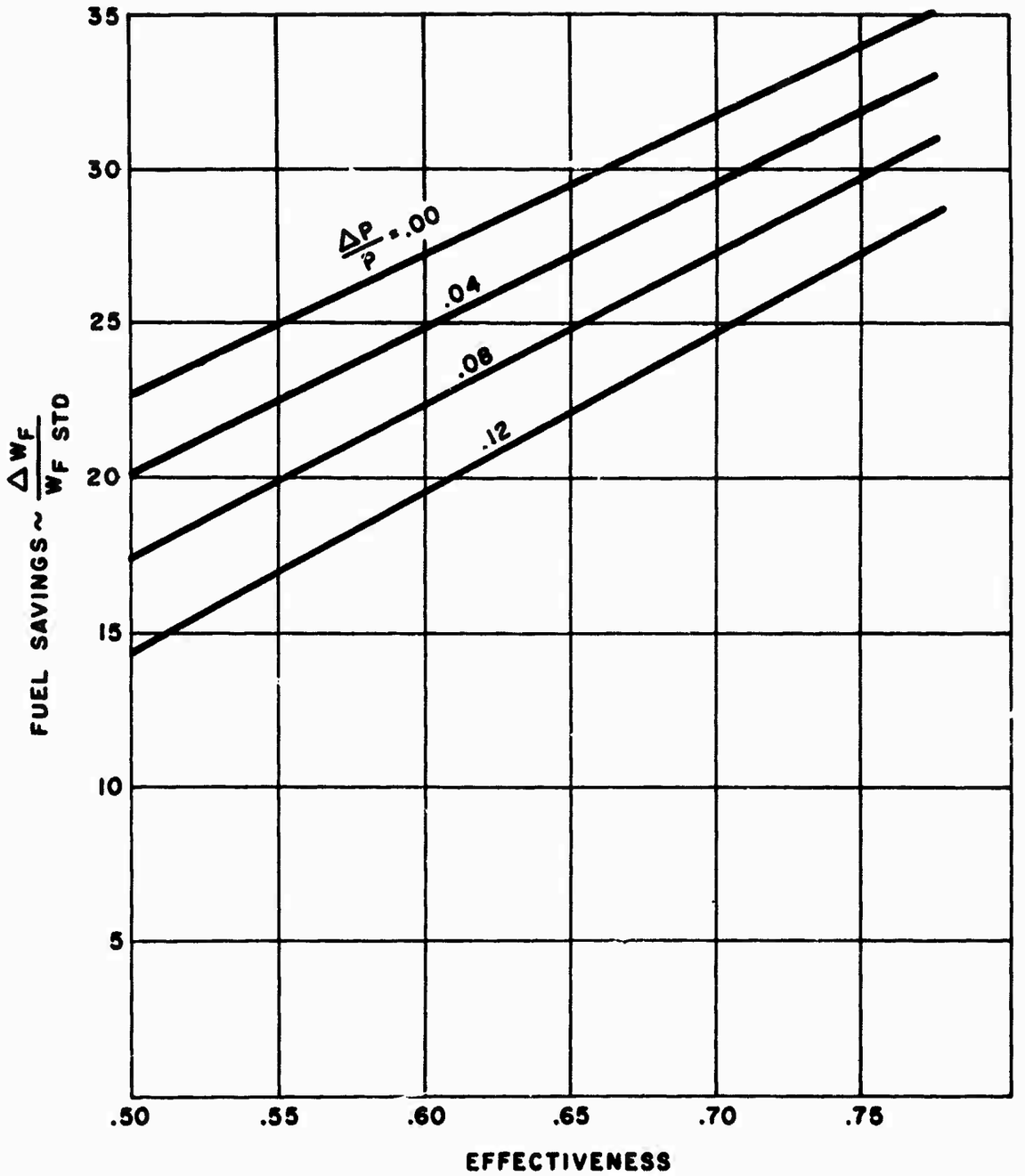

Figure 8. T53-L-9 Engine Regenerator Fuel Savings Benefit. (75% normal rated power at 15,000-foot altitude.)

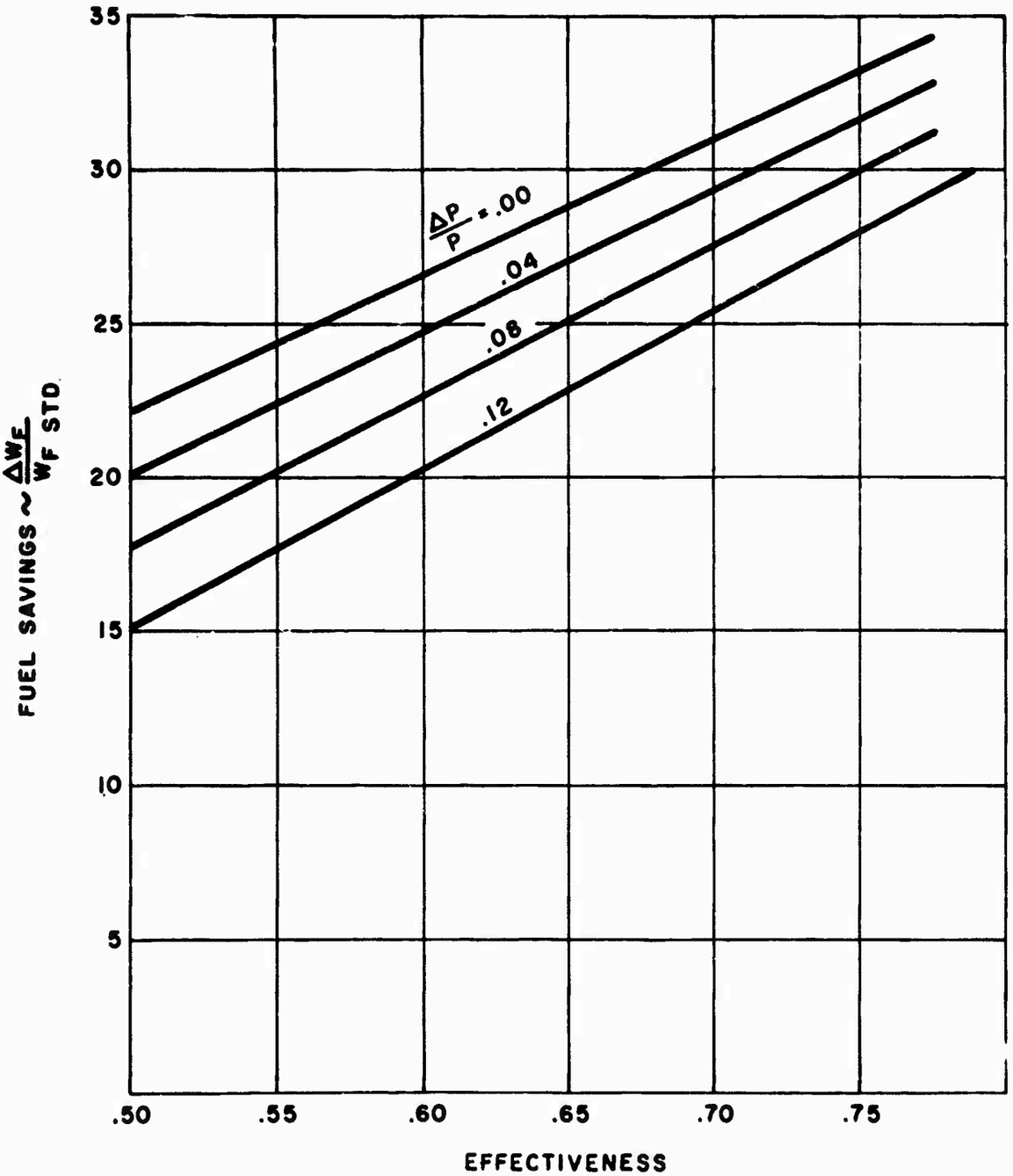

Figure 9. T53-L-9 Engine Regenerator Fuel Savings Benefit. (Military rated power at 15,000-foot altitude.)

Following is a list of the approximate trade-offs as concerns the T53-L-9 engine with a typical (ϵ = 0.75, Δ P/P= 10 percent) regenerator at the 75 percent power condition.

Trade-Off				To Maintain
1%	$\Delta P/P$	$\approx$	1.25% Effectiveness	Engine Fuel Savings
1%	$\Delta P/P$	$\approx$	1.8% Horsepower	Engine Burner Temperature
1%	$\Delta P/P$	$\approx$	10° Burner Temp.	Engine Horsepower
1%	$\Delta P/P$	$\approx$	.7% Fuel Savings	Regenerator Effectiveness

Figure 10 shows typical standard and regenerator fuel rates for the T53-L-9 engine. The plot of horsepower versus specific fuel consumption shows a comparison of the standard L-9 engine with the two hypothetical regenerators. Parameters of burner temperatures are also shown. At the normal rated power level (900 horsepower) the specific fuel consumption has been reduced from approximately 0.7 to 0.5 with an ϵ=0.70 and $\Delta P/P$ = 0.06 regenerator. It can be seen that the turbine inlet temperature was increased from 2040°R to 2100°R to maintain this normal rated power level.

4.3 SELECTION OF REGENERATOR TYPE

The discussion to this point has concerned only the effects of regeneration on the engine, with the measure of regeneration being defined in terms of effectiveness and pressure loss.

A type of regenerator must now be selected that will give the effectiveness and pressure loss performance envisioned. The most attractive regenerator will be, of course, that which will achieve a given performance with the smallest weight and size, other factors of cost, reliability, etc., being equal.

Lycoming has reviewed each of the various type regenerators; rotary, tube, plate-fin, and liquid metal. Each type of regenerator has particular advantages and disadvantages. Certain basic features that are desireable in any regenerator are listed in order of importance:

1) Small Hydraulic Diameters
2) Counterflow Arrangement
3) Zero Leakage
4) All Primary Surface

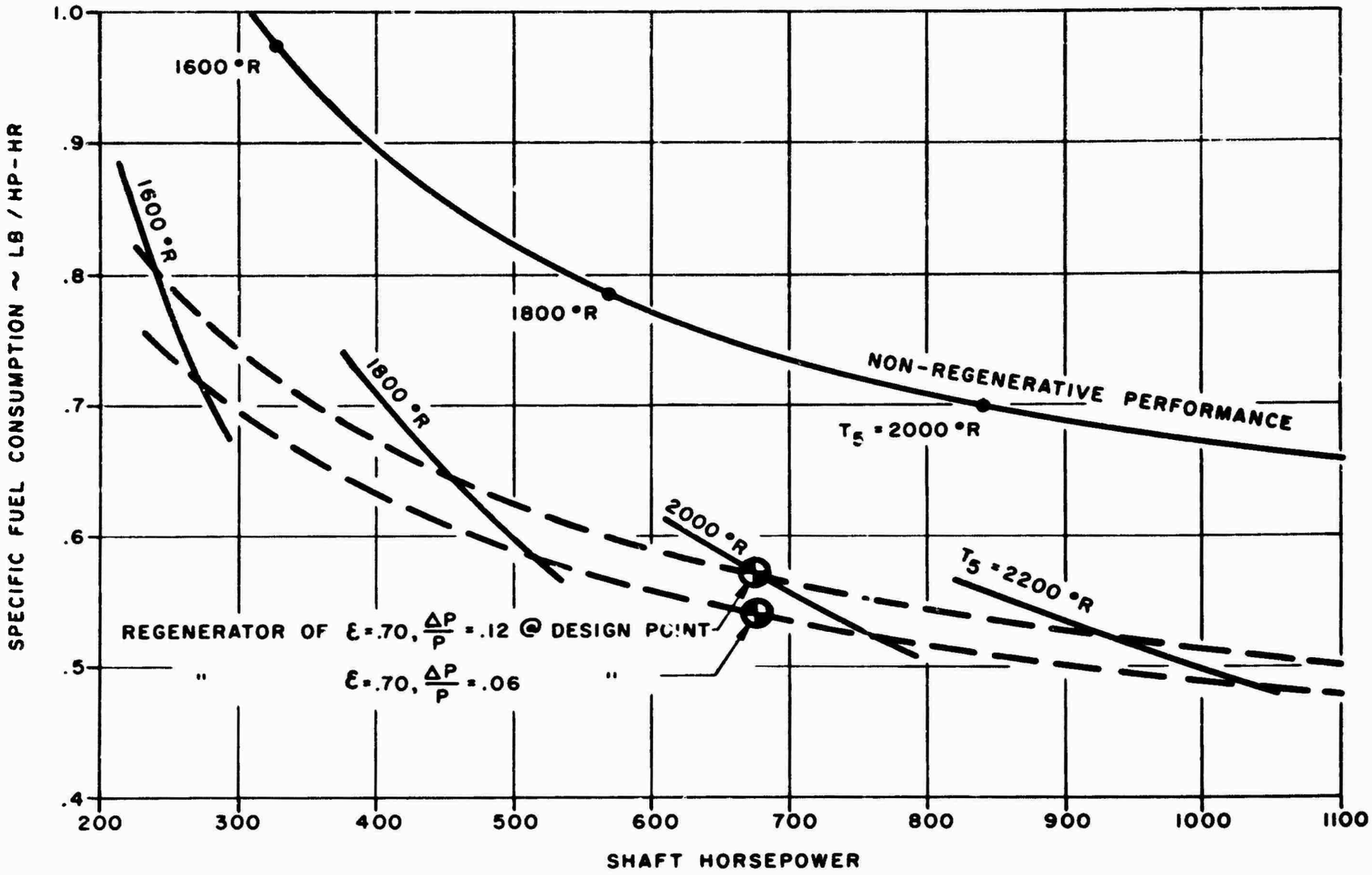

Figure 10. T53-L-9 Engine Typical Regenerator Effect on Specific Fuel Consumption.

It is these features that conduce to a small volume, lightweight heat exchanger matrix.

A brief synopsis of the design advantages and disadvantages for each regenerator type follows.

1) Lycoming Multiwave Plate

Characteristically achieves the four basic features of small hydraulic diameters, counterflow, all primary surface, and insignificant leakage. Possible disadvantages are high wrap-up weights with the individual core module design, and plate fabricating and brazing requirements.

2) Rotary

Easily achieves small hydraulic diameters with a primary surface counterflow arrangement, but suffers from an inherent problem of leakage and carry-over loss. Envelope dimensioning and headering may present problems.

3) Tube

Has generally a freedom of design (diameter to length) plus low wrap-up weight due to simplicity of the header system. Insignificant leakage can be achieved and maintained. To maintain simplicity, crossflow arrangements are generally settled for in place of the counterflow arrangement.

4) Liquid Metal

The advantages of this design include options of envelope dimensioning, flow arrangement, independence of hot to cold surface sizing, and freedom to locate "hot" and "cold" sides remotely. These options permit the construction of a compact heat regenerator with high effectiveness, so arranged as to minimize losses in ducting gas and air pressures. Greater total transfer area requirements, the complications of a coupling liquid circuit, and the need for a coupling liquid pump add complexity and weight.

4.4 MULTIWAVE PLATE REGENERATOR DESIGN OPTIMIZATION STUDY

This section deals with the aerodynamic design and optimum sizing of the Lycoming multiwave plate regenerator. A brief description of the multiwave plate core structure precedes the discussion of sizing work.

A multiwave plate pair (male and female plates) forms closed channels having either round or rectangular-like cross sections (Figure 11). All nodes or peaks of the male wave plate contact each mating wave peak on the female plate continuously along the entire length of the wave. The waves extend essentially the full length of the plate, except as otherwise specified. The waves are formed such as to follow each other in one "no flow" direction progressing from one side of the plate to the other. Pairing and stacking of the plates takes place in the remaining "no flow" direction, making a complete core module.

Each of the heat exchanging mediums flows alternately between plates. One fluid will pass through a plate pair, while the other fluid will pass between plate pairs. Therefore, each medium is encased between a male and female plate and is common to only one side of each sex plate. The hot fluid passes straight through the core from bottom to top. The cold fluid enters from a side near the plate top flowing perpendicular to its basic flow direction. This flow then turns 90 degrees so as to flow counter to that of the hot flow. The cold flow turns 90 degrees again in the same crossflow sense, leaving the core at the side opposite to that entered and near the core bottom. The cold flow thus has a small portion of its flow length defined as "crossflow". At both ends of the multiwave plates (top and bottom of both male and female) the waves or corrugations that form the cell passages for the cold flow blend away providing for this crossflow section. The area allowed for crossflow becomes larger as the exit or inlet point is reached, accommodating the progressively increasing mass flow rate being transformed from counterflow to crossflow.

Sealing the flows along the sides of the plates is accomplished by folding over or blending together pairs of plates that enclose the straight-through flowing fluids. The cold fluid is restrained by a final wave formed with a male and a female plate, one each from neighboring pairs. This final wave will blend away as the crossflow portions are reached. The wave will again form at the very top of these same two plates running along the periphery in a longitudinal manner, thus maintaining separation of the two flows at this point.

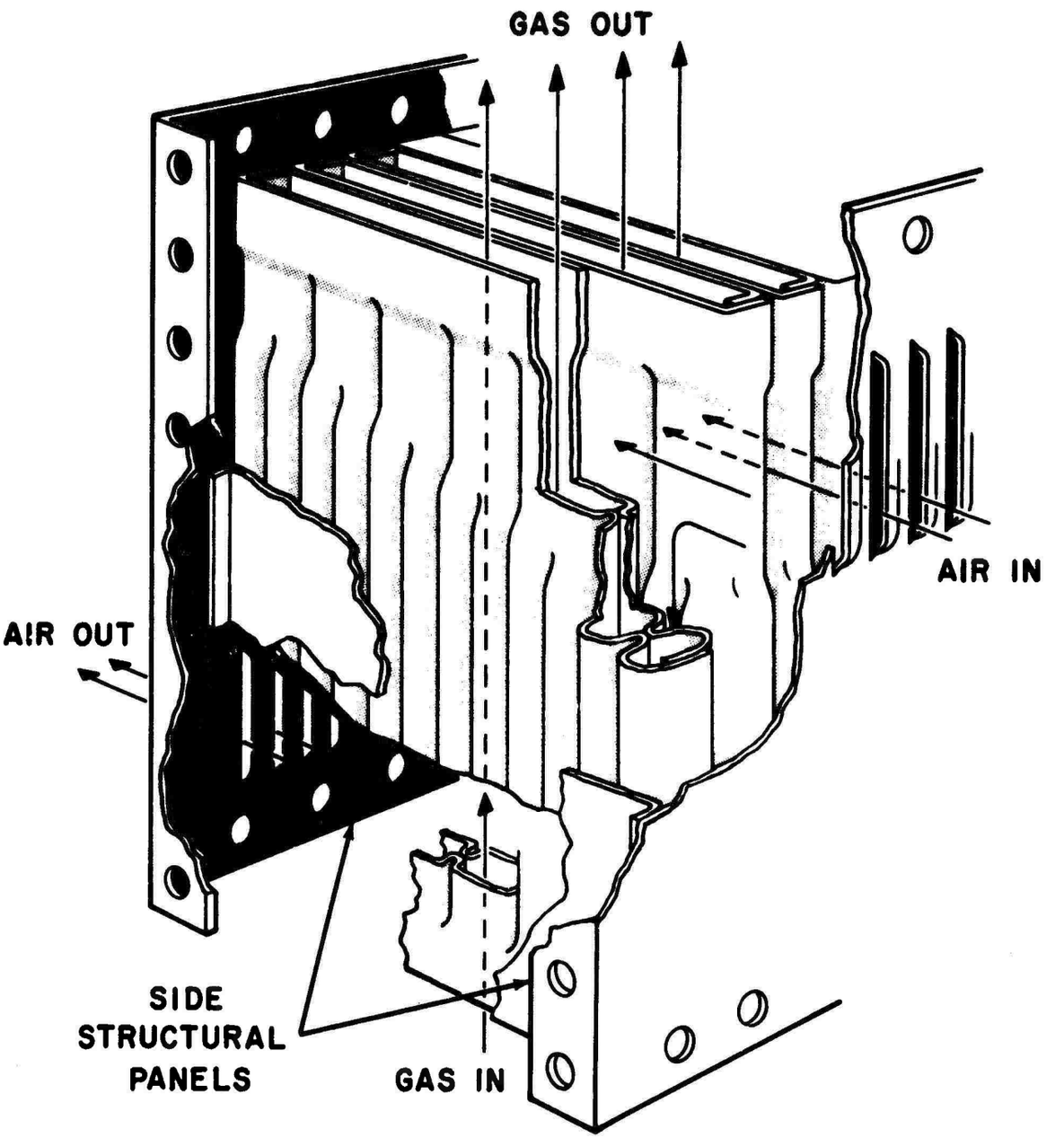

Figure 11. Matrix Core.

From the foregoing description, the primary asset of the multiwave plate concept can now be explained. The fact that a multitude of very small, all primary surface, tubelike passages can be made with a single pair of stamped wave plates has much significance. A heat exchanger matrix of extremely small hydraulic diameters can now be constructed without the prohibitive effort that would otherwise be required with the handling of an equivalent amount of separate tubes. The size of heat exchanger hydraulic diameters has a strong effect on performance; for a laminar flow heat exchanger matrix of a given volume, for instance, the heat transfer quantity quadruples when the hydraulic diameter is decreased to one half.

During initial investigations of the multiwave plate concept, carried on under a Contributing Engineering Program, some informative relations were established whereby the performance of a heat exchanger, effectiveness and pressure drop, was related to design and thermodynamic parameters. Upon establishing a fixed relation between air and gas cross-sectional flow area and passage aspect ratio, regenerator performance at a fixed engine operation is determined by three basic design parameters; hydraulic diameter, flow length, and frontal area. Likewise, for a fixed regenerator design, the performance is determined by the three basic thermodynamic parameters: temperature, pressure, and flow rate. The effect of thermodynamic and design parameters on regenerator performance is different, depending upon whether the flow is laminar or turbulent.

Tables 1 and 2 show the approximate effects of the design and thermodynamic parameters on regenerator performance. The value "NTU" is used to define the heat transfer magnitude since this term has, unlike effectiveness, a more direct relation to the controlling parameters.

TABLE 1
EFFECT OF HEAT EXCHANGER DESIGN PARAMETERS ON PERFORMANCE AT FIXED THERMODYNAMIC CONDITIONS

Laminar Flow:

$$NTU \propto \frac{AcL}{D_H^2} \qquad \frac{\Delta P}{P} \propto \frac{L}{Ac\ D_H^2}$$

Turbulent Flow:

$$NTU \propto \frac{L}{D_H} \qquad \frac{\Delta P}{P} \propto \frac{L}{Ac^2 D_H}$$

TABLE 2

EFFECT OF HEAT EXCHANGER THERMODYNAMIC PARAMETER ON PERFORMANCE FOR A FIXED DESIGN

Laminar Flow:	$NTU \propto \frac{T}{W}$	$\frac{\Delta P}{P} \propto \frac{WT^2}{P^2}$
Turbulent Flow:	$NTU \propto$ Const.	$\frac{\Delta P}{P} \propto \frac{W^2T}{P^2}$

The first objective in sizing the counterflow multiwave plate heat exchanger was to determine the air- to gas-side passage size and shape relationship. Here exists a compromizing problem since the gas- and air-sides cross-sectional flow areas, passage shape, and hydraulic diameters directly affect each other. The cross-sectional flow area, for example, can be increased on the gas side only at the cost of an equivalent decrease on the air side. A unique occurrence with the multiwave plate design is that the hydraulic diameters, air to gas, vary directly with the cross-sectional flow areas. This condition exists because of the fact that all the surface of one side of a single multiwave plate is common to the gas while all the surface on the other side of the same plate is common to the air. A consequence, then, is that equal amounts of both air and gas surface area and wetted perimeters exist in any multiwave plate design.

The effects of varying the air to gas crossflow section on a typical multiwave plate regenerator design are shown in Figures 12 and 13. As the gas to air cross-sectional flow area (A_c gas / A_c air) is increased from 1.20 to 1.80, it is noted that the gas pressure loss decreases while the air pressure loss rises. Since the predominant effect is that of the gas, a net reduction in pressure loss is obtained. The film coefficients, controlling the heat transfer, follow the same pattern as the pressure losses with a resultant slight disadvantage. The values of the film coefficients are diverging, resulting in a heat transfer controlled by the lower-valued gas film. The overall change of fuel savings is indicated in Figure 13.

The effect of reduced overall pressure losses is slightly stronger than the small disadvantage in unbalanced film coefficients in going to larger values of gas to air cross sections. However, the magnitude of fuel savings gain is so small that the design point of 1.50 was predicated upon the more important factor of wave plate forming problems which favor lower values of Ac gas/Ac air.

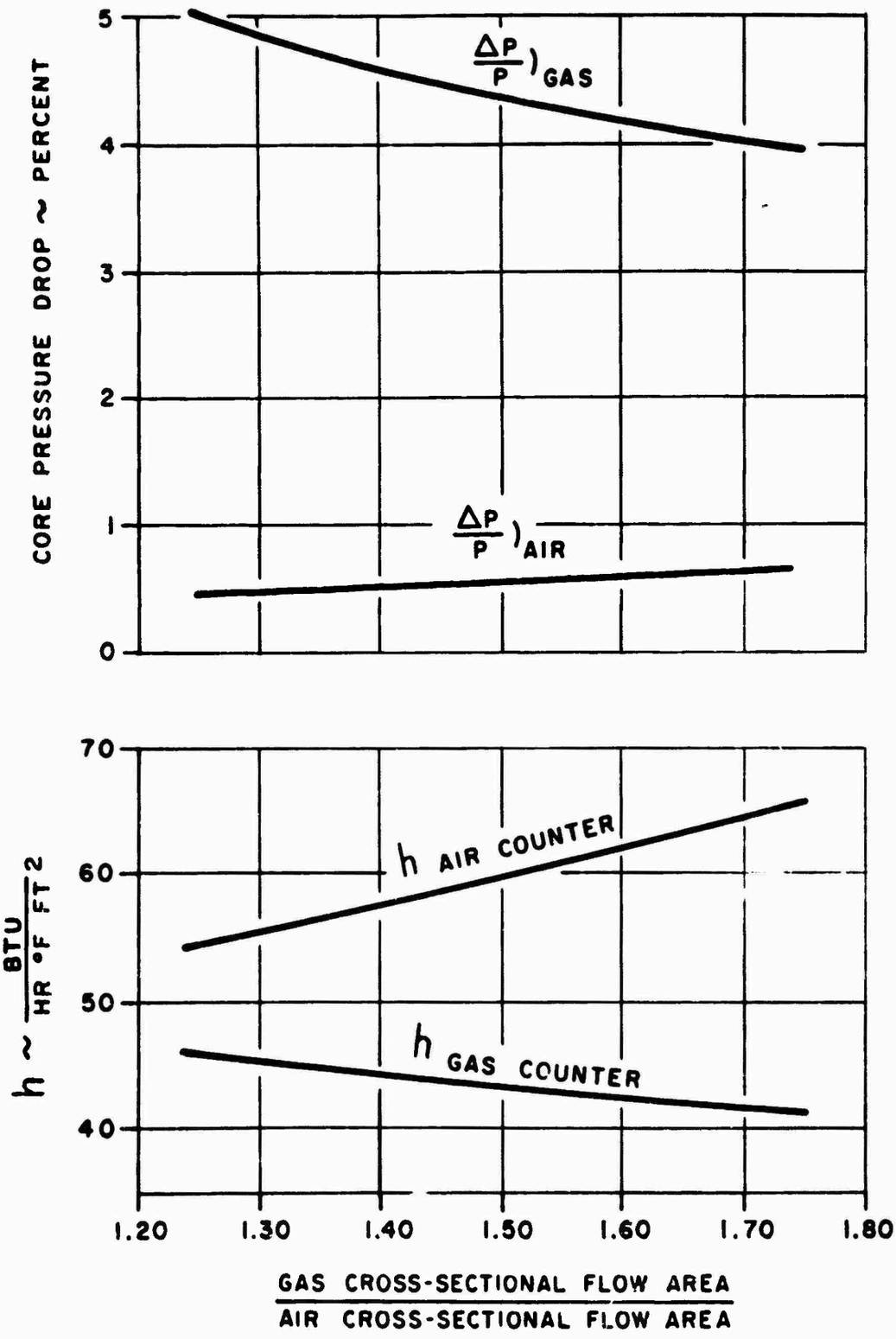

Figure 12. Multiwave Plate Regenerator. (Effect of air to gas flow area ratio on heat transfer coefficient and core pressure drop.)

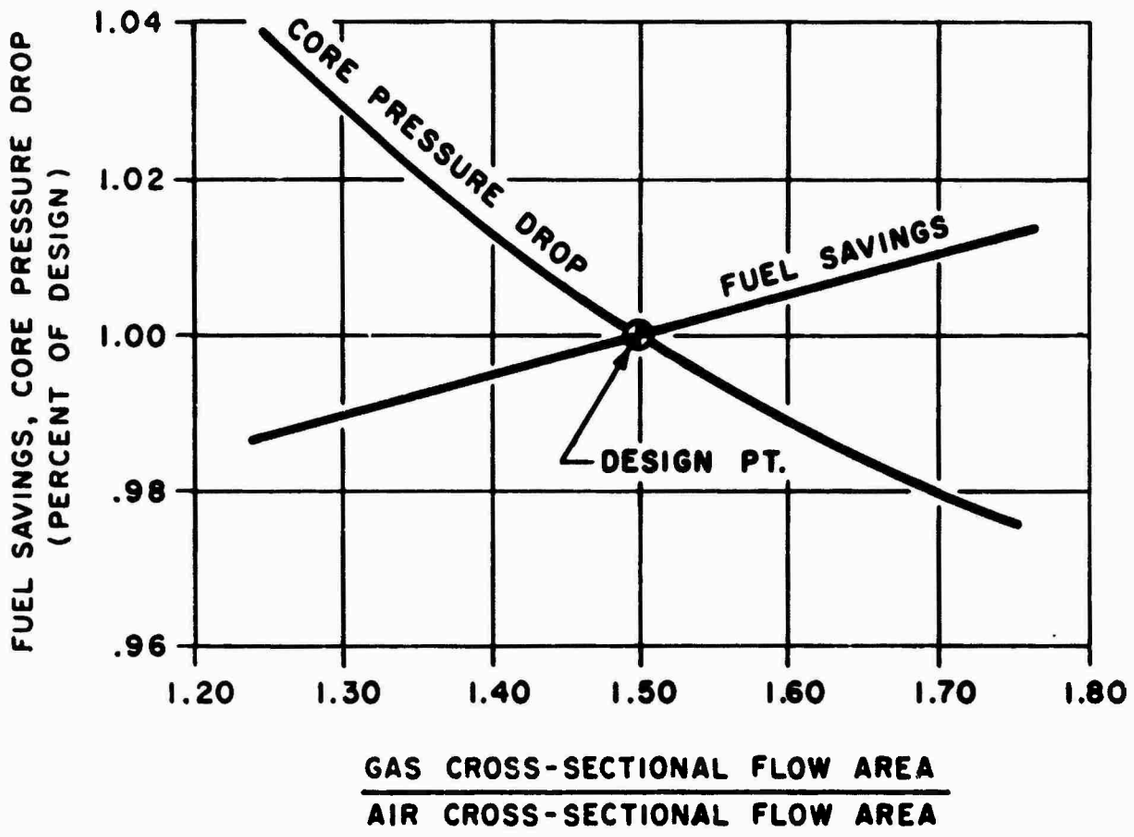

Figure 13. Multiwave Plate Regenerator. (Effect of air to gas flow area ratio on percent of change in fuel savings and total core pressure drop.)

Once the air to gas relationship within the multiwave plate regenerator matrix is established, a complete parametric study can be conducted by varying the aforementioned basic design parameters of hydraulic diameter, flow length, and frontal area. For this purpose, a digital computer program was written and used on the Lycoming IBM 7070 computer. The range covered by each variable is listed:

Hydraulic diameter = 0.030 mils to 0.090 mils
Flow length - 4 inches to 8 inches
Frontal area - 1.6 ft^2 to 14 ft^2

This coverage encompasses several hundred possible solutions used in the construction of Figures 14, 15, and 16, the last of which allows for the selection of the optimum regenerator design for a specified mission.

The range of variables was selected on the basis of covering all areas of performance interest, yet limited by a point of practicality from a size and fabrication standpoint. Figure 14 shows the regenerator performance (effectiveness and pressure drop) versus core frontal area in parameters of hydraulic diameter and core flow length. The range of variables has been limited on this graph for clarity. Some interesting observations can be made from this graph.

1) For a fixed-size regenerator (defined frontal area and flow length), the smaller the hydraulic diameter, the greater the heat transfer and pressure drop.

2) For a fixed hydraulic diameter and frontal area, the greater the flow length, the greater the heat transfer and pressure drop.

3) For a fixed hydraulic diameter and flow length, the greater the frontal area, the greater the heat transfer but the lesser the pressure drop.

4) For a hydraulic diameter of 60 mils and frontal areas of less than 3 ft^2, the flow becomes turbulent, indicating that further reduction in frontal area does not decrease effectiveness but increases pressure loss by the second power. Table 1 turbulent flow equations verify this.

If now a regenerator of $\epsilon = 0.71$ and $D_H = 0.030$ inch were examined, Figure 14 shows that values of $l = 6$ inches and $A_{fr} = 3$ ft^2, or $l = 4$ inches and A_{fr} - 4.5 ft^2 may be chosen. Either regenerator is of the same volume (1.5 ft^3) and weight; only the second choice with the shorter flow length has the lesser pressure drop, 6 percent versus 12 percent.

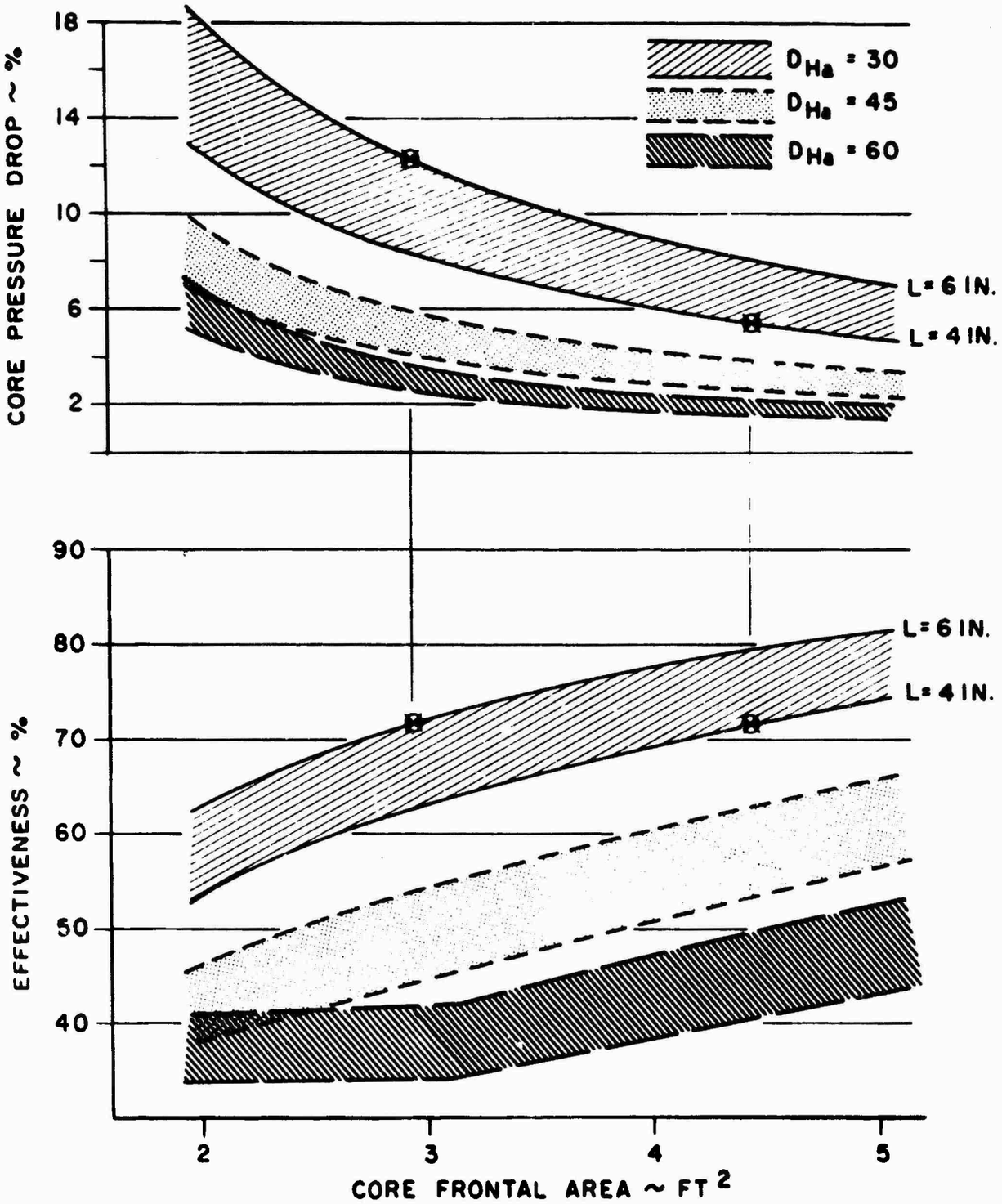

Figure 14. Multiwave Plate Regenerator Performance. (Parametric investigation.)

This then already indicates the direction to go for the best design. For a given volume heat exchanger matrix, the smallest possible hydraulic diameter should be used with a core configuration of largest frontal area and shortest flow length.

A more obvious selection of design can be made from Figure 15. Here it is possible to observe the quantitative effects in going to small D_H, large A_{fr}, and short l. For the range of design factors shown on this graph, it can be seen that with a D_H = 30 mils, l = 4 inches and A_{fr} = 9 ft^2, almost 40 percent fuel savings is possible with the T53-L-9 engine at 75 percent normal rated sea level power.

Figure 16 shows the final regenerator optimization curves. The optimum regenerator is defined as that one which will render the greatest net weight savings (fuel weight saved minus added weight of the regenerator) for a specified mission time. Figure 16 shows regenerator weight* versus percent fuel savings where the regenerators are arranged according to parameters of hydraulic diameters. A further parameter superimposed on the constant hydraulic diameter designs is flow length. Cross plotted on the fixed hydraulic diameter and variable flow length designs is frontal area. Again the advantage of the small hydraulic diameter and short flow length is emphasized, for these designs represent the lowest possible regenerator weight for any given fuel savings rate, or conversely the maximum fuel savings for any given regenerator weight.
Lycoming arbitrarily chose to optimize with a 4- to 5-hour mission. Optimization was done by first going to the smallest hydraulic diameter (D_H = 36 mils) and flow length (l = 5.2 inches) considered practical at the time, and by increasing the frontal area of the design until the greatest net fuel savings was reached. This point occurs where the ordinate distance between the regenerator weight for a line representing fixed D_H and l and the 4- to 5-hour mission line is a maximum. The resulting regenerator weight and frontal area are found to be roughly 300 pounds and 4.75 ft^2 giving a 27 percent fuel savings. The gross fuel

---

* The total regenerator weight is made up of core weight (wave plate plus braze), header and tube weight, and the structural wrap-up weight. Core weight is precisely determined by plate number, size and thickness, plus braze area times braze thickness. The fixed header weight was determined from known fixed header flow area and strength requirements. The wrap-up structure weight is somewhat ambiguous but was determined to be a function of core volume. The total multiwave plate regenerator weight as applied to the T53-L-9 engine is: Regenerator Weight = Core Weight + Interface Hardware Weight + Regenerator Wrap-Up Weight.

Interface hardware weight is estimated to be 75 pounds; regenerator wrap-up weight, in pounds, is estimated at 37 times the core volume in cubic feet.

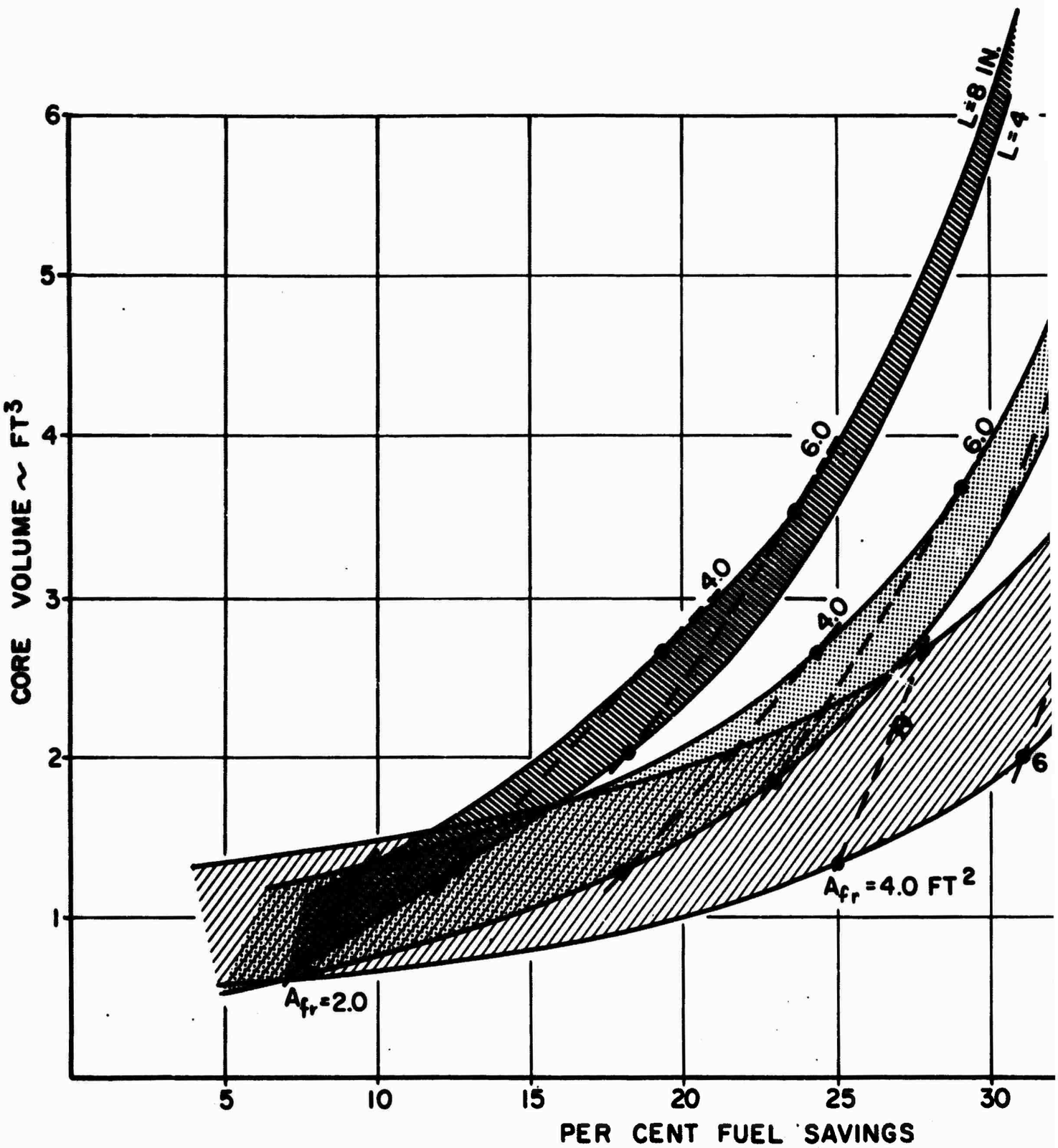

Figure 15. Multiwave Plate Regenerator Core Volume
(T53-L-9 engine at 75% normal rated powe

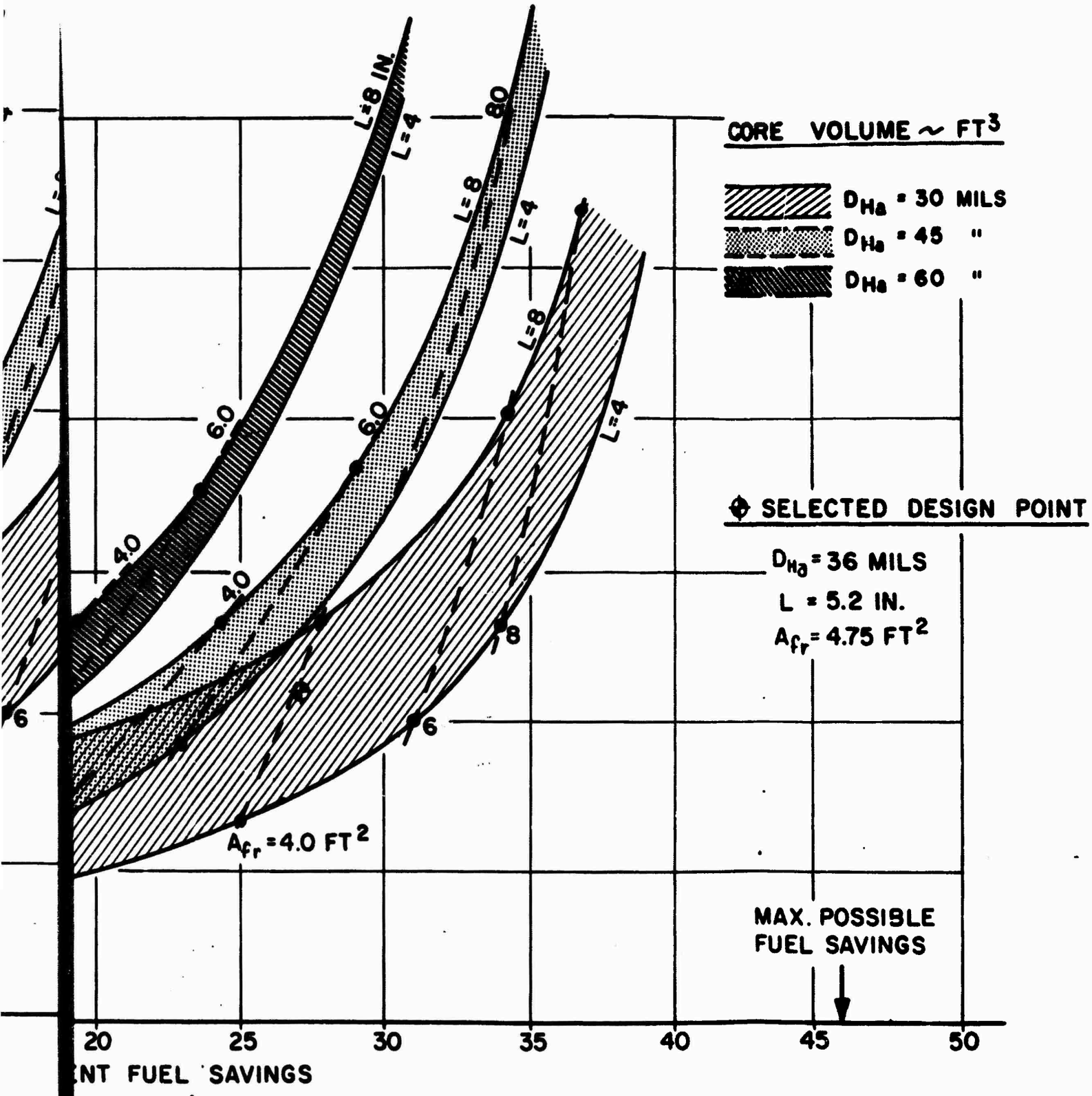

me V e Plate Regenerator Core Volume Vs. Fuel Savings.
ower engine at 75% normal rated power - sea level.)

B

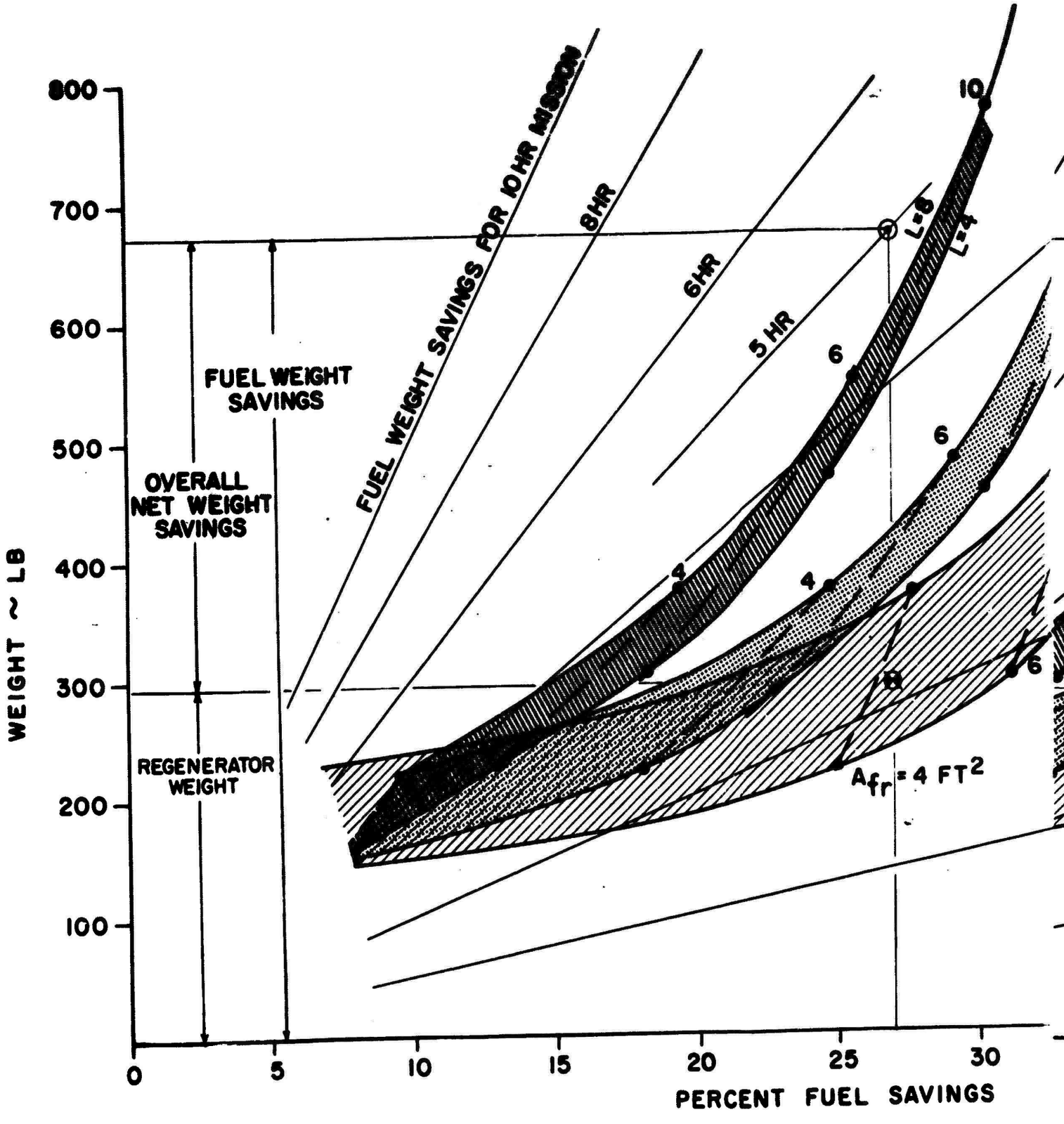

Figure 16. T53-L-9 Regenerator Sizing Optimization rated power - sea level. (Sizing for maxi payload increase.)

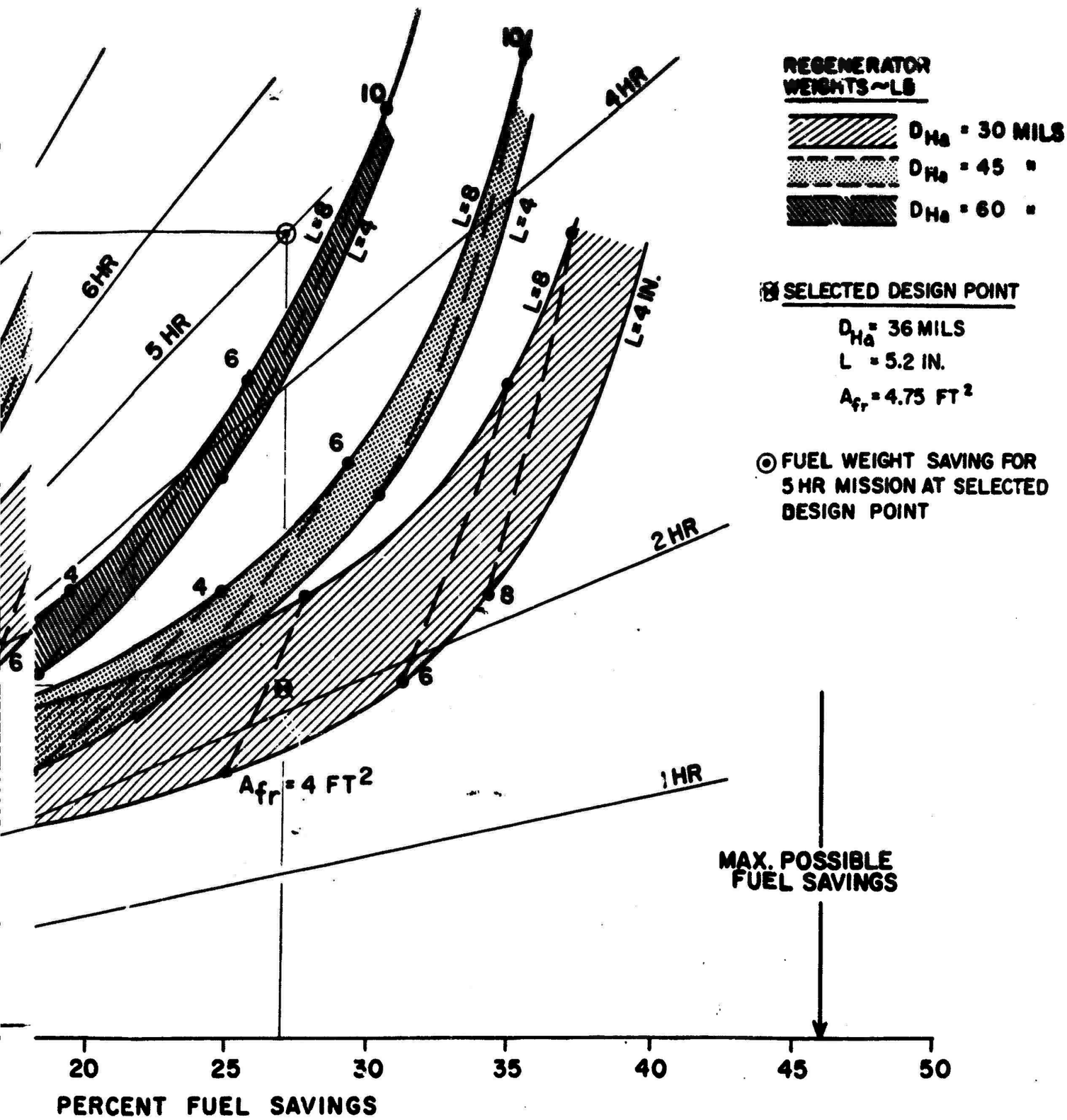

on
axi 9 Regenerator Sizing Optimization at 75% normal
ower - sea level. (Sizing for maximum mission
l increase.)

B

savings is 700 pounds for a 5-hour flight as indicated by a 5-hour fuel savings line at a 27 percent fuel savings rate. The net overall savings on weight would then be 400 pounds, approximately that of the entire engine.

If longer flight mission times are required, the optimum multiwave plate regenerator would require greater frontal areas, and net weight savings would become more impressive.

At this point the following general statements can be made about optimizing the multiwave plate regenerator:

1) Since reduced hydraulic diameter is always beneficial from a performance standpoint, the minimum size will be limited by the state of the art of plate forming and brazing techniques and by clogging and fouling considerations.

2) The flow length of the regenerator will be reduced to a point limited by practicality of overall regenerator envelope dimensions and wrap-up hardware requirements.

3) The frontal area of the regenerator is the one parameter that can be conveniently varied to optimize the regenerator for any given mission, again limited from the high end if impractical envelope dimensions occur.

Statement 3) has particular significance; the multiwave plate can be optimized for different missions by building essentially the same multiwave plate cores, but stacking together different quantities of plates. This allows for the correct frontal areas necessary for any mission optimization.

To this point all heat transfer performance studies have been limited to continuous, smooth-walled surfaces. It is well known that rough, dimpled, or herringbone surfaces have greater heat transfer and pressure losses per unit surface area. Only in the cases of extreme Reynolds numbers where flow is either strongly viscous or tremendously turbulent is this not so. The magnitude of pressure loss (friction factor) and heat transfer (Colburn factor) difference between typical dimpled and undimpled tubes of the same size is indicated in Figure 17. The more pronounced the dimpling, the greater this difference.

The first impression obtained from Figure 17 is that since the Colburn factor is higher for a dimpled surface than for a smooth surface, the use of the former will result in a smaller, lighter regenerator to meet a given effectiveness. However, the higher friction factor for the dimpled

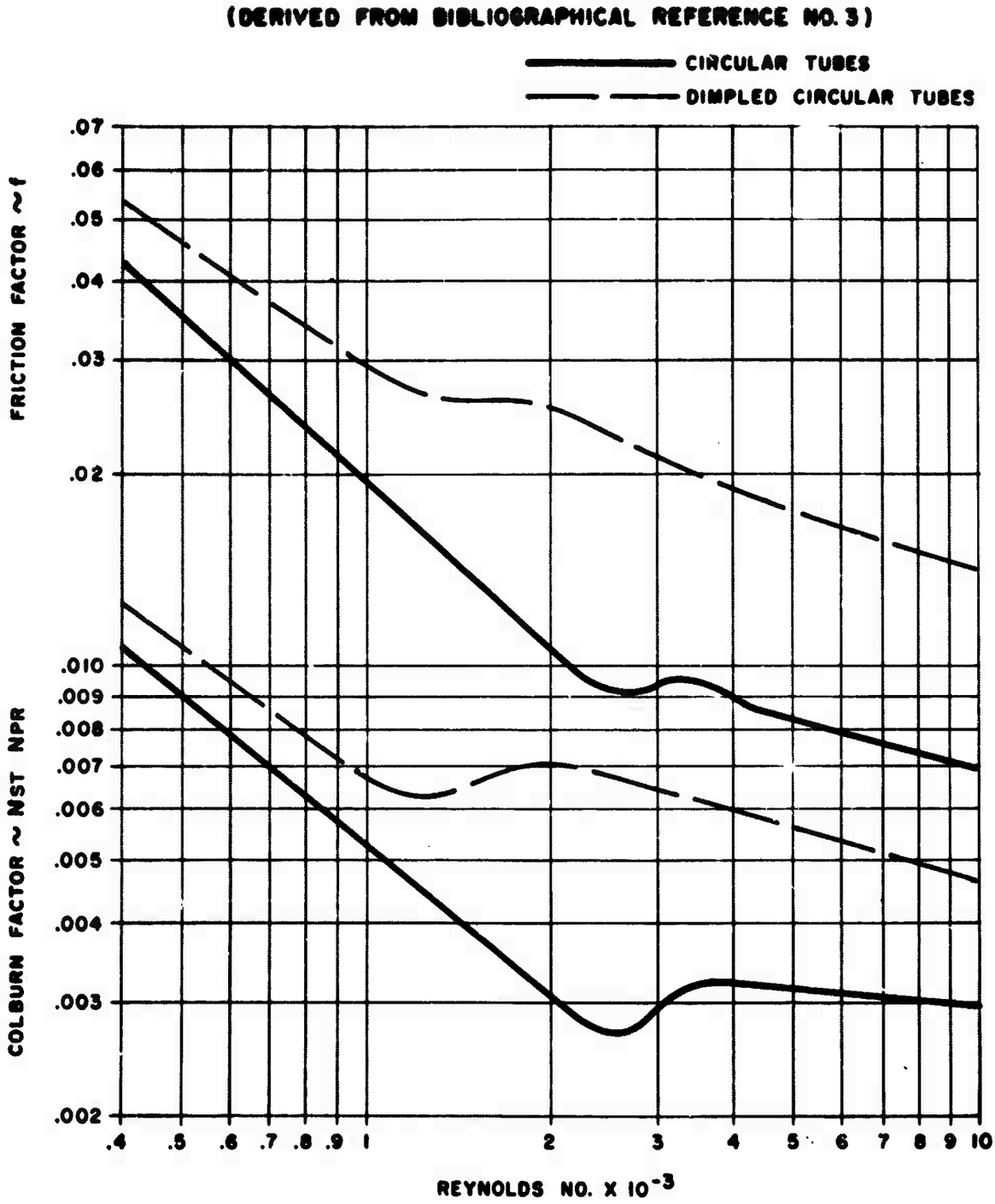

Figure 17. Heat Transfer and Friction Factors Vs. Reynolds Number. (Comparison of smooth and dimpled tubes.)

surface will cause increasing pressure loss through the regenerator. Therefore, even though the heat transfer area and volume required of the dimpled surface regenerator is smaller, a larger frontal area is required to maintain a given pressure loss. This larger frontal area may result in a final dimpled design which is larger than the smooth-surface design, depending upon the relative increase of the friction and the Colburn factors at the particular Reynolds number being considered.

Dimpling can be easily incorporated into the multiwave plate surface, but accurate determination of its value is dependent upon the acquisition of experimental performance data for both types of wave plate surfaces.

4.5 EVALUATION OF REGENERATOR OFF-DESIGN AND BYPASS PERFORMANCE

4.5.1 Off-Design-Point Performance

The regenerator design and performance has to this point been based on the Lycoming T53-L-9 gas turbine engine operating at 75 percent normal rated sea level power (675 horsepower). It is now necessary to examine the regenerator performance over a range of power settings and altitudes.

Looking first at the effects of different sea level power settings (Figure 18), tendencies in regenerator pressure losses can be seen in the weight flow parameter versus shaft power graph. An increase in power above the design point shows that the high-pressure or air-side flow parameter tends to drop off. Since the flow parameter is a direct indication of Mach number, and Mach number being a rough indication of pressure loss (varies depending on whether flow is turbulent or laminar), the general conclusion is that at higher than design power setting the air-side pressure loss diminishes. Contrary to this, the gas flow parameter increases significantly in going to full power. Excessive gas-side pressure loss would then be experienced under high-power operation. It becomes evident that a gas-side bypass valve is desirable for successful regenerative gas turbine operation unless the engine is designed for maximum power operation.

A more accurate picture of percent change of design pressure drop with power is shown in Figure 19. In this graph the air and gas theoretical friction pressure loss variation with power is shown in dashed lines for both turbulent and laminar flows. On the gas side it is noted that the laminar and turbulent flows show almost the same rate of increase in friction pressure loss with power. Normally, it would be expected that the turbulent flows would show a greater increase. However, with the particular action of the gas turbine exhaust gases, the exhaust temperature rises with power at a greater rate than does the mass flow, attributing to the condition shown.

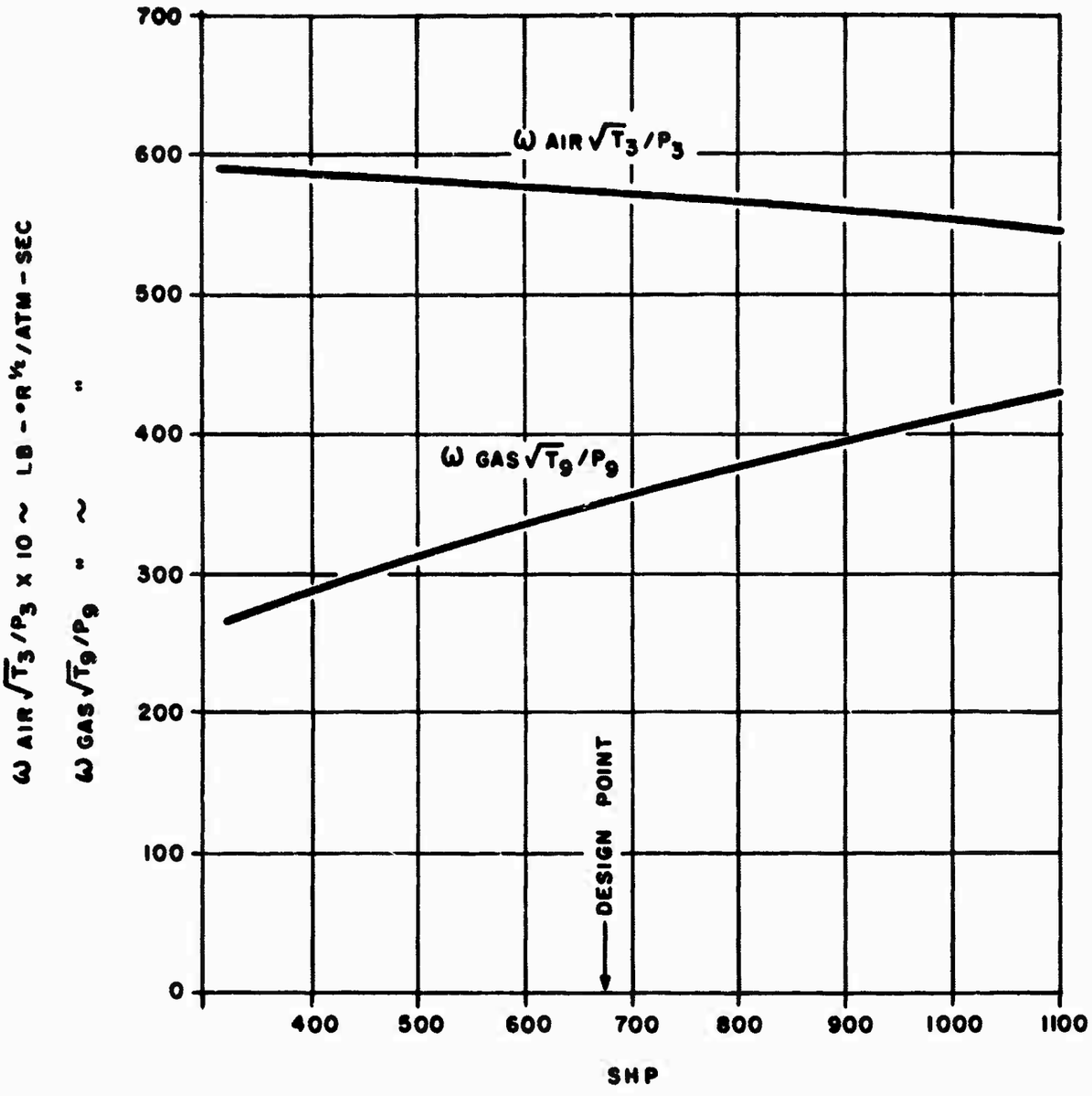

Figure 18. T53-L-9 Engine Flow Parameters Vs. Power at Sea Level.

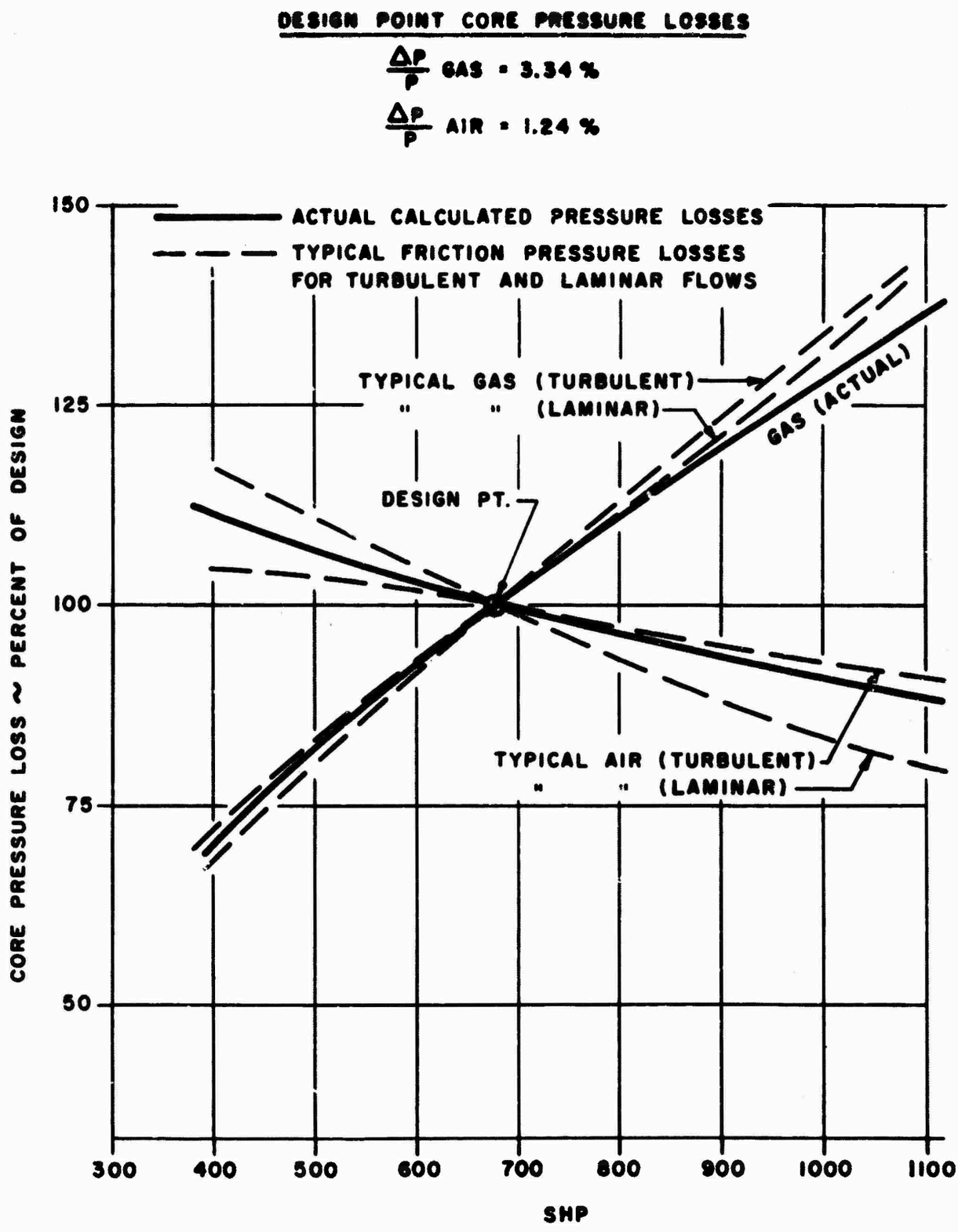

Figure 19. Multiwave Plate Regenerator. (Core pressure loss vs. power.)

The actual regenerator pressure losses shown in solid lines of the same figure include not only the effect of friction loss (approximately 80 percent of the total), but core entrance, exit, and momentum losses. At increased powers the effect of the overall gas losses follows closely, but is somewhat less than the predicted losses due to friction only. The actual air-side pressure losses follow the slope of the predicted laminar friction losses at low powers and that of the turbulent friction losses at higher powers. The reason is that at design powers and above, the air in the crossflow section of the regenerator matrix is not only turbulent but contributes a major portion to the total air-side pressure drop.

The changes in regenerator performance due to altitude will next be considered. The flow parameter versus altitude curve is shown in Figure 20. Figure 21 shows (in dashes) the theoretical friction pressure losses, laminar and turbulent, for both air and gas. It is to be noted that the laminar friction pressure losses show greater increases at altitude than do the turbulent flows. The air-side losses in general show only moderate increases in pressure loss versus altitude, while the gas side shows excessive loss with increasing altitude. The multiwave plate regenerator has essentially laminar flow except in the air crossflow section. Even the air-side cross-flow section becomes laminar at low powers and increased altitudes. The solid lines of Figure 21, representing the actual overall pressure loss change with altitude, follow the laminar friction loss lines. As can be observed, the gas-side pressure drop increases over twofold in going from sea level to 25,000 feet. From Table 2, the percent pressure loss change with changing thermodynamic states is $\Delta P/P \propto WT^2/P^2$. It is thus seen that the pressure of the exhaust gas, which drops off directly with the atmospheric pressure at altitude, is primarily responsible for the increased percentage in gas core pressure drop. Fortunately, the heat transfer effect also increases with altitude, thereby presenting the opportunity for exhaust gas bypassing at altitude, trading off heat transfer effectiveness against pressure losses.

4.5.2 Bypassing

From the off-design performance study, it was concluded that a regenerator exhaust gas bypass valve will be required to eliminate excessive gas-side pressure losses at altitude and high-power operation. This section will deal with the performance change (effectiveness and pressure drop) of a fixed-design regenerator as a function of the exhaust gas bypass.

In a given laminar flow heat exchanger, the performance is essentially a function of the air and gas mass flow, temperature, and pressure. With bypassing, the average temperature and pressure levels do not sig-

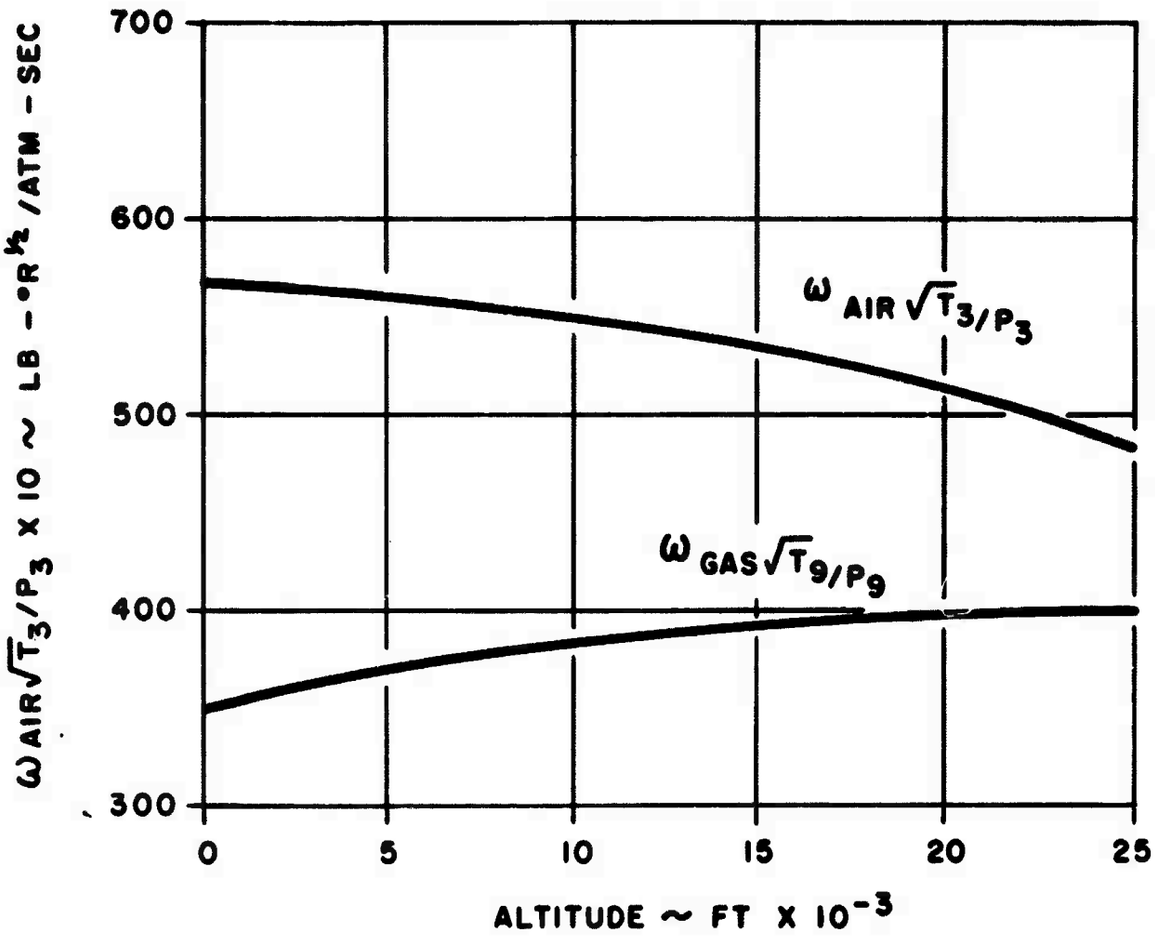

Figure 20. T53-L-9 Engine Flow Parameters Vs. Altitude at 75% Normal Rated Power.

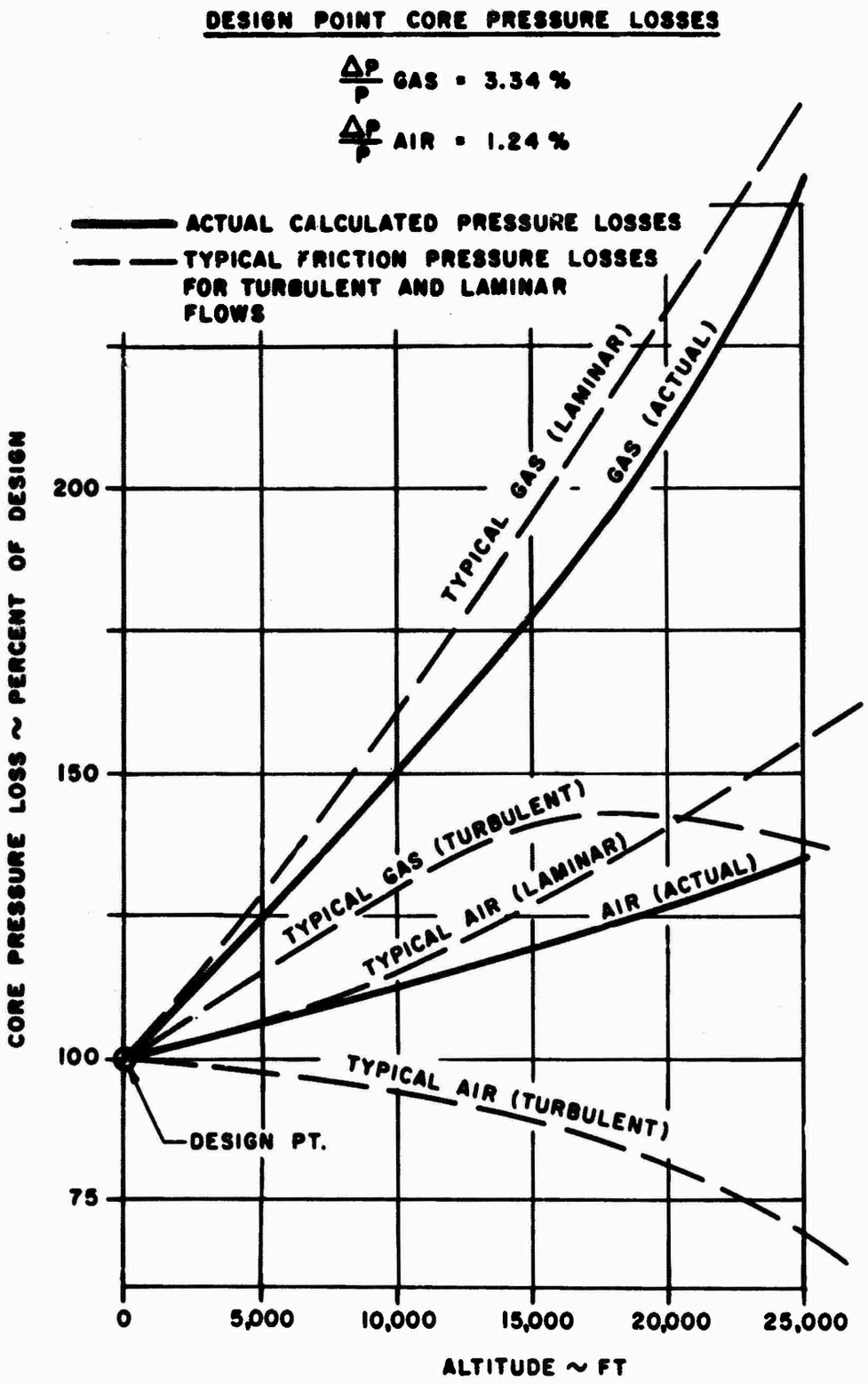

Figure 21. Multiwave Plate Regenerator. (Core pressure loss vs. altitude.)

nificantly change, reducing performance to a function of weight flow only. As increasing portions of exhaust gas are bypassed around the regenerator, the gas-side effectiveness, or temperature drop, increases with that proportion of gas that does go through the regenerator. The air-side effectiveness, however, decreases. This is due to the lesser quantity of gas that can transfer heat to the air. For any degree of gas bypassing, the temperature change of the air in passing through the regenerator (air-side effectiveness) is equal to the gas temperature change (gas-side effectiveness) times the ratio of the gas heat capacity rate to air heat capacity rate (C_{gas}/C_{air}). Figure 22 shows this effect. Beginning with a hypothetical regenerator design for an air-side effectiveness of 0.71 at zero bypass, and a $C_{air}/C_{gas} = 0.95$, both air-side and gas-side effectiveness values are shown as a function of the percent gas bypass. With bypassing, the gas-side effectiveness approaches 100 percent while the air-side effectiveness falls off zero percent.

A clearer picture of what is happening during gas-side bypassing is shown in Figure 23. Here the air and gas temperature change is given as the medium pass through a true counterflow regenerator. Curve A represents the full flow or zero bypass situation. Curves B and C have 40 and 60 percent gas bypass, respectively. It can be noted that at zero bypass, the gas temperature drops and the air temperature rises uniformly as they pass through the length of the heat exchanger core. Also to be noted is that with this condition the temperature difference between air and gas is the same at any length station attributing to the factor of uniform temperature change and uniform heat transfer at any section. Looking at Curve C (60 percent bypass), it is seen that at the air inlet (zero percent core flow length) the gas has already been cooled to a temperature approaching that of the incoming air.

This means that at a small temperature difference, air to gas, there is little heat transfer, and thus the slope of these lines is quite flat in this region. Further on through the core, at the gas inlet, it is seen that the air discharge temperature is still relatively low. Thus, at this point the slopes of the air and gas plots are steeper owing to the great temperature difference and resulting heat transfer. In all cases, with a certain percent gas bypass, the slopes of the gas temperature plot are greater than that of the air at any given station. The degree of slope difference is here related to the amount of gas being bypassed. The more gas being bypassed, the greater the slope of the gas temperature plot relative to the air temperature plot. Shown also in Figure 23 is the air and gas effectiveness for Curves A, B, and C. The effectiveness can be read from the discharge temperatures and the vertical adjoining effectiveness scale.

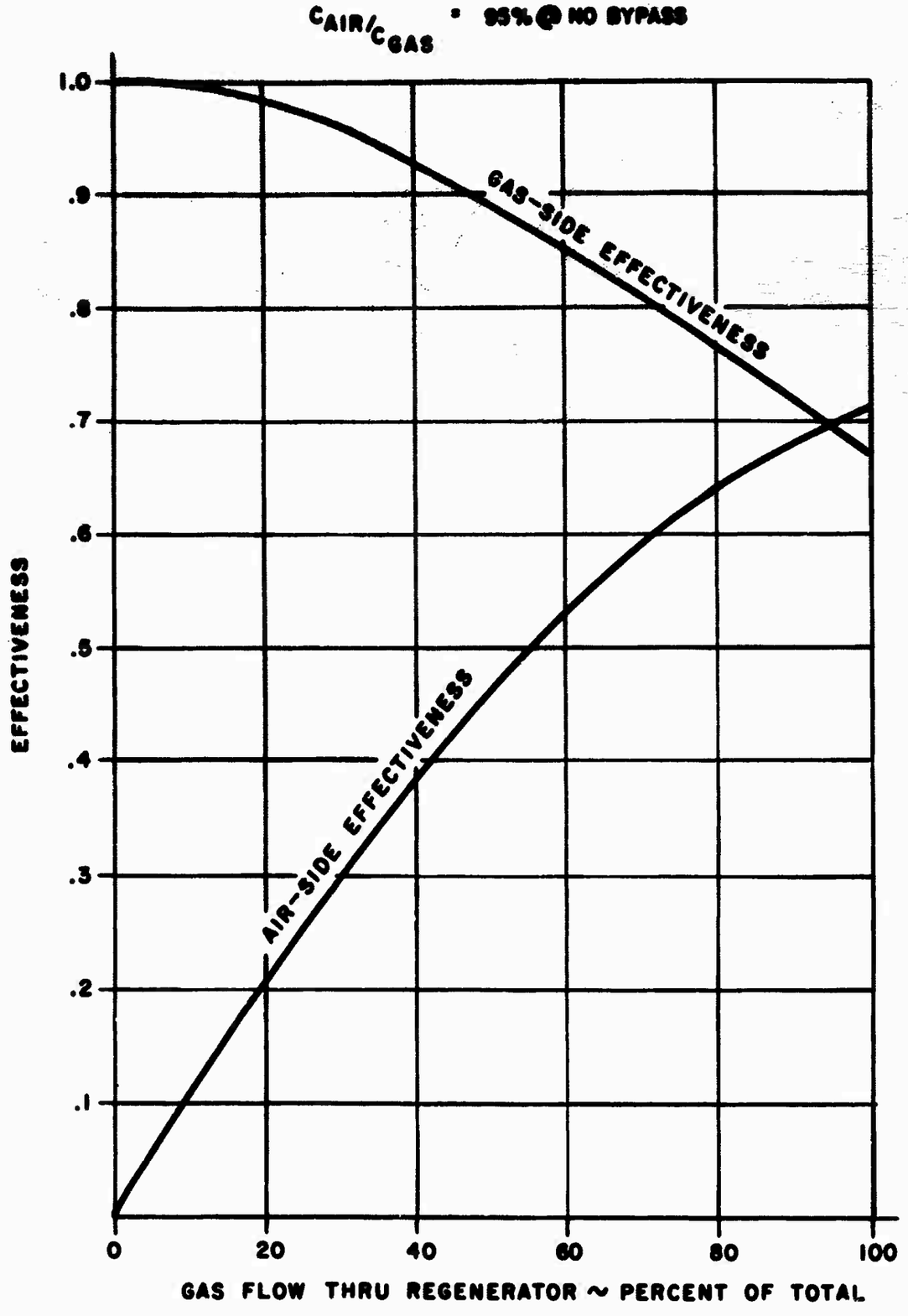

Figure 22. Effectiveness Vs. Gas Bypass.

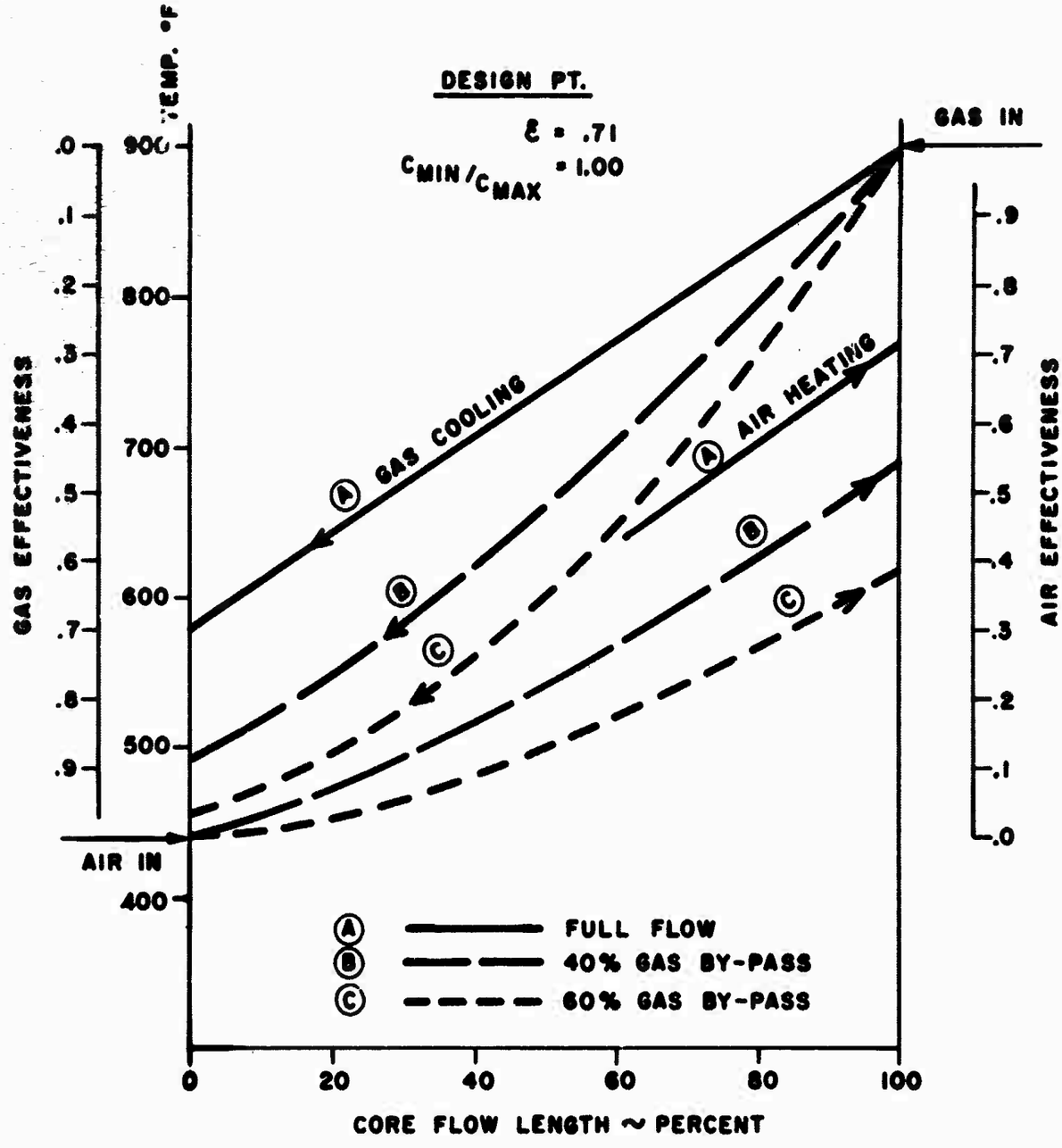

Figure 23. Core Temperature Distribution. (Effect of gas bypassing.)

As previously stated, the amount of decrease in pressure drop with bypassing varies directly with the decrease in weight flow through the core. Of course, with gas-side bypassing only, the gas-side pressure loss will be diminished. There remains now the problem of determining when and how much bypassing will be necessary to eliminate excessive pressure losses.

Considering first the regenerator performance at design power (75 percent normal rated) versus aititude, Figure 24 is presented. Plotted here is total regenerator pressure loss and air-side effectiveness versus altitude in parameters of percent gas bypassed. In going to 25,000 feet, the total pressure drop increases from approximately 8 to 14 percent in the nonbypass condition. The air-side effectiveness, however, goes from 0.71 to over 0.80. This effectiveness increase represents a significant increase in NTU's, and is basically a result of the decrease weight flow being handled at these altitudes. It was determined that total pressure losses caused by the regenerator should not exceed 10 percent under any condition in order not to upset the match between the engine components. From Figure 24 it is seen that a 10 percent total pressure drop occurs at zero bypass and 11,000-feet altitude. At 25,000 feet a 33 percent gas bypass is necessary to retain the 10 percent total pressure loss.

With the bypassing of up to 33 percent at 25,000 feet, the air-side effectiveness remains equivalent to or slightly better than that at sea level. Actually, the bypassing of gas has only served to lose what would have been an effectiveness gain at altitudes. This effectiveness loss plus the eliminated pressure drop is indicated by the shaded regions in Figure 24.

Gas bypassing requirements versus power setting at sea level is shown i. a different manner in order to present the overall picture of fuel savings, operating temperatures, and power limitations. Figure 25 shows a plot of fuel rate versus sea level power setting. The short dashed lines represent the nonregenerative T53-L-9 engine, while the long dashed lines represent the same engine with the regenerator design selected by Lycoming in the optimization study. Cross-plotted on this graph are parameters of turbine inlet temperatures and percent gas bypass, The difference between the nonregenerative and regenerative engines is the shaded area which represents the magnitude of fuel savings to be had over the power spectrum. It is to be noted that gas bypassing is initiated at the point where maximum allowed turbine inlet temperature is reached. With the full regenerator pressure loss this power point is approximately 975 horsepower versus 1100 horsepower

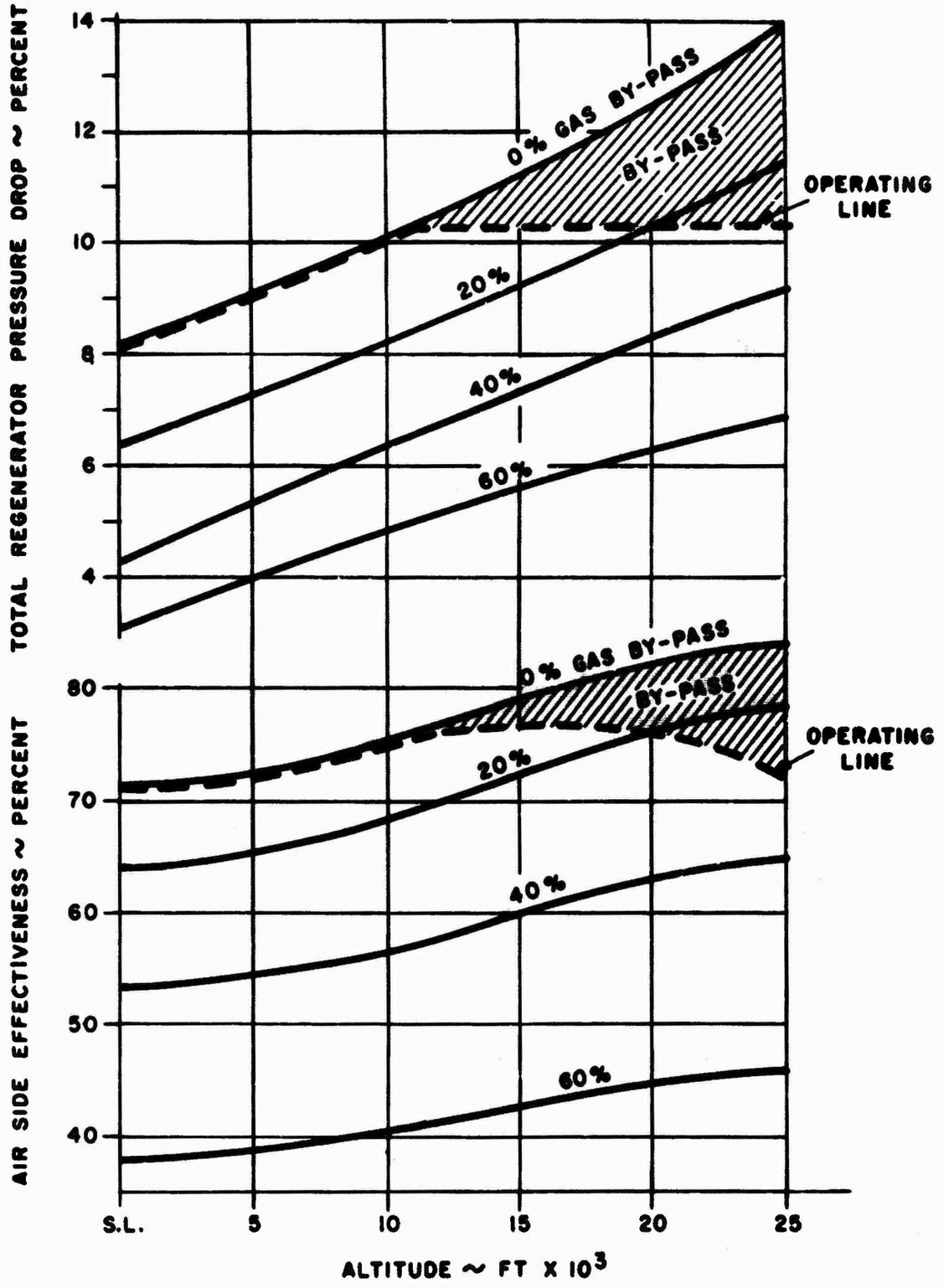

Figure 24. Multiwave Plate Regenerator. (Design point operation vs. altitude.)

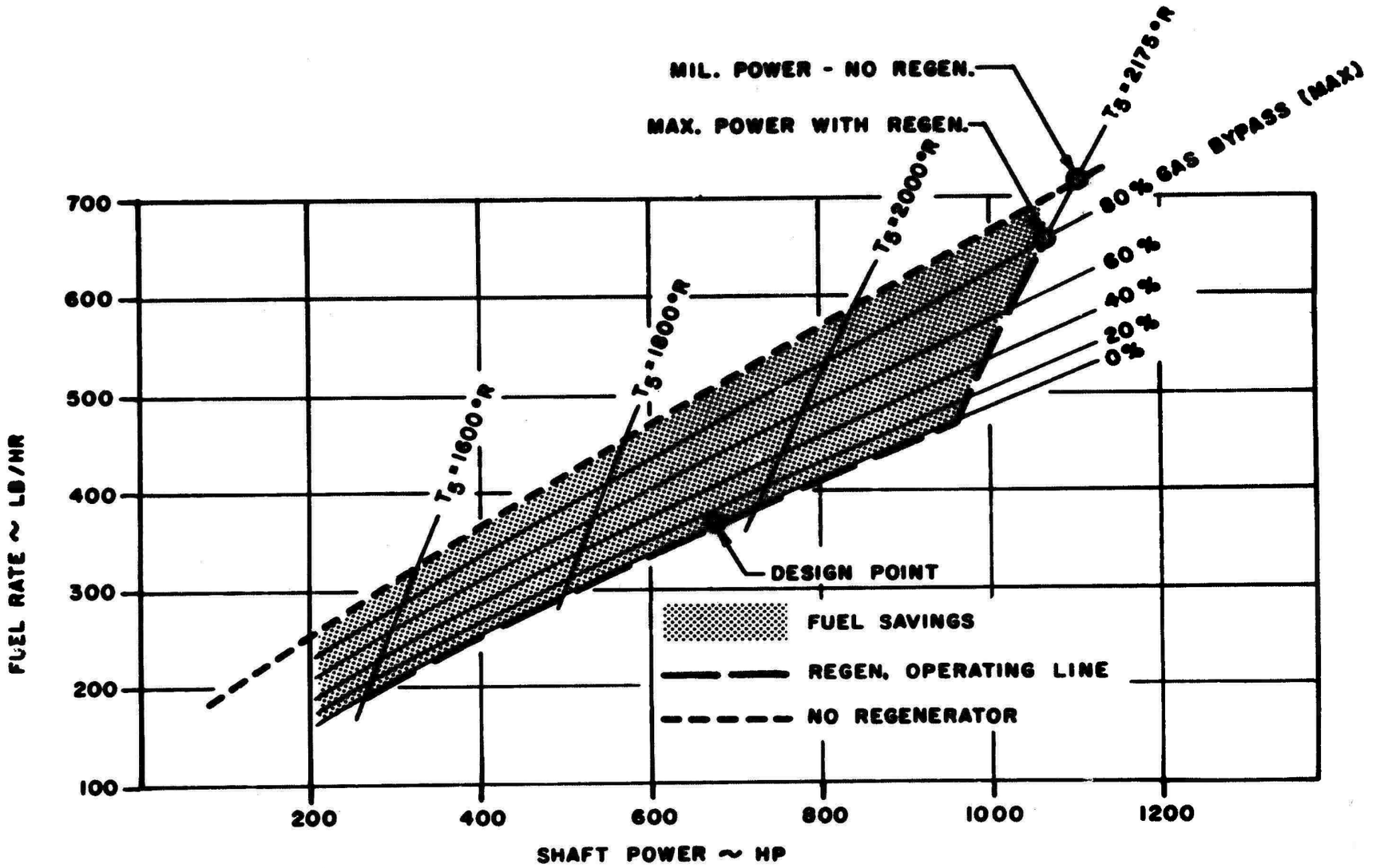

Figure 25. T53-L-9 Multiwave Plate Regenerator Engine. (Performance vs. power.)

for the nonregenerative version. At the fixed maximum temperature of 2175° R, increasing rates of gas bypass allow the power to increase to 1060 horsepower. This is now the new military power setting which corresponds to 80 percent gas bypass. The 80 percent value is the practical limit of bypassing. The original power of 1100 horsepower at a turbine inlet temperature of 2175° R will never be reached owing to the continuing air-side and remaining gas-side pressure losses.

Of importance here is the fact that military power was determined on the basis of a fixed maximum turbine inlet temperature. In actuality the turbine hardware life is controlled not by the average maximum turbine inlet temperatures but by the more local radial and circumferential peak temperatures. The magnitude of these peak temperatures is a function of the temperature rise in the combustor. Owing to the preheating of the air by the regenerator prior to entering the combustor, these peaks should experience a worthwhile reduction. This occurrence would lead Lycoming to believe that for the same turbine life, somewhat higher average turbine inlet temperature could be tolerated with the regenerative model engine, possibly elevating the regenerative military power to its original level.

4.6 SPECIFICATION SUMMARY OF FINALIZED MULTIWAVE PLATE REGENERATOR

At the onset of the regenerator analytical study a problem statement in the form of a preliminary regenerator specification (Spec. No. 105.23.1 dated 4 September 1962) was written using the T53-L-9 engine and its performance as a basis. This specification appears in Appendix I. The thermodynamic states of the engine that are required for the regenerator design are summarized in Table 3. These thermodynamic states are given for the design point of 75 percent normal rated power.

The performance of the optimized multiwave plate regenerator selected in Section 4.4 is given in Table 4. The basic performance is first listed, followed by a detailed breakdown of the accumulated pressure drops and additional heat transfer data. The pertinent dimensional data of the regenerator are tabulated in Table 5.

TABLE 3
THERMODYNAMIC STATES FOR REGENERATOR DESIGN POINT
OF 75% NORMAL RATED POWER

Regenerator Air Side			
Weight flow	W_{air}	=	9.6 lb/sec (less cooling)
Temperature, in	T_3	=	440° F
Pressure, in	P_3	=	74.5 psia
Spc. heat, avg.	c_p	=	0.25 Btu/lb-°F
Regenerator Gas Inlet			
Weight flow	Wgas	=	9.71 lb/sec
Temperature, in	T_9	=	902° F
Pressure, in	P_9	=	14.7 ΔP_{gas} psia
Spc. heat, avg.	c_p	=	0.26 Btu/lb-°F

TABLE 4
DESIGN-POINT PERFORMANCE

Basic Performance

Air-side temperature effectiveness	-	71.6%
Total pressure drop	-	8.10 %
Fuel savings	-	27 %

Detailed Pressure Drops

Core (air)	-	1.25%
Core (gas)	-	3.35%
Headers (air)	-	0.50%
Ducting and exhaust (gas)	-	3.00%
Total		8.10%

Heat Transfer Data

ϵ gas	-	66.5%
NTU	-	2.27
C_{min}/C_{max}	-	0.935
U	-	19.66 Btu/hr-^{o}F-ft^{2}
h air	-	44.9 Btu/hr-^{o}F-ft^{2}
h gas	-	34.9 Btu/hr-^{o}F-ft^{2}
N_R air	-	887
N_R gas	-	826
D_H air	-	36 mils
D_H gas	-	54.4 mils
A	-	936 ft^{2}
A_{fr}	-	4.75 ft^{2}
A_c air	-	1.62 ft^{2}
A_c gas	-	2.42 ft^{2}
A_c metal	-	0.71 ft^{2}

TABLE 5
DESIGN SPECIFICATIONS

Overall Dimensions

Maximum overall diameter	-	31 in.
Total length (from engine flange)	-	29 in.
Gross weight	-	294 lb

Core Dimensions

Number of cores	-	8
Core length, width, height	-	24 in. x 3.6 in. x 5.5 in.
Core weight	-	144 lb
Core volume	-	2.18 ft^3
Core frontal area	-	4.75 ft^2
Heat transfer surface	-	936 ft^2
Total number of plates	-	6,100
Number of plates per inch	-	32
Initial plate thickness	-	0.0032 in.
Avg. plate forming elongation	-	22%
Core porosity	-	85%

SECTION FIVE. EXPERIMENTAL MULTIWAVE PLATE CORE EVALUATION

5.1 EXPERIMENTAL CORE DESIGN

5.1.1 Design Criteria

The design of a gas-to-air regenerator suitable for use on aircraft gas turbine engines is based on a stationary type with counterflow passages and 100 percent primary heat transfer surfaces. An investigation of these two initial conditions defined a regenerator core construction of the tubular or multiwave plate type. The use of multiwave plates was chosen as the method of achieving a more compact, lighter, and more efficient regenerator.

The required aerodynamic and heat transfer characteristics that establish the counterflow cross-sectional conditions are:

1) A ratio of gas-to-air cross-sectional flow area of 1.5 to 1.
2) A hydraulic radius (the flow area divided by the wetted perimeter) for the gas side of 0.01125 inch and for the air side of 0.0075 inch.

Further mechanical design criteria are established by the following:

1) An 85-psi maximum pressure differential.
2) A need for minimum wall thickness to minimize core weight.
3) A need for low percentage of elongation of the material permitting it to be readily formed.
4) Varying temperatures from inlet to outlet areas creating thermal stresses.

5.1.2 Multiwave Plate Core Design

Two basic cross-sectional wave forms, the crest-on-crest and the crest-on-flat, were thoroughly investigated. A cross section of a typical crest-on-crest wave form is shown in Figure 26. Table 6 shows a comparison of the studies made for the crest-on-crest wave form, giving the effects on the heat transfer properties caused by changing one or more of the design parameters. "Figure 9" in this Table corresponds to the design illustrated in Figure 26.

A cross section of a typical crest-on-flat type of wave form is shown in Figure 27; a comparison of the studies for this type is shown in Table 7.

32 WAVES PER INCH
40 PLATES PER INCH

ELONGATION = 27.77 %

$A_G/P_G = .01075$

$A_A/P_A = .00743$

$A_G/A_A = 1.506$

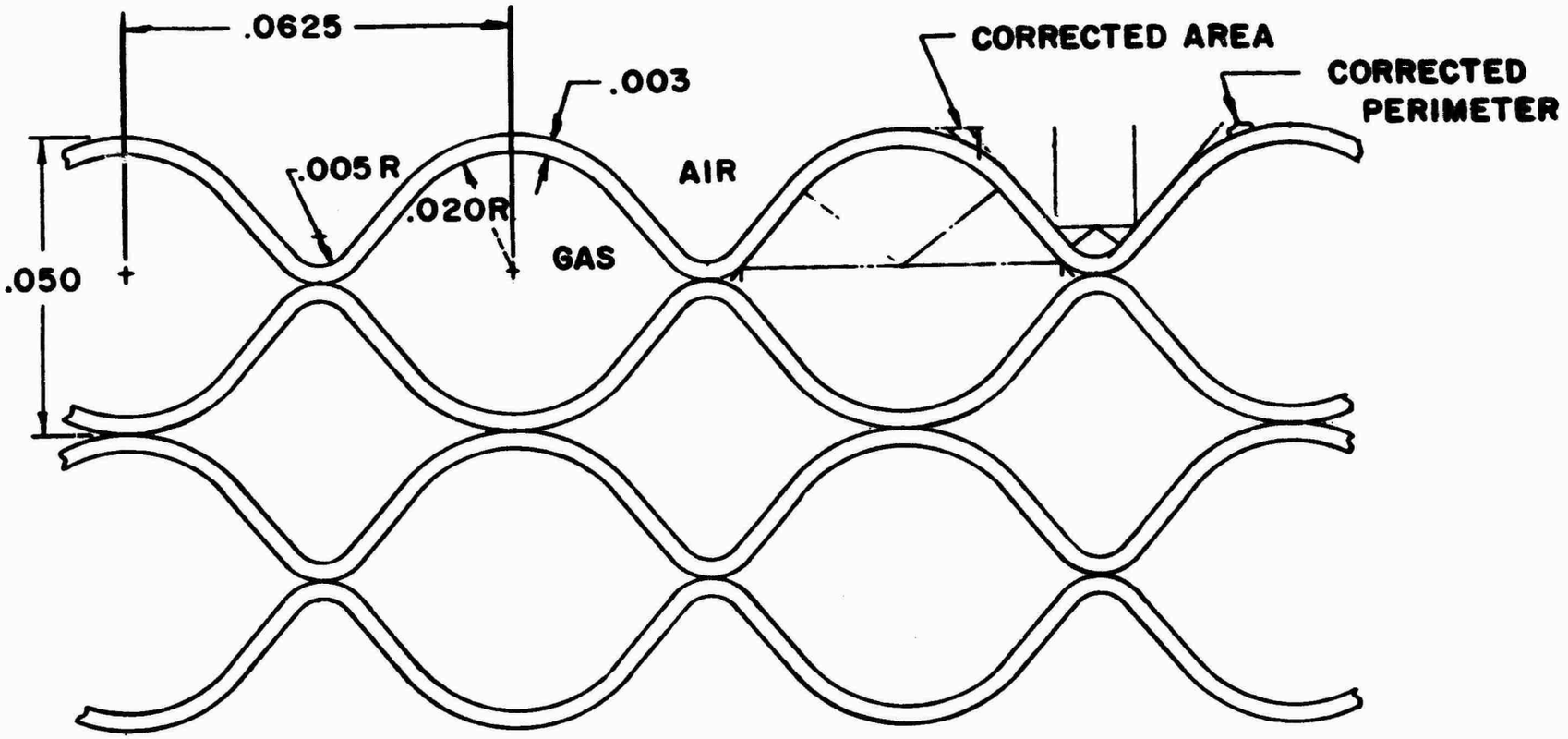

Figure 26. Crest-on-Crest Wave Form.

Design Parameters						
	Number of Waves Per Inch	40	40	40	40	40
	Number of Plates Per Inch	32	32	32	32	32
	Gas-Side Bend Radius (Inches)	.015	.016	.012	.010	.015
	Air-Side Bend Radius (Inches)	.007	.006	.007	.006	.006
Figure Number		1	2	3	—	4
Gas Hydraulic Radius		.01020	.01062	.01113	.00986	.0106
Air Hydraulic Radius		.00604	.00563	.00795	.00842	.00634
$\frac{\text{Gas-Side Area}}{\text{Air-Side Area}}$		1.463	1.659	1.356	1.239	1.721
Elongation (percent)		70.08	70.08	65.27	62.02	68.15
Actual Gas Flow Area Per Inch of Core Length		1.845	1.925	1.755	1.636	1.913
Actual Air Flow Area Per Inch of Core Length		1.167	1.087	1.274	1.344	1.206
Sheet Metal Surface Area Per Inch of Core (Both Sides)		2156	2156	2094	2054	2130
Weight Per Inch of Core Length		.922	.922	.895	.878	.911
$\frac{\text{Air Inlet Area}}{\text{Gas Flow Area}}$		.177	.170	.186	.192	.171
$\frac{\text{Air Inlet Area}}{\text{Air Flow Area}}$		.280	.300	.256	.243	.271
$\frac{\text{Sheet Metal Surface Area}}{\text{Sheet Metal Weight}}$		2338	2338	2340	2339	2338
$\frac{\text{Sheet Metal Surface Area}}{\text{Gas Flow Area}}$		1169	1120	1193	1211	1113
$\frac{\text{Sheet Metal Surface Area}}{\text{Air Flow Area}}$		1847	1983	1644	1528	1766

A

TABLE 6

CREST-ON-CREST WAVE-FORM DATA

	40	40	40	40	40	40	32	32	32	32
	32	32	32	32	40	40	40	40	40	40
5	.012	.010	.015	.014	.012	.013	.018	.019	.019	.020
6	.007	.006	.006	.007	.006	.006	.007	.006	.005	.005
	3	—	4	5	6	7	8	—	—	9
06	.01113	.00986	.0106	.01022	.00958	.00933	.01048	.01061	.01063	.01075
634	.00795	.00842	.00634	.00685	.00769	.00700	.00809	.00838	.00830	.00743
21	1.356	1.239	1.721	1.489	1.332	1.405	1.394	1.485	1.514	1.506
15	65.27	62.02	68.15	68.16	38.08	42.18	27.76	27.63	27.42	27.77
13	1.755	1.636	1.913	1.815	1.728	1.756	1.797	1.842	1.857	1.851
06	1.274	1.344	1.206	1.204	1.275	1.230	1.251	1.207	1.193	1.177
0	2094	2054	2130	2130	2186	2252	2024	2022	2018	2024
1	.895	.878	.911	.911	.935	.963	.865	.864	.863	.865
1	.186	.192	.171	.180	.189	.186	.182	.177	.176	.176
1	.256	.243	.271	.271	.256	.265	.261	.270	.274	.273
3	2340	2339	2338	2338	2338	2339	2340	2340	2338	2340
3	1193	1211	1113	1174	1265	1282	1126	1098	1087	1093
6	1644	1528	1766	1769	1715	1831	1618	1675	1692	1691

M DATA

2	32	32	32	32	32	32	32	30	34.04+	0
3.)	40	40	40	40	40	40	40	40	42.55+	50
40)18	.019	.019	.020	.022	.022	.020	.022	.022	.019	–
.(07	.006	.005	.005	.005	.003	.008	.008	.008	.005	–
.(	–	–	9	10	11	–	–	12	14	13
10 1048	.01061	.01063	.01075	.0110	.0110	.01072	.0110	.0110	.01006	.0102
.(0809	.00838	.00830	.00743	.00729	.00717	.00841	.00777	.00810	.00708	.0068
.(										
394	1.485	1.514	1.506	1.662	1.708	1.502	1.769	1.428	1.5000	1.500
1..76	27.63	27.42	27.77	28.55	27.77	29.00	30.16	25.37	27.55	0
2E										
797	1.842	1.857	1.851	1.884	1.917	1.846	1.893	1.798	1.818	1.836
1.										
251	1.207	1.193	1.177	1.161	1.131	1.197	1.145	1.260	1.196	1.224
1.										
24	2022	2018	2024	2036	2024	2044	2062	1986	2149	1980
20,5	.864	.863	.865	.870	.865	.874	.882	.849	.919	.846
.8										
2	.177	.176	.176	.173	.170	.177	.172	.182	.180	.178
.1										
1	.270	.274	.273	.281	.289	.273	.285	.259	.373	.267
.2										
0	2340	2338	2340	2340	2340	2339	2338	2339	2338	2340
23										
6	1098	1087	1093	1081	1056	1107	1089	1105	1182	1078
10										
8	1675	1692	1691	1754	1790	1708	1801	1576	1797	1618
17										

C

10 PITCHES PER INCH
40 PLATES PER INCH

MAX TOTAL ELONGATION 18%

$P_G / A_A = 1.234$

A_G / P_G = (HYD. RAD.)= .0121

A_A / P_A = (HYD. RAD.)= .0106

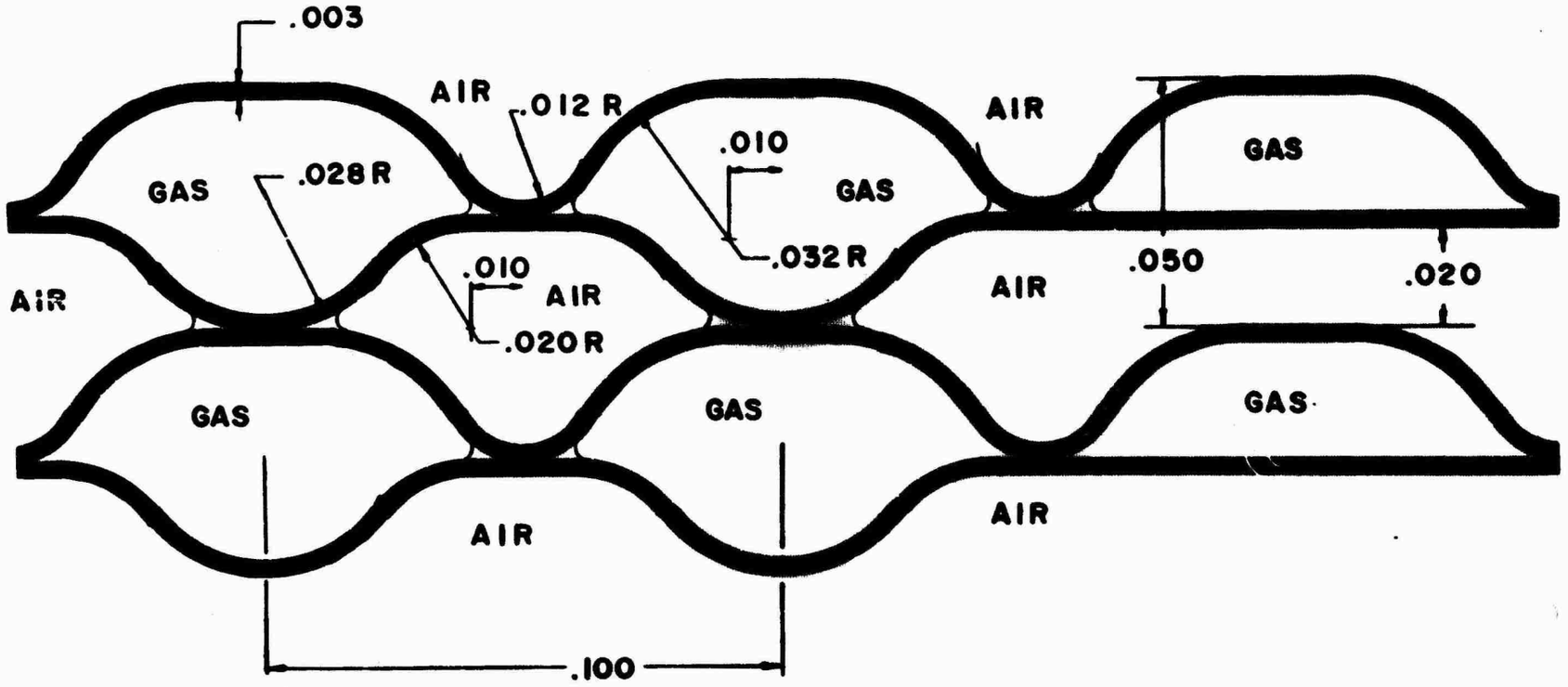

Figure 27. Crest-on-Flat Wave Form.

TABLE 7
CREST-ON-FLAT WAVE-FORM DATA

Design Parameters										
	Number of Waves Per Inch	10	10	10	10	10	10	10	10	10
	Number of Plates Per Inch	40	40	40	40	40	40	40	40	40
	Min. Gas-Side Bend Radius (Inches)	.007	.017	.017	.007	.012	.015	.020	.025	.012
	Min. Air-Side Bend Radius (Inches)	.007	.012	.012	.007	.012	.007	.012	.012	.012
Figure Number		15	16	17	18	19	20	21	22	23
Gas Hydraulic Radius		.01182	.0105	.0123	.0124	.01185	.0118	.01167	.0121	.0122
Air Hydraulic Radius		.0091	.0099	.0095	.00866	.00873	.0091	.01115	.0106	.0982
$\frac{\text{Gas Side Area}}{\text{Air Side Area}}$		1.31	1.20	1.35	1.515	1.358	1.46	1.11	1.234	1.258
Elongation (Percent)		16	23	23	26	15.2	20.3	16	18	18
Actual Gas Flow Area Per Inch of Core Length		1.79	1.66	1.757	1.86	1.766	1.820	1.613	1.69	1.699
Actual Air Flow Area Per Inch of Core Length		1.325	1.387	1.303	1.227	1.301	1.250	1.454	1.370	1.350
Sheet Metal Surface Area Per Inch of Core (Both Sides)		1737	1789	1759	1730	1735	1769	1708	1761	1707
Weight Per Inch of Core Length		.8054	.8054	.8054	.8054	.8054	.8054	.8054	.8054	.8054
$\frac{\text{Air Inlet Area}}{\text{Gas Flow Area}}$		.1934	.2889	.2732	.1806	.2718	.1846	.2976	.284	.2825
$\frac{\text{Air Inlet Area}}{\text{Air Flow Area}}$		.254	.346	.3684	.2646	.3690	.2688	.3301	.3504	.3556
$\frac{\text{Sheet Metal Surface Area}}{\text{Gas Flow Area}}$		958	1077	1001	9301	9824	972	1059	1042	1005
$\frac{\text{Sheet Metal Surface Area}}{\text{Air Flow Area}}$		1295	1289	135	1410	1334	1415	1175	1285	1264

The crest-on-flat wave configuration studies were undertaken in anticipation of misalignment problems which might occur in the crest-on-crest wave forms. The crest-on-flat form allows some misalignment without changing either cross-sectional flow area or wetted perimeter. Preliminary fabrication and assembly studies showed that misalignment was not a serious problem and led to the adoption of a crest-on-crest configuration.

The multiwave plate assembly consists of rectangular plates mated to form closed channels similar to those shown in Figures 28 and 29. The long faces are corrugated as shown in cress section. Two matching plates are placed together and joined by either brazing or resistance welding the internally matched crests. This is done to form a rigid assembly and to avoid possible fretting at these locations. The quality of these joints does not affect leakage or heat transfer.

Similarly, the assembled pairs of wave plates are brazed together at their matching surfaces to form the regnerator matrix. The exhaust gas is contained within the paired assemblies, whereas the air passes between the wave plate assemblies in the channels formed by the corrugations.

At both ends of the multiwave plate assemblies, the corrugation pattern is changed to provide the inlet and exit crossflow portion of the regenerator core. In this section, the width of the channel is reduced, which allows the air to move in a crossflow direction into and out of the core matrix. At the extreme ends of the multiwave plate assemblies, the full width of the channel is restored so the channels can be joined together to seal the air from the exhaust gases. These brazed surfaces at the ends which join the multiwave plate paired assemblies together are the critical brazed joints in the matrix. In the counterflow region, the crests of the multiwave plate assemblies are brazed to the corresponding points on the adjacent plates to unitize the matrix and to prevent possible fretting at these points. These joints are not critical from the leakage or heat transfer viewpoint.

5.1.3 Regenerator System - Initial Design

The next phase is the fabrication of the core module and the arrangement necessary to form a complete regenerator system. This system is determined by the following design requirements:

1) Air inlet and outlet areas and their related sealing problems.
2) A gas bypass area allowance of 220 square inches, which eliminates the gas-side pressure loss and its effect on full-power engine operation.
3) The thermal stresses incurred in a structure of varying tem-

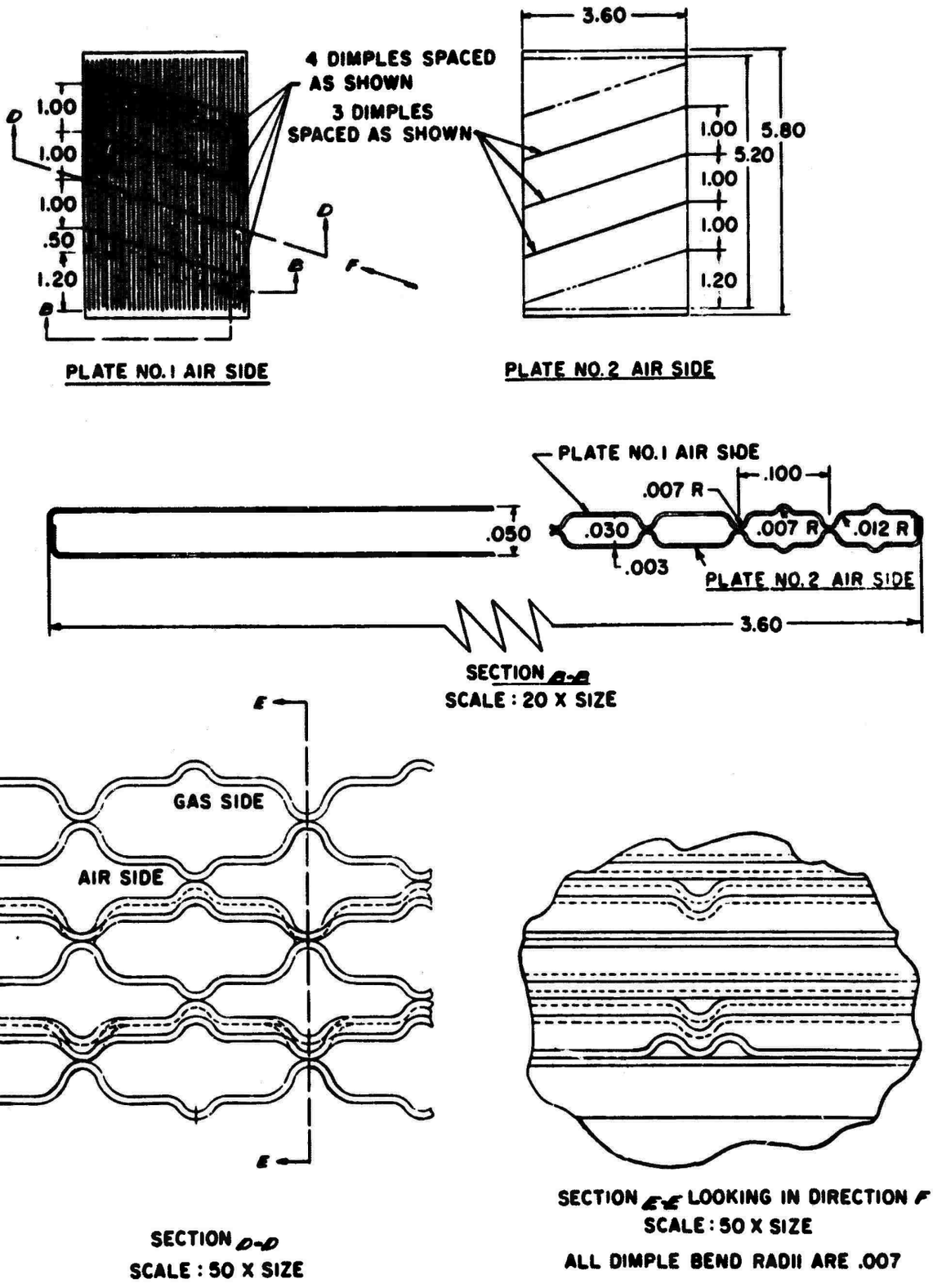

Figure 28. Multiwave Plate Pair.

Position	Gas-Side Radius		Air-Side Radius		Counterflow Area		Hydraulic Rad	
	External	Internal	External	Internal	Gas Side	Air Side	Gas Side	Air
small end	.137	.134						
1	.136	.133	.040	.037	.0166	.01004	.03311	.0
2	.134	.131	.039	.036				
3	.129	.126	.039	.036	.01754	.0106	.0338	.0
4	.128	.125	.038	.035				
5	.125	.122	.038	.035				
6	.122	.119	.037	.034				
7	.120	.117	.037	.034	.01915	.0120	.0366	.0
8	.119	.116	.036	.033				
9	.118	.115	.035	.032				
10	.117	.114	.035	.032				
11	.116	.113	.034	.031	.02112	.01283	.0388	.0.
12	.115	.112	.034	.031				
13	.114	.111	.033	.030	.0221	.01317	.04017	.0.
14	.113	.110	.033	.030		.01321		.0.
15	.110	.107	.034	.031	.0225	.01384	.0407	.0.
16	.109	.106	.034	.031		.01398		.0.
17	.108	.105	.035	.032				
18	.105	.102	.035	.032				
19	.103	.100	.036	.033	.02469	.01591	.04287	.0.
20	.101	.098	.037	.034				
21	.100	.097	.037	.034				
22	.098	.095	.038	.035				
23	.097	.094	.038	.035	.02608		.04416	
24	.096	.093	.039	.036		.01744		.0
25	.095	.092	.039	.036				
large end	.094	.091	.040	.037	.02672	.01785	.04468	.0

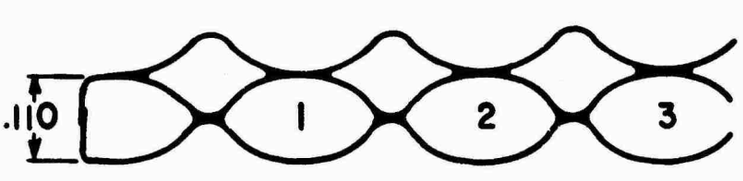

WAVE PLATES 6.625 IN. LONG (RADIALLY)

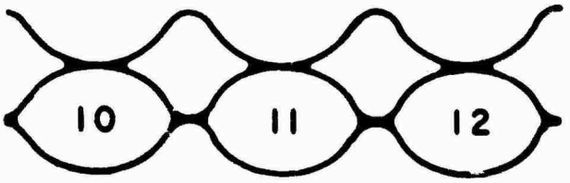

CIRCULAR CORE SECTIONS OF

Figure 29. Multiwave Plate Pair; Study.

A

unterflow Area		Hydraulic Radii		Counterflow Area Ratios (Gas/Air)		Counterflow Section	
Side	Air Side	Gas Side	Air Side	Pos - 1/2	Pos + 1/2	Ext. Gas-Side Radius	Air-Side Dimension
							0
66	.01004	.03311	.02342	1.653		.152	.014
						.152	.017
.754	.0106	.0338	.02369	1.655		.152	.022
						.152	.025
						.152	.026
						.152	.029
.915	.0120	.0366	.0252	1.596		.152	.033
						.152	.036
						.152	.037
						.152	.038
:112	.01283	.0388	.0262	1.646		.152	.041
						.152	.043
:21	.01317	.04017	.02710	1.678		.152	.044
	.01321		.02719		1.673	.147	.045
:25	.01384	.0407	.02758	1.626		.146	.046
	.01398		.02759		1.609	.145	.047
						.142	.048
						.133	.049
:469	.01591	.04287	.02907		1.552	.131	.050
						.129	.051
						.127	.052
						.124	.053
:608	.01744	.04416	.03067		1.495	.123	.054
						.122	.055
:672	.01785	.04468	.03139		1.497	.121	.056
						.120	.057

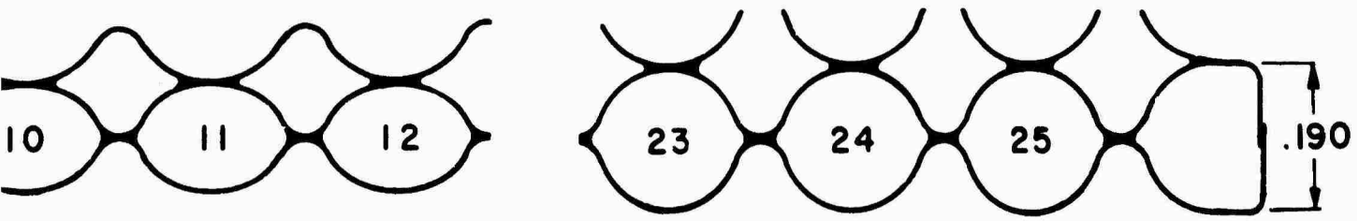

:IRCULAR CORE SECTIONS OF 31.50 O.D. & 18.25 I.D. SCALE: TEN X

:9. Multiwave Plate Pair; Study.

B

perature conditions.

4) The stresses imposed by the high-pressure conditions.
5) The structural rigidity as affected by vibration and "G" loadings.
6) The most efficient usage of the support structure with reference to weight considerations.

Consideration of these conditions led to the development of a regenerator made up of eight rectangular core modules, as shown in Figure 30. These modules utilize rectangular wave plates such as those shown in Figure 28. The plates shown are dimpled across the flow cross-sectional areas, obstructing the gas-side flow with a decreased area. These dimples make the plates rigid across their surface and are to be used to create turbulence in the flow. Tests to determine whether the turbulent flow improves the heat transfer sufficiently to offset the accompanying pressure losses must decide the case for or against the use of dimples across the flow. Initial development will consider only the undimpled plates to facilitate the forming of the wave plates.

In the arrangement shown in Figure 30, each core module with its compressed air ducting acts as a small pressure vessel. Louvered plates over the exhaust gas inlet and outlet areas counteract the compressed air pressure in the manifolds which exerts tangential loads on the core. In addition to these loads, the manifold exerts a compressive loading to the matrix which must be compensated for by a support structure which is located within the core flanges. To provide a chamber from which the exhaust gas is directed through the matrix, the core modules are connected to each other by a sheet metal wall. This wall is formed at the inside diameters locating the core modules, to connect the flanges from adjacent modules. This gives added rigidity to the structure and seals the exhaust gas passage.

The fore and aft closures are heavy plates to take the axial pressure loads. The forward closure also acts as the main support member for the regenerator. The rear of the core modules are allowed to pivot, assuming the position necessary to compensate for the thermally induced distortion. The gas bypass area determined the location of the inner flanges of the core matrices. Since the dimensions for a rectangular wave plate were determined by the desired heat transfer properties, the number of cores about the bypass area diameter could subsequently be ascertained. From the number of cores and the desired gas flow area, the length of the cores was determined. The gas flow exhaust area gave the necessary external diameter which completed the dimensional packaging.

The air inlet tubes are to be used as rigid coupling members for the engine and regenerator, while the outlet tubes are to have bellows-type connections to allow for expansion due to temperature differentials. The mounting of the combined units is proposed to be at the forward engine mounts and at the flange of the forward wall of the regenerator.

The rectangular wave plates shown in Figure 28 provide the best aerodynamic and heat transfer properties. This led to the design of a small test section utilizing this configuration as is shown in Figure 31. Close examination and test results of this section have revealed an excessive leakage of air to the gas side, in the area of the support flanges and along the mating flanges of the plates, on all core assemblies. Since this is mainly a result of fabrication, the resolution of this problem lies largely within the area of improved brazing and welding techniques.

5.1.4 Regenerator System - Alternate Design

The fabrication problems associated with this construction led to a parallel investigation to develop a new design which shows promise of obtaining a leakproof core. This design eliminates the need for the side flanges on the plates which cause the difficult mating, brazing and sealing problems. The same basic wave plates are used with the flanges being replaced by metal spacers sandwiched between the plates. Two spacers are required, one for enclosing the air and one for enclosing the exhaust gas.

In order to simplify fabrication of the full core module, the spacers are made into rectangular frames as shown in Figures 32 and 33. This makes it possible to position and hold the spacers relative to each other and to the plates. The assembly procedure consists of alternately stacking the gas-side and air-side plates and spacers to form a solid block which is held tightly in a fixture during the brazing cycle.

At this stage of fabrication the air and gas inlet and outlet ports are sealed by the spacers. To obtain the air inlet and outlet ports, the air enclosure frames are recessed in this area (Figure 32) so that by machining the sides of the core slightly beyond the recess the air inlet and outlet ports are opened. To obtain the gas inlet and outlet ports, the gas enclosure frames are formed (Figure 33) with a larger internal vertical dimension than the air enclosure frames. By machining the top and bottom of the core slightly beyond the internal vertical dimension of the gas enclosure frames, the gas inlet and outlet ports are opened. After final machining of the core, the spacers will only be from 0.025 to 0.030 inch wide.

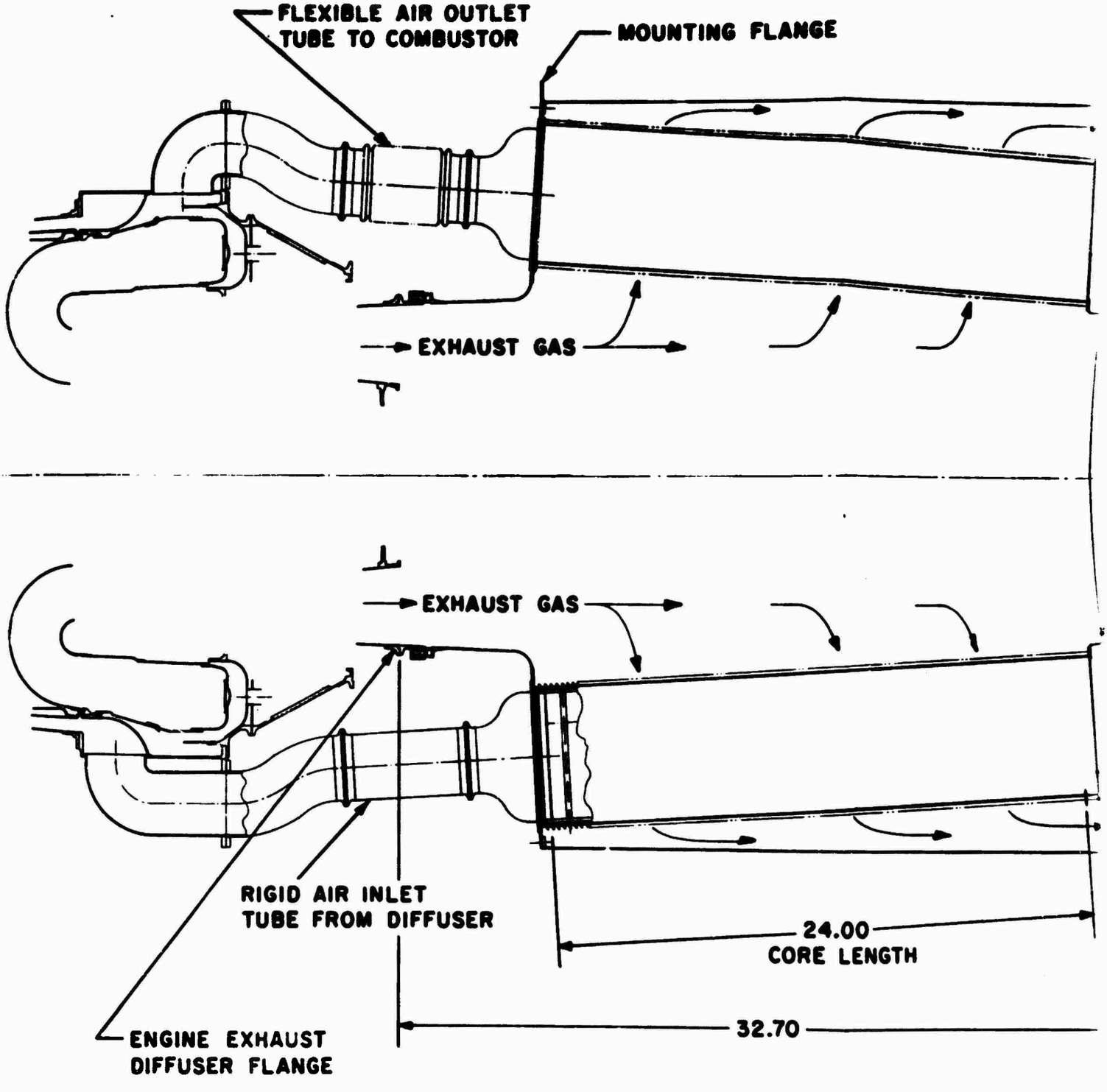

Figure 30. Regenerator-Engi

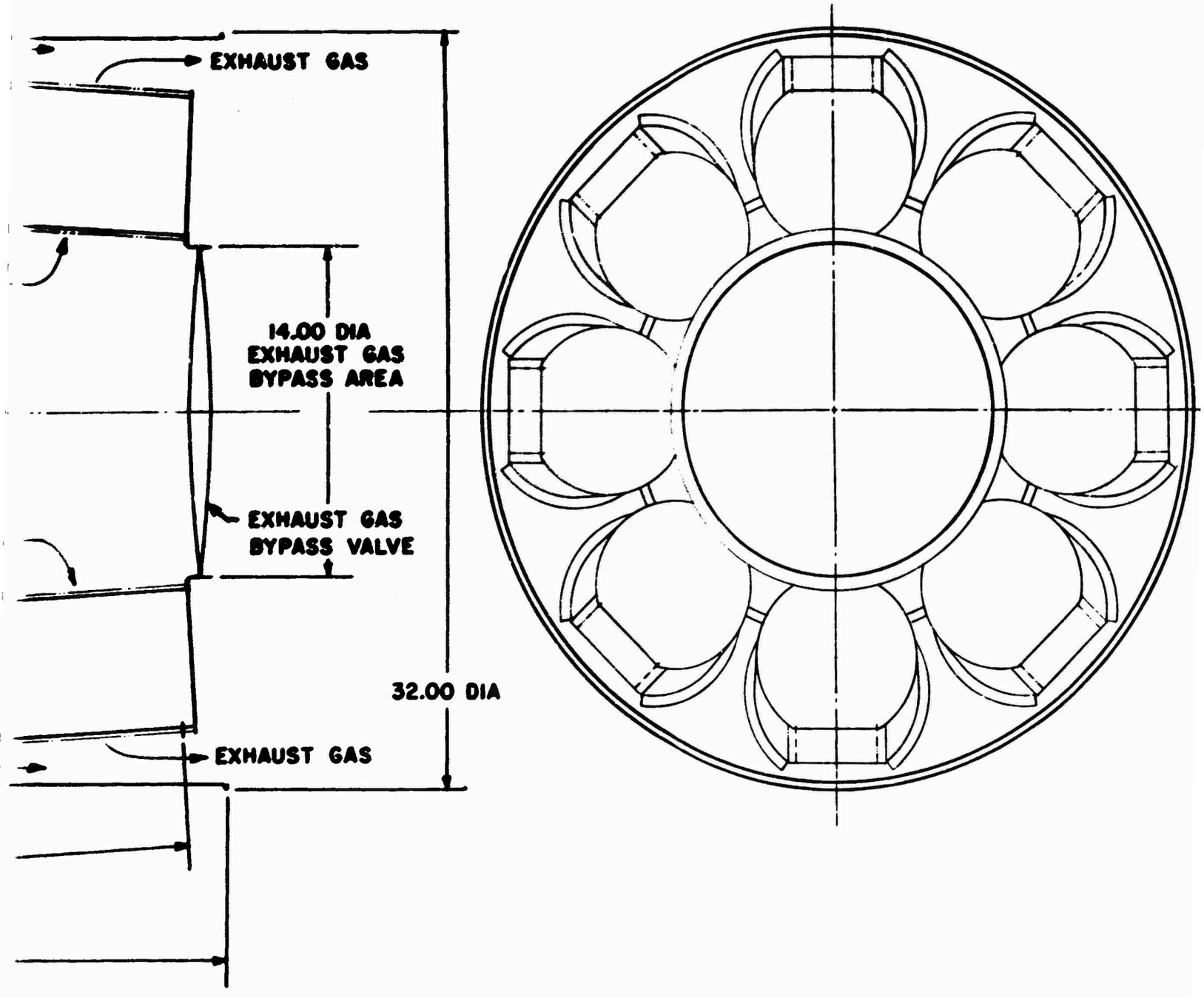

:generator-Engine Integration.

B

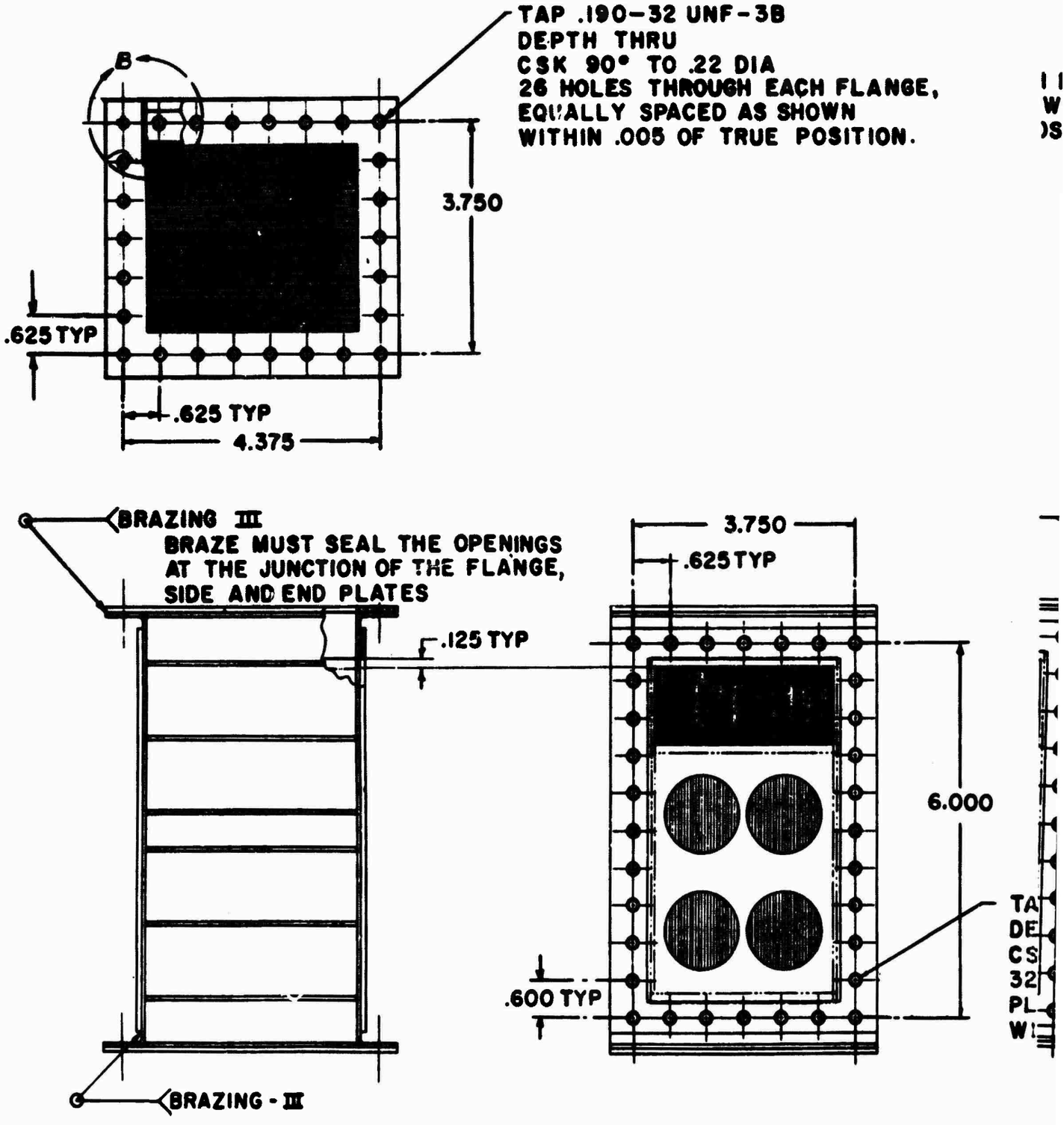
TAP .190-32 UNF-3B
DEPTH THRU
CSK 90° TO .22 DIA
26 HOLES THROUGH EACH FLANGE,
EQUALLY SPACED AS SHOWN
WITHIN .005 OF TRUE POSITION.
B
3.750
.625 TYP
.625 TYP
4.375
BRAZING III
BRAZE MUST SEAL THE OPENINGS
AT THE JUNCTION OF THE FLANGE,
SIDE AND END PLATES
.125 TYP
3.750
.625 TYP
6.000
.600 TYP
BRAZING - III

A

Figure 31.

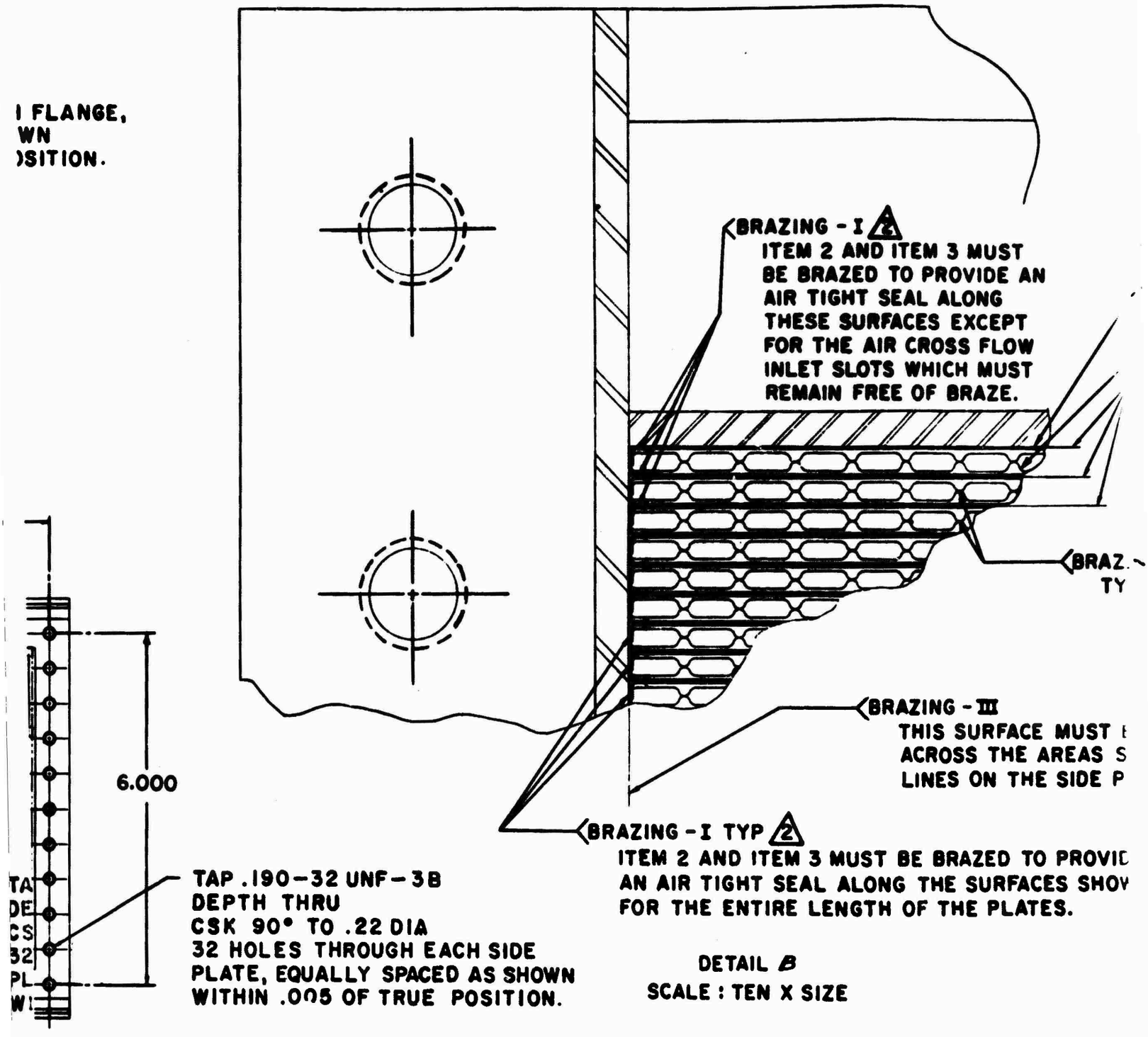

Figure 31. Regenerator Case Test Section Assembly.

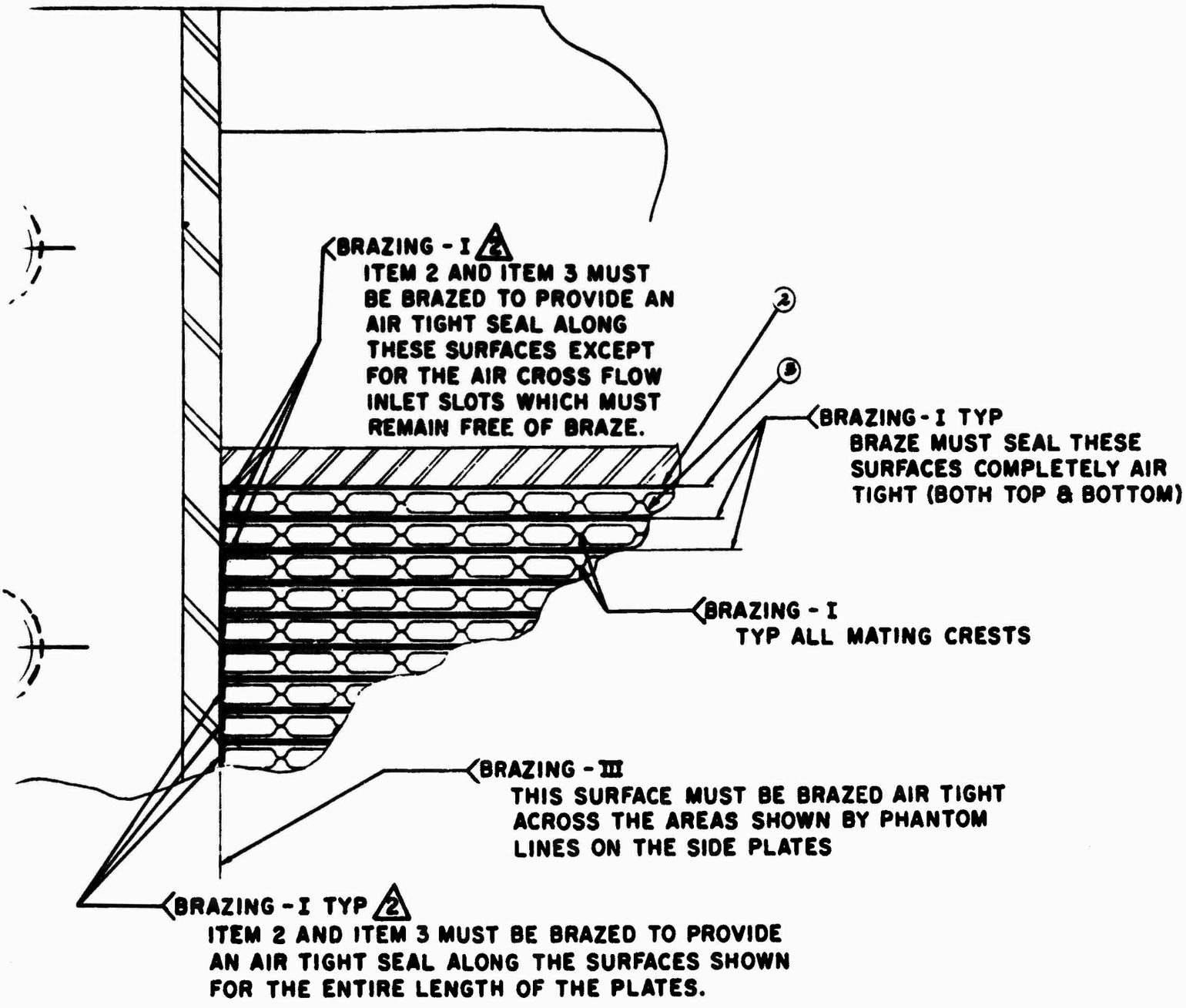

ACH SIDE
D AS SHOWN
POSITION.

DETAIL B
SCALE : TEN X SIZE

Test Section Assembly.

C

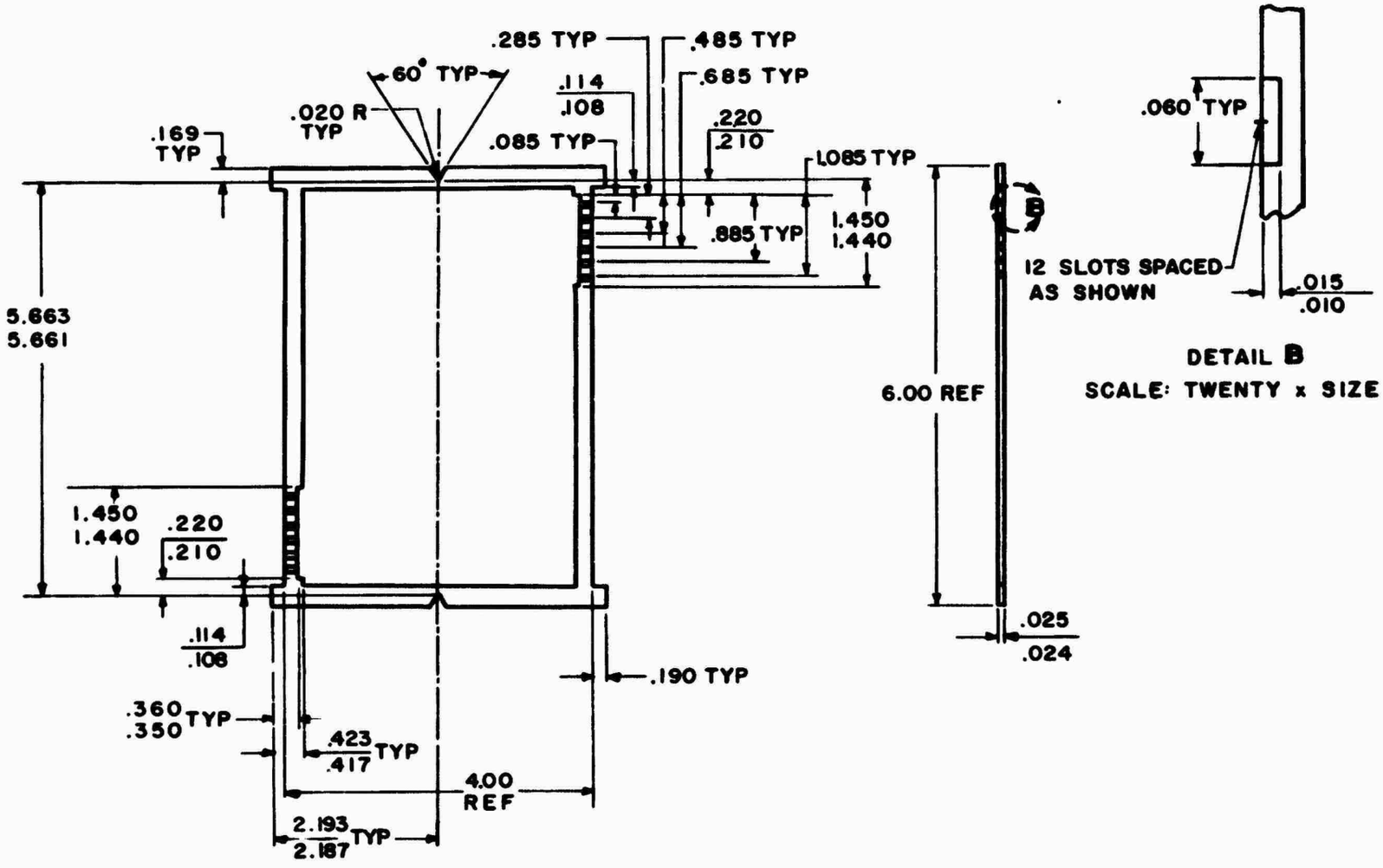

Figure 32. Pressure Air Passage Sealing Spacer.

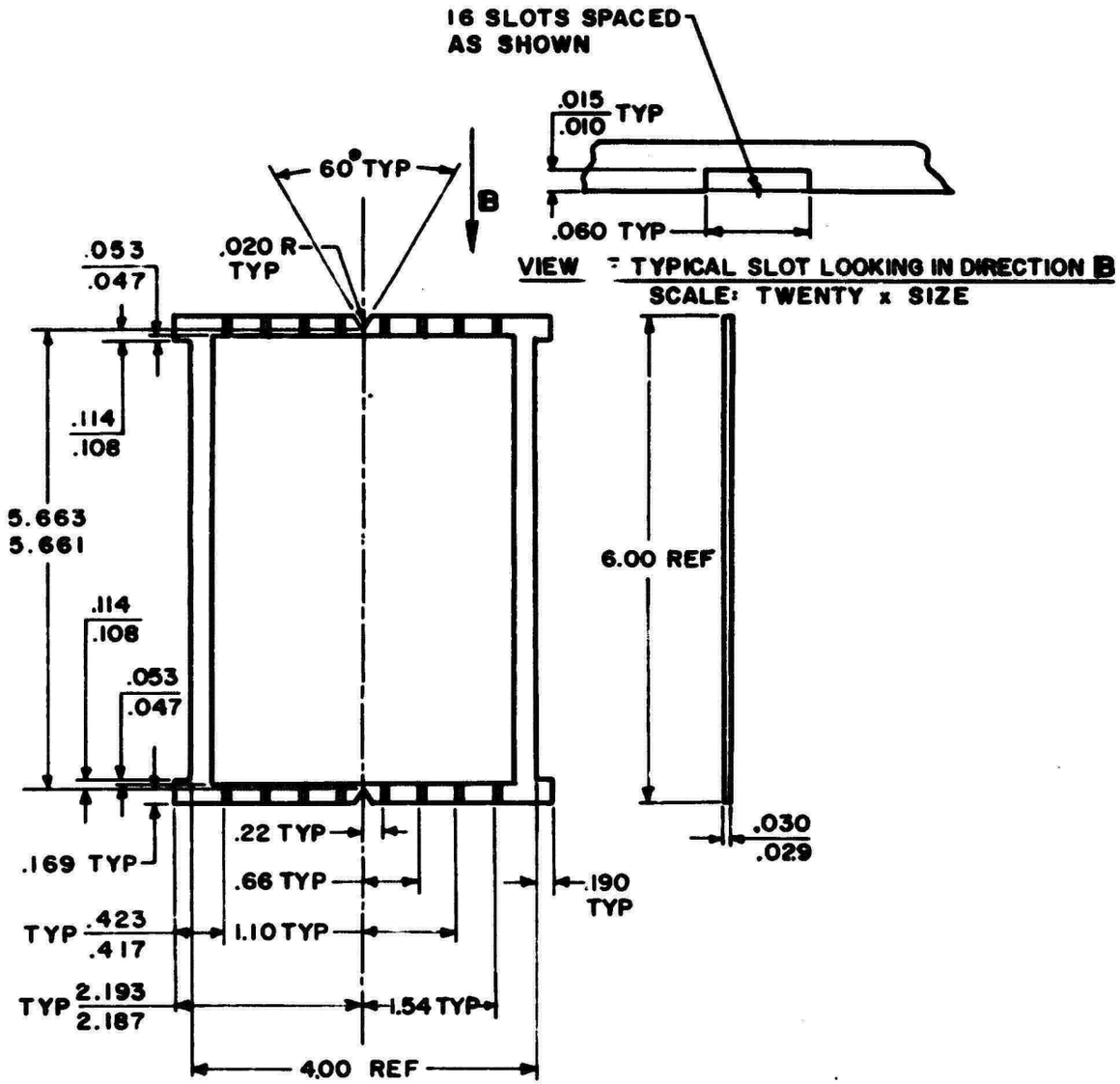

Figure 33. Exhaust Gas Passage Sealing Spacer.

A small test section utilizing these features, shown in Figure 34, has been designed to provide a test vehicle similar to the one developed for the original multiwave plate construction.

The many similarities of these two types of construction allow for readily adapting the sealing frame arrangement to the original regenerator assembly shown in Figure 30. The use of the frames for sealing, rather than the overlapping flanges, eliminates the need for a secondary support structure to withstand the loads induced by the high-pressure air. The frames have the required rigidity to support the tensile and compressive loads which the compressed air manifolds transmit to the core matrix. The elimination of these support structures not only constitutes a weight savings but eliminates some of the bolted flanges, thereby reducing the areas for possible leakage.

The extensive thermally induced distortion of the core modules in this type of regenerator led to development of an annular ring arrangement of the wave plates in a manner shown in Figure 35. This arrangement necessitated the use of wave plates having a cross-sectional configuration similar to the one shown in Figure 29.

Since the temperatures vary mainly in an axial direction, the stresses due to thermal growth lie within the range of the material. The high-pressure air can be contained within cylindrical pressure vessels providing the best possible structure. This arrangement also provides the most compact core from a standpoint of overall dimensions. Despite the inherent advantages displayed by this system, certain negative factors have been found to outweigh the advantages. First is the problem of radially sealing concentric diameters under high pressure. Assuming a solution for this problem, the next problem lies with the wave plate cross-sectional area variations. To maintain the desired aerodynamic and heat transfer characteristics, the wave plates must assume the shapes shown in Figure 29. As readily seen, the cross-sectional area is correspondingly greater at increasing distances from the regenerator centerline. This has little or no effect on the gas-side flow. However, the compressed air inlet and outlet areas are at the outermost diameters and will force most of the air to flow through the sections of larger area and least counter flow length, short-circuiting most of the wave plate heat transfer surface.

The compressor air ducting can be arranged as in either Figure 35 or Figure 36. As shown in Figure 35, the manifold consists of tubular ducts from the compressor to the regenerator and from the regenerator back to the combustion chamber. Another ducting arrangement is shown in Figure 36, having the manifold integrated with the basic engine structure. Struts are provided for support of the power turbine section and for

accessibility to the thermocouples, oil and fuel lines. This type of construction offers a good method of mounting the combined units, and provides a reasonably rigid coupling between the engine and the regenerator.

5.2 EXPERIMENTAL CORE FABRICATION

5.2.1 Process Parameters

Fabrication of the experimental test core proceeded with the selection of wave plate and joining materials appropriate to design criteria. Table 8 lists the process parameters for each of the cores manufacture; twelve 3-inch cores and one 12-inch core were manufactured. The development effort for each manufacturing phase is described in the paragraphs which follow.

5.2.2 Wave Plate Base Metal

Selection of a wave plate base metal was based on the following requirements:

1) Oxidation resistance at 1350° F
2) Resistance to thermal fatigue
3) Mechanical strength at elevated temperatures
4) Compatibility with vacuum brazing
5) Availability as 0.0035-inch foil
6) Adequate deep drawing properties.

A preliminary study suggested the use of three materials: Hastelloy X, Inco 718, and Type 304L (low carbon) stainless steel. These three alloys, which fulfilled requirements 1) through 3) above, were evaluated with regard to plate fabrication and brazing qualities to ascertain compliance with the remaining base metal requirements.

Foil test specimens of Hastelloy X and Type 304L were successfully vacuum brazed using two braze alloys (Au-Ni and Ni-P plating). Inco 718 was dropped from consideration because it was not readily wet by the brazing alloys and it required an extensive heat treatment to impart desired physical properties.

Hastelloy X stock of 0.003-inch thickness was formed into plate pairs with a resultant convolution depth of only 0.027 inch (0.032 inch was desired). When a new die, which was designed to produce deeper convolutions, was employed to fabricate additional Hastelloy X plates, the base metal fractured during drawing.

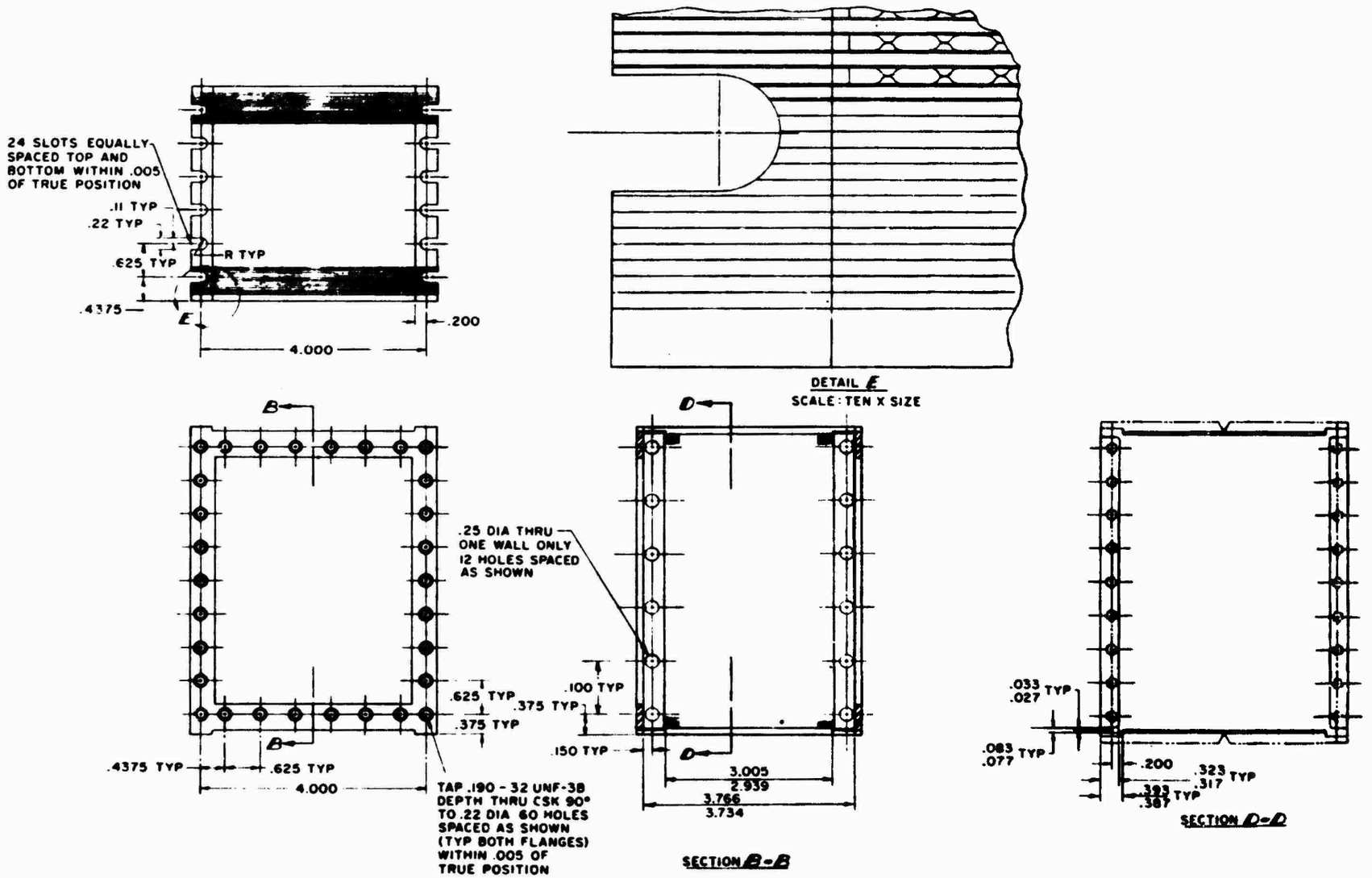

Figure 34. Regenerator Core Test Module Assembly.

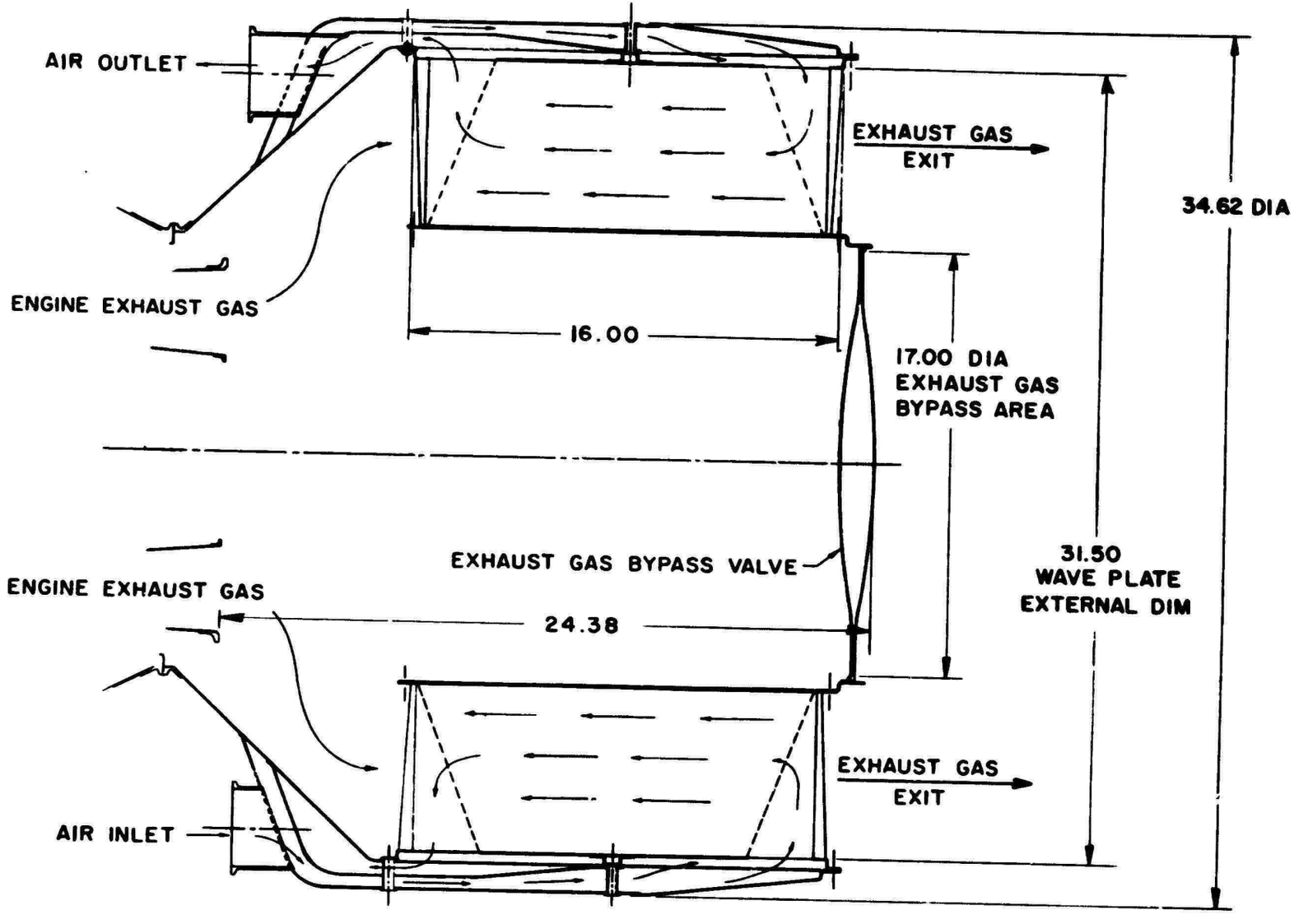

Figure 35. Regenerator Flow Arrangement.

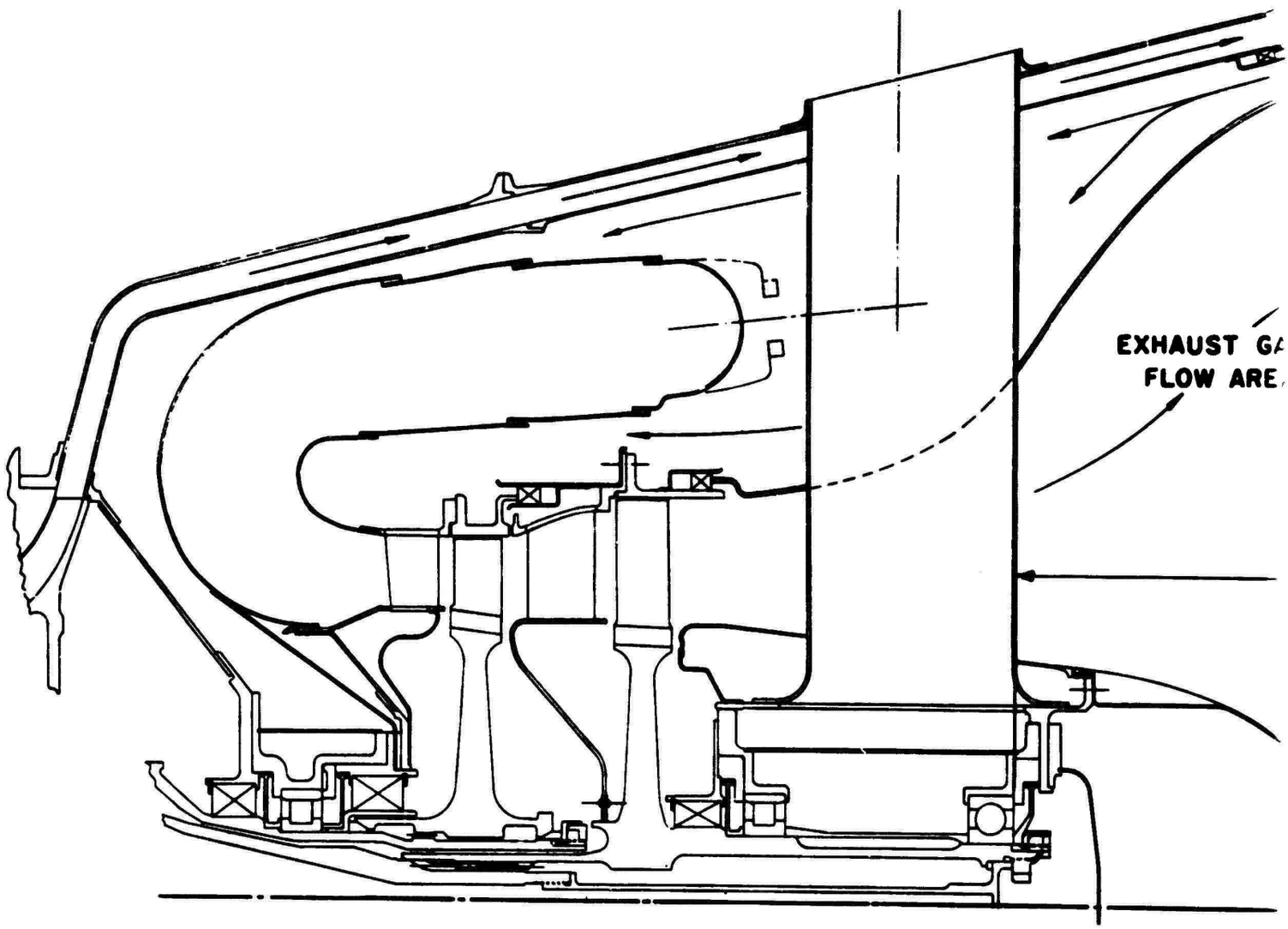

Figure

A

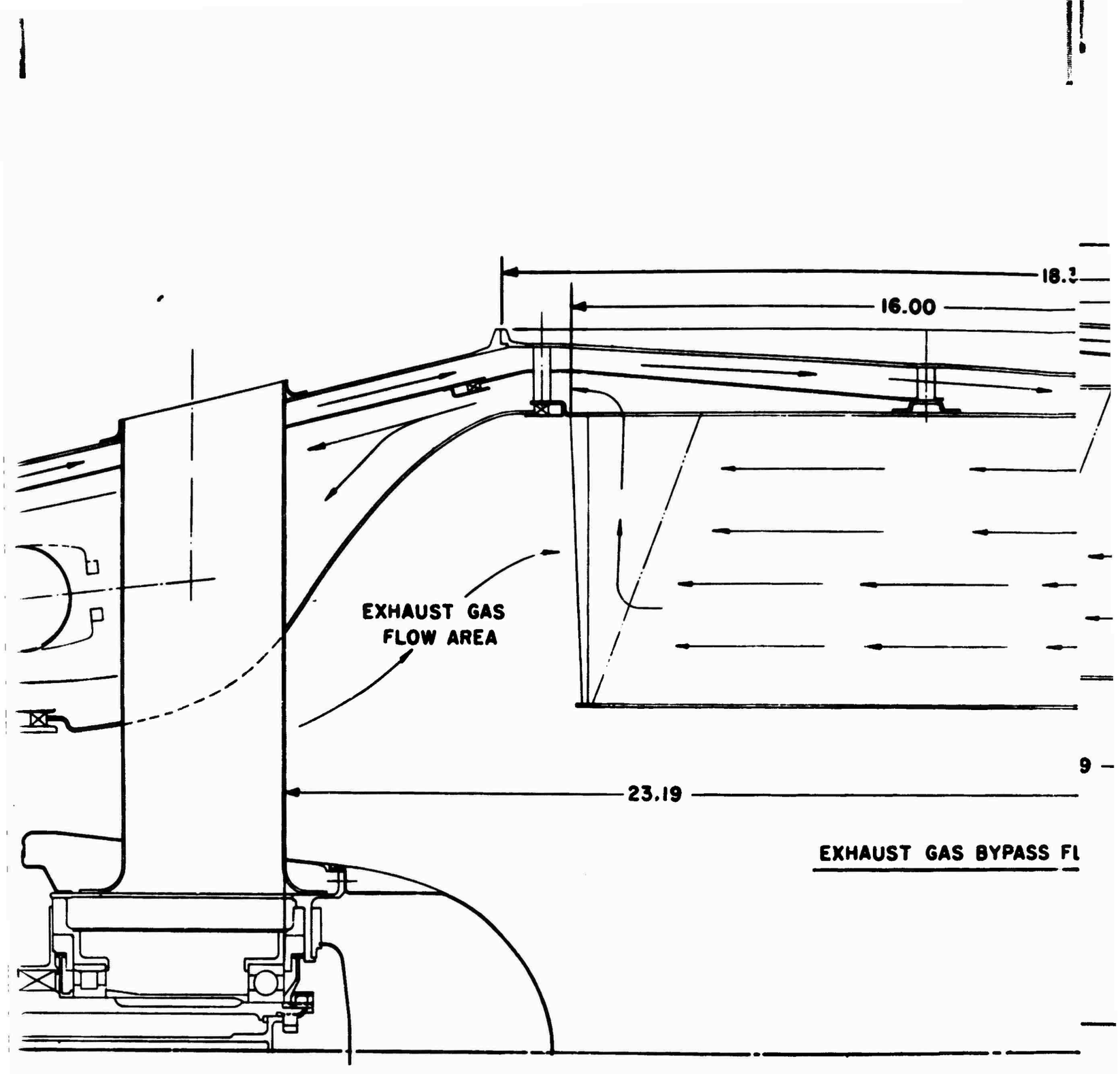

Figure 36. Regenerator-Engine Assembly.

B

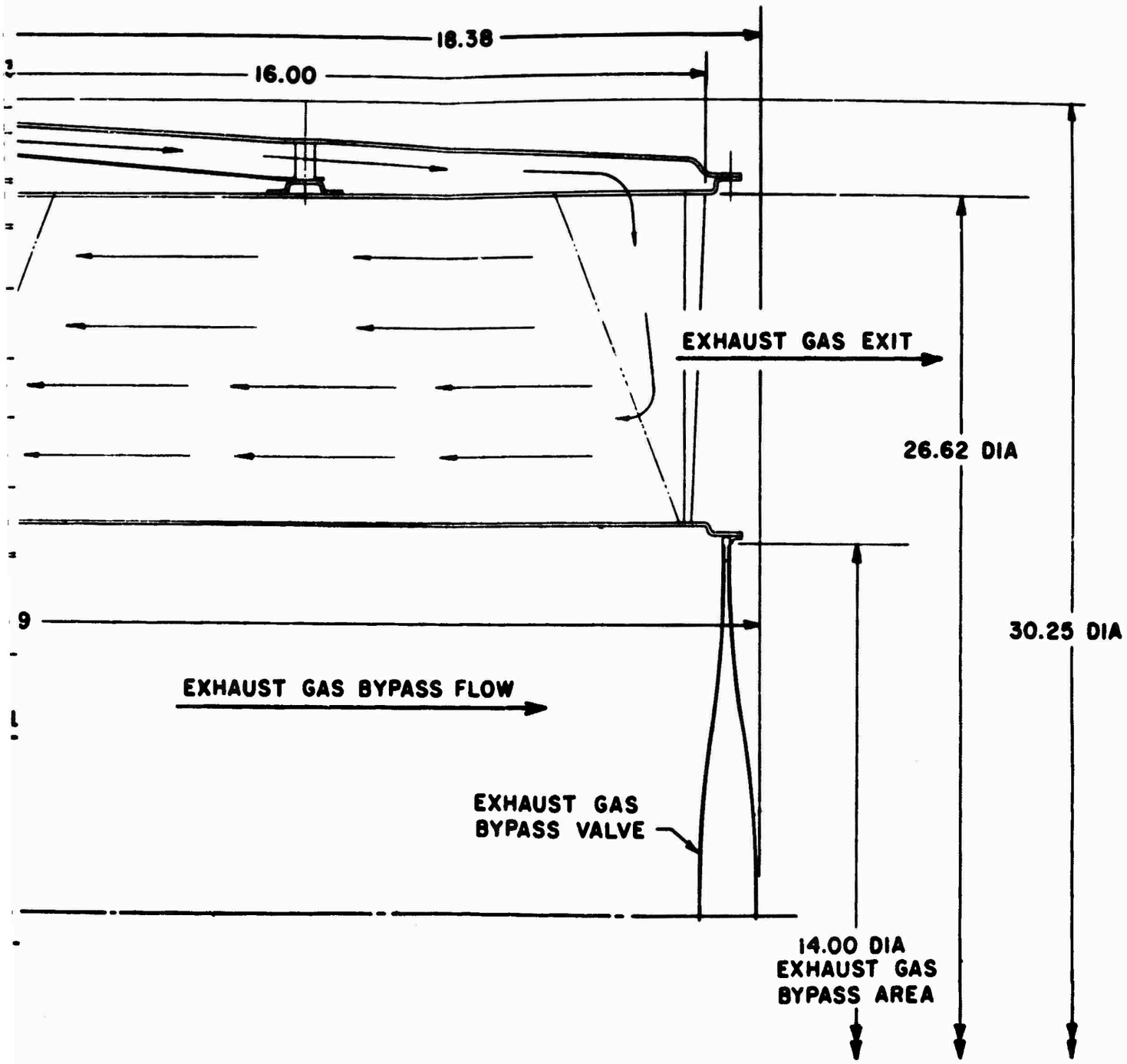

-Engine Assembly.

C

TABLE 8

PROCESS PARAMETERS OF REGENERATOR TEST CORES

Core	Base Metal	Type	Braze Alloy	Alloy Placement	Pair Assembly	Stack Assembly	Braze Cycle	Integrity	Box Type	Box Assy.	Final Disposition
I	Hast. X	Large flange conv. depth .027	AuNi	All over	Conv. fixtures, spot tacked, 1/2 as "H" section 1/2 as Box section	Elox Vee in 1-in. groups W/M 3860 foil-stacked in vee post fixture with top weight	1925°F, 15 min. 1925°F, 15 min.	Air entries closed, leaks at flanges & air entries	Rigid Hast. X	E.B. weld braze	Leaks at edge and end flanges
II	Hast. X	Trimmed flange conv. depth .027. Vee notch dimpled air plenum	AuNi	Hi-lites	Pin fixture, spot tacked, box section	Stacked in vee post fixture with top weights	1925°F, 15 min.	Edge flange leaks	Rigid Hast. X	Rolled flange	Flanges cracked.
III	304L	Trimmed flange conv. depth .031 Vee notch dimpled air plenum	AuNi	Hi-lites	Pin fixture, spot tacked, box section	Stacked in vee post fixture with top weights	1925°F, 15 min.	Edge flange leaks	Flex.	Fixtures W/M 3860 foil	Leaks at edge and end flanges.
IV	304L	Trimmed flange conv. depth .031. Vee notch dimpled air plenum	AuNi	Hi-lites	Pin fixture, spot tacked, box, E.B. welded flanges W/.051 wire spacers	Clamped, E.B. tacked ends stacked in vee post fixture with straddle weights	1925°F, 15 min.	Edge flange leaks	Flex.	-	Leaks at edge and end flanges. Dimensions poor.
V	304	Trimmed flange conv. depth .031. Vee notch flat air entry	AuNi	Hi-lites	Pin fixture, spot tacked, box, E.B. air entry W/wire .051 spacer	Clamped, E.B. tacked ends and edges stacked in vee post fixture with straddle weights	1925°F, 15 min. 1700°F, 1 hour	Saddle-shaped core. Edge flange leaks	-	-	Dimensions poor.
VI	304	Trimmed flanges vee notches, conv. depth .031, flat air entry.	NiP	All over	Pin fixture, spot tacked, box .051 wire spacers	Stacked in vee post fixture with straddle weights	1925°F, 15 min.	Edge flange leaks	-	-	12-in. display core.
VII	304	Retrimmed flanges, vee notch, conv. depth .031, flat air entry.	AuNi	Hi-lites	Pin fixture, spot tacked, box .051 wire spacers	Clamped, E.B. tacked edges and ends, stacked in vee post fixture with straddle	1925°F, 15 min.	Edge and end flange leaks	-	-	Edge and end flange leaks. Dimensions poor.
		flanges vee			spot tacked,	vee post	15 min.	leaks			core.

		flanges vee notches, conv. depth .031, flat air entry.			spot tacked, box .051 wire spacers	vee post fixture with straddle weights	15 min.	leaks			core.
VII	304	Retrimmed flanges, vee notch, conv. depth .031, flat air entry.	AuNi	Hi-lites	Pin fixture, spot tacked, box .051 wire spacers	Clamped, E. B. tacked edges and ends, stacked in vee post fixture with straddle weights	1925°F, 15 min.	Edge and end flange leaks	-	-	Edge and end flange leaks. Dimensions poor.
VIII	304	Retrimmed flanges, vee notch, conv. depth .031, flat air entry.	AuNi	Hi-lites	Pin fixture, spot tacked, box .051 wire spacers	Clamped, E. B. tacked edge and ends, stacked in vee post fixture with straddle weights	1925°F, 15 min.	Edge and end leaks	-	-	Edge and end leaks. Dimensions poor.
IX	304	Retrimmed flanges, vee notch, conv depth .032 flat air entry	AuNi	Hi-lites	Pin fixture, spot tacked, box .055 wire spacers	Edge clamp E. B. tacked edges and ends, stacked in vee post fixture with straddle weights	1925°F, 15 min.	Edge and end leaks	-	-	Edge and end leaks. Dimensions fair.
X	304	Retrimmed flanges, vee notch, conv. depth .032 flat air entry	AuNi	Hi-lites	Pin fixture, spot tacked, .055 wire spacers- E. B. flanges	Edge clamp E. B. tacked edge and end	Clamped, 1925°F, 15 min.	Collapsed pair, edge leaks	-	-	Edge and end leaks. Dimensions good.
XI	304	Retrimmed flanges, vee notch, conv. depth .032 flat air entry	AuNi	Hi-lites	Pin fixture, spot tacked, .055 wire spacers E. B. air entry	Edge clamp E. B. tacked edge and end	Clamped, 1925°F 15 min.	Collapsed pair, edge leaks	-	-	Edge and end leaks. Dimensions good.
XII	304	Retrimmed flanges, vee notch, conv. depth .032 flat air entry	NiP (hvy woods) nickel	All over	Pin fixture, spot tacked, box .055 wire spacers	Edge clamp E. B. tacked edge and end	Clamped, 1925°F, 15 min.	Poor flow, many leaks	-	-	Edge and end leaks
XIII	304	Retrimmed flanges, vee notch, conv. depth .032 flat air entry	NiP	All over	Pin fixture, spot tacked, box .055 wire spacers	Edge clamp E. B. tacked edge and end	Clamped, 1925°F, 15 min.	Edge flange leaks	-	-	Edge leaks.

Intermediate draws with vacuum anneals up to 2150° F prior to the final draw did not correct the problem. The amount of stretch required to form the convolution base exceeded the capability of Hastelloy X. Foil blanks of 0.0035-inch-thick Type 304L stainless steel were formed to the desired depth of 0.032 inch using an intermediate vacuum anneal. Type 304 stainless steel, cheaper than the extra low carbon variety and readily available, also formed satisfactorily.

5.2.3 Braze Alloy

Selection of a braze alloy system presented the twofold problem of alloy placement technique and selection of a low-penetration alloy in association with 0.0035-inch-thick base metal. Alloy placement using foil pre-forms did not appear applicable to the complex wave plate assembly in that a thin brazing foil (e. g., 0.0005-inch-thick) in a lace-like pattern presented a difficult handling problem.

If solid foil were used, the increased core weight and the reduction of area of the core passages with the excess brazing alloy would have been objectionable. A search for alternate placement procedures yielded two possible alloys that could be plated upon the base metal and used for brazing: a gold-nickel eutectic alloy M3860 (82 percent Au, 18 percent Ni) melting at 1740°F, and a nickel-phosphorus alloy (89 percent Ni, 11 percent P) melting at 1610°F.

In order to ascertain whether an interaction of these plated braze alloys with the foil base metals would occur during brazing, wave plate samples were prepared with various thickness layers of the brazing alloys and brazed in vacuum at various temperatures. Table 9 presents the results of this study. Typical brazed joints of Au-Ni and Ni-P on Hastelloy X base metal appear in Figures 37 and 38. Based upon the findings of this investigation, the braze alloy selected was the 82 percent gold, 18 percent nickel alloy plated 0.00020 to 0.00025-inch thick.

5.2.4 Plate Fabrication

Wave plate stampings were fabricated in closed dies. These plates comprised mating pairs stacked together to form alternate layers of air and gas passages. The initial plate configuration was not supported in the air crossflow area and control of that dimension was difficult; therefore, the plate design was revised to include support piers (dimples) in this zone. A number of Hastelloy X plates were manufactured to this configuration, and subsequent processing of these plates revealed the need for a) more accurate and deeper convolution forming in order to match pairs, b) a method of aligning the pairs and core stack, and c) precision-sized edge flanges with the dimples removed from the air entry to both

TABLE 9
VACUUM BRAZING TESTS

Base Metal	Braze Alloy [1]	Thick. (mils)	Temp (°F)	Time (min)	Bond Integrity[2]	Bend Ductility[3]	Gap Coverage[4]
Hast. X	AuNi	0.05	1925	15	P	P	P
Hast. X	AuNi	0.10	1925	15	G	E	P
Hast. X	AuNi	0.25	1925	15	E	E	E
Hast. X	AuNi	0.50	1925	15	E	E	E
Hast. X	NiP	0.20	1800	2	F	P	F
Hast. X	NiP	0.40	1800	2	E	P	E
Inco 718	NiP	0.40	1800	2	E	P	E
Hast. X	NiP	0.05	1875	2	None	-	-
Hast. X	NiP	0.10	1875	2	G	P	P
Hast. X	NiP	0.50	1875	2	E	P	E
Hast. X	NiP	1.00	1875	2	E	P	E
304	NiP	0.25	1925	15	E	G	E

1 AuNi - Electrolytic plating of 82% gold and 18% nickel alloy
NiP - Electroless plating of 90% nickel and 10% phosphorus alloy
2 Visual continuity of braze
3 Ability to withstand twisting of plate pair
4 Fillet at edge flanges and nodes

Code

E - Excellent
G - Good
F - Fair
P - Poor

Figure 37. Gold-Nickel (M3860) Braze Joint.

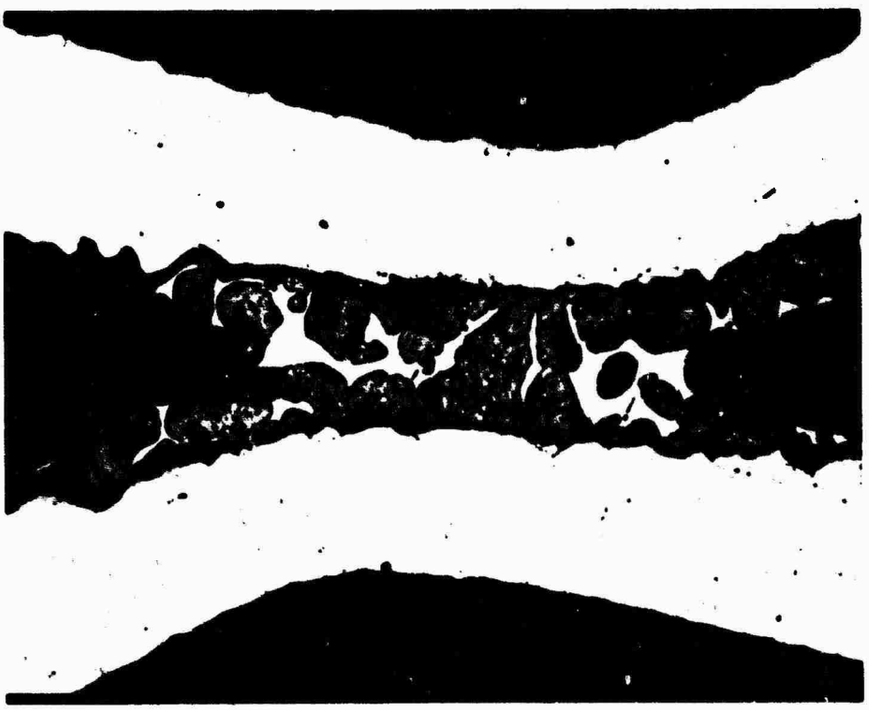

Figure 38. Nickel-Phosphorus Braze Joint.

control pair dimensions and produce a brazeable fit-up. Figure 39 illustrates plates with and without dimpled air entries.

New dies with increased convolution depth and improved alignment were fabricated. A die set was also fabricated for punching vee's which would permit alignment of plate pairs. A guillotine shearing setup was utilized to size the edge flanges. Hastelloy X could not be formed to the new configuration (deeper convolutions) without cracking; however, Type 304 possessed the required forming properties. A typical wave plate pair manufactured by the revised method appears in Figure 40. Even these changes did not eliminate all problems with convolution matching, edge flange engagement, and thickness of end convolutions. Subsequent tooling adjustments attenuated the problems, but did not eliminate them. Figure 41 illustrates the convolutional matching problem.

5.2.5 Braze Alloy Placement

Application of the braze alloys required the development of cleaning, masking, and plating procedures to obtain uniform alloy layers on the 0.0035-inch-thick wave plates. The procedures selected included the application of brazing alloy only on the contacting surfaces (nodes) of the wave plates in order to reduce the possibility of base metal erosion during brazing and to reduce weight and cost. The sequence of procedures is outlined below:

1) Cleaning to remove oils and die forming compound
2) Painting and baking on an effectual mask
3) Hi-liting (removing the paint layer from the surface where alloy placement is desired)
4) Cleaning and surface activation prior to plating
5) Plating the brazing alloy
6) Stripping the mask without affecting the plating
7) Final cleaning

Tables 10, 11, and 12 present the processes in detail.

The masking compound was required to be impervious to the cleaning and activation solutions and not to absorb contaminating compounds which could reduce the effectiveness of the alloy plating solution. Of several paint systems studied, Fidelity EX43 stop-off appeared to fulfill the process needs. Hi-liting consisted of lightly wiping the node areas with paint solvent to remove most of the paint, then lightly vapor blasting to expose the base metal. Although this method was effective, it required excessive time and handling. A second and more successful procedure consisted of machine abrading the node areas to remove the paint.

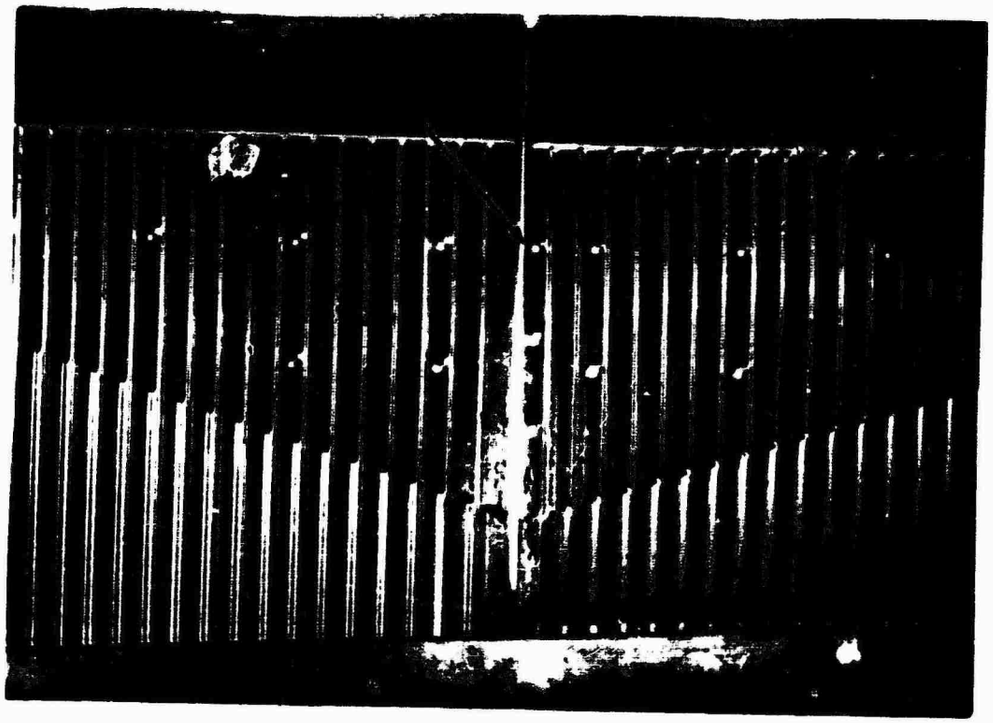

Figure 39. Dimpled Air Passages Showing Revision of Air Entry. Arrows show deformation caused by air entry dimples.

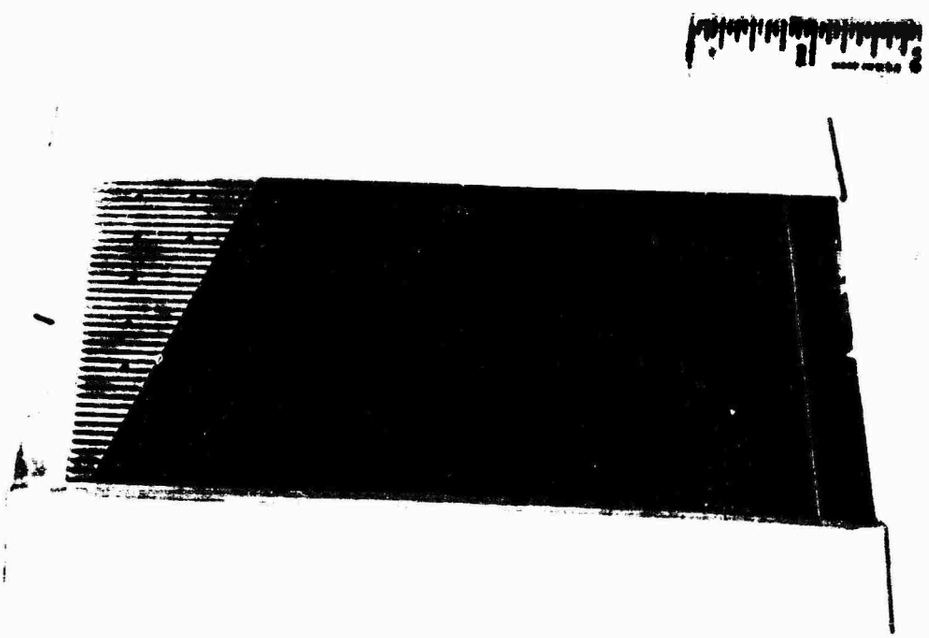

Figure 40. Typical Redesigned Plate Pair.

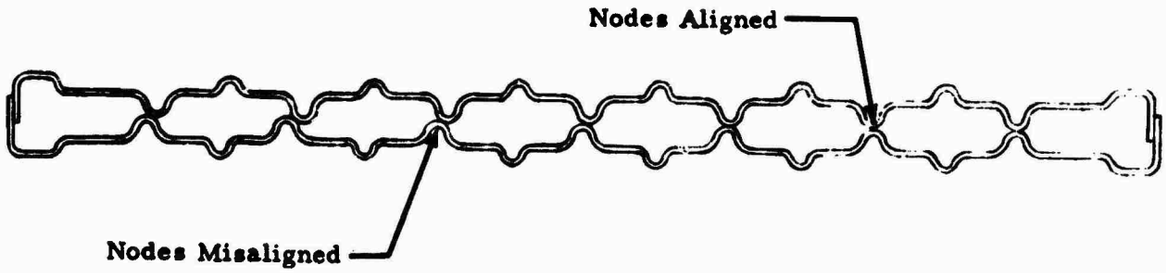

Figure 41. Plate Pair Cross Section Illustrating Node Alignment.

TABLE 10
PROCESS OUTLINE FOR PLATING REGENERATOR PLATES

(Gold-Nickel)

1. Place in racks
2. Vapor degrease (180°F trichlorethylene)
3. Anodic clean (hot caustic soda, until no water breaks occur)
4. Rinse in hot and cold water
5. Pickle for 1/2 to 1 min. (2 parts HNO_3, 1 part HF, 3 parts water)
6. Rinse in cold water
7. Clean for 2 min., periodic reverse (remove on anodic cycle)
8. Rinse in hot and cold water
9. Dip in chromic acid (20 to 30 sec.)
10. Rinse in cold and hot water
11. Mask and Hi-lite if required (see Table 11)
12. Cathodic clean for 1 min. (hot caustic soda)
13. Rinse in cold water
14. Pickle in HCl for 1 min. (room temp. 1% solution)
15. Rinse in cold water
16. Activator pickle for 1 min. (KNiCN solution)
17. Rinse in cold water
18. Dip in HCl for 5 sec. (room temp. 1% solution)
19. Rinse in cold water
20. Woods nickel plate for 1 min. (5 volts)
21. Rinse in cold water
22. Dip in H_2SO_4 for 2 sec. (room temp. 1% solution)
23. Rinse in cold water
24. Gold-nickel plate (Karatklad 528, 10 amp/ft^2 at 5 volts)

TABLE 11
PROCESS OUTLINE FOR REGENERATOR PLATE HI-LITING AND CLEANING AFTER PLATING

These steps follow Operation No. 10 of Table 10 process:

1. Rack with taped edges and ends
2. Spray paint (Ex 43 stop-off)
3. Bake for 3 min. at 100°F
4. Repeat operations 2 and 3
5. Reverse plate surfaces and repeat operations 1 through 4
6. Remove tape
7. Fixture the work, then abrade protruding surfaces
8. Perform operations 12 through 24 of Table 10
9. Strip paint (Fidelity 548 or MEK)
10. Cathodic clean for 1 min. (hot caustic soda)
11. Rinse in cold water and gently brush
12. Activator dip for 15 sec. (KNiCN solution)
13. Rinse in cold and hot water
14. Dry

TABLE 12
PROCESS OUTLINE FOR PLATING REGENERATOR PLATES

(Nickel-Phosphorus)

1. Place in racks
2. Vapor degrease (180°F trichlorethylene)
3. Anodic clean (hot caustic soda, until no water breaks occur)
4. Rinse in hot and cold water
5. Periodic reverse clean for 2 min. (remove on anodic cycle)
6. Rinse in hot and cold water
7. Dip in chromic acid (20 to 30 sec.)
8. Rinse in cold and hot water
9. Pickle in HCl for 1 min. (room temp., 1% solution)
10. Rinse in cold water
11. Woods nickel plate for 1 min. (5 volts)
12. Rinse in cold water
13. Electroless nickel plate

Both procedures were assisted by development of racking and fixture methods for each operation. Some of these fixtures included cast rubber replicas, vacuum chucks, and sheet metal snap clamps. Examples of the fixtures appear in Figures 42, 43, and 44.

Base metal surfaces required activation to be receptive to plating; a meticulous preparation was necessary because as little as 3 parts per million of a chloride would alter the gold-to-nickel ratio of the plating bath to a point beyond its useful function. The Au-Ni plating bath, a solution of Karatclad 528 and nickel salts, was prepared according to vendor instructions; however, current density and plating rates had to be established. Plating thickness versus time for a current density of 10 amperes per square inch appears in Figure 45.

Following plating, the masking was removed and the plates were ready for assembly.

The electroless nickel plating technique involved plating of a nickel-phosphorous alloy on the entire component. This technique was used as an expedient to study assembly techniques and check new plate configurations.

5.2.6 Plate Assembly

Plate pairs were joined prior to stacking for brazing because the individual plates lacked rigidity for handling during assembly. Pairs of plates were tack welded as an "H" section (Figure 46) so that stacking and alignment would be accomplished by interlocking adjacent edge flanges. To facilitate pair assembly for tacking, plastic replica fixtures were manufactured to align the convolutions. A precision electronic welder with electrodes designed to engage convolutions was employed for tacking plate pairs. Initially, the operation was disrupted with burning and tearing of the plates. The difficulty was traced to residual masking, which was subsequently removed with an additional chemical cleaning step after the braze alloy plating process.

When it became evident that stack assembly of the "H" sections was not feasible because the flange widths were not uniform in basic dimensions, the plate pairs were assembled as a box section shown in Figure 47. The pairs were aligned initially in a replica-type fixture for tacking, but when plates with stamped locating vee notches became available, a pin-type fixture (Figure 48) was manufactured to expedite pair assembly. The procedure consisted of fitting a plate pair against the pins, then interlocking the edge flanges, and finally clamping the cover.

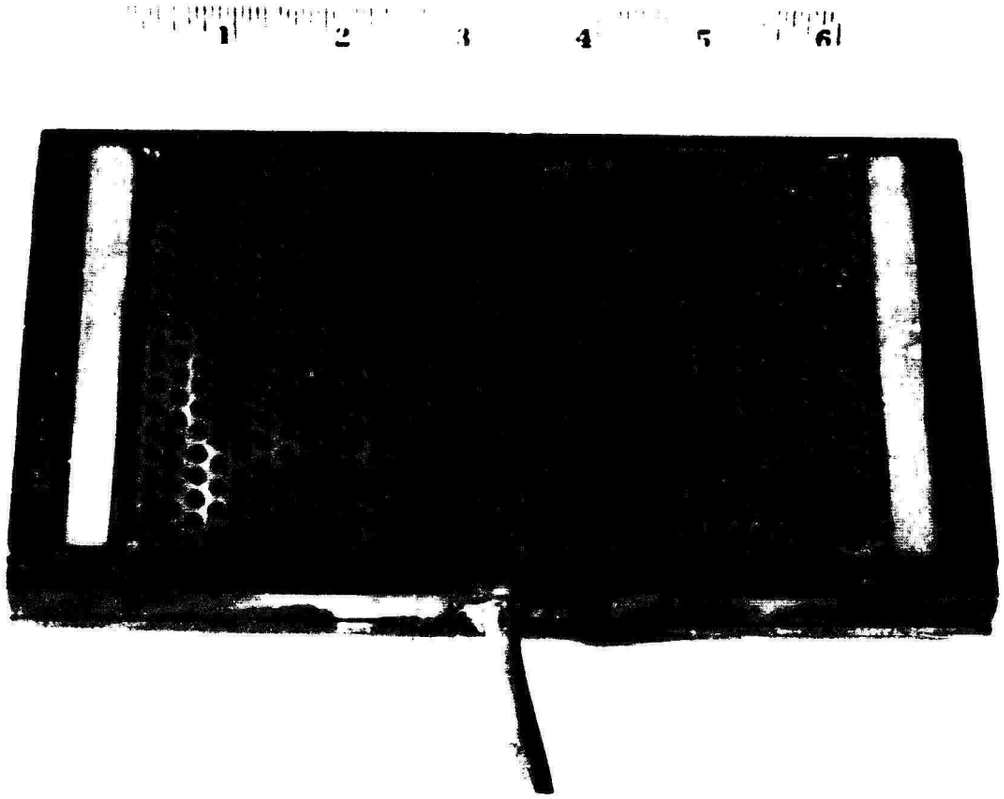

Figure 42. Vacuum Chuck Used During Hi-Liting.

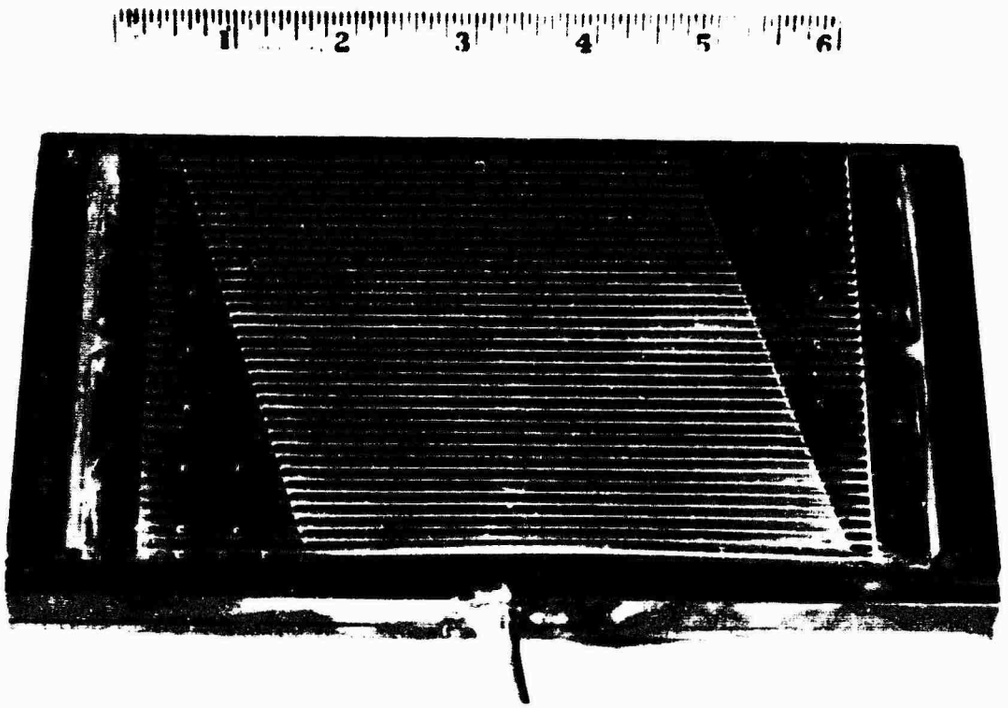

Figure 43. Plate Placed on Vacuum Chuck.

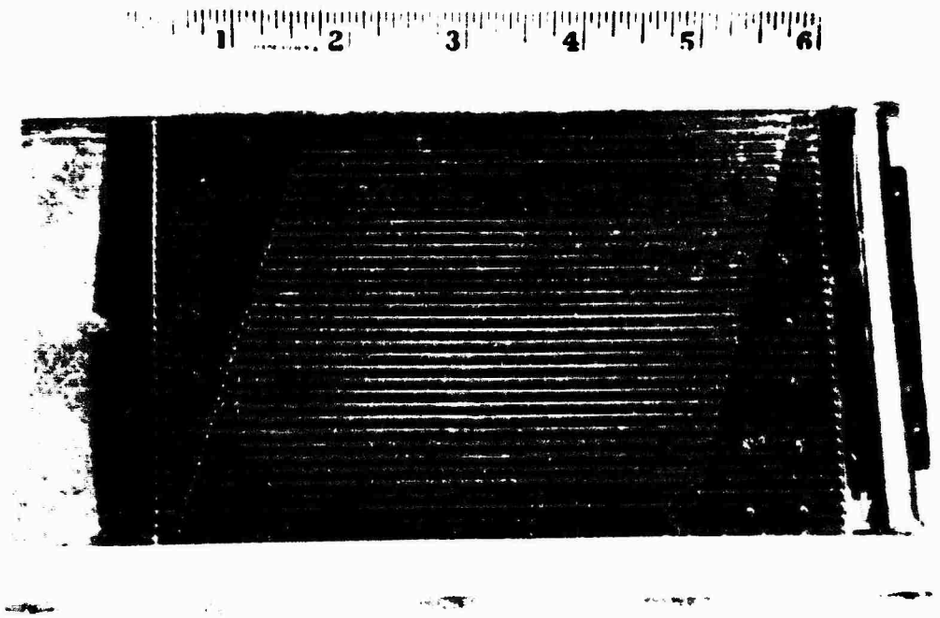

Figure 44. Plate in Sheet Metal Snap Clamp.

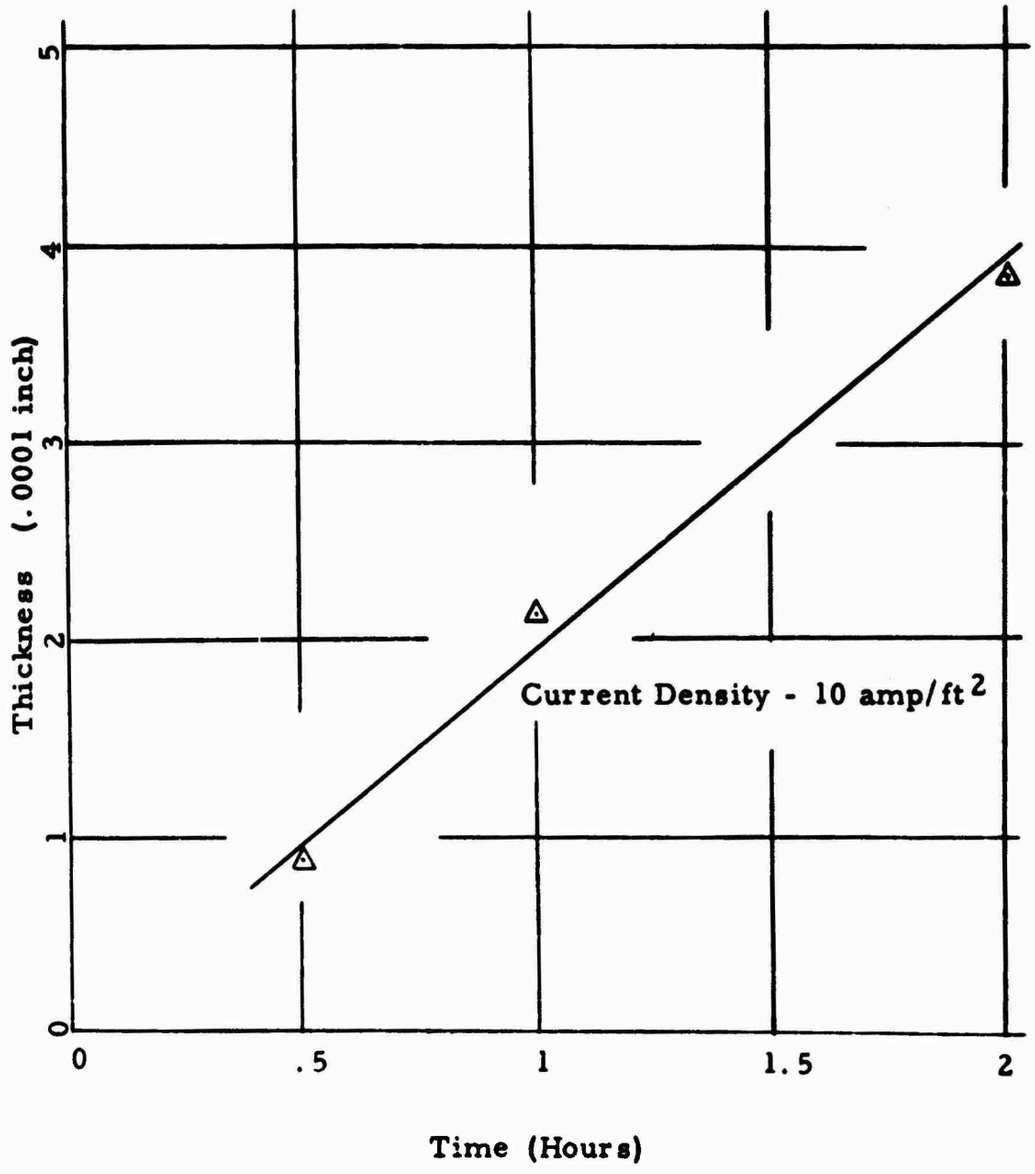

Figure 45. Plating Rate for Gold-Nickel Bath.

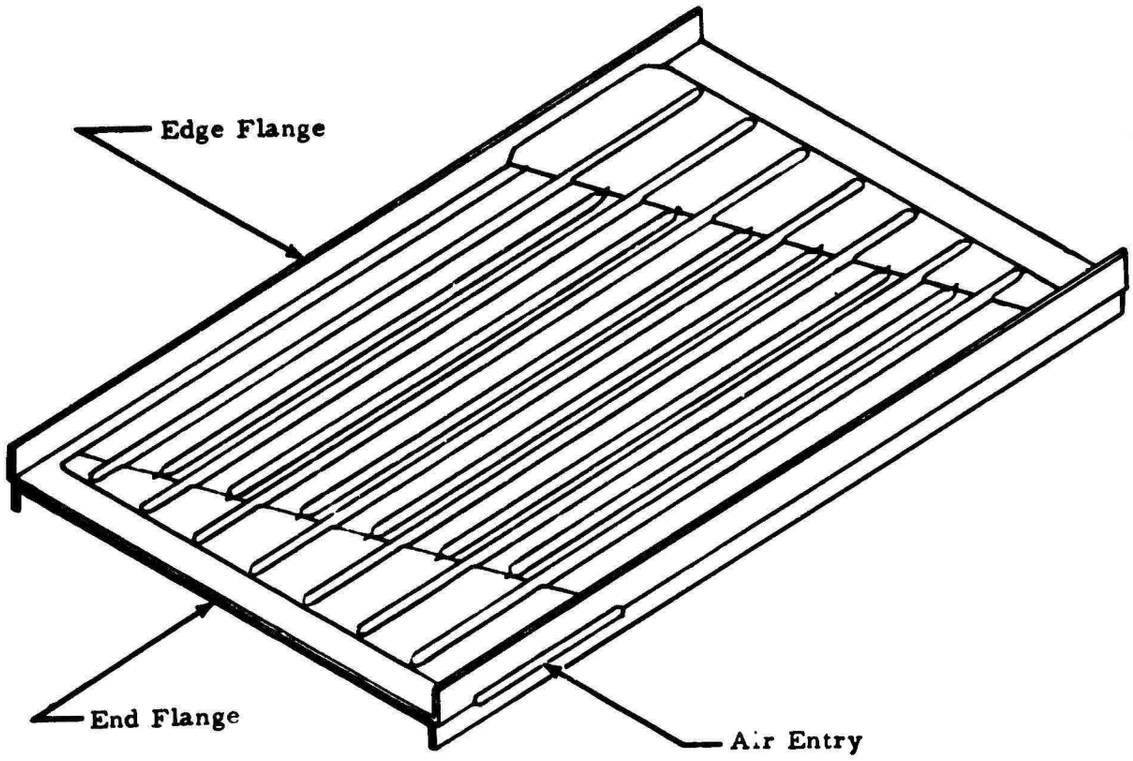

Figure 46. Plate Pair as "H" Section.

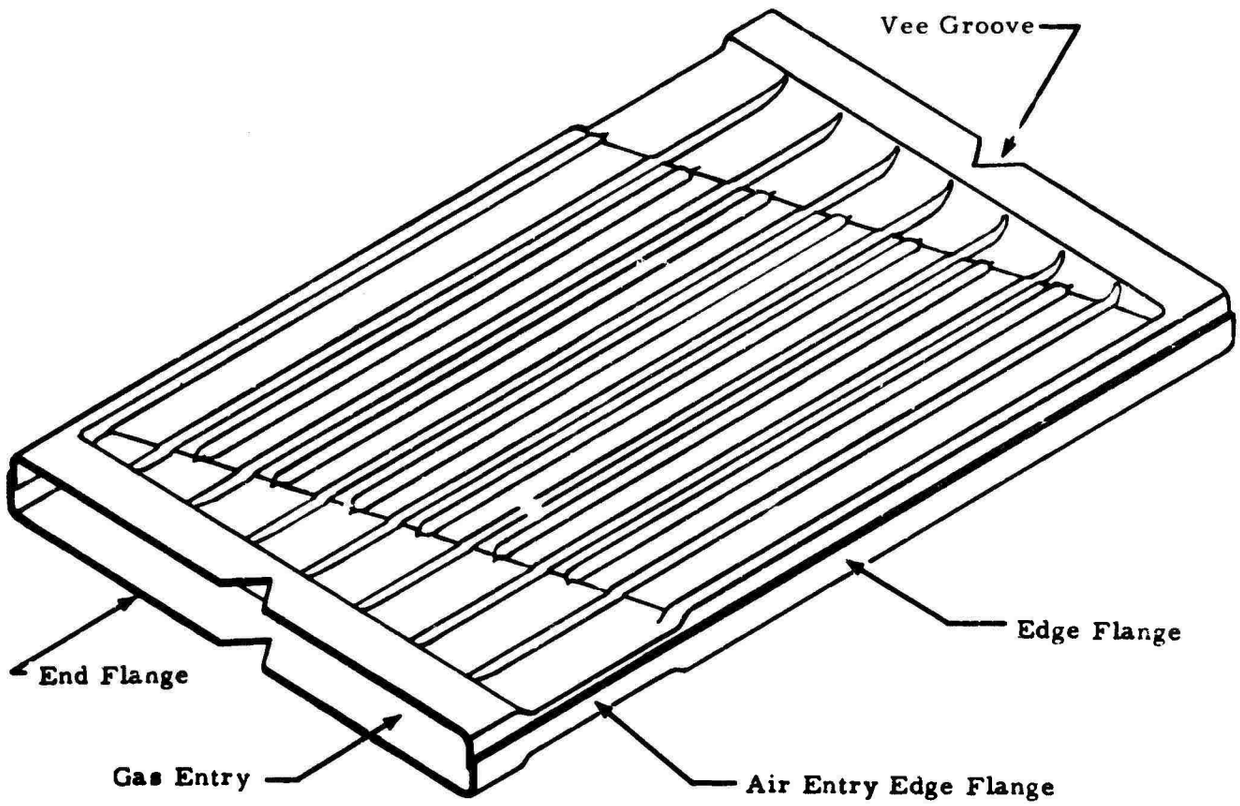

Figure 47. Plate Pair as Box Section.

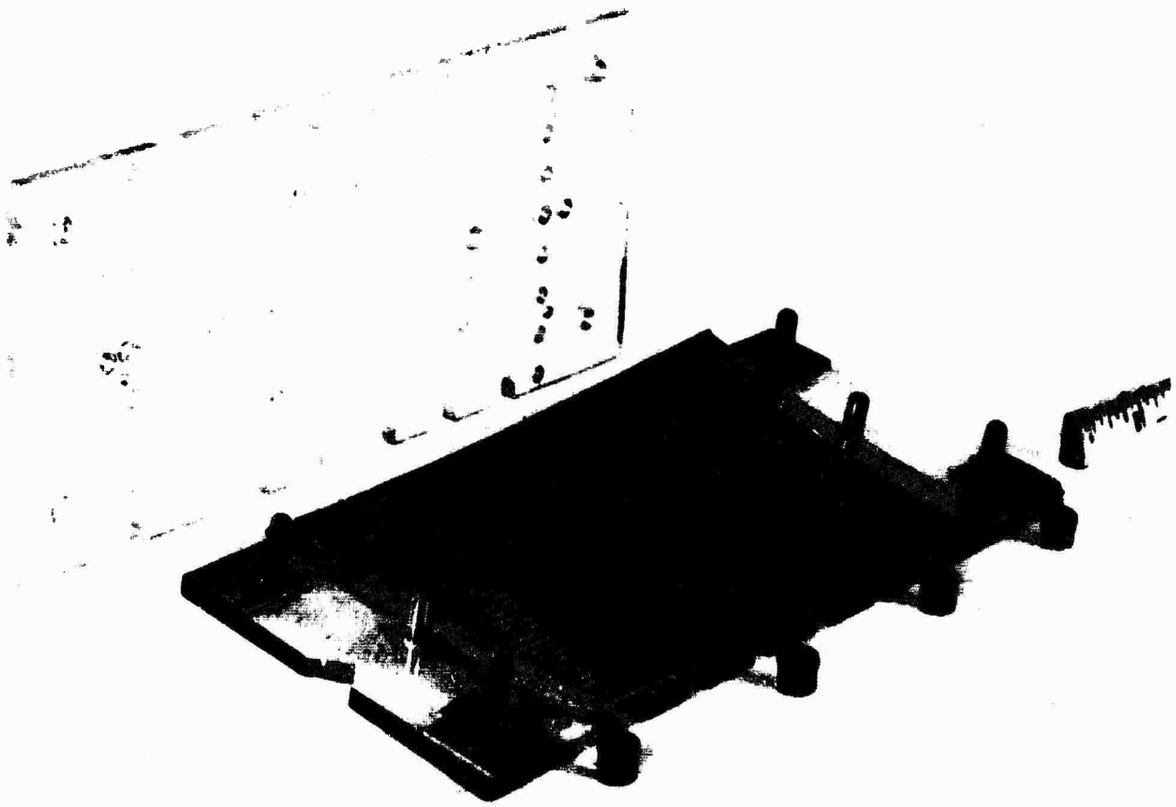

Figure 48. Pin Fixture for Resistance Spot Tack Welding Plate Pairs.

However, manufacturing tolerance buildup did not allow a straightforward procedure in that the edge flanges did not interlock without considerable hand reworking.

5.2.7 Core Stacking

Tack welded pairs of "H" sections without end flange notches were stacked in a fixture which supported and guided the stack laterally and compressed the stack with a weighted platen. The frictional drag of the side supports and lack of vertical alignment resulted in a dimensionally poor core.

In order to maintain plate alignment it was necessary to utilize fixed locating notches in the plates to guide and control plate movement during stacking and brazing. Plate notching was accomplished by stacking and clamping together tacked pairs, sufficient to form a 1-inch core, with two rods separating each adjacent pair. The pseudo-assembly was then adjusted manually, utilizing an optical comparator to position the pairs. After firmly clamping the assembly, locating notches were machined centrally at each end of the 0.0035-inch-thick plates with an electrical discharge machine using a brass electrode. Final assembly was performed by stacking plate pairs in a brazing fixture with vee end posts (Figure 49). The addition of a weighted top platen to compress the core to a height determined by the support legs completed the brazing assembly. Figure 50 shows a typical assembly. Four 1-inch-high core sections were processed according to the described method. The first and second cores were comprised of H-section plate pairs. Edge flange engagement was difficult to maintain during assembly and brazing; subsequent plate pairs were therefore prepared as box sections to assure flange engagement.

Upon stacking box sections for notching, it was noted that the end flanges required internal support to maintain a constant gas opening and to produce contact with adjacent end flanges during brazing. Figure 51 shows preformed wire supports for insertion into the gas openings. With wires in position the pairs were prepared for brazing. Following brazing, it was noted that both top and bottom pairs were displaced in relation to the remainder of the stack. This was attributed to thermal gradients between the plates and fixture. To alleviate the situation, dummy pairs (containing no braze alloy) were placed at the bottom and top of each core.

Assembly of subsequent cores was expedited by using prenotched plates to form the matched pairs, so that stacking pairs in the brazing fixture and applying the weighted top plate completed the assembly procedure.

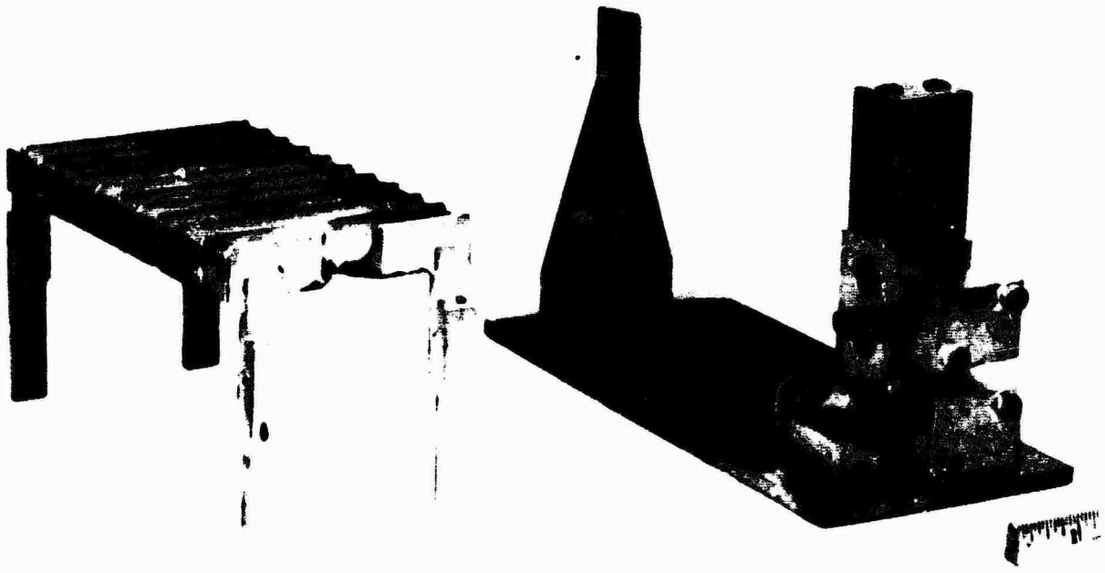

Figure 49. Vee-Post Brazing Fixture.

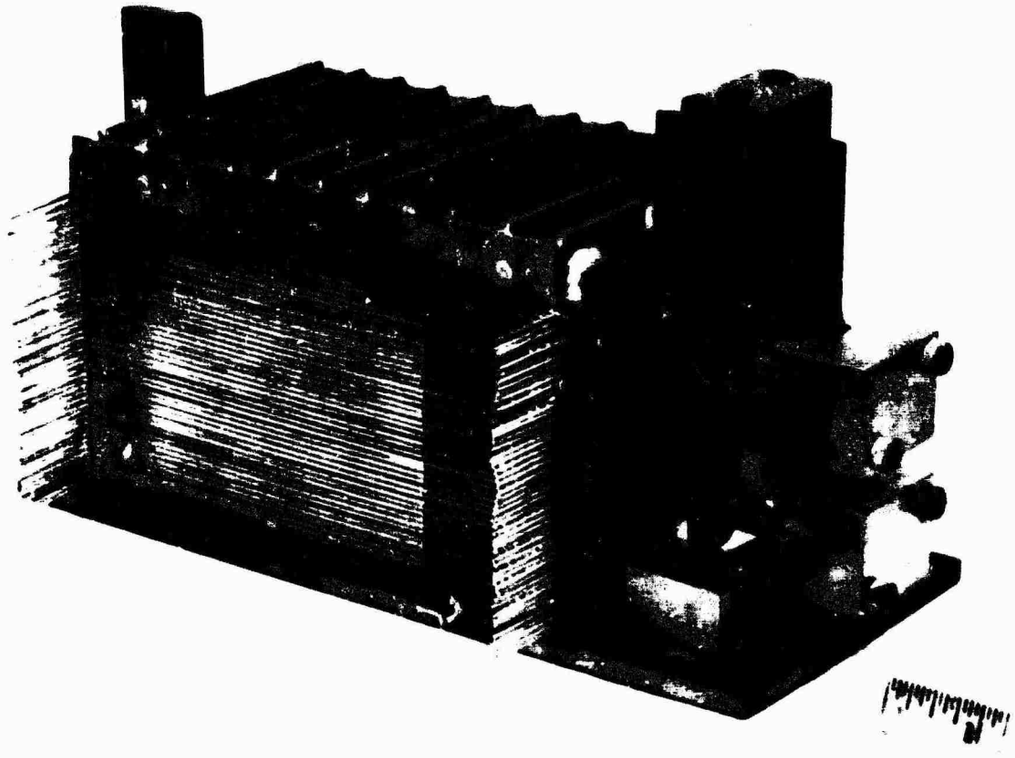

Figure 50. Core Stack Assembled in Brazing Fixture.

The dead-weight compression technique was not successful in producing cores to precise dimensions because of manufacturing tolerance buildup. An attempt was made to compress a stack to final dimension and tack weld the pairs together to lessen the amount of settling during brazing. This method did improve the dimensional quality of the core.

The procedure consisted of fixturing plate pairs on the edge flanges, which were aligned by locating notches during tacking, and then longitudinally adjusting the pairs to a reference line. A clamp held the pairs for electron beam tack welding at the pair corners. Figure 52 shows a core stack in the clamp fixture. Upon release from the clamp, the stack required recompression to fit the brazing fixture. Subsequent stacks received additional electron beam tack welds in three places on each edge flange to reduce springback; however, these cores also experienced considerable springback upon release from the clamp fixture. The most recent assembly method consisted of clamping assembled pairs to the desired final height, and brazing in the clamp. Figure 53 shows a clamped assembly ready for brazing. Although the resultant core dimensions appeared to be improved, it was noted that at least one plate pair collapsed during clamping and/or brazing.

5.2.8 Brazing

From the brazing test data and results of additional brazing trials, a stack brazing temperature of 1925° F was selected for both Au-Ni and Ni-P plated alloys. The additional superheat assured melting of a broader alloy composition in the platings. Also, the high brazing temperature and relatively long time (15 minutes) accelerated diffusion to raise remelting temperature. Brazing was performed in a cold-wall vacuum furnace. Fixtured 3-inch cores were vacuum brazed by heating to 1590° F (below the solidus of the braze alloys) to equalize the temperature of the heavier components (fixture), then heating rapidly to 1925° F and holding for 15 minutes. Vacuum cooling to 1550° F (below the solidus) followed by cooling to 200° F in an argon atmosphere completed the braze cycle.

5.2.9 Core Integrity

The brazed cores required reworking prior to application of the structural frames to seal leaks and adjust critical dimensions. Leaks persisted throughout the program and constituted the major problem in producing a sound regenerator core. Three specific areas were afflicted with leakage: edge flanges, air entry edge flanges, and end flanges. Figure 54 indicates the problem areas.

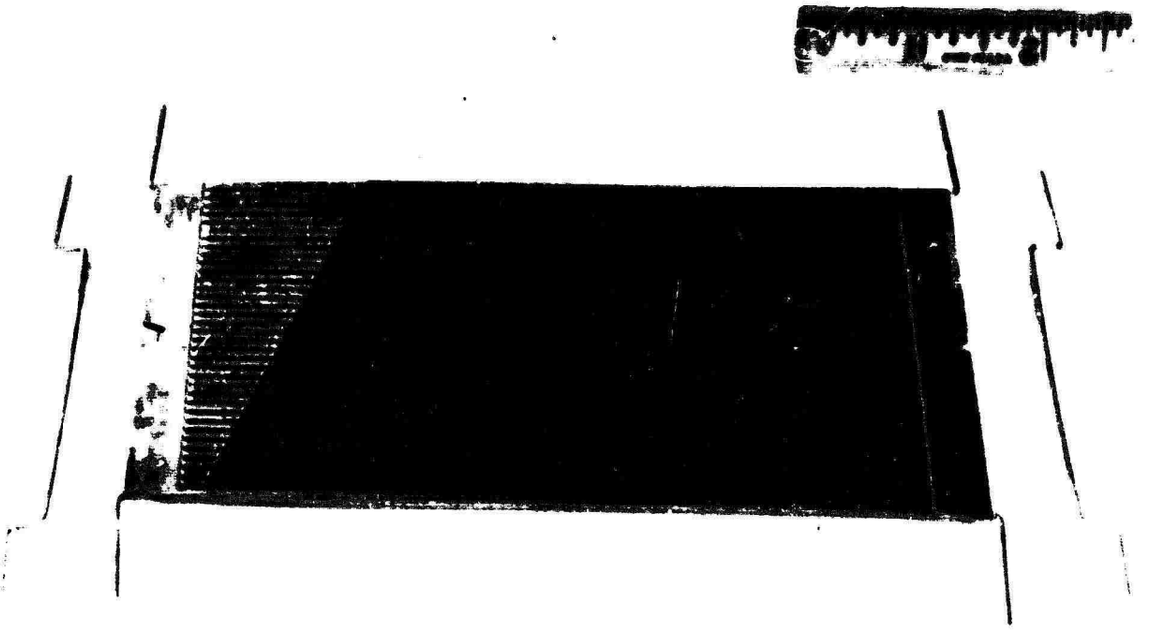

Figure 51. Gas Opening Spacer Wires.

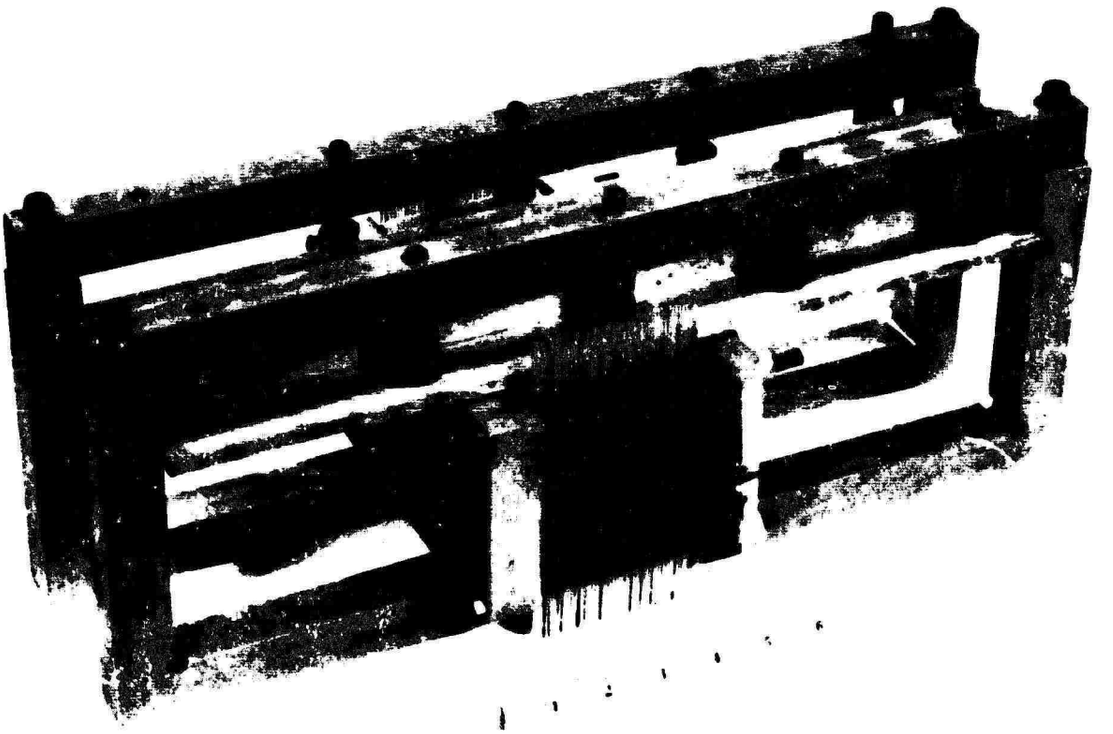

Figure 52. Clamp-Type Stack Assembly Fixture.

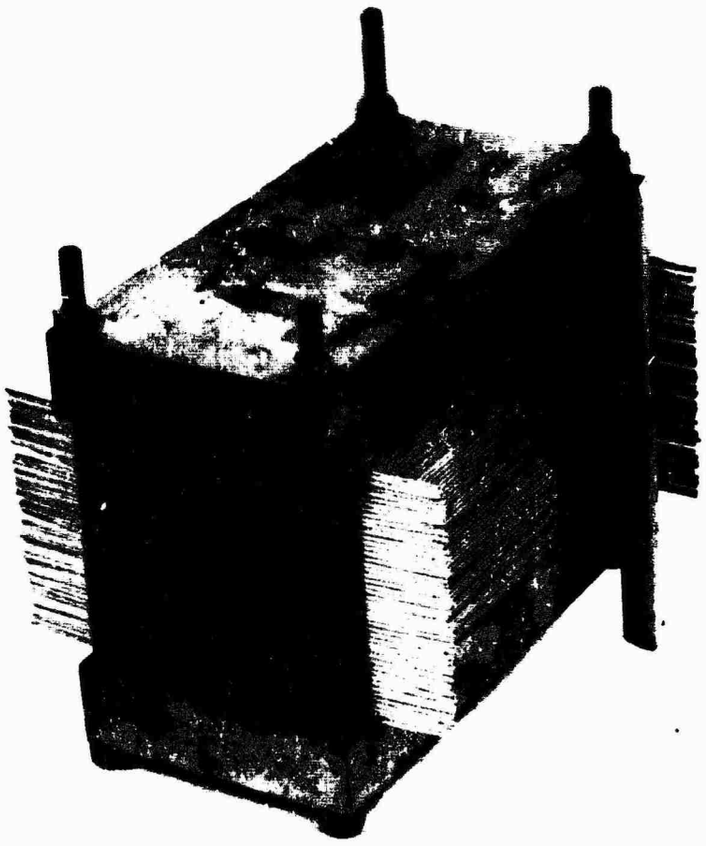

Figure 53. Core Stack in Clamp-Type Braze Fixture.

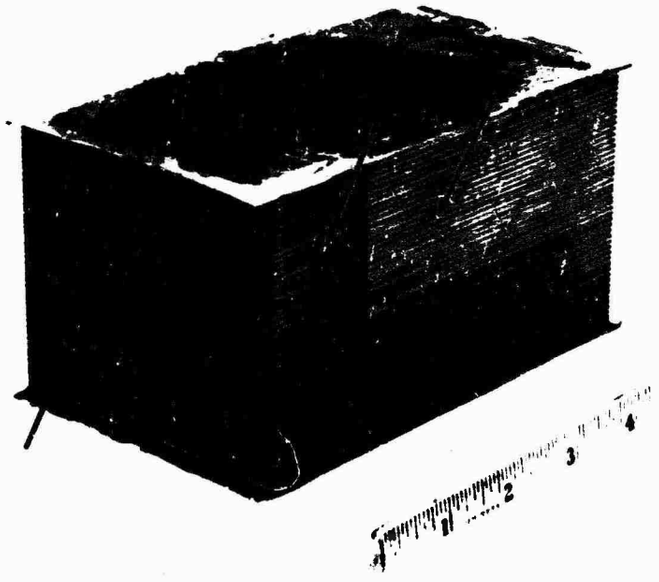

Figure 54. Typical Core With Arrows Showing Areas of Leakage.

Improvements of plate dimensions (sheared flanges) and assembly methods (box section pairs) significantly reduced the number and size of edge flange leaks. These smaller voids were sealed by dusting a thin layer of braze alloy powder on the edge flanges and vacuum brazing at 1875° F for 2 minutes. Generally, the resultant brazes were sound; however, in a few instances erosion from excess braze alloy produced large nonrepairable voids. A second method of producing leak-tight edge flanges involved the process of plasma flame spraying a pure nickel layer on the flanges and dusting braze alloy on the surface to infiltrate the sprayed metal during brazing. This procedure also was utilized to produce a uniform surface for box assembly (by grinding the buildup surface flat). A third method involved the electron beam fusion welding of the tacked pairs on the flanges utilizing internal wire spacers to standardize the edge thickness. The procedure consisted of inserting wire spacers into the edge gas passages of spot welded pairs, alternately stacking pairs and 0.020-inch stainless steel spacer plates in a welding clamp, then longitudinally electron beam welding at 80 kv, 0.325 ma, and 30 inches/sec.

The average yield of plate pairs with sound weldments was 40 percent because the contact of the flange overlap was irregular so that the beam would strike a single plate thickness and burn through. Figure 55 illustrates this condition. It was noted that the air entry flange welds had a yield close to 70 percent resulting from more uniform fit-up by using external spacer shims in the air passages. Therefore, it was decided to seal the air entry flanges by electron beam welding and to depend upon the dusting method to seal any edge flange leaks.

Leaks at end flanges appeared to have resulted from insufficient contact between plate pairs during brazing, and repair attempts to insert plated shims and/or braze alloy sheet failed to seal these leaks. The most promising approach was to utilize wire spacers in the gas openings large enough to produce sufficient pressure across the end flange so that the resultant brazement would be sound.

5.2.10 Core Boxing Preparation

The edge flange dimension fit-up of early cores was not amenable for brazing to a flat box plate. Several methods were employed to improve fit-up for brazing. The first procedure was to press rods transversely into the core edges at both ends and adjacent each air entry, braze the rods in place, then grind the rods. However, upon press fitting the rods, the plate edges cracked causing a serious leakage problem.

A second attempt to improve the edge surfaces was to clamp the core on a milling machine table and feed it under a sizing roller. This method was successful in flattening the edge surfaces of the core, but the resultant plate deformation closed off the air entry. Efforts to reopen the air entry passages resulted in fracturing the base metal and brazed joints. Another method, mentioned previously, was plasma flame spraying of nickel and grinding the surface flat. However, the resultant surface spalled off.

5.2.11 Core Boxing

Securing the core into a rigid box frame was accomplished by electron beam welding a plate-type frame, which was plated with brazing alloy, around the core and vacuum brazing at 1850° F. Thermal gradients across the heavy and thin sections of this assembly caused cracking of flange joints that subsequent repairs could not seal. It was then decided to manufacture a sheet metal frame to alleviate thermal expansion problems in fabrication and in operation. The redesigned frame, illustrated in Figure 56, consisted of a reinforced sheet metal top and bottom plate, to which Au-Ni braze alloy foil was tack welded, and corner tie bars to complete the structural member. Electron beam tack welding was utilized to preassemble the test core, and the components were preloaded against the core in a brazing fixture. Vacuum brazing at 1850° F joined the structure. Leakage problems developed across the corners between the air and gas entries; repair brazing, using braze alloy foil and powder dusting and vacuum brazing at 1800° F, did not seal the leaks.

5.2.12 Fabrication Results

Phase I has progressed through the basic stages of fabricating a test core utilizing wave plates with interlocking edge flanges: a plate material (Type 304 stainless steel) and braze alloy (gold-nickel eutectic) were selected, a technique for braze alloy placement (plating on the plate nodes) was devised, and a core assembly method was evolved. Many additional procedures were developed to cope with the problems of dimensional control and leakage encountered during this study. Leakage at edge flanges and end flanges persisted throughout the program and was the major deterrent to the fabrication of an acceptable test core.

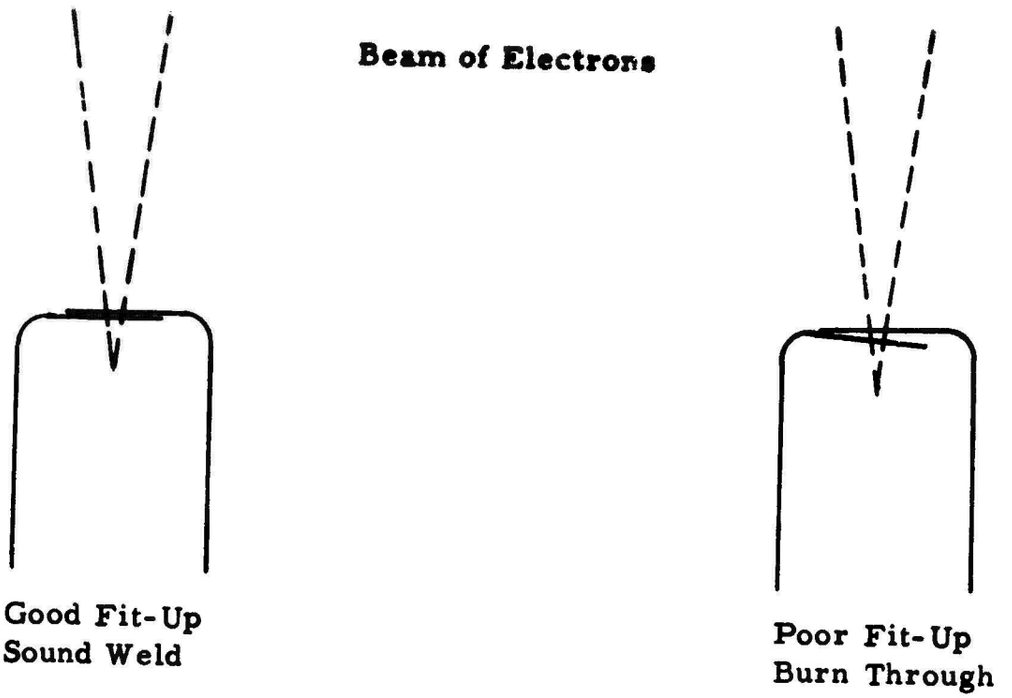

Figure 55. Edge Flange Condition During Electron Beam Welding.

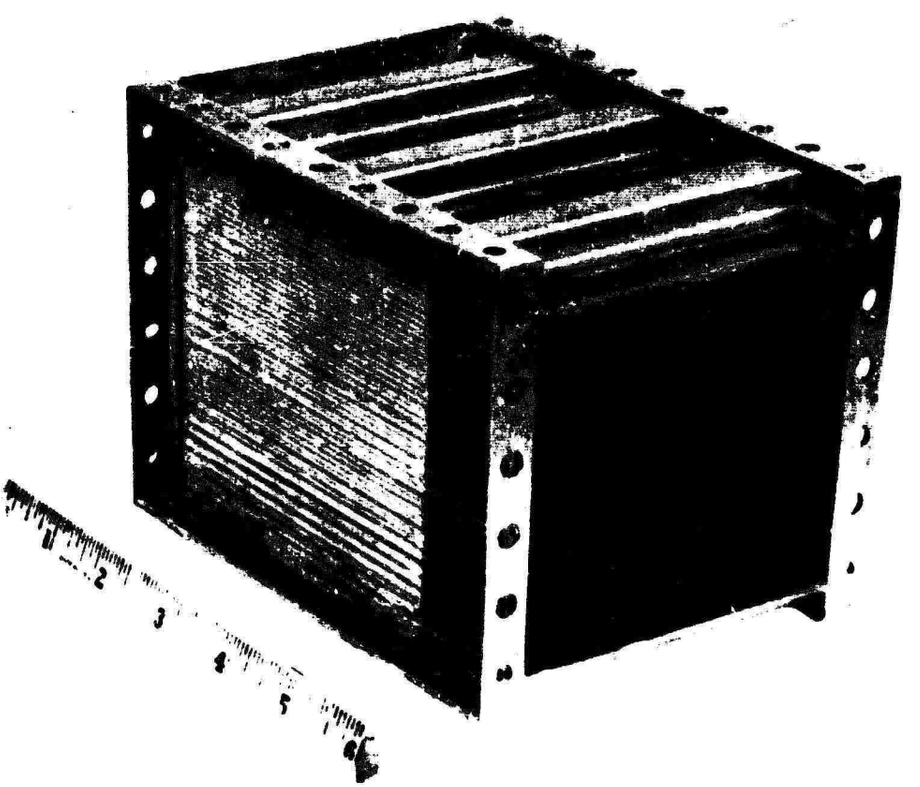

Figure 56. Core With Sheet Metal Box.

5.3 EXPERIMENTAL CORE TEST

5.3.1 Test Modules

Several test core modules were fabricated for test as described in Section 5.2, of which three modules were of sufficient quality for testing. The modules were sized to be of 3 inches in the no-flow length, ample for the determination of performance yet convenient to handle from a fabrication facility and instrumentation standpoint. Pertinent design values for the core are given below:

Test Sample (3 inch) Core Specifications

Core length (no flow)	- 3 inches
Core Width	- 3.6 inches
Core Height	- 5.5 inches
Number of Plates Per Inch	- 32
Air Side Hydraulic Diameter	- 36 mils
Gas Side	- 54.4 mils
Gas to Air Cross-Sectional Flow Area	- 1.50
Initial Plate Thickness	- .0032 inch
Average Plate Forming Elongation	- 22 percent
Core Porosity	- 85 percent
Representative Size (compared to full regenerator	- 1/64 (1.56 percent)

The modules were built for the performance evaluation of effectiveness and pressure loss only. It was intended to perform the tests at exact engine operating conditions to eliminate any errors in extrapolating from reduced test results. This was not possible because of core leakage; however, several runs were conducted at full engine operating conditions.

5.3.2 Test Equipment

Core module testing was conducted in the Lycoming heat exchanger test laboratory shown in Figures 57 and 58. Figure 57 is a view of the control room panel; Figure 58 shows a core module mounted in the test cell. The facilities are capable of handling heat regenerator sections ranging from small core samples to large (1/6) sections of a T53 engine regenerator. (With test cell modifications, a full-size T53 regenerator can be tested at actual engine conditions.) A schematic diagram of the laboratory for both core module and larger (1/6) sections is shown in Figure 59.

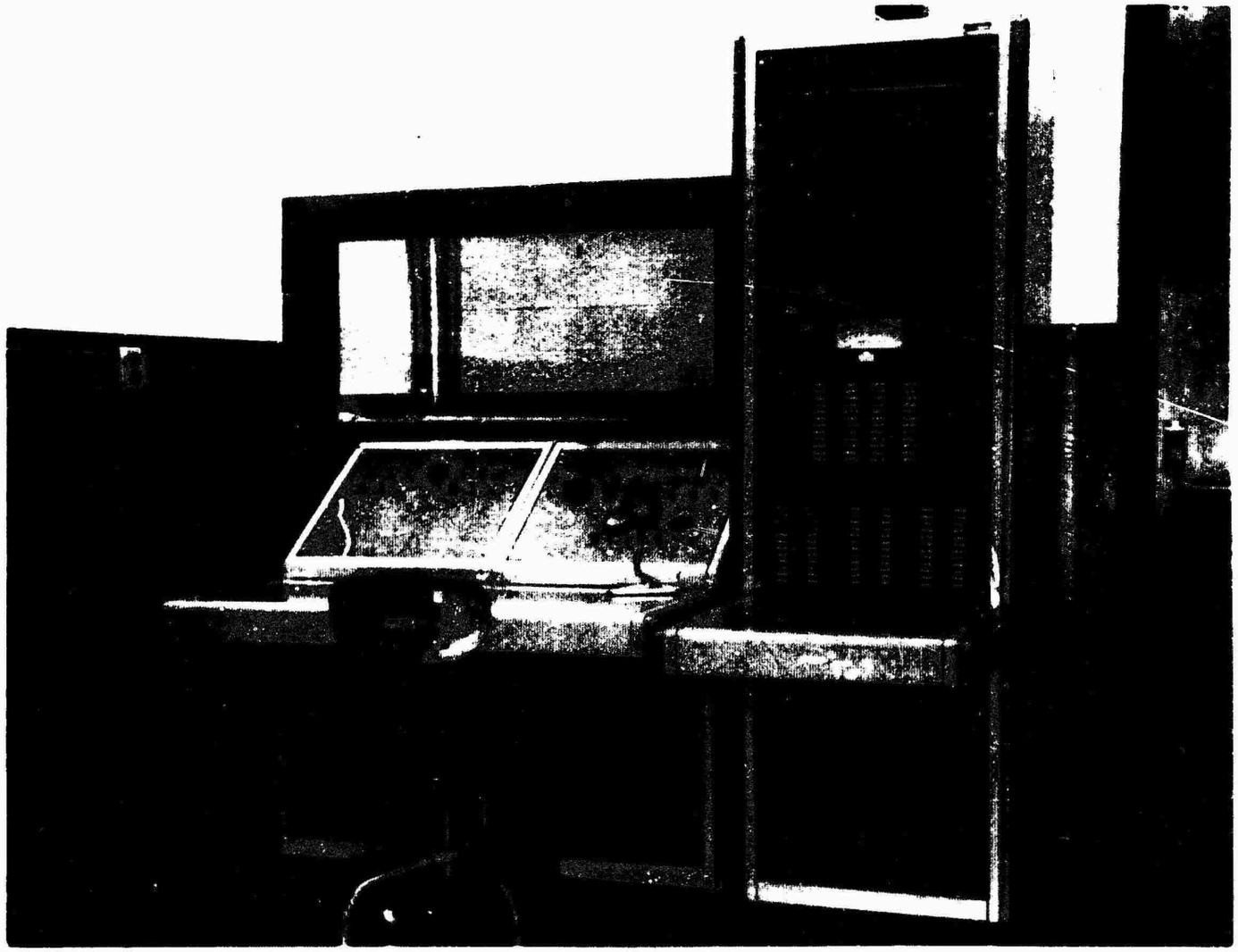

Figure 57. Test Cell Control Panel.

Figure 57. Test Cell Control Panel.

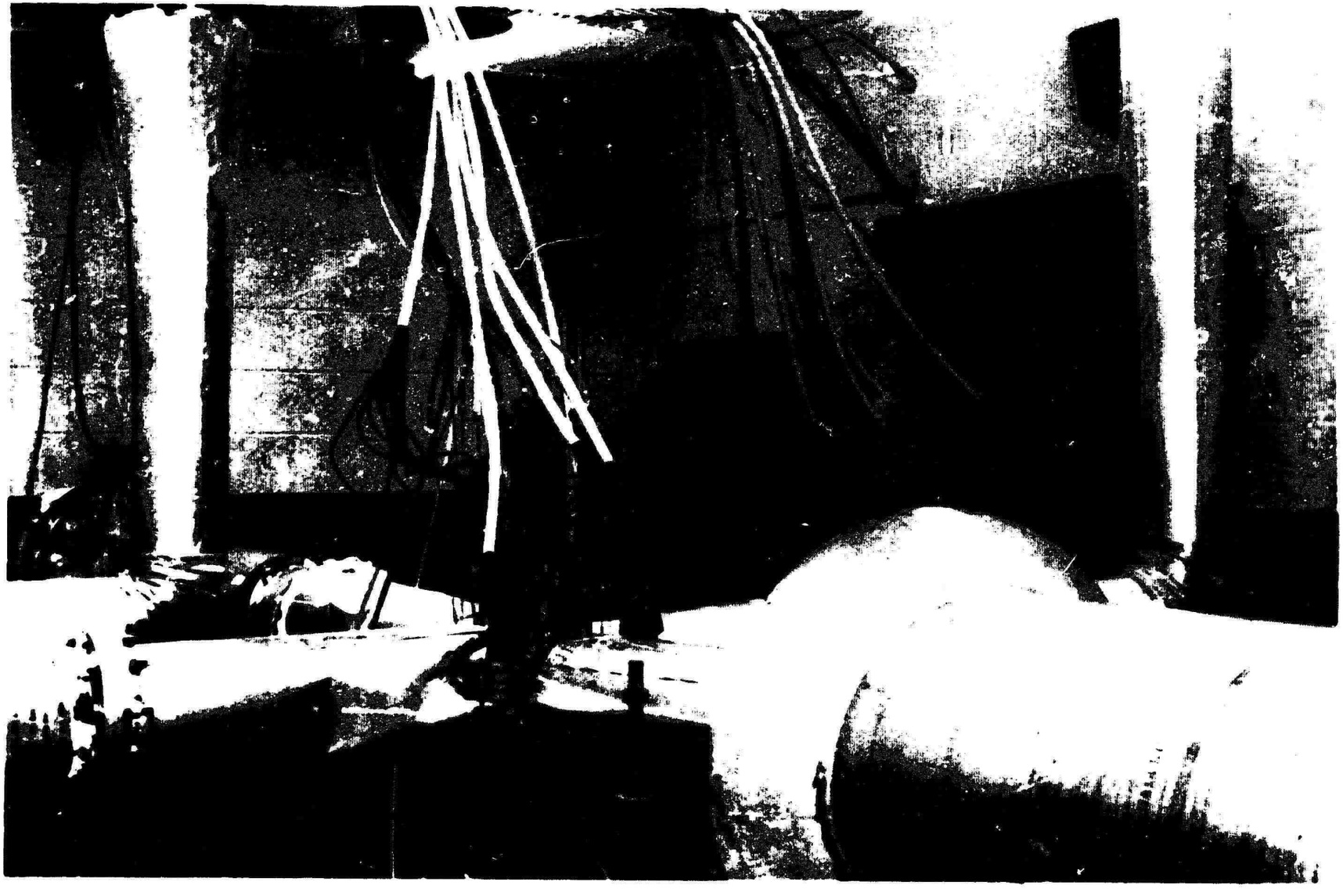

Figure 58. Core Module Mounted in Test Cell.

CORE MODULE SYSTEM

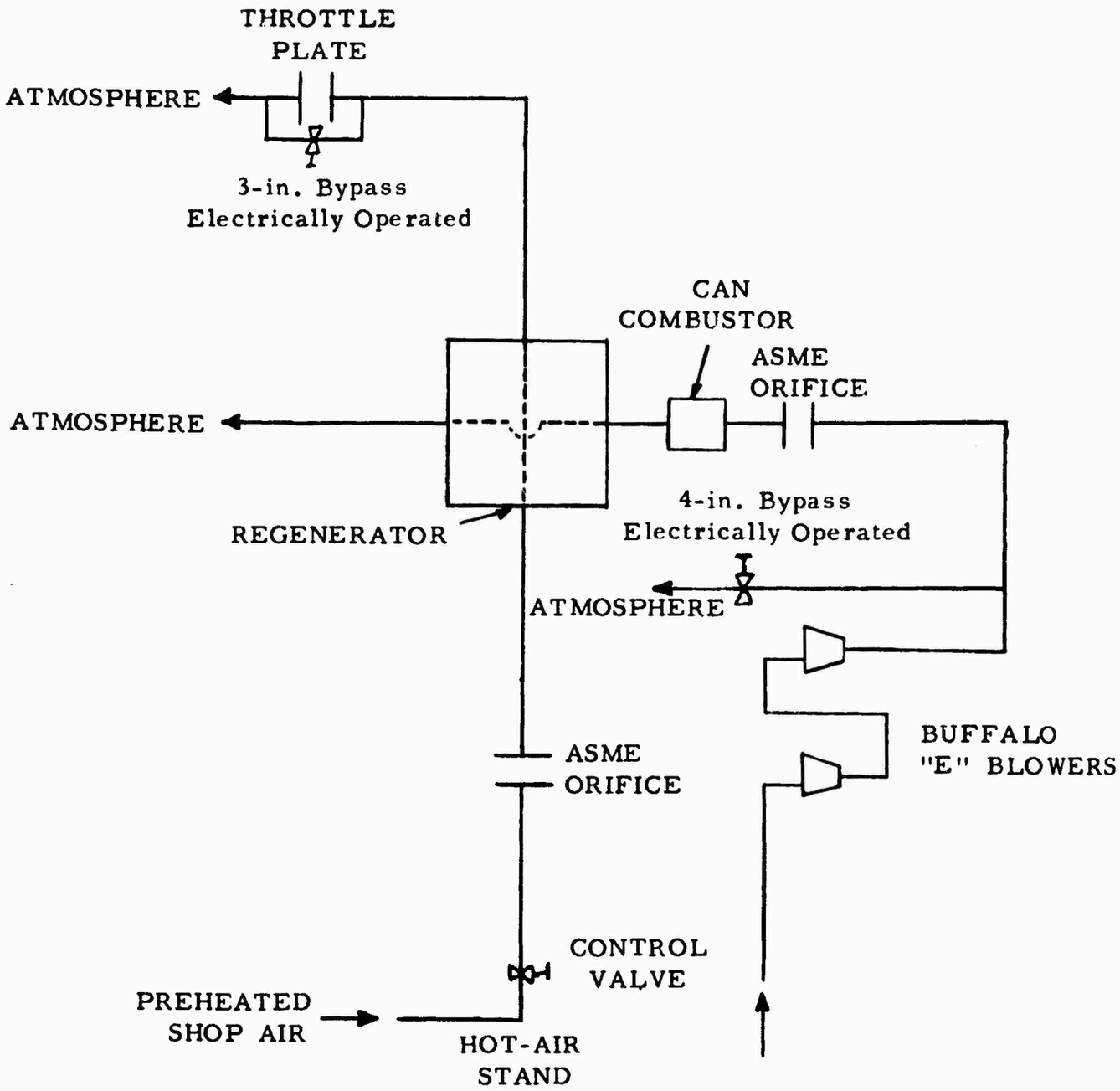

Figure 59. Core Mo

1/6 - 1/8 SECTION SYSTEM

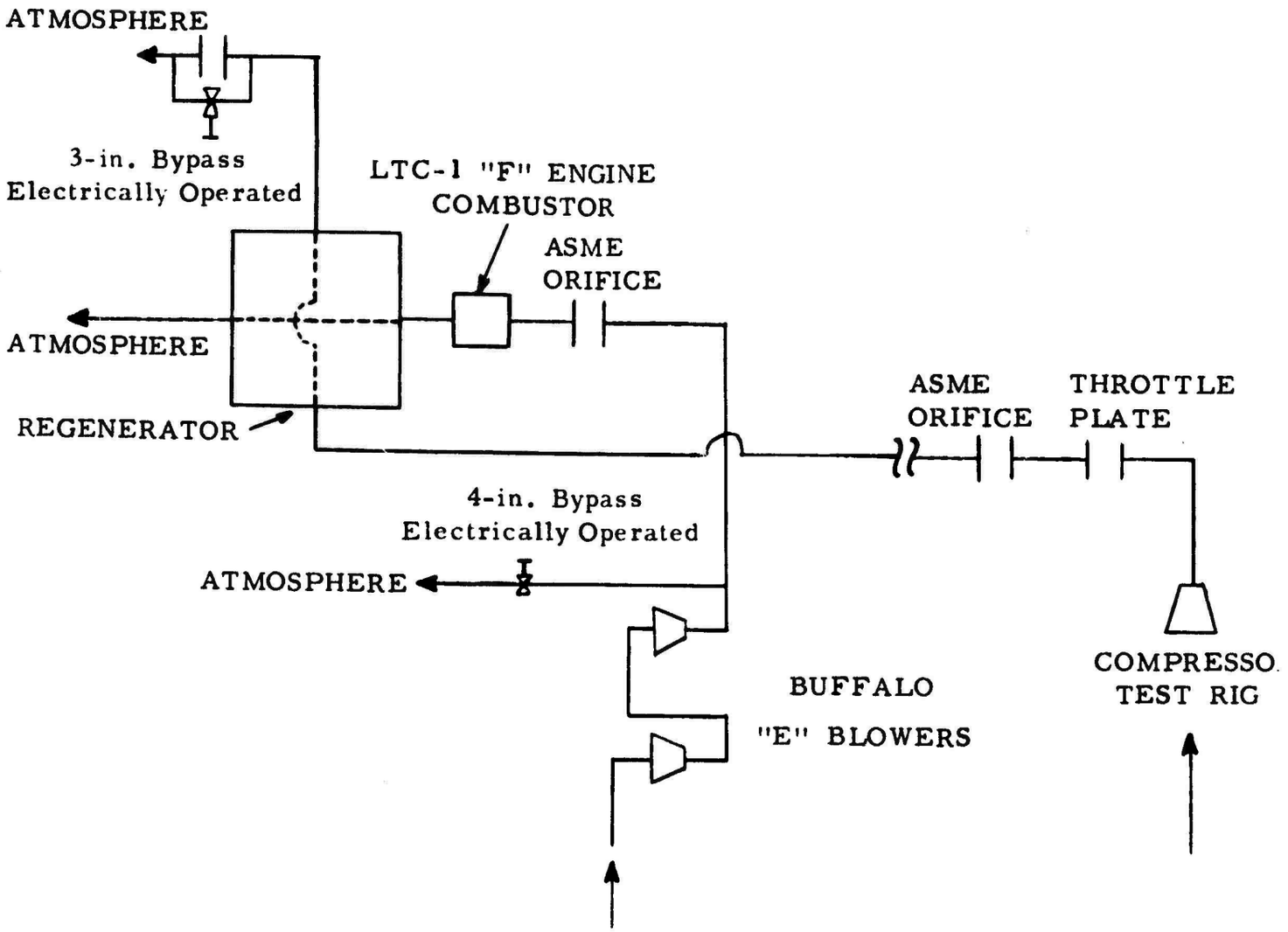

lodule Test Schematic.

B

The core module air-side flow is provided by electrically heated shop air. Control of both the air pressure level and flow rate requires control valves at upstream and downstream sides of the core. The downstream valve is placed in parallel with a fixed throttle plate that is blanked off at the low flow rates associated with core module testing. The core gas-side flow is provided by a Buffalo blower followed by a small can combustor burning JP-4 or any other gas turbine fuel. The flow of hot gases is regulated by a bypass valve between the blower and the combustor. The gas flow leaving the core is dumped directly to atmosphere.

When testing large core sections, the following changes are made to the test system.

Air Side:
1) Shop air and electrical heater replaced with a T53 engine compressor and throttle plate driven in the compressor test cell.

2) Downstream valve used in parallel with a fixed-size throttle plate.

Gas Side:
1) Can combustor replaced with a T53 engine combustor.

The test apparatus is completely instrumented to insure proper operation of the pumps, combustor, electric valves, etc. The performance of the core is accurately determined with instrumentation, including ASME orifice plates upstream of the core, measuring both air and gas weight flows. Core air and gas pressure drops are measured with upstream and downstream wall static pressure taps (4 each). Temperature changes of fluids passing through the core require detailed sampling across the flow streams. A grid of 16 thermocouples is located in the hot gas flow stream at the inlet to the core; a similar pattern of 16 thermocouples is located at the core exit. This arrangement allows for some indication of varying performance within a single core. The air-side temperature changes are measured with a similar arrangement using the same technique, but with only 12 thermocouples because of the smaller inlet and exit areas. All test instrumentation and apparatus functioned satisfactorily throughout the test program.

5.3.3 Test Description

Testing of the three core modules is described in chronological order. Core performance varied significantly depending upon discrepancies in core construction. Performance results (Table 13) indicate the development problems encountered during the program. The best results were

obtained from the third core, which had the lowest leakage rate and a wave form most closely approaching design requirements. In order to maintain low leakage rates and, therefore, more meaningful performance results, the core was tested at reduced pressure and temperature, and the results were corrected to engine conditions.

TABLE 13
TEST CORE MODULE NOS. 1 TO 3

Physical Characteristics	Module No. 1	Module No. 2	Module No. 3
Construction	Structure collapsed throughout	Structure approximately correct	New packaging design, internally unchanged
Frontal Area	Reduced 20% by collapse, 2.39 x 3.6 in.	3 x 3.6 in.	3 x 3.6 in.
Flow Area	Partly filled by braze	Unobscured	Partly filled by braze
D_{Ha}, Inches	.0325	.036	.036
D_{Hg}, Inches	.0488	.0544	.0544
Leakage	High	High	$\simeq$ 8% of design airflow
Test Conditions and Results			
T air in, °F	73	-	193.5
T gas in, °F	900	905	567.5
P air in, psia	29.1	-	20.25
W air in, lb/sec	.1218	-	.1431
W gas in, lb/sec	.1218	.120	.1531
Δ P air, percent	13.0	-	26.2
Δ P gas, percent	6.36	5.00	2.53
Effectiveness	Not determined	Not determined	.662

Core Module No. 1

Testing of the first wave plate core module began on 26 February 1963. Due to manufacturing problems encountered in constructing the core module, discrepancies in the design dimensions were present. The largest discrepancy was a reduction in overall width from a design value of 3 inches to 2.39 inches, thereby reducing the overall frontal area and hydraulic diameters on both the air and gas sides. The air-side openings were further reduced by an excessive amount of braze which was used in an attempt to eliminate crossflow leakage within the core. The gas-side openings also contained an excessive amount of braze material accumulated during attempts to reduce leakage.

The initial test was a pressure check to determine the amount of flow leakage. The test rig for pressure checking the module is designed to measure pressure decay rate. The large leakage rate of the module prohibited determination of an absolute value for the leakage.

Effectiveness testing was not possible because of the large internal leakage rate in the core module and therefore only pressure drop studies and gas-side contamination tests could be conducted.

The initial pressure loss test on the air side showed a drop of 38.4 percent at the design W_a and T_T. A visual inspection of the air-side inlet and outlet indicated that a large amount of pressure loss was due to the excessive amount of braze on the outer edge of the plates. To eliminate this condition, the plates were opened with an electrical discharge machine. It was found that in order to obtain a reasonable air-side opening, it was necessary to cut back two convolutions. This operation resulted in opening the air side to the gas side thus providing two flow paths for the high-pressure air. This problem was eliminated by blocking the opening between the air side and the gas side with an epoxy material. The module was again tested, and a pressure loss of 13 percent at design conditions was obtained. The design pressure loss across the air side was 6.63 percent at test conditions of W_a = 0.021 lb/sec and a temperature of 440° F.

A contamination test of 10 cycles using combustion gas was conducted on the gas side. Each cycle was of 1-hour duration with a combustion ignition and test temperature of 900° F. It was found that the initial pressure loss was 6.38 percent and that there was no increase in pressure loss throughout the 10-hour period. The design pressure loss across the gas side was 5.60 percent at a "no heat transfer" condition of W_a = 0.121 lb/sec and a temperature of 902° F. A plot of the gas-side pressure drop versus running time is presented in Figure 60.

Figure 60. Multiwave Plate Core Module No. 1; Gas-Side Contamination Test.

Core Module No. 2

This core module also had excessive leakage rates but looked quite clean in the gas-side passage area. A "no heat transfer" gas-side pressure drop test was again made by blanking off the air-in and air-out openings. Pressure drop readings of 5.00 percent were observed. This value indicated an improvement over the previous core No. 1 test but was still somewhat higher than the design value, which in this case is 3.35 percent due to the now correct hydraulic diameters.

No further testing was done with this test piece.

Core Module No. 3

Testing of the third core module began on 29 April 1963. This module incorporated a new packaging design to eliminate a portion of the brazing cycles that were required in manufacturing and to provide the means of using one external package for any number of modules.

The initial test was a check of the leakage rate. At the test pressure of 20.25 psia the leakage of the module was 5.5 percent (Figure 61). This was the minimum pressure at which the required mass airflow could be passed. The leakage problem was partially eliminated by using a ceramic cement ("H" cement) to block visible leakage voids, reducing the leakage at the same pressure from 5.5 to 2.1 percent. After two preliminary heat transfer test runs and subsequent leak tests, the leakage increased to a greater value than it was originally. The high temperatures of the heat transfer test had distorted the wave plates enough to break off the ceramic cement and open other braze points that were only marginally sealed.

After the leakage rate appeared to stabilize with further testing, a final effectiveness test was conducted at 20.25 psia, $T_{T\ air\ in}$ of 193.5° F, and $T_{T\ gas\ in}$ of 567.5° F. The cold-side effectiveness under these conditions was found to be 66.2 percent, with a gas-side exit temperature variation of 57° F. This variation was caused by both flow leakage and inlet temperature distortion. The pressure loss at the test conditions was found to be 26.2 percent on the air side and 2.53 percent on the gas side. A large amount of the air-side pressure loss was due to the reduced frontal area of the air opening caused by excessive braze material.

A leakage test was repeated and showed that the module leakage rate was 8 percent at test conditions. Depending upon the location of the leaks within the core, varying effects on performance would result in that the

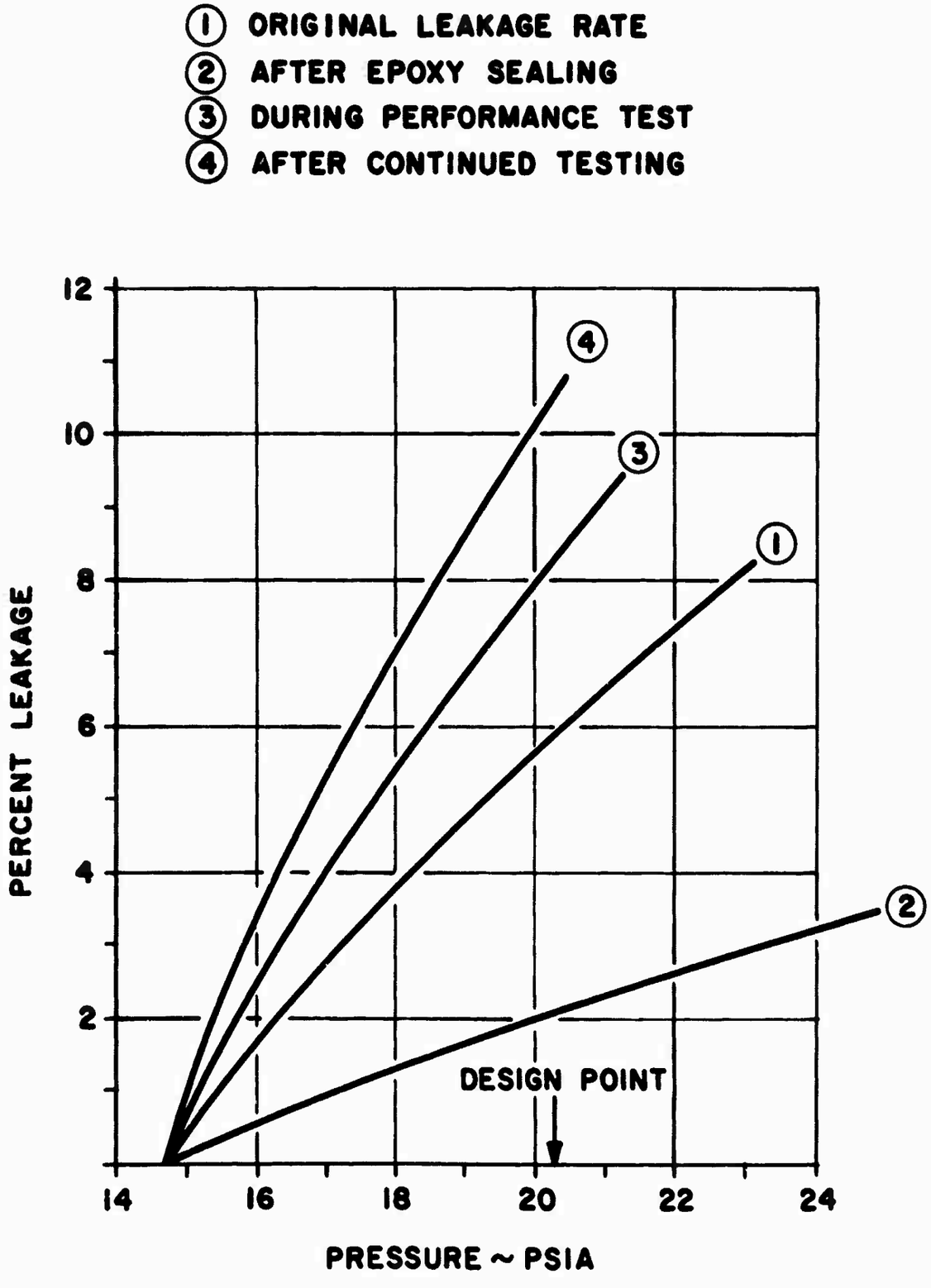

Figure 61. Multiwave Plate Core Module No. 3; Air-Side Leakage vs. Pressure.

C_{min}/C_{max} ratio through the core could change, the air could dilute the gas temperature, high gas-side pressure drops could be created, etc. Since it is not known where the leaks occurred, no adjustments to the measured performance was made due to leakage.

5.3.4 Test Results

The testing of core module No. 3 gave the most complete and reliable information of the three modules tested. The results of this test are given in Table 14. Column 1 lists the design values at engine conditions. The engine thermodynamic conditions follow the performance values. Column 2 gives the test results and the test thermodynamic conditions. Column 3 lists the performance of core module No. 3 when extrapolated from the test conditions of Column 2 to the engine conditions of Column 1. The method of extrapolation is described in Section 5.3.5.

TABLE 14
TEST RESULTS OF MODULE NO. 3

	Design Engine Condition	Test Values*	Test Extrapolated* to Engine Condition
Effectiveness	.71	.662	.698
$\Delta P/P_{air}$	1.24%	26.2%	2.53%
$\Delta P/P_{gas}$	3.34%	2.53%	4.00%
T_{air} in (°F)	440	193.5	440
T_{gas} in (°F)	902	567.5	902
P_{air} in (psia)	74.5	20.25	74.5
W_{air} (lb/sec)	.15	.1431	.15
W_{gas} (lb/sec)	.15	.1531	.15

* Approximately 8% air-side to gas-side leakage

It is seen that the effectiveness of this test core module is close to the design or predicted value. The pressure drops, however, are on the high side. The gas-side pressure loss may be high due to the air leakage. The air-side pressure drop could only be decreased by the leakage effect. The high reading here must then be attributed to the visible distortion in the core air-side crossflow entrance and exit area.

5.3.5 Method of Extrapolating Test Results

General

The core performance, extrapolated to engine conditions, is listed in Table 14, Column 3. This performance is determined by modifying the test results of Column 2 to account for the different thermodynamic states that prevail during engine operation. The reduced temperatures and pressure used for testing were necessary to avoid creating additional core leaks and to minimize the leakage rate at existing leak points.

The predominant part of the heat transfer and pressure drop in the multiwave plate regenerator occurs in the counterflow section, which is designed to be in the laminar flow regime. Consequently, the friction factor and heat flow parameter (Colburn factor) vary inversely with Reynolds number.

For laminar flow in tubes

$$(N_{st}N_{pr}^{2/3}) \propto N_R^{-1.0} \tag{1}$$

where

$$N_R = \frac{DW}{\mu A_c} \tag{2}$$

and

$$h = \frac{(N_{st}N_{pr}^{2/3})\, W c_p}{N_{pr}^{2/3} A_c} \tag{3}$$

Assuming that film coefficients on both sides of the exchanger are equal, which is approximated in this design,

$$U \simeq \frac{h}{2} \tag{4}$$

Therefore,

$$NTU = \frac{UA}{(Wc_p)_{min}} = \frac{hA}{2Wc_p} = \frac{(N_{st}N_{pr}^{2/3})A}{2N_{pr}^{2/3}Ac} \tag{5}$$

But

$$\frac{A}{Ac} = \frac{4L}{D} \tag{6}$$

and substituting (1), (2), and (6) into (5),

$$NTU = \frac{2(N_{st}N_{pr}^{2/3})h}{N_{pr}^{2/3}D} = \frac{2\mu AcL}{N_{pr}^{2/3}WD^2} \tag{7}$$

Within the temperature range of interest the variation in transport properties of air may be represented as power functions of temperature as follows:

$$\mu \propto T^{.68}, \quad c_p \propto T^{.13}, \quad N_{pr} \propto T^{-.0622}$$

Therefore

$$\boxed{NTU \propto \frac{T^{0.72}AcL}{WD^2}} \tag{8}$$

For laminar flow in tubes, the Hagan-Poiseulle law for calculating pressure drop is applicable.

$$\frac{\Delta P}{P} = \frac{32\mu LW}{PD^2\rho Ac} \tag{9}$$

but

$$\rho = \frac{P}{RT}$$

$$\frac{\Delta P}{P} = \frac{32\mu LWRT}{P^2D^2Ac} \tag{10}$$

Upon eliminating constants and representing viscosity as a function of temperature, the relationship for pressure loss is obtained:

$$\frac{\Delta P}{P} \propto \frac{T^{1.68}\, WL}{P^2\, AcD^2} \qquad (11)$$

Equations (8) and (11) show the effect of changes in regenerator thermodynamic states and design on regenerator performance. The equations given in Tables 1 and 2 for laminar flow and pressure drop, if combined, would be equations (8) and (11) with the exponents rounded off to the nearest integer.

Core Module No. 3 Extrapolation

The method of extrapolating test results to engine conditions for test core module No. 3 is given below.

The air-side pressure drop is calculated as follows:

From Test Results -

Inlet P_a	= 20.3 psia	Inlet T_a	= 653° R
Outlet P_a	= 14.9 psia	Outlet T_a	= 910° R
Average P_a	= 17.6 psia	Average T_a	= 781° R

At Engine Conditions -

Average P_a = 74.1 psia Average T_a = 1063° R

With the use of equation (11), the air-side pressure drop at engine conditions is found to be

$$\left(\frac{\Delta P}{P}\right)_{engine} = \left(\frac{\Delta P}{P}\right)_{test} \left(\frac{T_{engine}}{T_{test}}\right)^{1.68} \left(\frac{W_{engine}}{W_{test}}\right) \left(\frac{P_{test}}{P_{engine}}\right)^2$$

$$\left(\frac{\Delta P}{P}\right)_{engine} = .262 \left(\frac{1063}{781}\right)^{1.68} \left(\frac{.15}{.14}\right) \left(\frac{17.6}{74.1}\right)^2 = 2.53\%$$

The gas-side pressure drop is calculated as follows:

From Test Results -		At Engine Conditions -	
Inlet T_g	= 1027° R	Inlet T_g	= 1362° R
Outlet T_g	= 787° R	Outlet T_g	= 1052° R
Average T_g	= 907° R	Average T_g	= 1207° R

With the use of equation (11), the gas-side pressure drop at engine conditions is found to be

$$\left(\frac{\Delta P}{P}\right)_{engine} = 0.0253 \left(\frac{1207}{907}\right)^{1.68} \left(\frac{.15}{.1531}\right) = 4.00\%$$

The effectiveness is calculated as follows:

From Test Results -

$T_{average,\ air} = 781° R = 321° F, \quad C_p = .242$

$T_{average,\ gas} = 907° R = 447° F, \quad C_p = .250$

$\frac{C_{min}}{C_{max}} = \left(\frac{.1431}{.1534}\right)\left(\frac{.242}{.250}\right) = .905, \quad E = .662$

$(NTU)_{test} = 1.77$, from relationship for counterflow heat exchanger

$T_{average\ in\ exchanger\ at\ test} = \frac{781 + 907}{2} = 884° R$

$T_{average\ in\ exchanger\ at\ engine\ conditions} = \frac{1063 + 1207}{2} = 1135° R$

From equation (8)

$$(NTU)_{engine} = (NTU)_{test} \left(\frac{W_{test}}{W_{engine}}\right) \left(\frac{T_{engine}}{T_{test}}\right)^{.72}$$

$$= 1.77 \left(\frac{\frac{.1431 + .1531}{2}}{.15}\right) \left(\frac{1135}{844}\right)^{.72} = 2.16$$

At $\frac{C_{min}}{C_{max}} = .95, \quad E = 0.698$

SECTION SIX. ANALYTICAL STUDIES FOR TUBE-TYPE REGENERATION

6.1 INTRODUCTION

The analytical studies leading to the selection of an optimum regenerative version of the T53-L-9 engine were covered in detail in the Phase I study. This selection was the Lycoming multiwave plate counterflow design and took into account various mission profiles. As a result of fabrication experience, the decision was made to proceed with the program utilizing the tube-type regenerator for the Phase II activity, and a firm basis for selection of the regenerator core was required. The following paragraphs describe these considerations and their resolution which resulted in the present regenerator.

Two performance criteria were considered significant: fuel savings and power penalty. Fuel savings is a direct function of effectiveness and an inverse function of system pressure loss. Additionally, for a given maximum burner temperature, the power penalty is a direct function of the additional system pressure loss.

One of the considerations was to minimize the additional pressure drop $\Delta P_t/P_t$ of the regenerator cycle. At 75 percent power operating conditions, preliminary analysis indicated that the ducting for a typical tube-type regenerator installation would cause a pressure drop of 4 percent above normal engine losses.* Since the fuel savings are an inverse function of the total pressure drop, the additional pressure drop of the cycle must be held as low as possible. For these reasons, the core pressure drop was selected to be not greater than 4 percent at the design condition. A review of regenerator designs showed that this pressure drop limitation would still allow the selection of regenerators which are attractive both from an effectiveness standpoint, and suitably compact in overall size. The design value of total pressure drop will then be 8 percent (4 percent ducting loss and 4 percent core loss).

The second consideration was to select the effectiveness value. Here, several considerations were involved: fuel savings, time to recover the added system weight, envelope dimensions, and flow configuration. To provide the possibility of installing the regenerative system in an existing T53 engine/aircraft application, selection was made of a two-pass cross-counterflow core of 28-inch maximum diameter. This core size would

*At military power, the regenerator would operate in a bypassing condition to reduce the gas-side pressure loss to maintain the military power as high as possible for a given maximum turbine inlet temperature limit.

yield an attractive effectiveness of 66 percent. The maximum core diameter could have been maintained with a higher effectiveness but would have imposed the penalties of higher pressure loss, requiring an increased number of smaller tubes, and would have added to the complexity, weight, and cost of the final product.

6.2 DETERMINATION OF REGENERATION SPECIFICATIONS

The preliminary regenerator specification No. 105.23.1 (Appendix I) was written using the T53-L-9 engine performance as a basis. This specification was based upon the available knowledge in aircraft regenerator practice at the time. Reasonable requirements on effectiveness, pressure loss, length, weight, tube size and spacing parameters were arrived at by discussion with AiResearch (References 8 and 9).

An initial parameter to be established was the inside diameter of the regenerator. This diameter selected was such that the exit gas Mach number leaving the regenerator in a bypass condition would not be appreciably increased over present engine values. This resulted in a basic core inside diameter of 17.0 inches.

Core pressure loss, which is only part of the total pressure loss, must be held to as low a figure as practical and, as previously stated, was selected to be 4 percent. The system pressure losses at this time were estimated to be:

Core air-side losses	1.8 percent	
Core gas-side losses	2.2	
Total Core Loss		4.0
Duct air-side losses	1.0	
Duct gas-side losses	3.0	
Total Duct-side losses		4.0
Total System Losses		8.0 percent

Regenerator effectiveness was now reviewed in light of the envelope objective of 28-inch maximum core diameter and a pressure loss not greater than 4 percent at the design condition. It was determined that an effectiveness of 0.66 (see paragraph 6.1) would meet these objectives and that a value greater than this would be justified only for a mission time greater than 4 hours (Figure 62). Lower effectiveness values present the problem of diminishing returns for the effort expended.

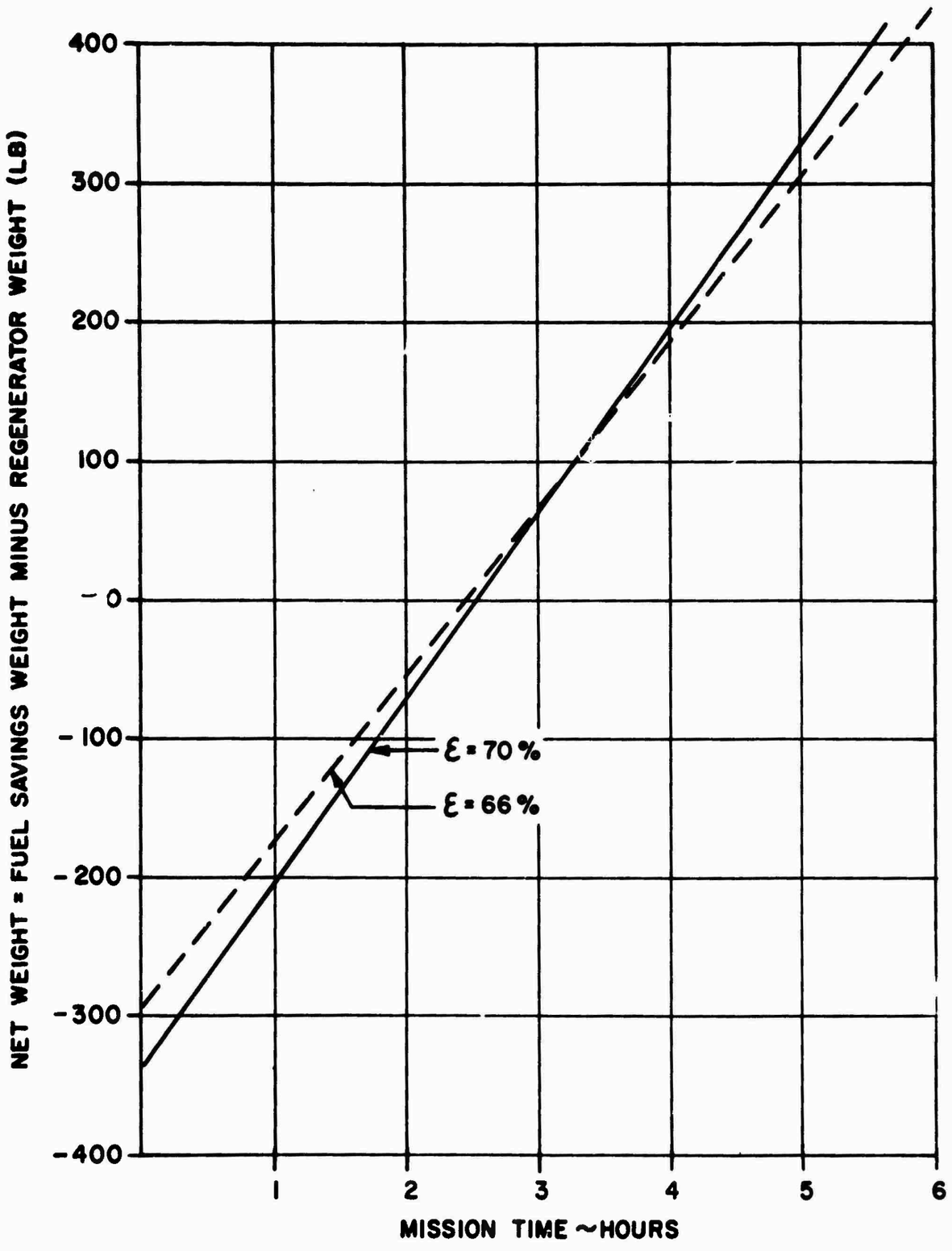

Figure 62. Net Weight Saving Regenerator System Vs. Mission Time.

Analysis of data supplied by AiResearch indicated that a spacing between tube center lines of 1.25D circumferentially and 1 D radially (spacing condition SBT 5) as well as a core pressure loss split of 45 percent air side/55 percent gas side would tend to yield a minimum package size.

Typical "carpet" plots of AiResearch IBM data for an effectiveness value of 0.66, spacing between tube configuration 5, and a 45 percent air/55 percent gas pressure drop split are given in Figures 63 and 64. An example of the use of these plots is given as follows; note that in these carpet plots, all divisions of parameters are made on the abscissa projection:

1) Enter Figure 63 at Station (1) and determine the coordinates of the 18-inch diameter and $\Delta P/P = 4$ percent intersections. Note that because of the necessity to allow a 1-inch radial gap between the group of outer and inner tubes in a U-tube bundle configuration, an actual dimension of 17-inch inside diameter is equivalent to a carpet plot inside diameter of 18 inches. The basic tube diameter (D_t) of 0.25 inch is established.

2) The Station (2) location determining the outside core dimension of 28 inches is now established by transposition of the 0.25-inch-diameter tube and 4 percent $\Delta P/P$ coordinates to the outside diameter carpet plot. For the reason given in 1), a core outside diameter of 27 inches on the carpet plot is equivalent to an actual outside diameter of 28 inches.

3) In a similar fashion, Station (3), (4), and (5) locations are established from Figures 63 and 64 and yield the effective core length, core weight, and tube number, respectively. Note that this length and weight does not include tube bend considerations.

Final parameters describing the tentative regenerator design were thus determined to be as shown in Table 15.

Using the parameters given in the table, the performance of the regenerator was evaluated independently by Lycoming. Both effectiveness and pressure drops were in agreement with the predictions by AiResearch.

The target weight of the regenerator was estimated by multiplying the effective core weight by 1.45 to allow for core packaging. Thus, a total regenerator weight of 188 pounds was specified. In determining the above weight specification, an allowance for the weight of the U-bends was inadvertently omitted. U-bends would have added 17.5 pounds, bringing the total minimum weight of the regenerator to 205.5 pounds.

TABLE 15
TUBE-TYPE REGENERATOR PARAMETERS

Effectiveness (air side)	0.66
Core total pressure loss	4%
Pressure drop split	45% air side/ 55% gas side
Core inside diameter	17 in.
Core outside diameter	28 in.
Tube diameter	0.25 in.
Core effective length (not including U-bend)	35 in.
Number of U-tubes	2050
Spacing between tube configuration	SBT 5
Core weight (effective length only)	130 lb

Table 16 presents the operating conditions for different power settings of a Lycoming T53-L-9 engine.

The above parameters were incorporated in Lycoming Experimental Component Specification XCS3R.1.1 (Appendix II), to which the AiResearch tube-type regenerator was manufactured.

A prediction of the variation in specific fuel consumption as a function of horsepowers for the U-tube regenerative engine is given in Figure 65. A maximum allowable turbine inlet temperature of 1720° F is assumed. Operation with and without the regenerator bypass above the design point is included. Regenerator design-point conditions are as given in Tables 15 and 16.

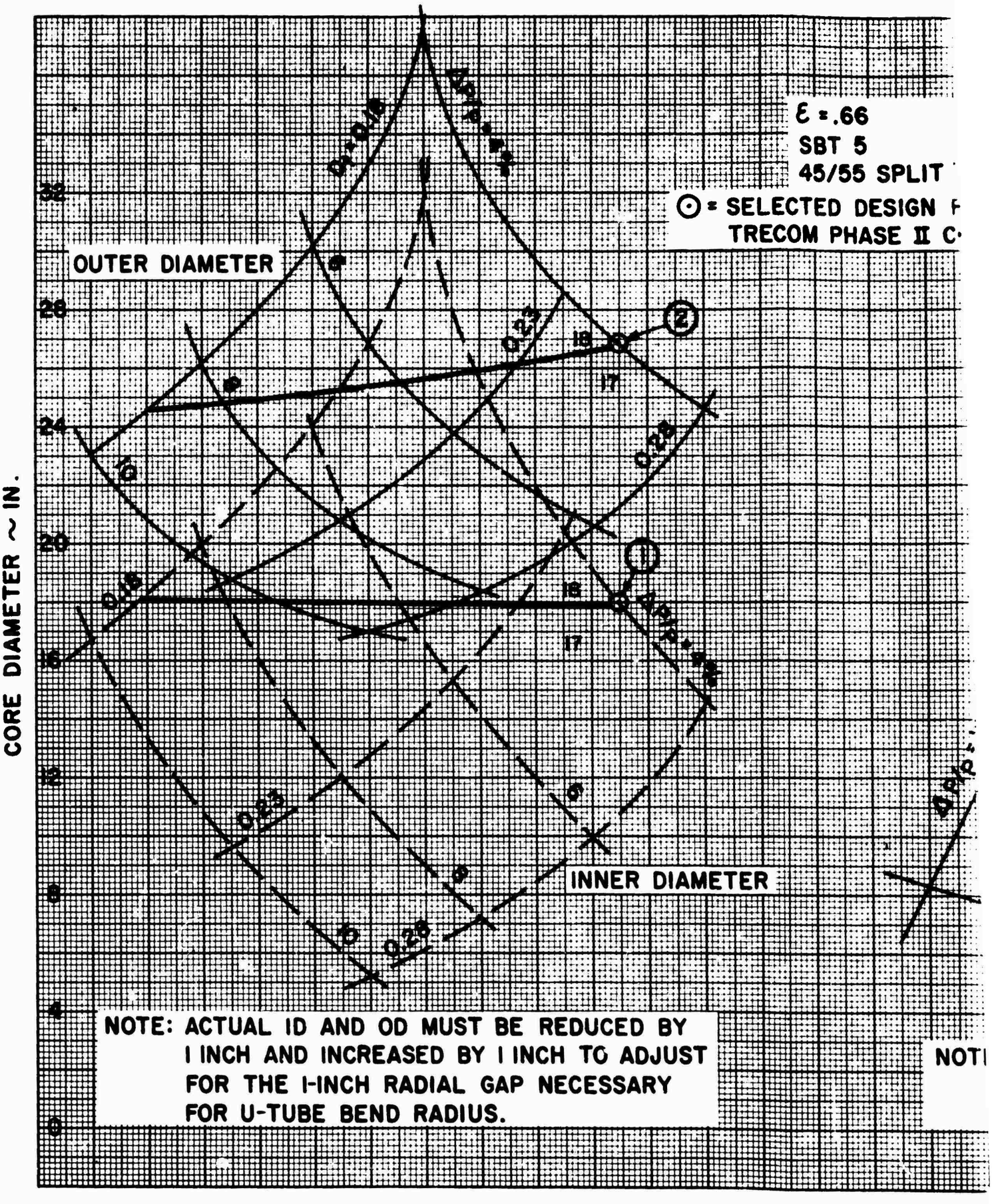

A

Figure 63. Regenerator IBM Data Carpet Plot; Cor

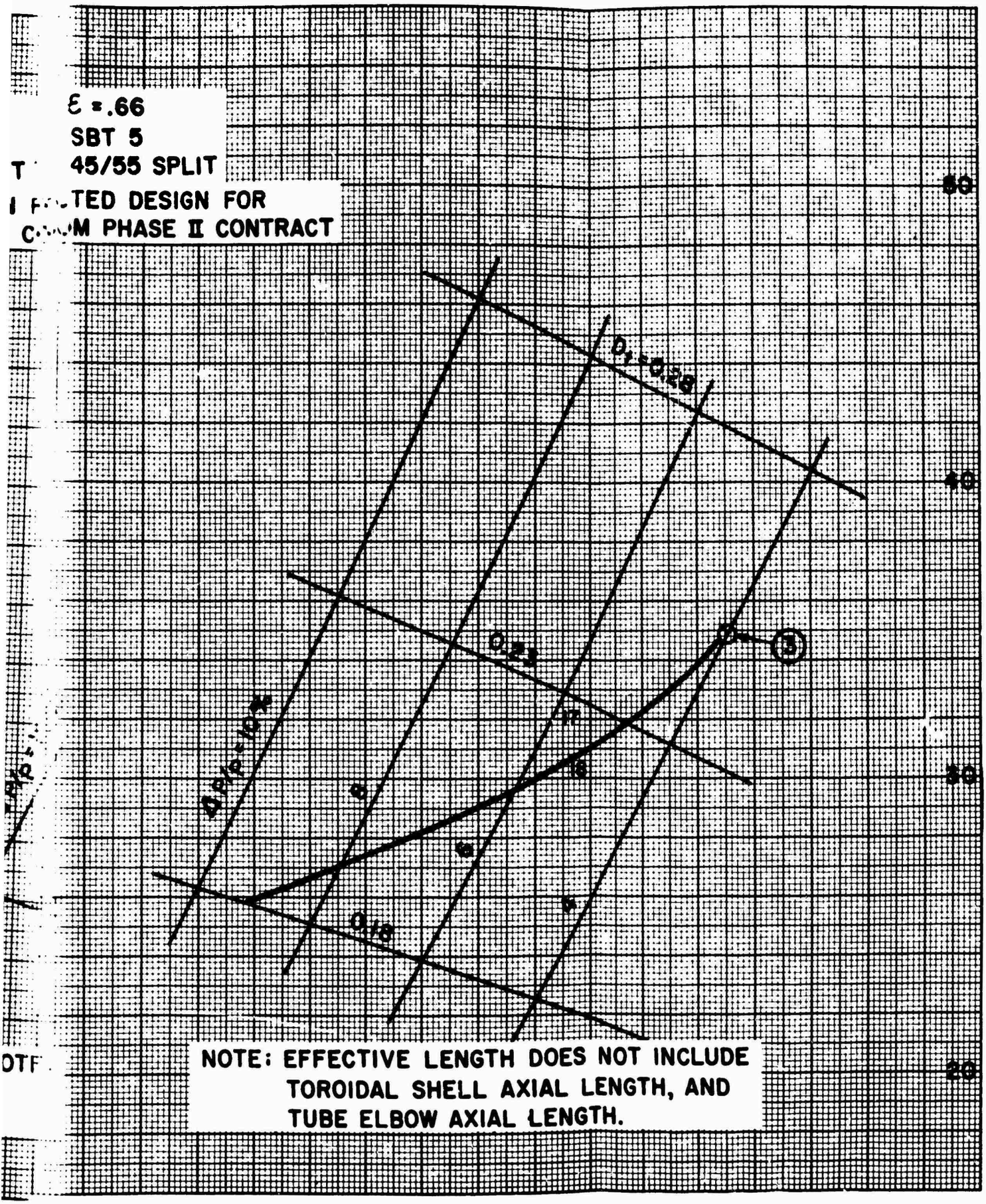

Carpet Plot; Core Diameter and Effective Length.

B

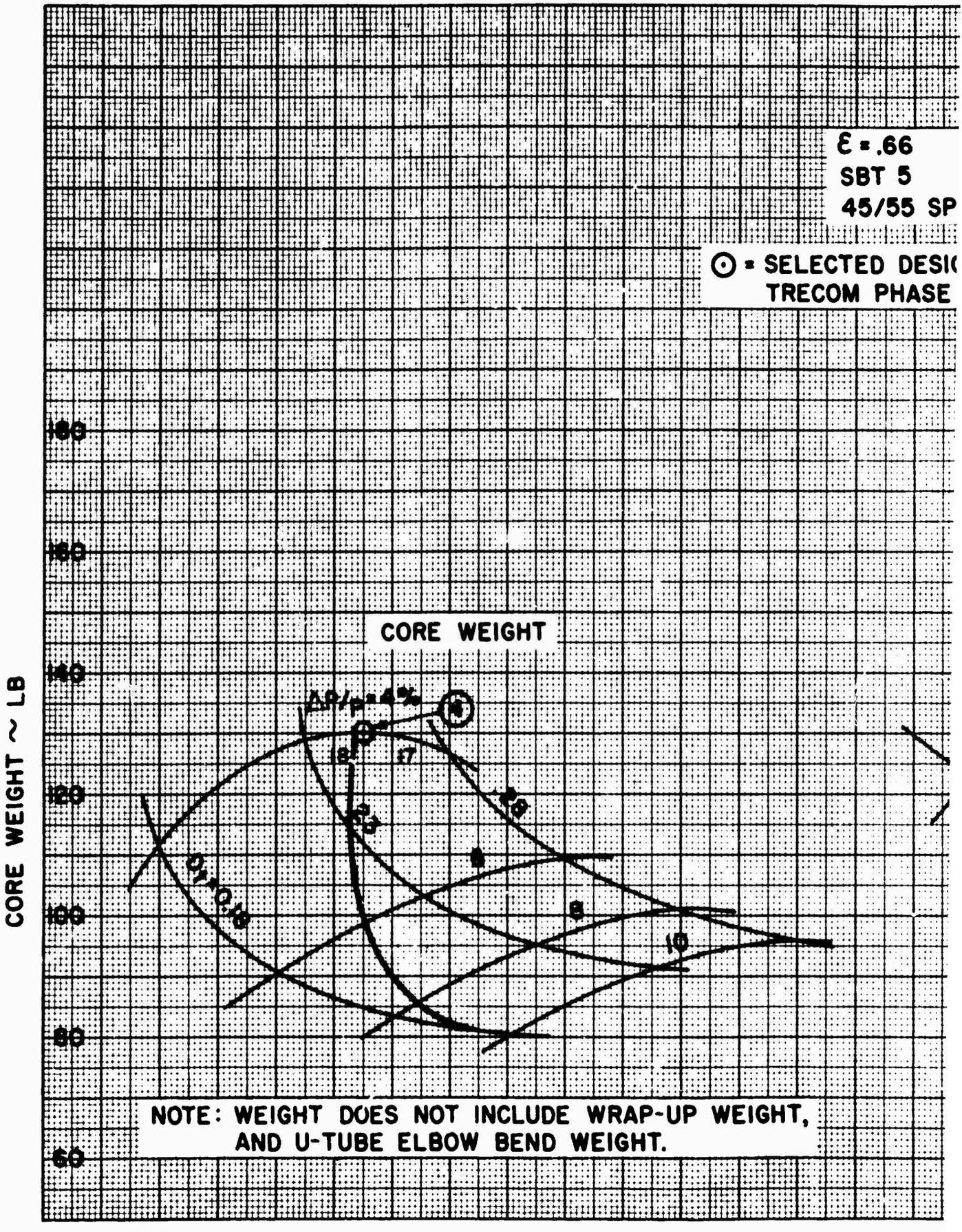

Figure 64. Regenerator IBM Data Carpet

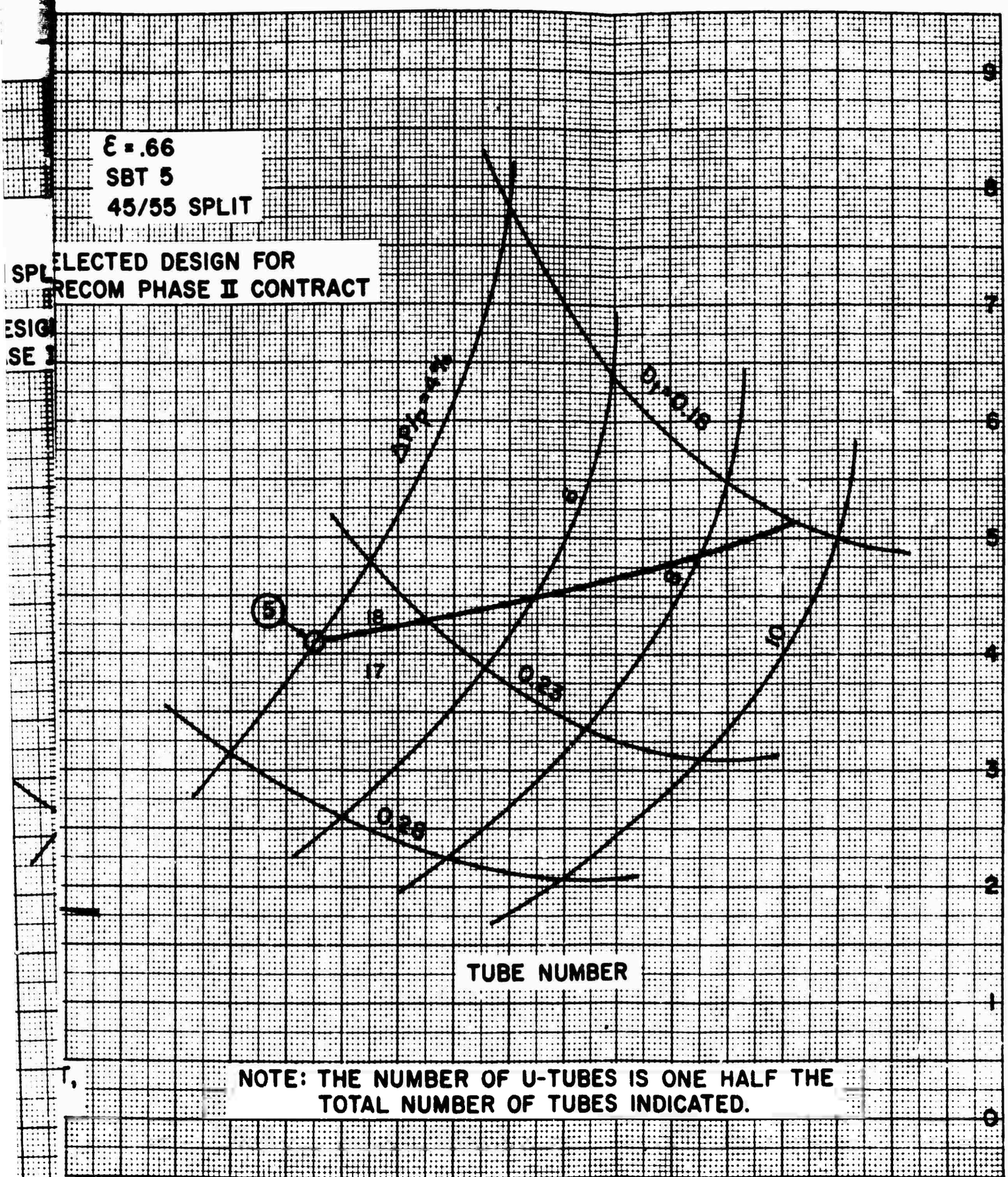

M Data Carpet Plot; Core Weight and Tube Number.

B

TABLE 16
REGENERATOR DESIGN POINT CONDITIONS FOR
VARIOUS T53-L-9 ENGINE OPERATING CONDITIONS

	1 Flight Idle 110 HP		2 75% 675 HP		3 Normal Rated 900 HP		4 Takeoff 1100 HP	
	Air	Gas	Air	Gas	Air	Gas	Air	Gas
Inlet Total Pressure, Atmos.	2.60	-	5.07	-	5.73	-	6.27	-
Exit Static Pressure, Atmos.	-	1.0	-	1.0	-	1.0	-	1.0
Inlet Total Temperature, ^{o}F	275	730	440	900	480	995	513	1085
Mass Flow Rate, lb/sec	5.44	5.59	9.45	9.71	10.1	10.4	10.73	11.06
Inlet Mach Number (approximate)	0.05	0.10	0.05	0.19	0.05	0.21	0.05	0.24

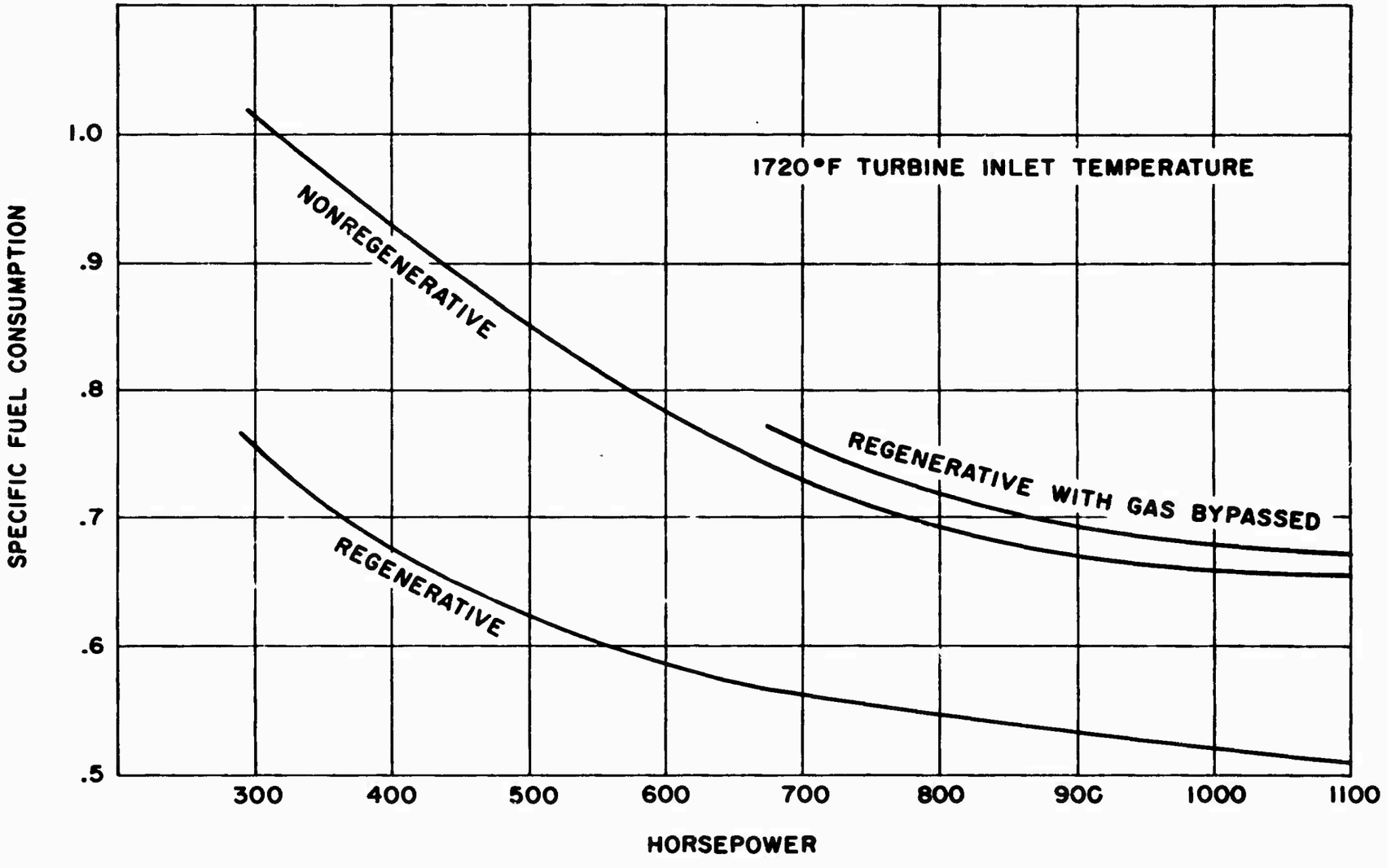

Figure 65. Specific Fuel Consumption for Regenerative and Nonregenerative Engines.

SECTION SEVEN. DESIGN FOR TUBE-TYPE REGENERATION

7.1 REGENERATOR DESIGN

The basic regenerator (Figure 66) consists of a bunder of U-tubes arranged in an annular pattern. It is classified as a two-pass cross-counterflow type; the compressed air makes two passes through the tubes, and the turbine exhaust gas makes one pass outside of and perpendicular to the tubes. This annular core design is well adapted to the engine application in its inherent flexibility, in the way it lends itself to the inclusion of an exhaust gas bypass valve, and in the ability of the tubes to adjust to thermal expansion without restraint.

7.1.1 Core

The regenerator core (Figure 67) consists of:

1) A circular steel header plate 0.060 inch thick, with 3840 tube holes drilled throughout its toroidal profile.

2) Four baffle plates fabricated from 0.032-inch steel plate.

3) Two support plates 0.063 inch thick.

4) U-tubes, 1920 in number.

   a) 240 tubes of 0.217-inch OD and 0.004-inch wall thickness, the centerline bend radius ranging from 0.788 inch to 0.895 inch.

   b) 1440 tubes of 0.250-inch OD and 0.004-inch wall thickness, the centerline bend radius ranging from 1.186 inches to 2.327 inches.

   c) 240 tubes of 0.250-inch OD and 0.007-inch wall thickness, the centerline bend radius ranging from 2.426 inches to 2.555 inches.

The core is supported in the shell by the two support plates each having six equally spaced bearing brackets (Figure 68). The bearings are of slotted construction and allow for both axial and radial movement of the core relative to the shell due to differential expansion.

The tube hole pattern (Figure 69) in the header, baffles, and support plates is based on a nominal transverse spacing of 1.5 diameters and a longitudinal spacing of 1.0 diameter. There are one and one half rows on the air outlet side corresponding to each row on the air inlet side. This spacing is a slight departure from the specified SBT5 selection.

7.1.2 Outer Shell

The outer shell (Figure 70) is fabricated from 0.025-inch sheet stainless steel, reinforced by two rings fabricated from welded elements forming a hat section and seam welded to the shell. The purpose of the rings is to stiffen the shell in the support areas. These areas are further reinforced by a 0.090-inch-thick doubler, which is spot-welded to the shell.

The shell has a 0.120-inch-thick flange welded at either end. The transition duct, which connects the core to the shell, consists of a 0.032-inch-thick body and two flanges. The shell side flange is 0.120 inch thick, and the turbine side flange is 0.160 inch thick.

A divider assembly used to separate the "cold" regenerator air from the "hot" regenerator air is formed from 0.032-inch sheet and attached to the header at six places. A 1/64-inch-thick gasket and heat-treated spring washers are provided to minimize leakage.

7.1.3 Weight and Dimensions

The weight of the completely assembled regenerator is 224 pounds. This difference of 18.5 pounds from the analytically determined weight of 205.5 pounds resulted from a) an increase in outside tube wall thickness from 0.004 to 0.007 inch for handling protection (12.5 pounds), b) an increase in aft flange size to support exhaust instrumentation (2.5 pounds), and c) an addition of hat stiffener sections to the outer shell (3.5 pounds).

The overall length of the regenerator from the header flanges to the shell exhaust side flange is 39.88 inches. The maximum diameter of the shell flange on the header side is 33.53 inches.

7.1.4 Final Design-Point Estimated Performance

Table 17 gives the estimated performance at the design point (75 percent normal rated power) on the basis of the following assumptions:

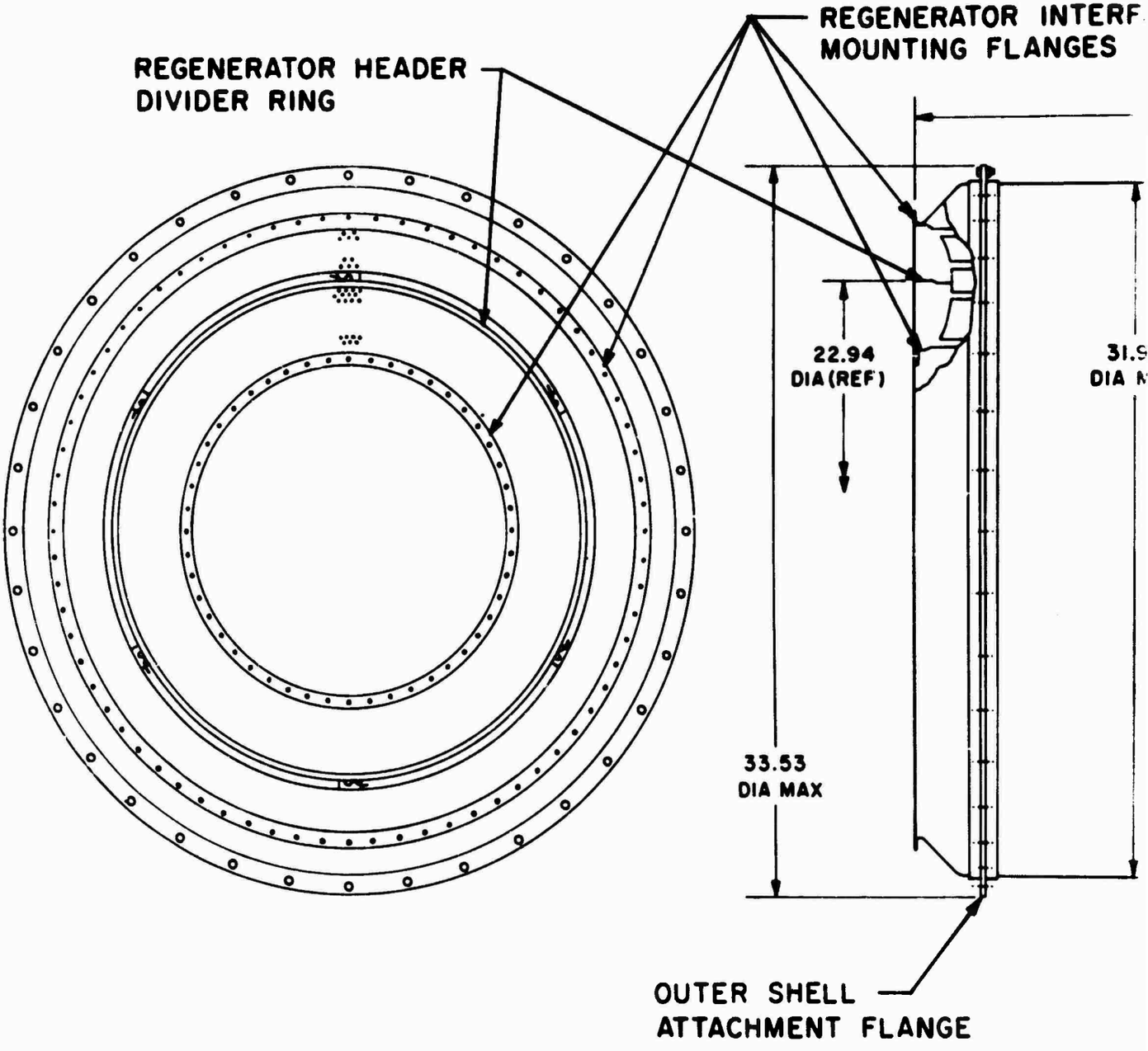
REGENERATOR INTERF
MOUNTING FLANGES
REGENERATOR HEADER
DIVIDER RING
22.94
DIA (REF)
31.9
DIA M
33.53
DIA MAX
OUTER SHELL
ATTACHMENT FLANGE

Figure 6

A

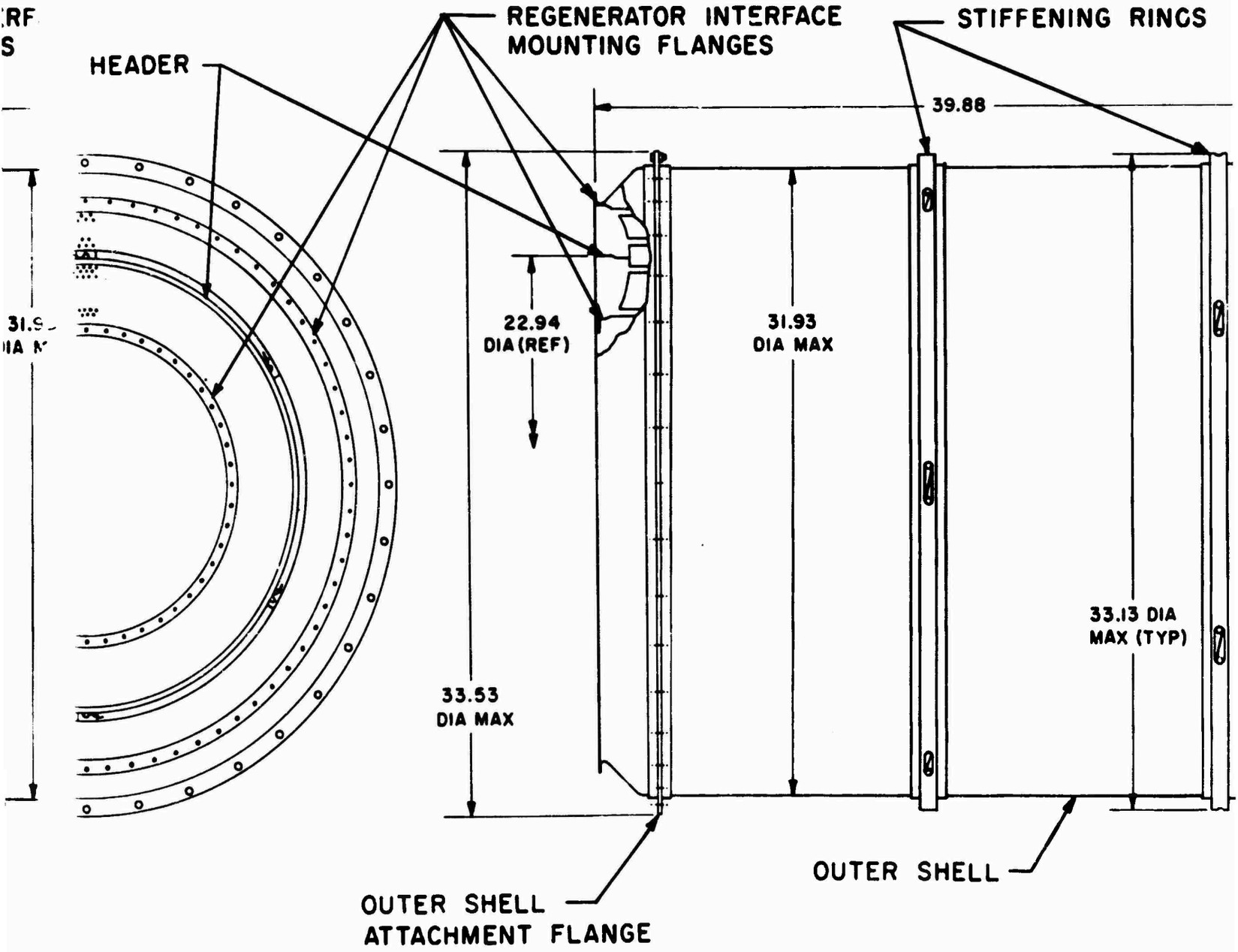

Figure 66. Regenerator Assembly.

B

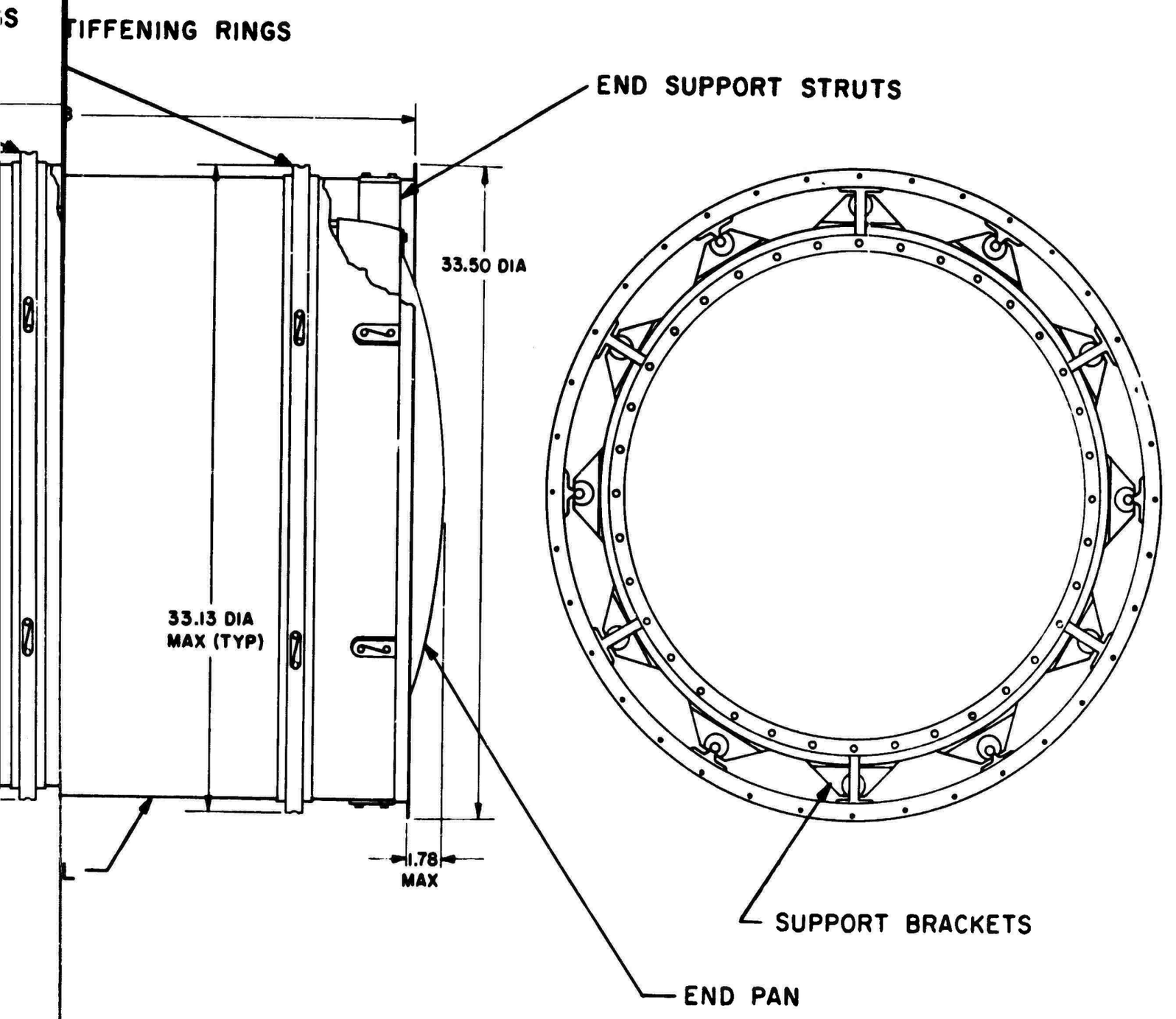
TIFFENING RINGS
END SUPPORT STRUTS
33.50 DIA
33.13 DIA
MAX (TYP)
1.78
MAX
SUPPORT BRACKETS
END PAN

r Assembly.

C

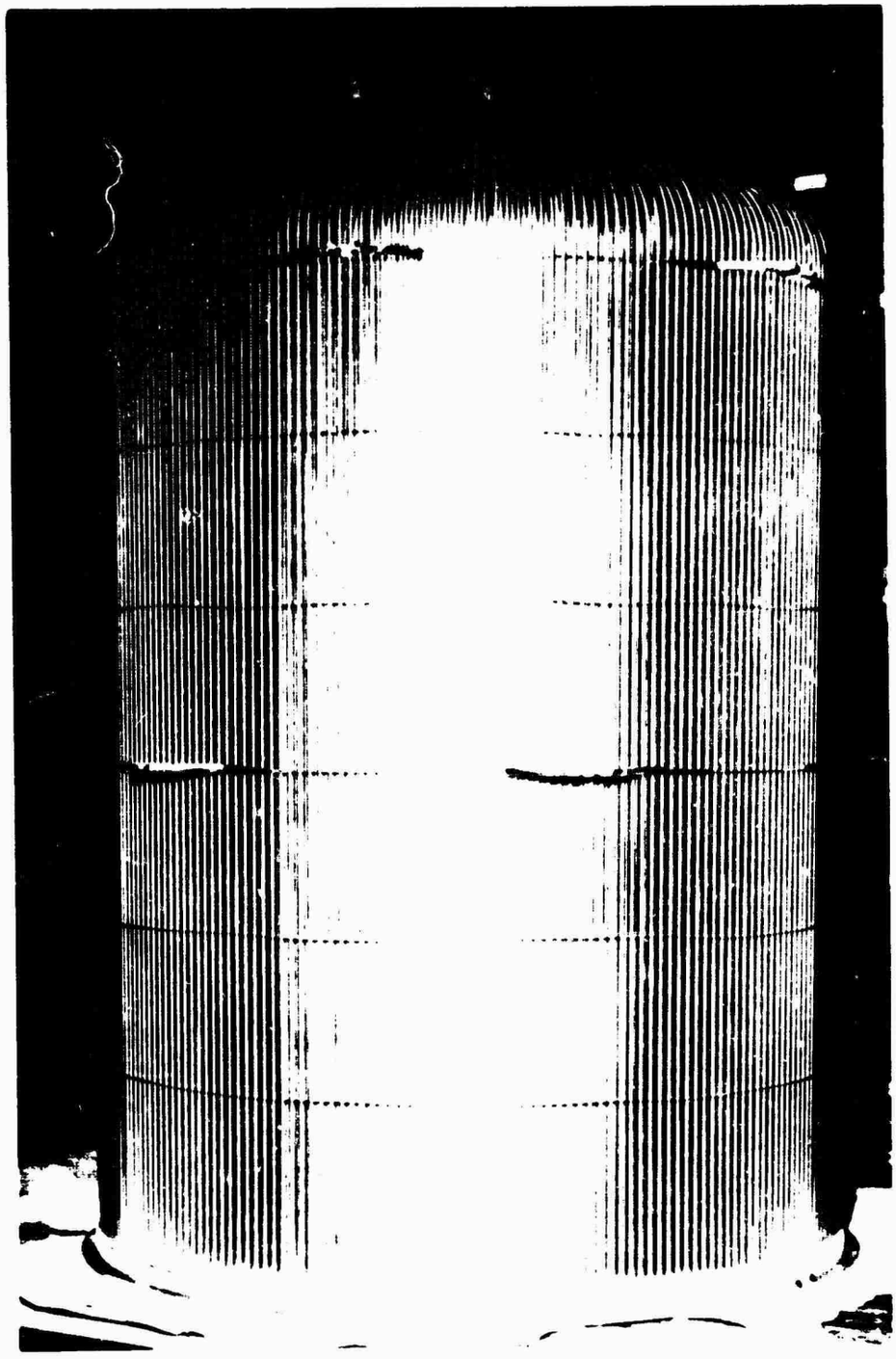

Figure 67. Regenerator Core.

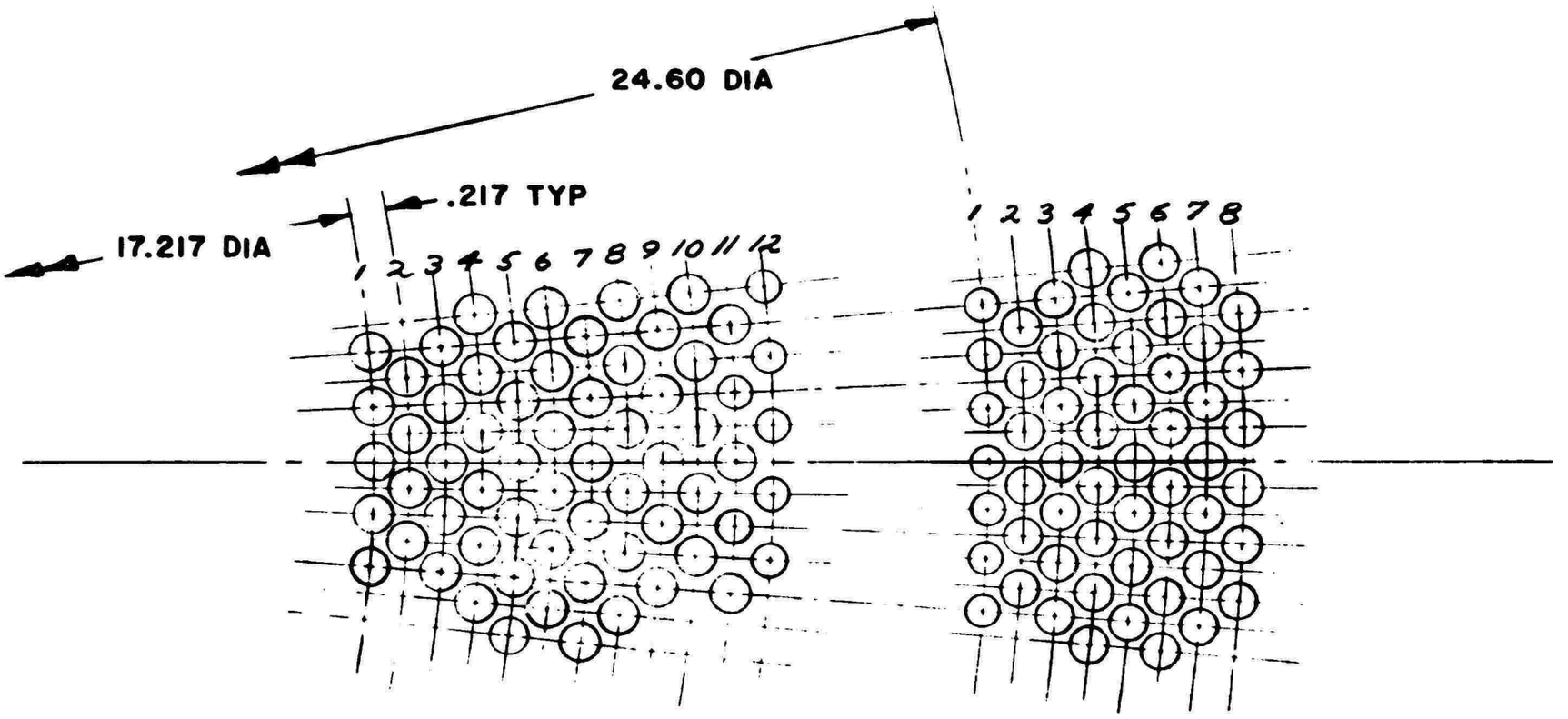

1st BAND - HOT AIR OUTLET PATTERN
12 ROWS OF 160 HOLES
EQUALLY SPACED AS SHOWN
1st THRU 10th ROWS - 160 HOLES .250 DIA
11th ROW - 160 HOLES ALTERNATELY
.217 DIA AND .250 DIA
12th ROW - 160 HOLES .217 DIA

2nd BAND - COLD AIR INLET PATTERN
8 ROWS OF 240 HOLES
EQUALLY SPACED AS SHOWN
1st ROW - 240 HOLES .217 DIA
2nd THRU 8th ROWS - 240 HOLES .250 DIA

Figure 69. Regenerator U-Tube Hole Pattern.

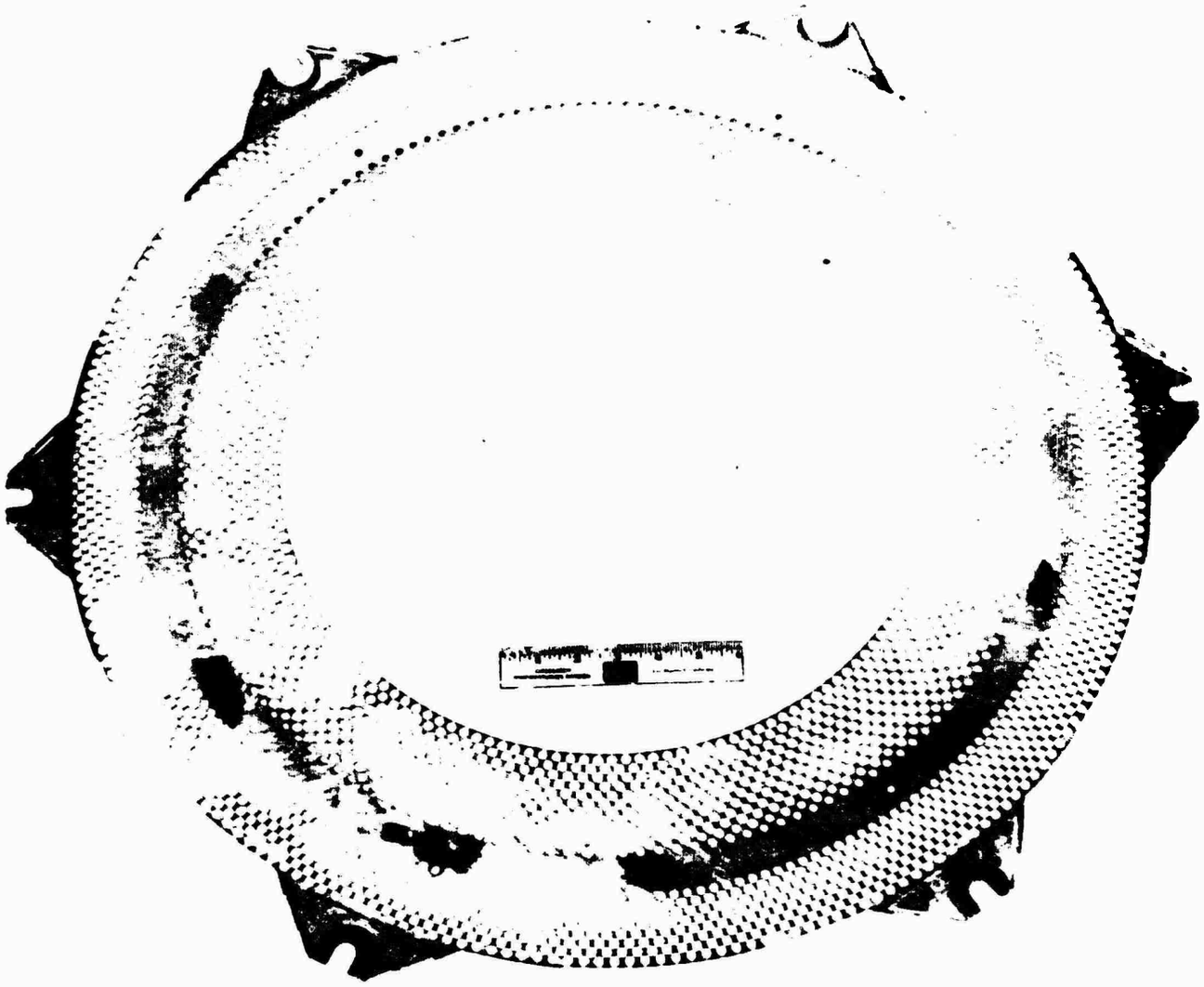

Figure 68. Regenerator Support Plate Assembly.

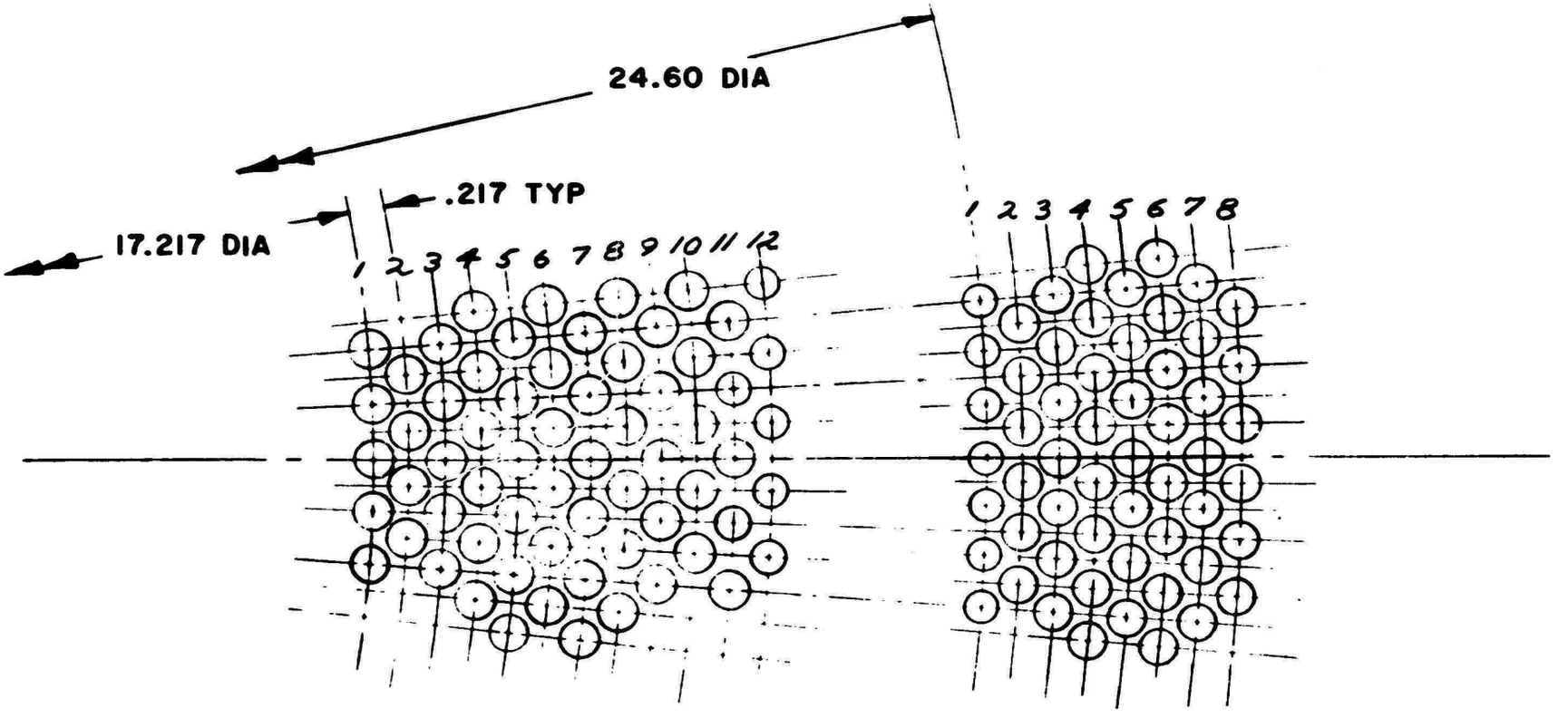

1st BAND - HOT AIR OUTLET PATTERN
12 ROWS OF 160 HOLES
EQUALLY SPACED AS SHOWN
1st THRU 10th ROWS - 160 HOLES .250 DIA
11th ROW - 160 HOLES ALTERNATELY
.217 DIA AND .250 DIA
12th ROW - 160 HOLES .217 DIA

2nd BAND - COLD AIR INLET PATTERN
8 ROWS OF 240 HOLES
EQUALLY SPACED AS SHOWN
1st ROW - 240 HOLES .217 DIA
2nd THRU 8th ROWS - 240 HOLES .250 DIA

Figure 69. Regenerator U-Tube Hole Pattern.

Figure 70. Regenerator Outer Shell Assembly.

TABLE 17
DESIGN-POINT ESTIMATED PERFORMANCE
LYCOMING T-53 REGENERATOR 180530

Air Side	Inlet	Average	Outlet
Flow rate, lb/sec	9.45	9.45	9.45
Temperature, ^{o}R	900	1051.8	1203.6
Pressure, psia	74.529	73.758	72.987
Core pressure drop*, psi		1.542	
Core pressure drop, %		2.07	
Total pressure drop, %		2.07	
Reynolds number		14524	
Coefficient of heat transfer, Btu/ft^2 sec ^{o}F		0.014798	
Friction factor		0.007143	
Mass velocity, lb/ft^2 sec	15.409	15.409	15.409
Velocity, ft/sec		81.6	
Gas Side			
Flow rate, lb/sec	9.71	9.71	9.71
Pressure, psia	15.834	15.338	14.841
Core pressure drop, psi		0.40	
Core pressure drop, %		2.52	
Total pressure drop, %		6.25	
Reynolds number		1073	
Coefficient of heat transfer, Btu/ft^2 sec ^{o}F		.0138	
Friction factor		.06727	
Mass velocity, lb/ft^2 sec		3.244	
Velocity, ft/sec		96	

NOTE:

(UA) Required = 4.76 Btu/sec ^{o}F
(UA) Available = 5.06 Btu/sec ^{o}F
(UA) Available Margin = 5.92 %

* Includes 20% increase because of U-tube bends

1) The exhaust gas flow is evenly distributed in the manifolds and core of the heat exchanger.

2) No pressure drop margin is allowed for the airflow or the exhaust gas flow.

3) The friction factor and the Colburn modulus for rectangular tube spacings also apply to the actual tube arrangement in the annular envelope.

4) The amount of heat transfer surface area of the tubes at the bends beyond the support plate at the aft side of the regenerator is neglected.

5) The lost coefficient $K = \Delta P_t/q$ for 90-degree bends and sudden expansions is 1.0.

6) The pressure drop given for the gas side takes into account the core and the ducting. The pressure drop given for the air side is that of the core only.

7.1.5 Stress Considerations

The stress design required that the regenerator be capable of withstanding vibrations according to Lycoming Specification No. XCS3R.1.1 (Appendix II, Figure 118). This specification was later considered to be too severe because it represented the maximum permissible vibration for a T53 engine normally mounted entirely from the inlet housing. Since a three-point regenerator support installation was to be used in this application, the original specification requirement was considered to be no longer applicable to the program. Lycoming's structural analysis of interface hardware based upon a 5g nonvibrating loading was considered satisfactory design criterion for the test regenerator, which is to be supported in the plane of the foreward header flanges. To withstand 10g flight loading will require a slightly increased wall thickness for the tubes, shell, flanges, and casing of the interface hardware. AiResearch states that if 10g loading requirements have to be met, there is flexibility in design for the modification of the shell structure and of the support plates. The regenerator shell structure should include at least six longerons 3/8 inch deep and 1/4 inch wide. The regenerator support plate should be integral with the support brackets, and should have a circumferential edge turned up in the direction of the gas flow and a thickening of the support bracket area, which should gradually taper from the local thickness of 0.120 inch to the support plate thickness of 0.063 inch.

7.1.6 Regenerator Pressure and Leakage Test

A hydrostatic pressure test, core air leakage test, divider seal air leakage test, and shell pressure test were performed on the regenerator.

The hydrostatic pressure test was made by filling the core and toroidal shell with water, then applying a 93-psig pressure for 5 minutes and observing the leakage. This was only a proof test and no provisions were made to collect or weigh the minute amount of water which dripped from the unit.

The core leakage test was made by determining air leakage as a function of pressure. Core leakage was determined by measurement of the amount of air necessary to maintain a given core pressure. Results obtained both at AiResearch prior to shipment of the core and at Lycoming upon receipt of the regenerator indicated core leakage rates less than the specification value of 0.10 percent of nominal flow at the 90-psig pressure level (Figure 71).

The divider seal leakage test performed at AiResearch was to determine the header divider ring air leakage across the assembly (P/N 179899-1) and the core toroidal shell. Results indicated that the divider, when assembled with an asbestos gasket and sealed with an RTV high temperature silicone compound, minimized the leakage rate to a value of 0.2 pounds of air per minute at a pressure differential of 3.0 inches mercury (Figure 72).

The shell of the regenerator assembly was pressurized to approximately 4 psig. No leakage was observed at the tube-to-header joints. Two tubes out of the total of 1920 U-tubes were found to have minor "feather" leaks.

7.1.7 Handling and Mounting

The regenerator incorporates two header flanges to allow mounting to the engine. In order to facilitate handling and moving of the regenerator, a handling plate is provided for bolting to the unit's outer header flange. This plate has three eye-bolts for cable attachment.

While being mounted to the engine, the regenerator should be supported at three equally spaced points on both the forward and aft flanges. Under no circumstances should it be supported at the shell body.

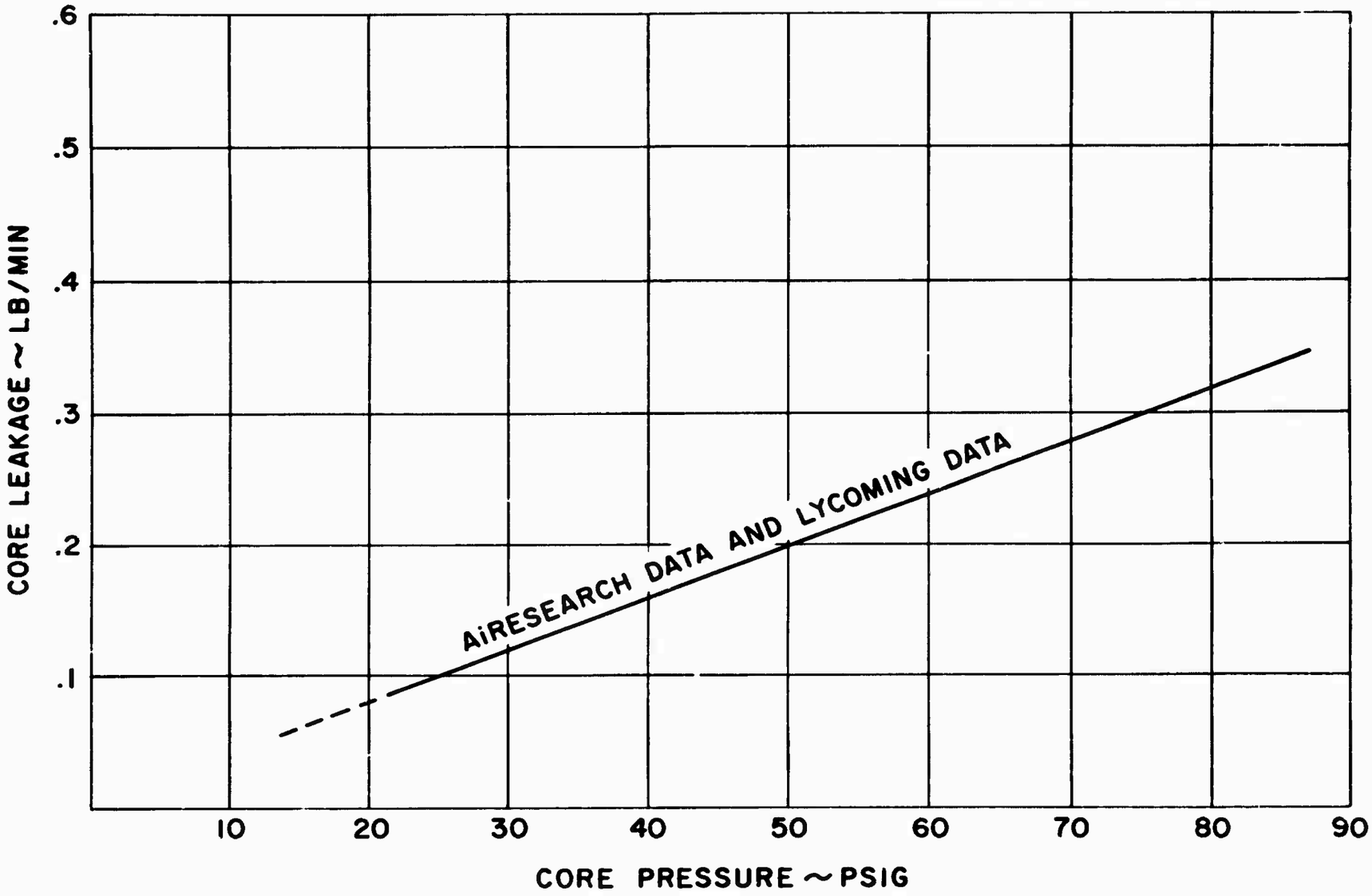

Figure 71. Regenerator Core Leakage Vs. Core Pressure.

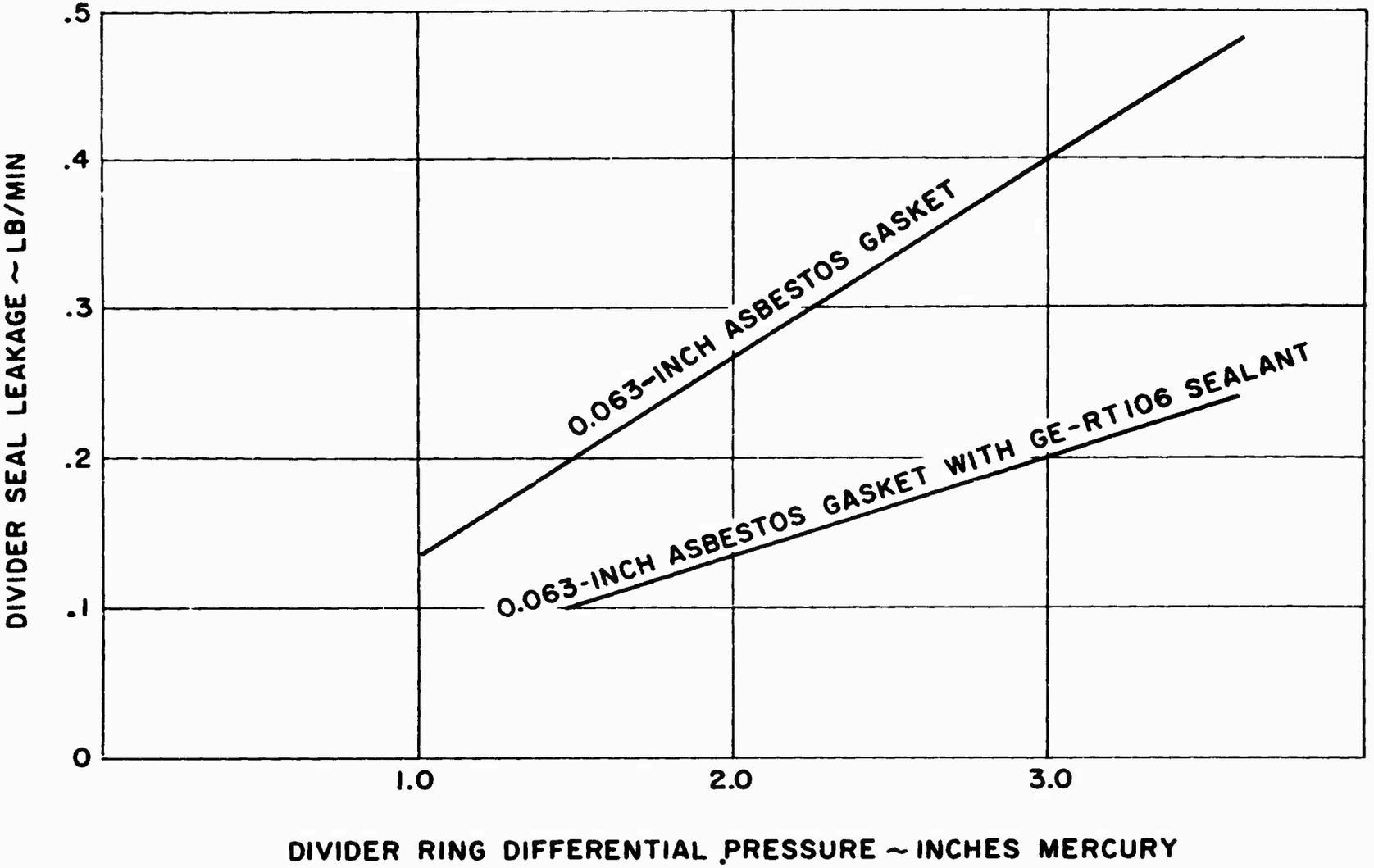

Figure 72. Divider Seal Leakage Vs. Differential Pressure.

7.1.8 Maintenance

Cleaning

The regenerator is designed to be maintenance free. However, should excessive fouling occur, the unit may be cleaned ultrasonically or by chemical solution cleaning methods. An example of the latter method makes use of a steel blackening bath solution, which consists of caustic soda and oxidizing agents such as sodium nitrate, sodium dichromate. etc., at an operating temperature of 300° to 400° F. The core is removed from the engine, immersed in the solvent, cleaned with water, and dried.

Plugging

Leaking tubes can be detected by pressurizing the shell to between 3 and 4 psig and applying a soap solution with a brush to the header surface. Bubbles will appear over any tubes that leak. The steel plug shown in Figure 73 should be inserted in the leaking tube and soldered in position with a high-temperature silver solder in accordance with AMS 4772. Care should be taken not to overheat the braze joints of the neighboring tubes.

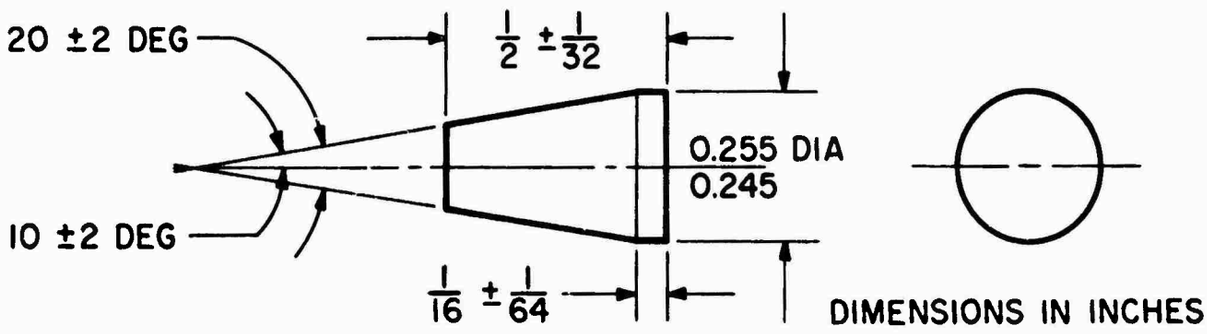

Figure 73. Steel Plug.

7.2 INTERFACE DESIGN

The engine-regenerator installation is shown schematically in Figure 74. Design of the engine-regenerator interface was oriented toward minimal changes to the existing T53-L-3/11 engine in order to minimize costs and the need for specialized engine parts.

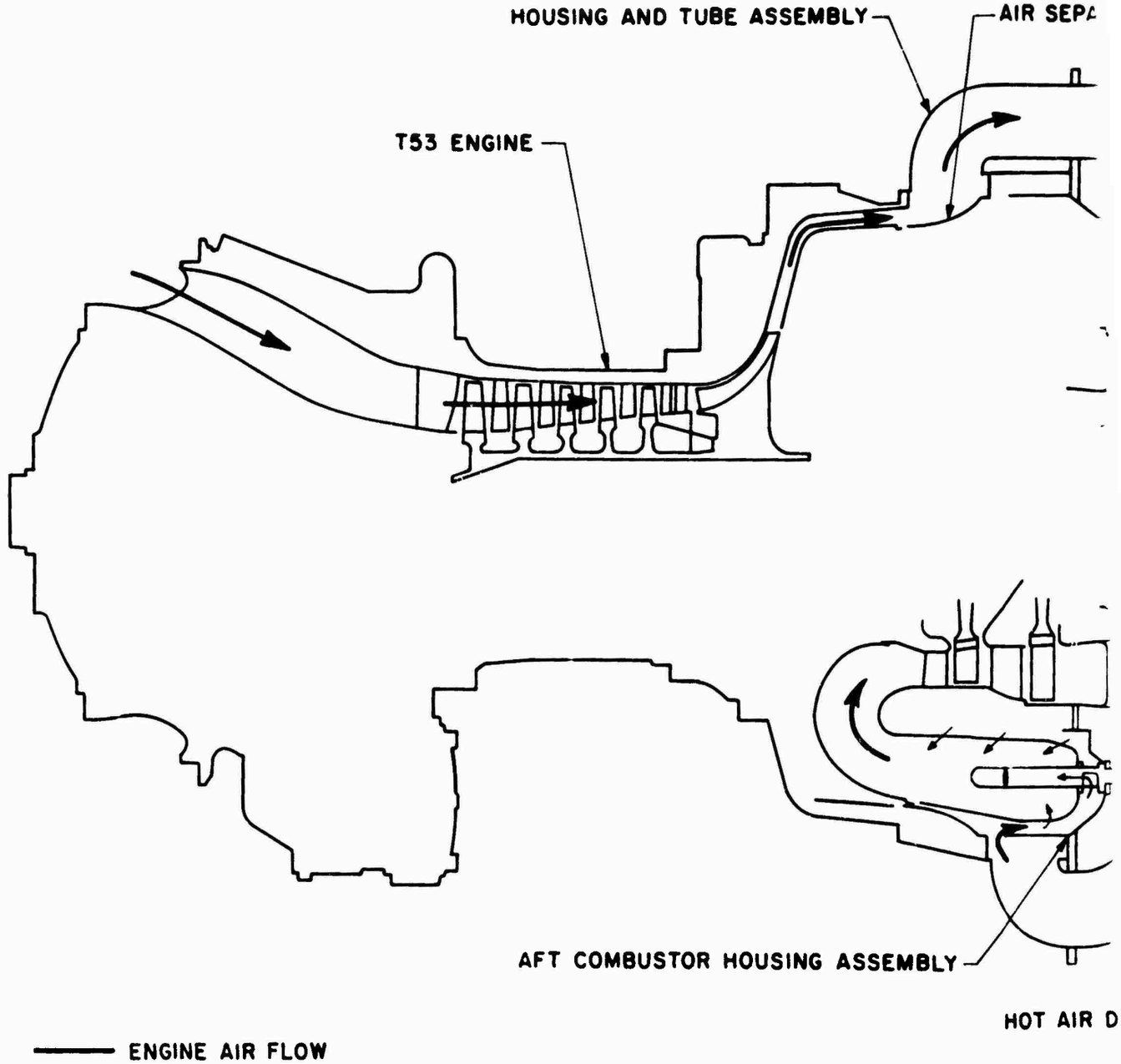
HOUSING AND TUBE ASSEMBLY
AIR SEPA
T53 ENGINE
AFT COMBUSTOR HOUSING ASSEMBLY
HOT AIR D.
ENGINE AIR FLOW
EXHAUST GAS FLOW

Figure

A

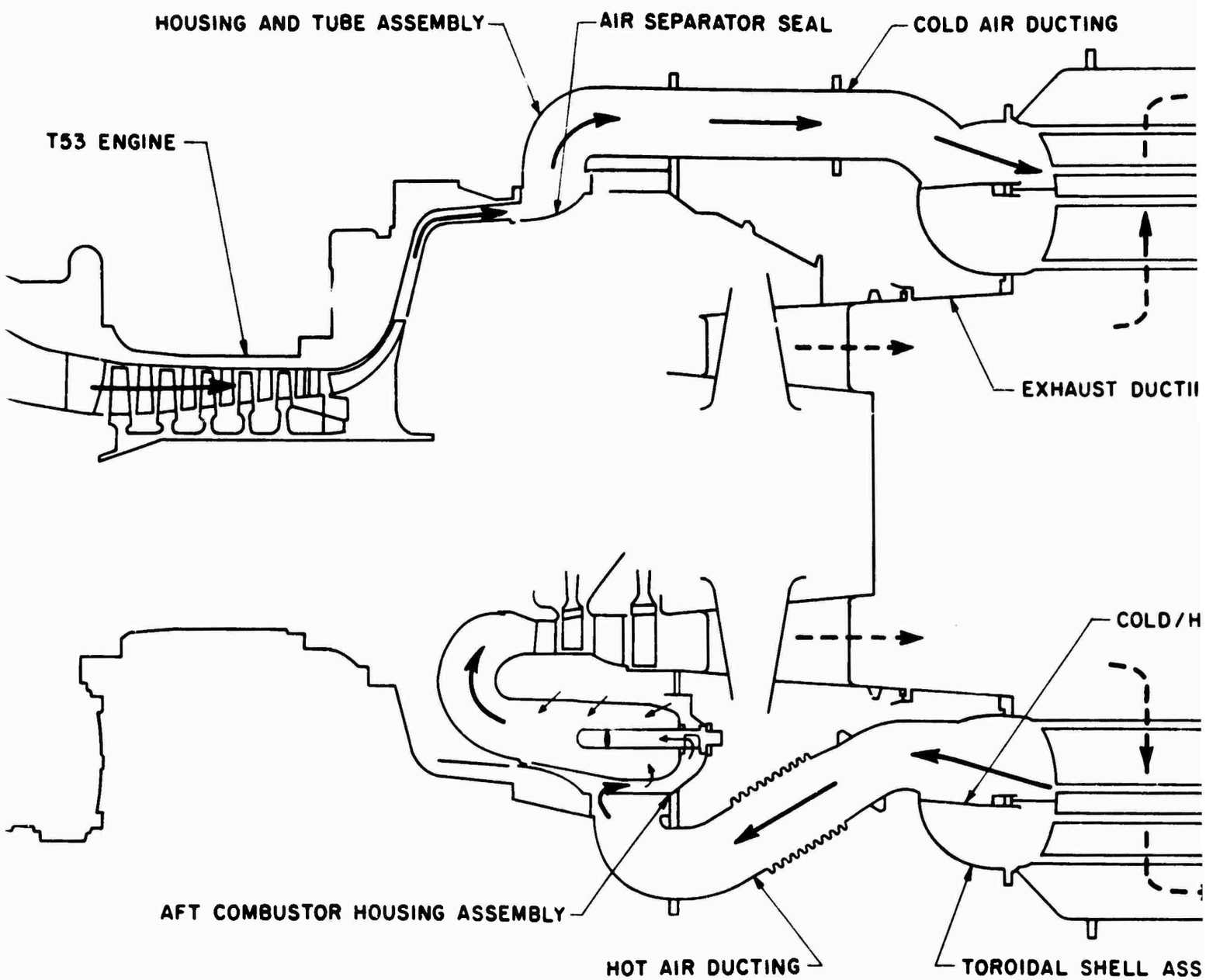

Figure 74. Engine-Regenerator Installation.

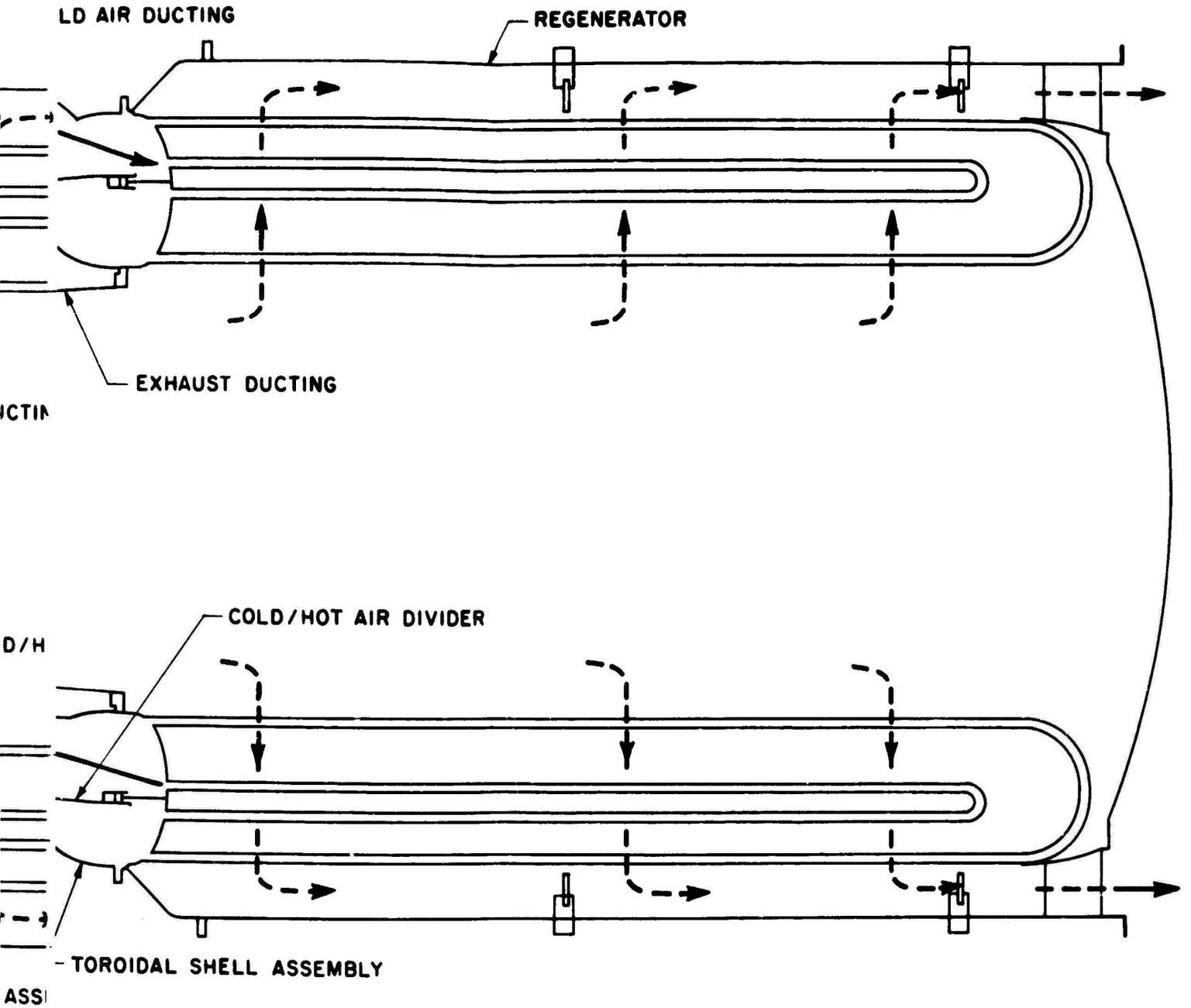

nerator Installation.

on.

C

Several designs were reviewed to determine methods of supporting the regenerator package aft of the engine turbine section. Of the several potential methods for connecting the regenerator to the engine, the use of individual cylindrical tubes was felt to be superior. This method allows access to the engine fuel manifold ignitors and facilitates exhaust duct cooling air circulation. In addition, hydraulic and fuel lines may be readily routed between the tubular connecting ducts.

7.2.1 Combustor Housing

The outer combustor wall was modified to accommodate the housing and tube assembly for the ducting of diffuser air to and from the regenerator.

The ducting is shown schematically in Figure 75. The aft combustor wall was modified slightly to make provision for the addition of two starting fuel nozzles.

7.2.2 Housing and Tube Assembly

The housing and tube assembly (Figures 76 and 77) includes eight cold-air inlet tubes and eight hot-air outlet tubes, which provide approximately 43 square inches of area per tube set. The air separator seal (Figures 74 and 75) of the housing and tube assembly diverts diffuser exit air to the regenerator outer tube rows and directs regenerator outlet air from the inner tubes rows to the combustor. Return air from the regenerator flows into the combustor entrance plenum chamber around a deflector to maintain combustor airflow direction as in the basic T53 engines. This plenum chamber provides even circumferential air distribution to prevent localized hot spots.

Cold-air inlet tubes, mounted in the aft flange of the housing and tube assembly, provide rigid structural members to support the regenerator. The hot-air outlet tubes are similarly mounted in the housing and tube assembly. One of these tubes is fitted with a fuel control temperature sensing probe boss and guide assembly. Since some of these tubes are located at the lowest point on the combustor assembly, provisions have been made at these locations to drain fuel which may accumulate during false starting. Lightening holes in the aft flange of the housing and tube assembly reduce weight and provide a means for routing hose assemblies.

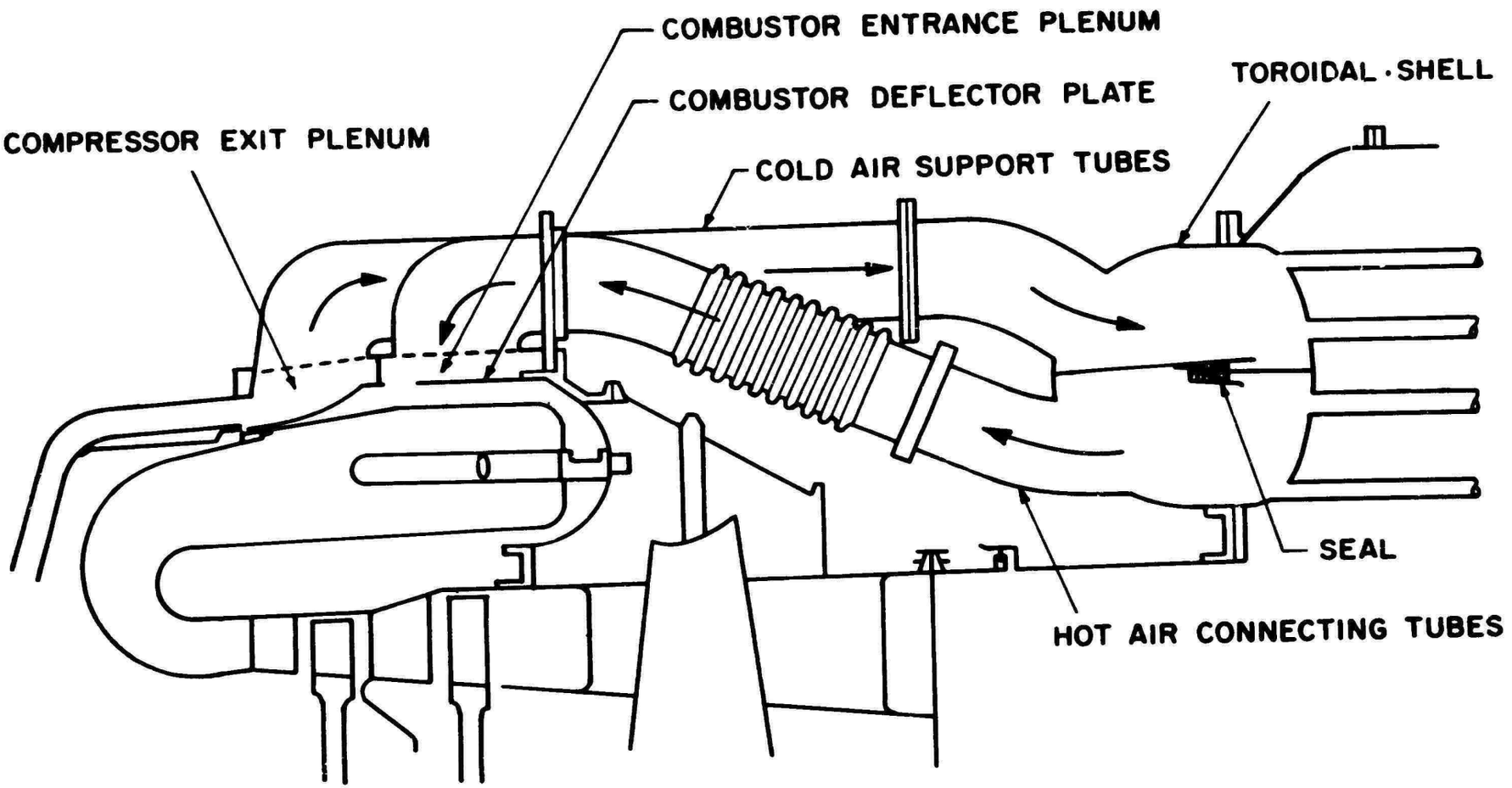

Figure 75. Combustor-Regenerator Ducting.

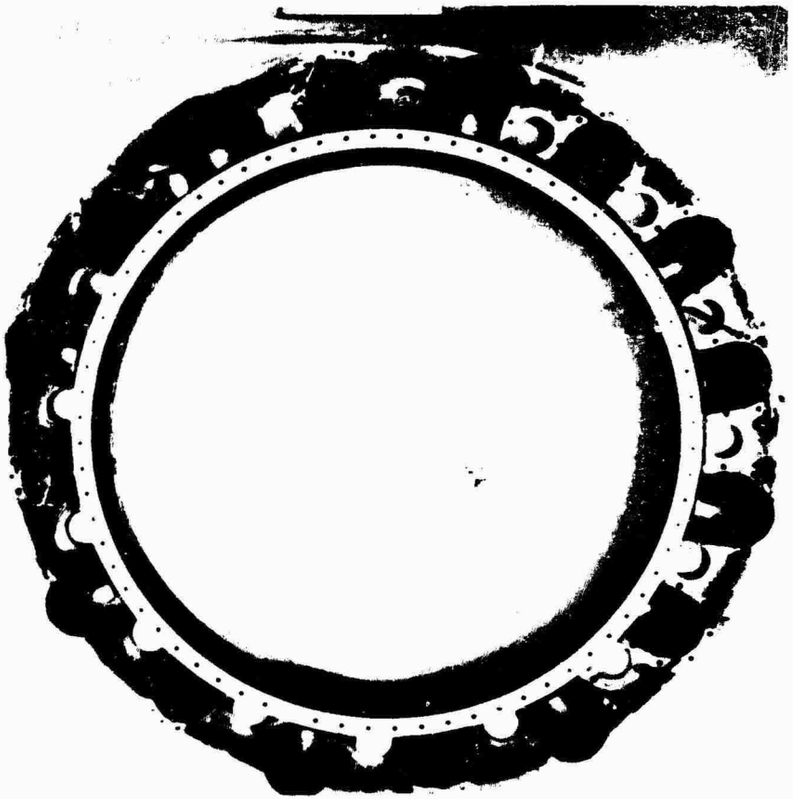

Figure 76. Housing and Tube Assembly; Front View.

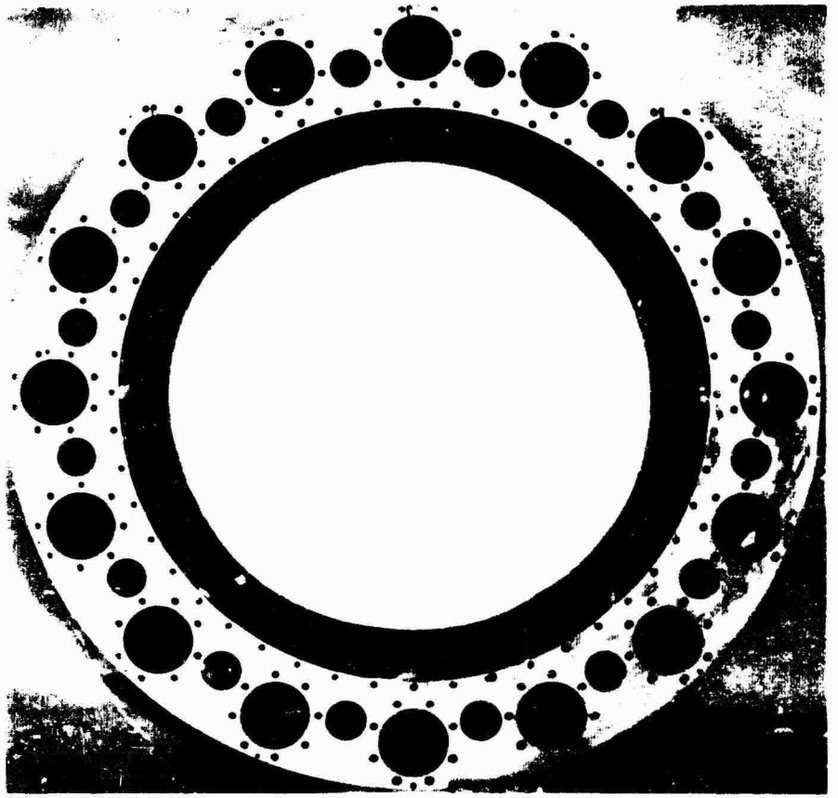

Figure 77. Housing and Tube Assembly; Aft View.

7.2.3 Tube Connecting Members

The cold-air tube connectors and the hot-air tube connectors (Figure 78) are located between the housing and tube assembly and the toroidal shell assembly. The cold-air tube connectors are mounted by bolts on their forward and aft flanges. Quick-disconnect clamps are used on the aft flange of the hot-air tube connectors. Allowance for differential thermal expansion is made by means of a flexible bellows section on the hot-air tube connectors.

7.2.4 Toroidal Shell Assembly

The toroidal shell assembly (Figures 79 and 80) provides the regenerator mounting structure. The shell portion is divided into two annular compartments by means of a seal configuration which separates regenerator inlet and outlet air flows. The seal configuration (Figure 81) consists of an asbestos seal contained by retainers which are spring-loaded to make positive contact with the regenerator header divider ring.

7.2.5 Exhaust Duct Assembly

The exhaust duct assembly (Figure 82) provides a connecting duct from the basic engine exhaust diffuser to the regenerator gas entrance. The forward section of the exhaust duct assembly incorporates a piston-ring-type seal to allow for axial motion (thermal growth between sections) and to compensate for axial and radial manufacturing differential tolerances. The engine exhaust diffuser aft flange is clamped to the seal support and permits the utilization of the existing T53 basic exhaust diffuser hardware. A Marmon-type quick-disconnect clamp provides ease of assembly.

7.2.6 Engine Hose Assemblies

Several engine-level hose assemblies were reworked by increasing their lengths and/or providing different end connectors to compensate for the interface hardware additions. Two additional hose assemblies connect the fuel control and the temperature-sensing element.

7.2.7 Interface Hardware Weight

The weight of the interface hardware was calculated to be 85 pounds, which is the weight difference between the basic T53 engine and the modified engine exclusive of the regenerator. The actual weight is 99 pounds; the additional weight results from added flange material and provisions for instrumentation.

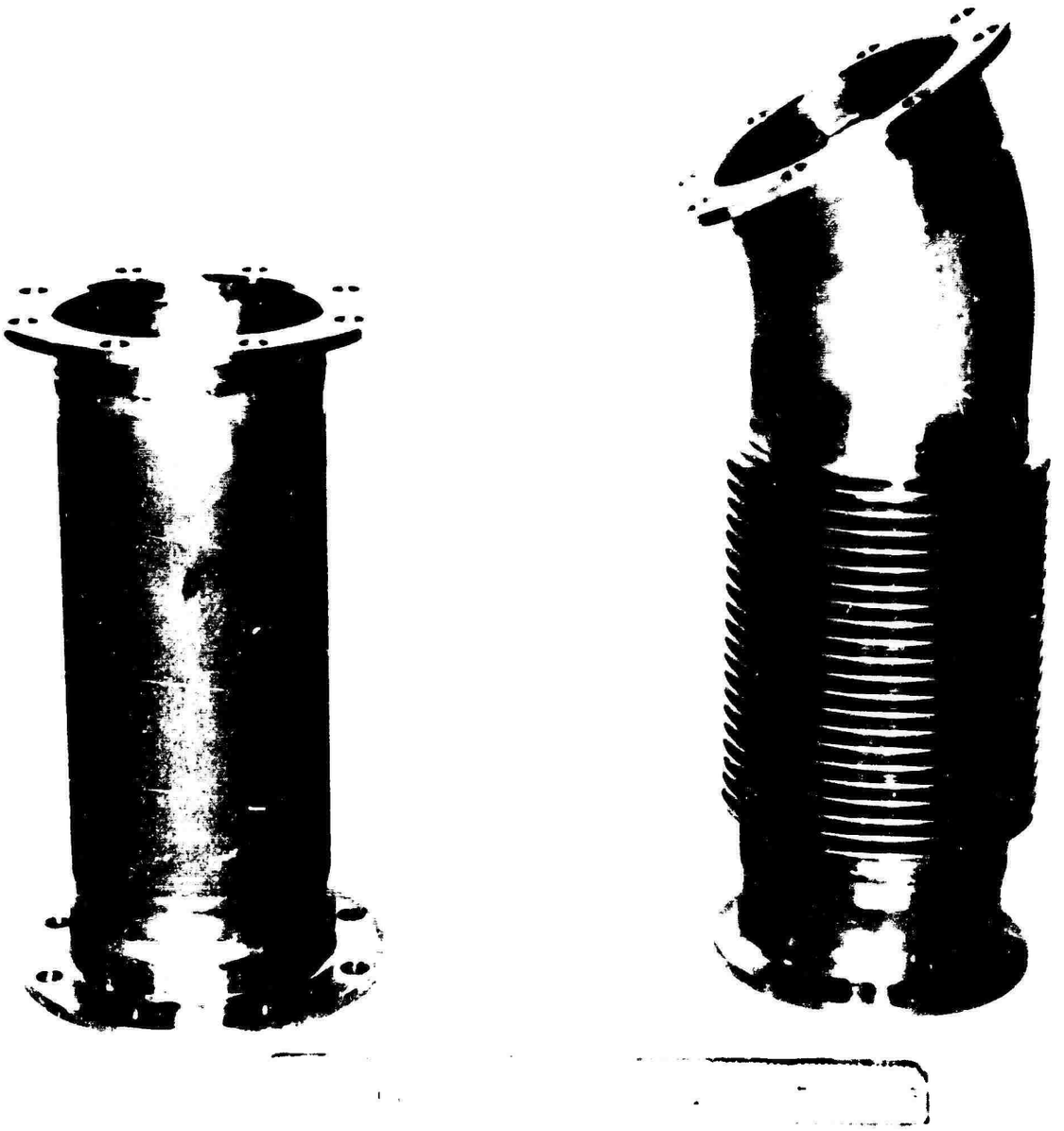

Figure 78. Tube Connecting Members.

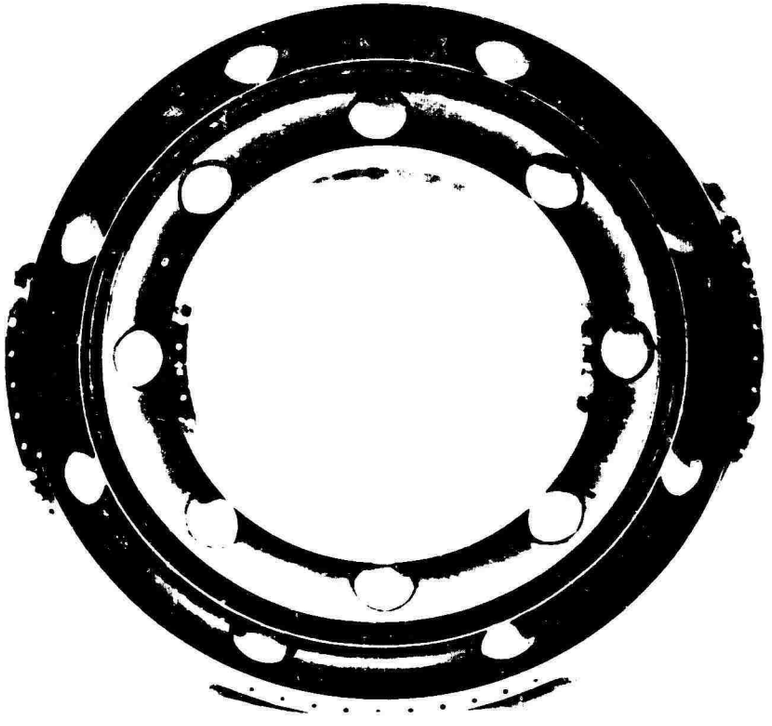

Figure 79. Toroidal Shell Assembly; Front View.

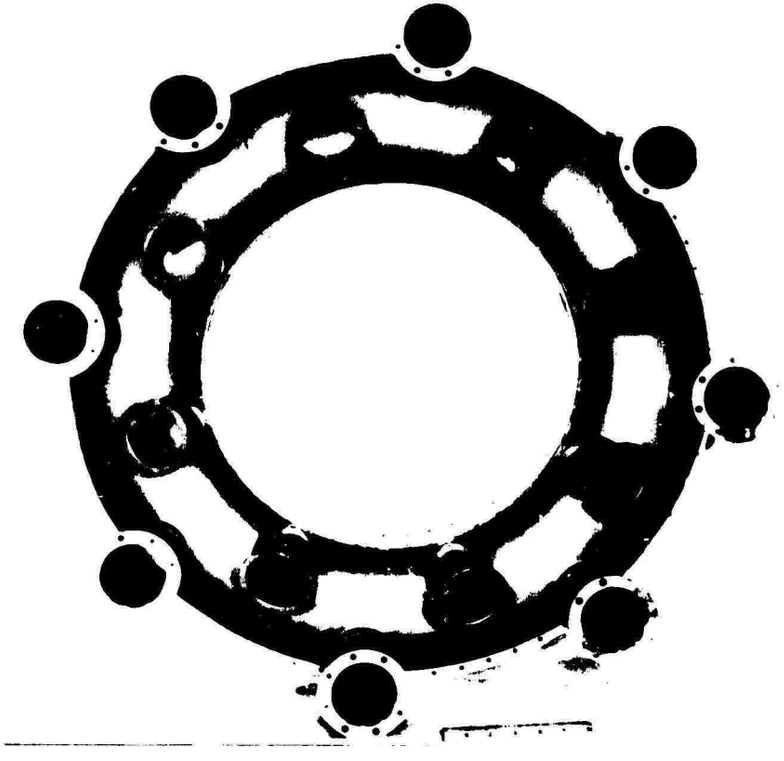

Figure 80. Toroidal Shell Assembly; Aft View.

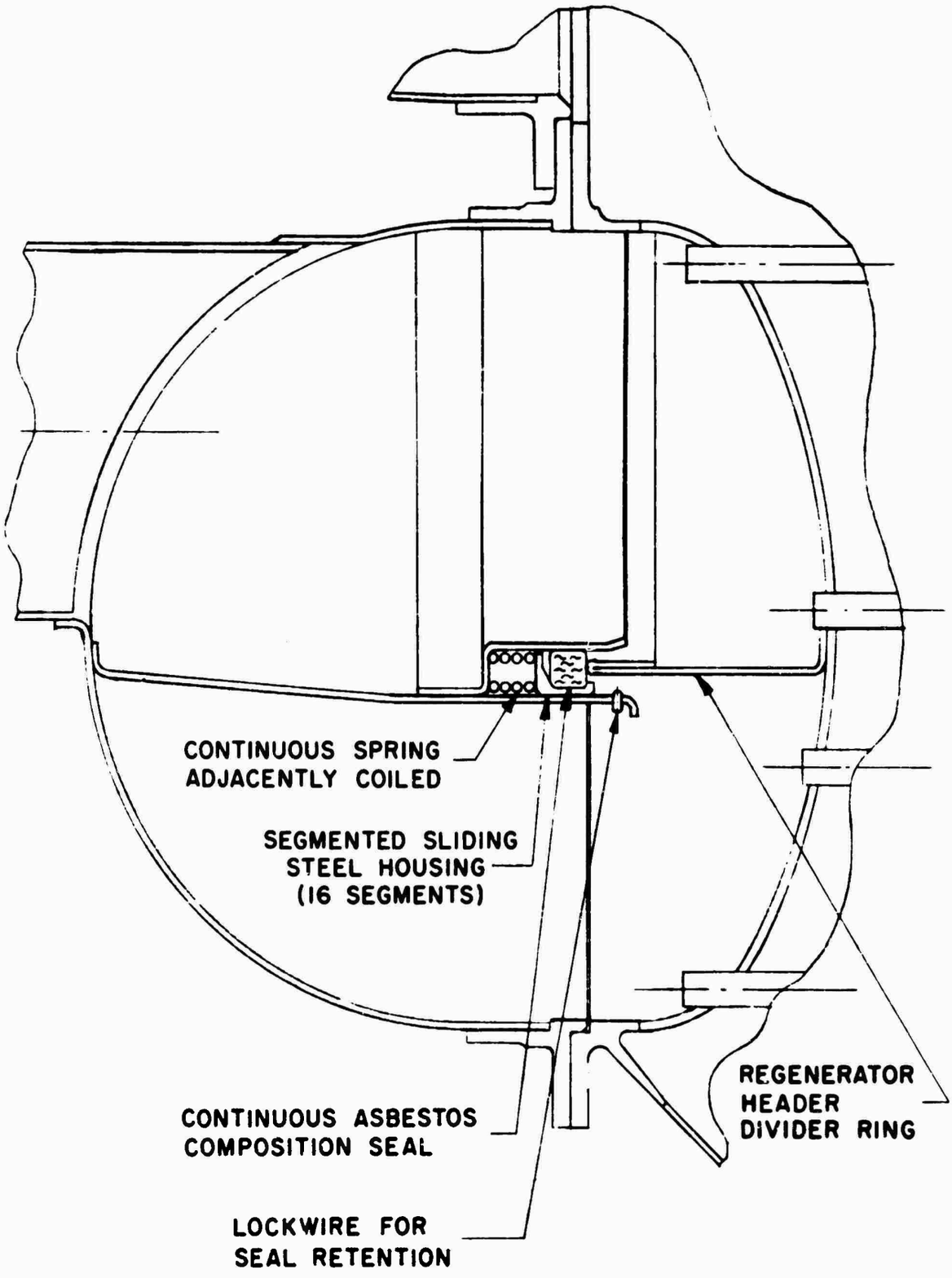

Figure 81. Toroidal Shell Seal Assembly.

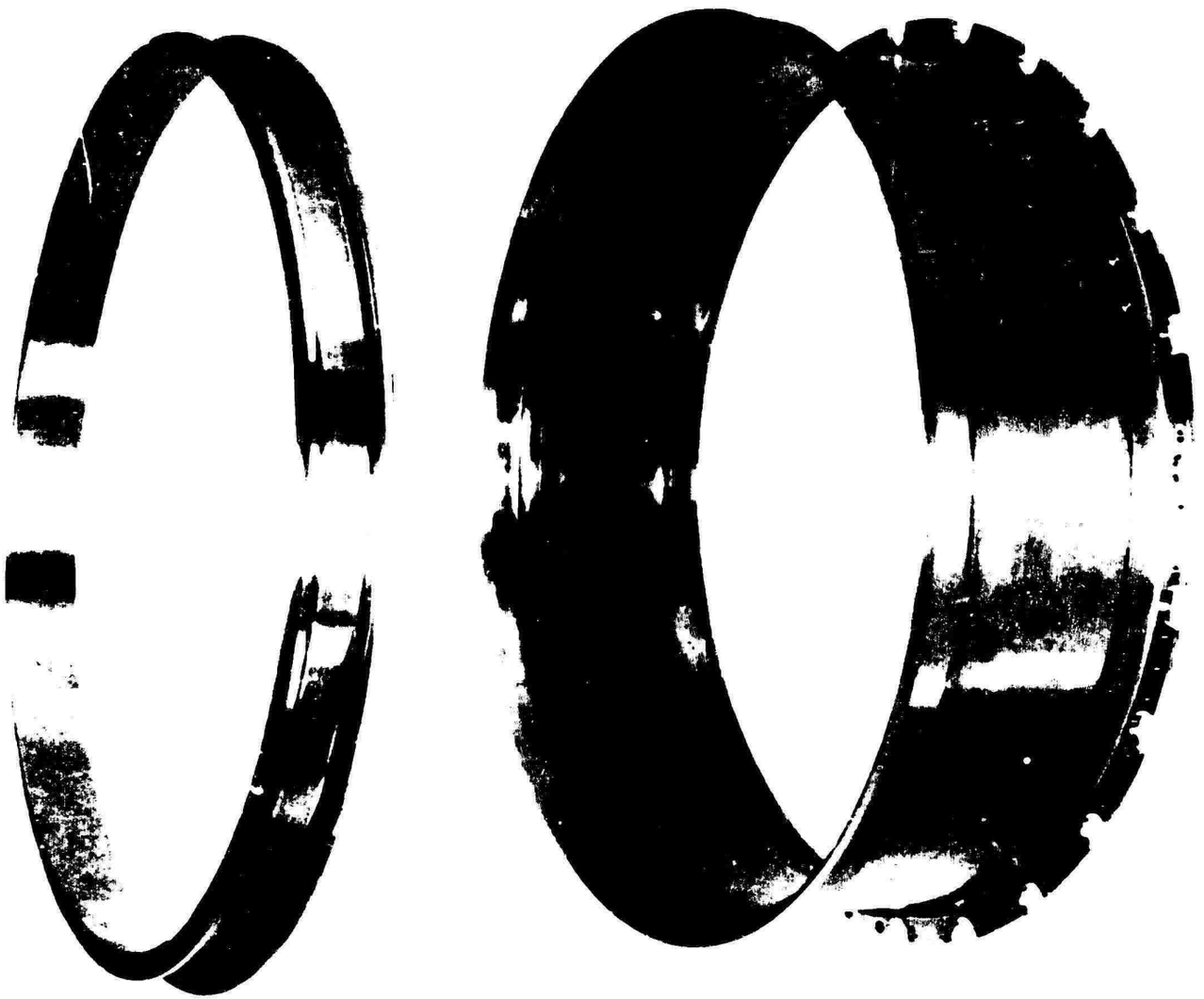

Figure 82. Exhaust Ducting.

A weight reduction of approximately 12 pounds could be obtained by reducing flange thicknesses and eliminating the special instrumentation provisions.

7.3 ENGINE MODIFICATIONS

7.3.1 Engine Model Modification

A basic T53-L-3 engine, S/N LE-02023, was provided by the Army in support of the regenerative engine program. The reduction gearing of the allocated T53-L-3 turboprop engine was replaced with that of the T53-L-11 turboshaft engine. The L-11 gearing will accommodate the installation of a water brake for power absorption and means for precise measurements of torque, and a bellmouth nozzle for the measurement of engine airflow required for performance calculations. With this gearing and the additional modifications described below, the test engine is capable of operating at T53-L-11 power levels of 1100 shaft horsepower.

7.3.2 Combustor

A satisfactory long-life combustor for reliable operation in a regenerative engine is, by its nature, the product of extensive development effort. Adaptation of the existing design and available hardware resulted in a combustor based on the assumption that modest life and performance of combustor hardware is acceptable within the scope of anticipated evaluations.

The difference between the standard combustor and the regenerative engine combustor is shown in Figure 83. Fuel vaporizers of reduced surface area are required during regenerative operation since the fuel flow through the vaporizer is reduced while inlet air temperature has increased. The standard production T53-L-11 vaporizers were reworked to shorten both inlet and exit legs, recoated with ceramic, then baked. Estimates of engine flame-out characteristics are presented in Figure 84.

To compensate for the loss in vaporizer surface, additional heat is required to assist flame propagation during the starting cycle. This heat is obtained by using two starting fuel nozzles at the 2:00 and 10:00 o'clock positions in addition to the two existing nozzles at the 4:30 and 7:30 o'clock positions. Provisions to supply fuel to the two additional nozzles were made by installing an additional upper fuel manifold assembly and providing two additional installation holes in the fireshield assembly.

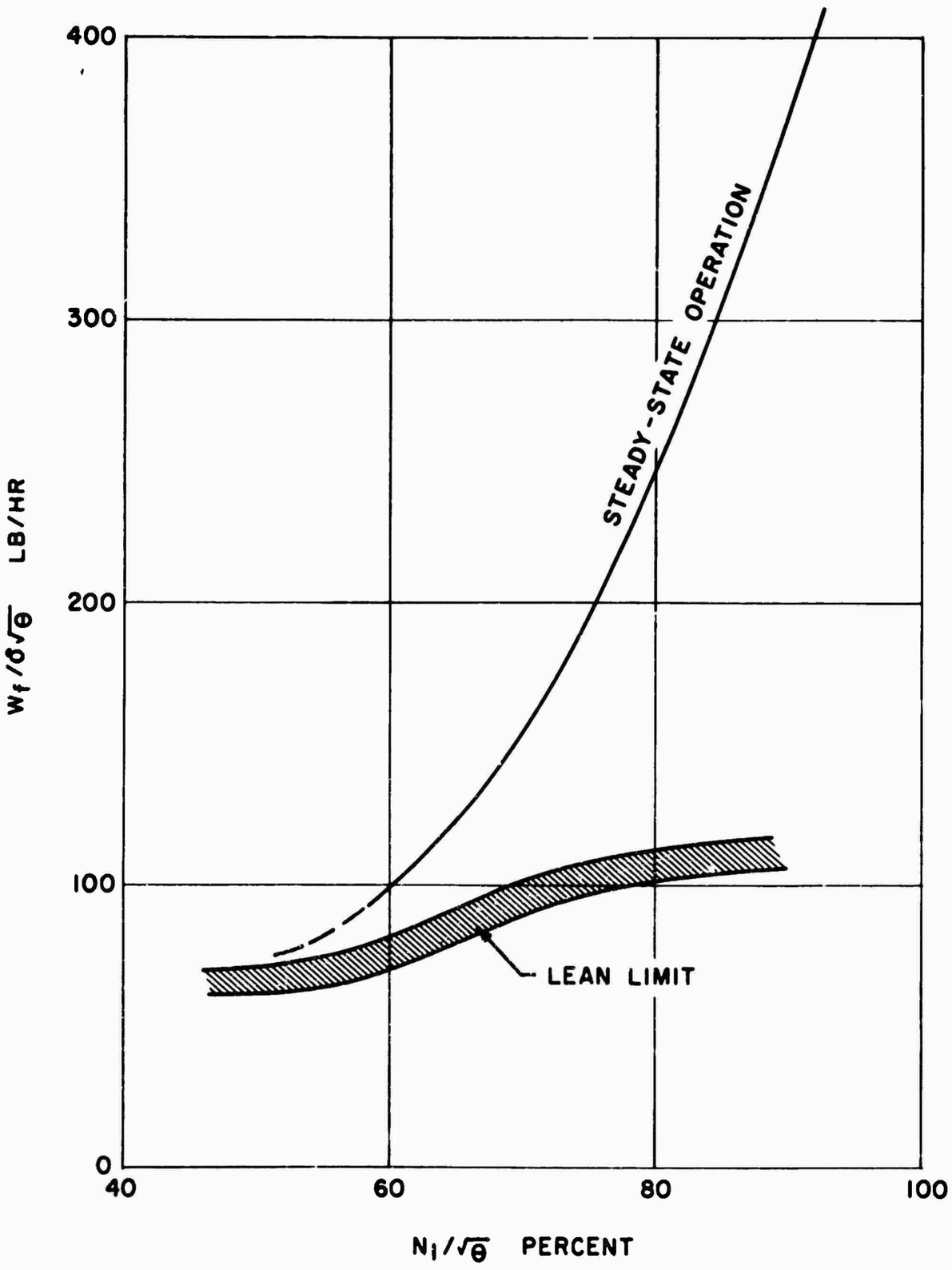

Figure 83. Engine Flame-Out Characteristics.

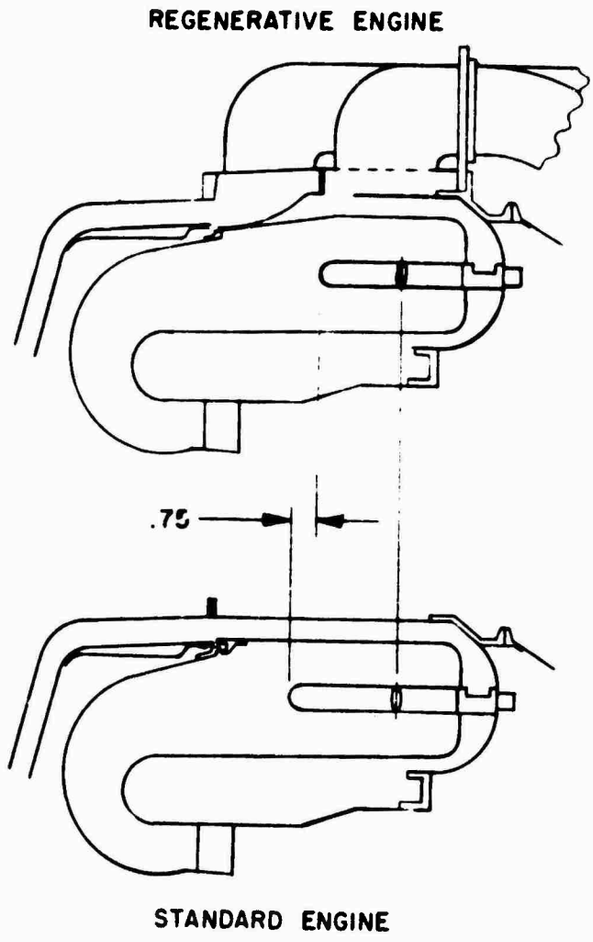

Figure 84. Engine Combustor Configurations.

7.3.3 Fuel Control

An analysis of the dynamic characteristics of the engine and the regenerator revealed that a control device is needed to vary the fuel flow schedules as required to compensate for the various initial states of the regenerator. Accordingly, the design of the production-type T53-L-11 fuel control was modified to incorporate a fuel schedule bias device (Figure 85). This device biases the control main metering valve metering head regulator as a function of the regenerator air outlet temperature to vary the fuel flow schedules. The fuel control metering head bias regulator is mounted on the fuel control housing in the area normally occupied by the regulating valve cover. From this housing, two fuel lines are run to the regenerator outlet temperature sensor housing. This sensor housing is mounted on a boss welded to one of the hot-air return tubes in the housing and tube assembly. A bimetal temperature-sensing probe is supported within the hot-air tube by a separate guide assembly. The above control unit modifications were made as an accessory package to be added to the fuel control and to the housing and tube assembly. It should be noted that this accessory package would not be required for the production type of engine since the regenerator exit temperature compensation can be added to the original fuel control by means of simple control cam modification. The accessory package will add 2.3 pounds to the existing fuel control weight of 29 pounds.

7.3.4 Gas Producer Nozzle and Power Turbine Nozzle

The effective flow areas of the gas producer nozzle and the power turbine nozzle were increased approximately 5 percent to compensate for the reduced available pressure drop across turbine stages and to maintain a normal engine operating line.

OPERATION

In the absence of a regenerator function, the main pressure regulating valve directly senses the fuel pressure drop across the main metering valve and maintains this drop essentially constant so that metered fuel flow to the engine is proportional to metering valve area. In order to achieve the fuel flow schedule modulation demanded by the regenerator, the construction illustrated schematically is used. This construction varies the pressure drop across the metering valve as a function of the regenerator outlet temperature (T_r).

A flowpath is provided in parallel with the main metering valve. In this flowpath is a fixed orifice of a small effective area, followed by a spring-loaded regenerator pressure relief (P_r) valve in series with the orifice. The spring pressure loading of the P_r valve is applied through a lever as a decreasing function with increasing T_r. The main pressure regulating valve senses the pressure difference across the fixed orifice, and maintains this pressure drop at a constant value. The P_r valve, now passing a constant flow, provides an additional pressure drop in accordance with increasing T_r and decreasing P_r spring force. The result is that the metering head pressure drop across the main metering valve is equal to a constant plus an amount dictated by T_r. In this manner, as the regenerator temperature increases, the metered flow to the engine decreases.

FROM
FUEL PU

MAIN
PRESSURE
REGULATING
VALVE

A

ction, the main
senses the fuel
ering valve and
stant so that metered
al to metering valve
low schedule modula-
the construction
This construction
metering valve as
temperature (T_r).

ith the main metering
rifice of a small
-loaded regenerator
with the orifice. The
alve is applied through
h increasing T_r. The
ses the pressure
and maintains this
The P_r valve, now
n additional pressure
T_r and decreasing
the metering head
ering valve is equal
d by T_r. In this
ature increases, the
s.

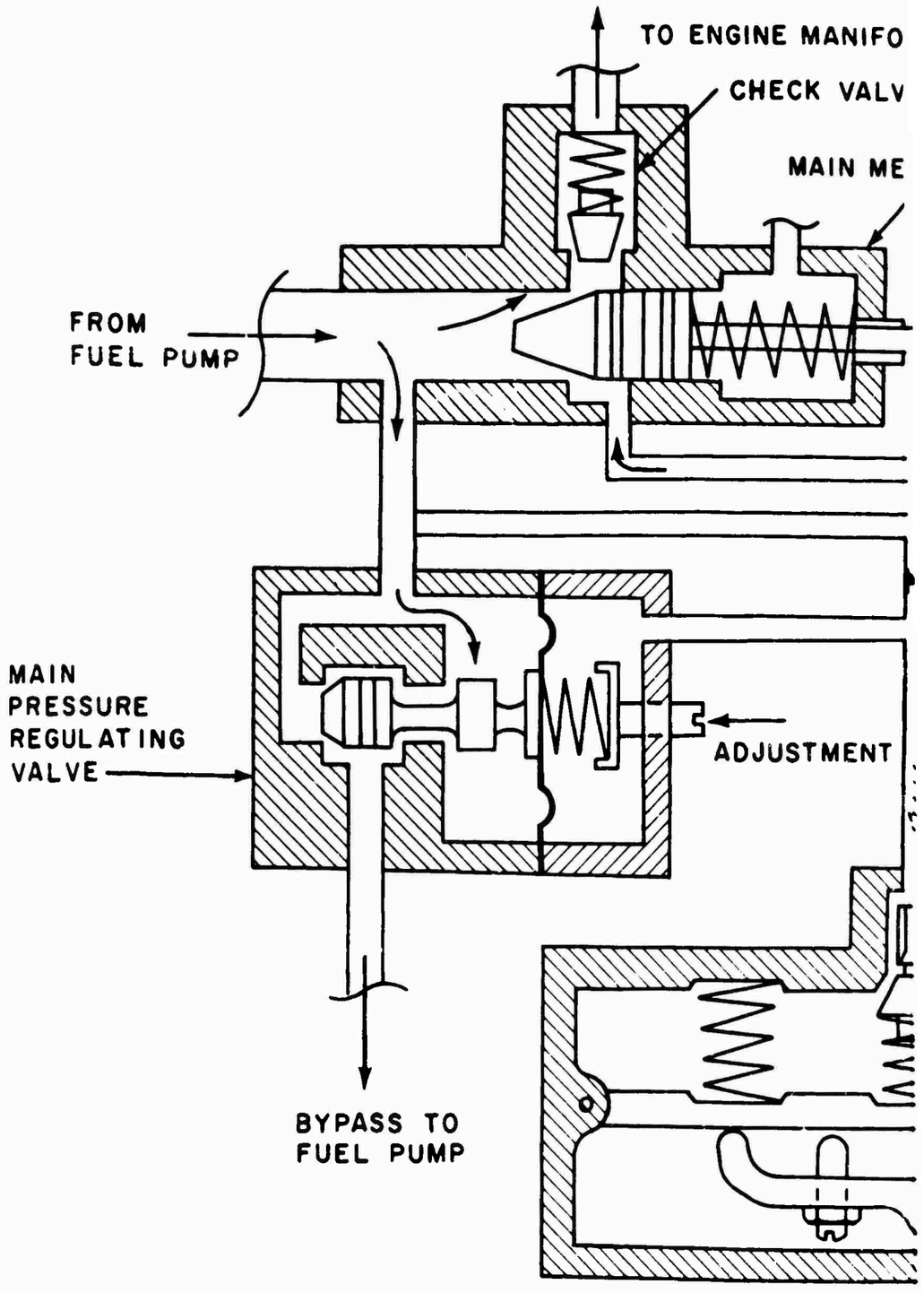

Figure 85. Regenerator Temperature Mo

B

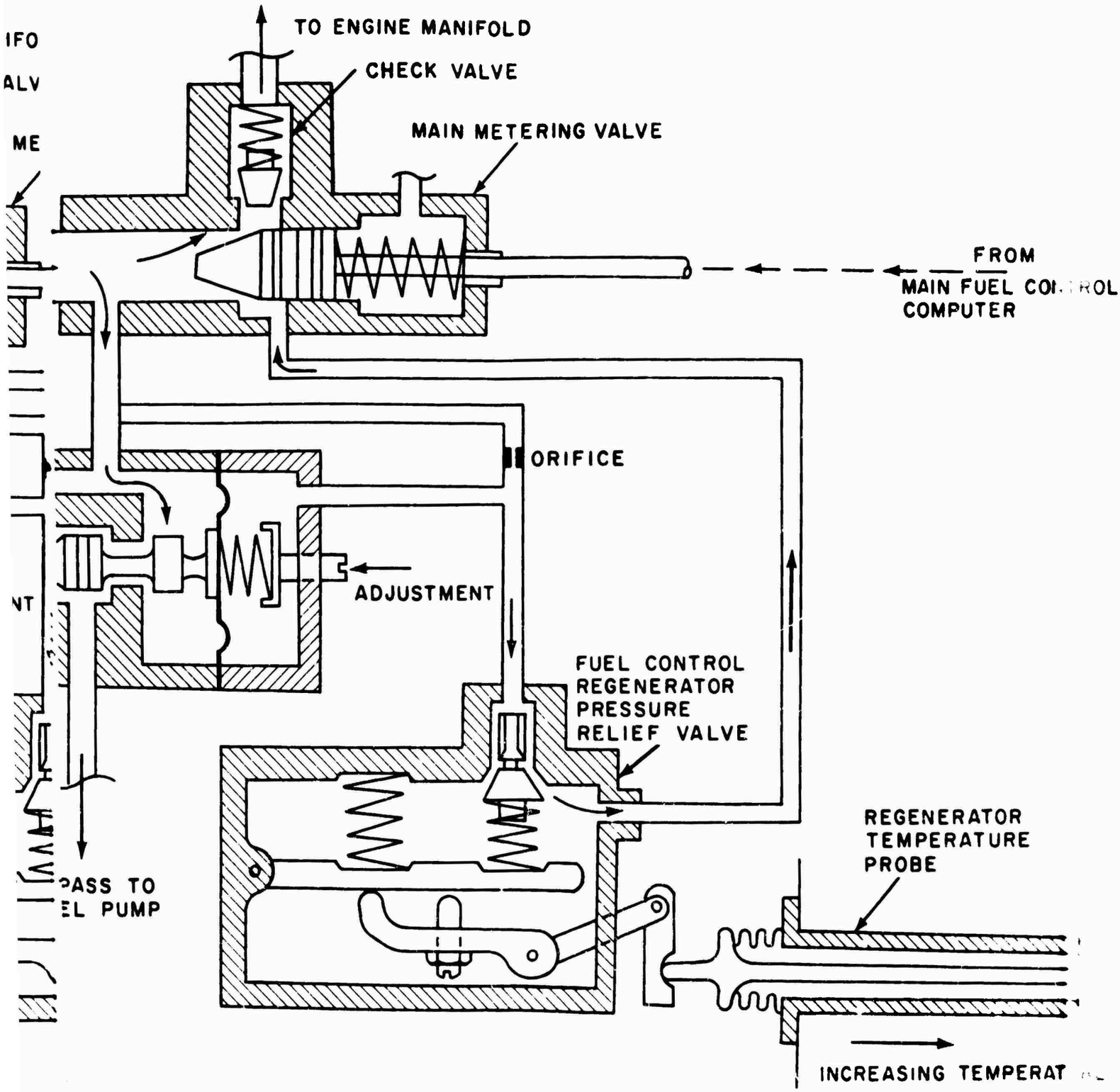

Figure 85. Regenerator Temperature Modulator, Engine Fuel Control.

SECTION EIGHT. HARDWARE FABRICATION FOR TUBE-TYPE REGENERATION

8.1 REGENERATOR HARDWARE

8.1.1 Material

All steel parts were fabricated from No. 347 (AMS 5512 and AMS 5646) steel except the shell doublers, which were fabricated from No. 321 (AMS 5510) steel. The bolts are according to AN 3C 3A, AN 3CH 4A, and AN 465A; the washers, according to AN 960 C10 and AN 960 C416; and the lockwire according to MS 20995 C32.

8.1.2 Tube Bending

Development work was performed to bend tubes to small radii without excessive thinning, wrinkling, or flattening in the bend area, but in spite of special tooling and the use of an established bending technique, about 10 percent of the tubes were found to be unsatisfactory after the bending operation and had to be scrapped.

8.1.3 Core Stacking

A special fixture was constructed to facilitate the core stacking operation (Figure 86). To establish the most suitable stacking sequence and the stacking height at the tube bends, an aluminum model, full size in section, was fabricated (Figure 87). After assembly, the tubes were mechanically secured so that they would be retained in position during the brazing operation; then they were trimmed. Tube support and spacing was provided by two support plates, four baffle plates, and six spacer rods spaced along the axis of the regenerator (Figure 88).

8.1.4 Core Brazing

To ensure a good penetration, the brazing alloy was applied to both sides of the header. Suitable stop-offs were painted in order to prevent the alloy from flowing into locations where it was not wanted. The unit was subjected to a specially designed, rigidly controlled brazing cycle. Visual inspection, confirmed by pressure test, revealed a leak in only one brazed joint. This leak was at the spacer rod boss and was repaired with high-temperature solder.

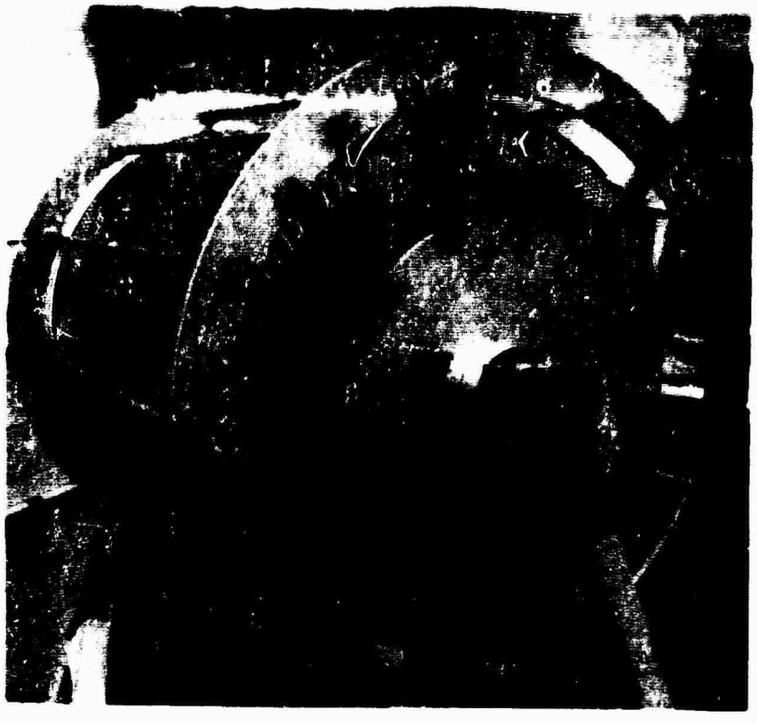

Figure 86. Core Stacking in Fixture.

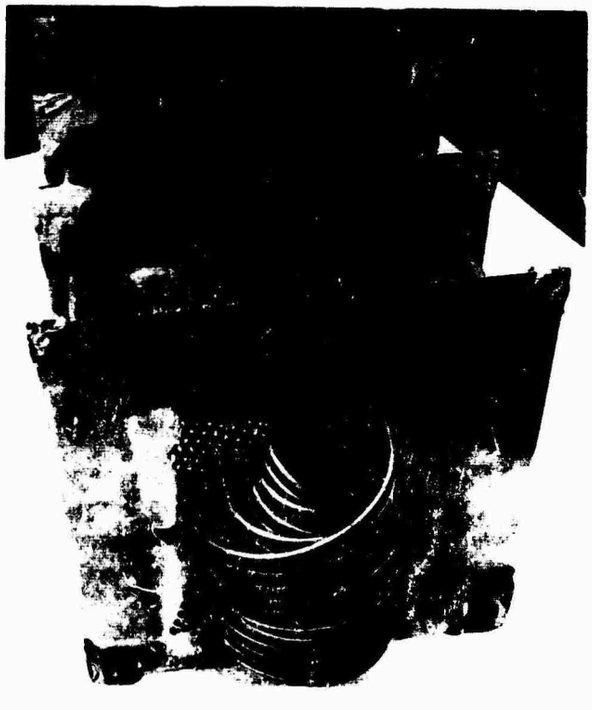

Figure 87. Tube Assembly Mockup.

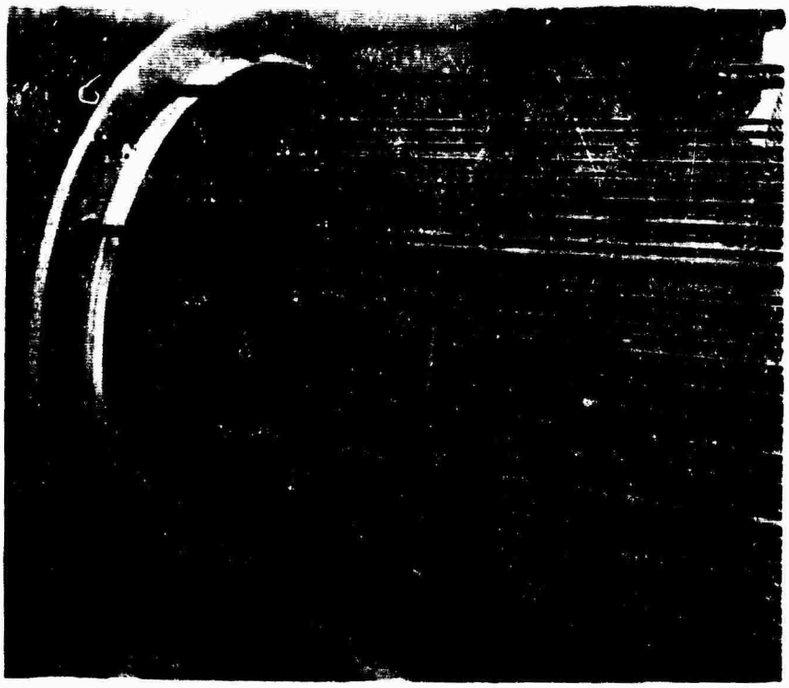

Figure 88. Core Baffle Plate and Support Plate Arrangement.

8.1.5 Flange Fabrication

Flanges were fabricated from unmachined stock which was rolled and welded. All except the two header flanges were machined to their final dimensions. Header flanges were rough-machined and welded to the header. To hold the required tolerance, final machining was performed on the assembled unit.

8.1.6 Header Fabrication

The header was formed from a 0.063-inch plate. There was little thinning of the outer diameter; the minimum measured thickness was 0.050 inch. The drilling technique for the header and support baffles is illustrated in Figure 89. The final machined header assembly is shown in Figure 90.

8.1.7 Shell Construction

The shell (Figure 70) was fabricated from 0.025-inch-rolled sheet and welded in a direction parallel to its axis. The doublers on the shell were made from No. 321 stainless. Each of the two reinforcing rings was fabricated from five elements, which were welded together and seam-welded to the shell body.

Figure 89. Drilling of the Header Plate.

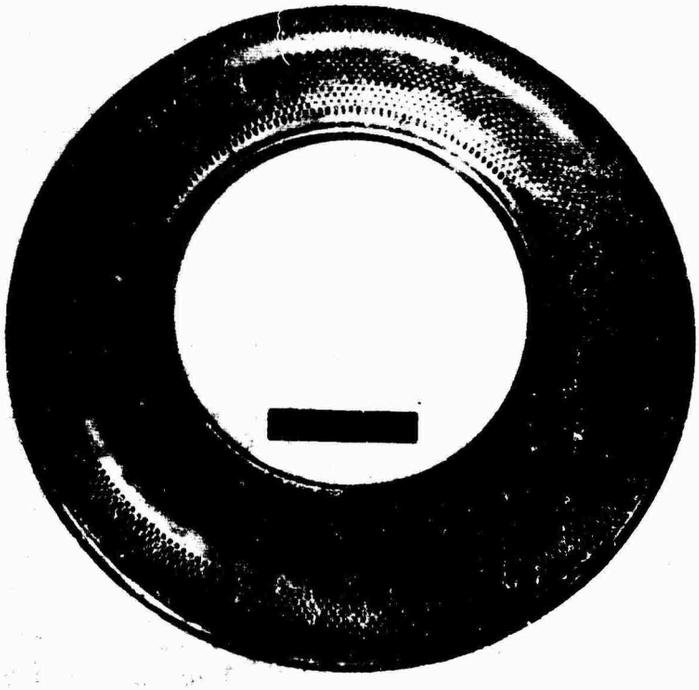

Figure 90. Header Plate.

8.1.8 Exhaust Gas Outlet Duct Assembly

The duct assembly on the exhaust gas side is fabricated from 0.032-inch sheet steel and formed into a curved baffle, to which a slotted 0.016-inch plate is seam-welded along the entire circumference. Six fin-like support brackets are fabricated from 0.040-inch sheet. They are welded to the baffle on one end and attached to the shell by means of a pair of bolts on the other end. Shims fitted between the support brackets and the shell assist in positioning the duct assembly concentrically with the core. Asbestos tape, tightly packed, was used in the space between the duct assembly and the tube bundle (Figure 91). The end pan, fabricated from 0.040-inch plate, is attached to the duct assembly by means of bolts and nut plates. This thickness was twice the design value to allow for instrumentation support. The shell and divider plate bolts are lockwired to ensure retention at all times.

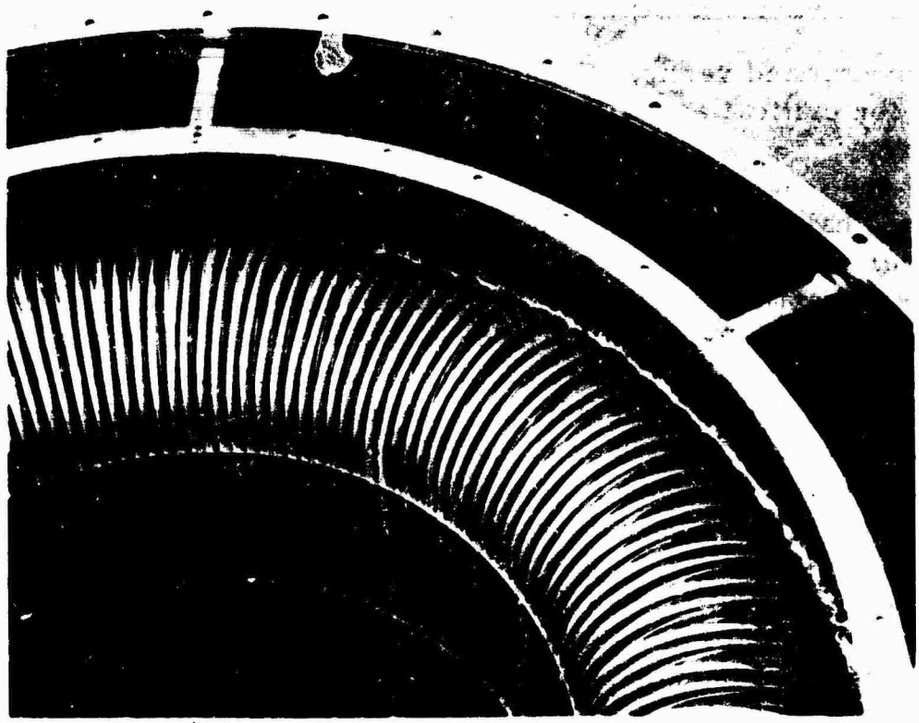

Figure 91. Regenerator Aft View Showing Asbestos Sealing Arrangement.

8.2 INTERFACE HARDWARE

The Lycoming interface regenerator hardware was fabricated primarily from AM 350 (AMS 5548) sheet and AM 355 (Lycoming Engineering Specification M 3703) plate and forgings. Both materials are

heat-treatable stainless steels. AM350 sheet is more difficult to draw or spin than type 300 series stainless due to its work-hardening characteristics. However, this material has excellent welding and brazing characteristics and good mechanical properties to 1000°F. Another adverse processing variable which occurs with both AM350 and AM355 is a size transformation or growth of approximately 0.003 inch per inch during the heat-treatment (hardening) cycle. This condition is accounted for during the processing of detail components. Many component assemblies were heat-treated (hardened) and nickel-brazed in one operation using a vacuum furnace. Other details heat-treated for mechanical properties but not requiring brazing are performed in vacuum or inert gas atmosphere furnaces to prevent oxidation. AM355 is more difficult to machine than type 300 series stainless; however, proper machining techniques produce excellent surface finishes.

8.2.1 Housing and Tube Assembly - EXP 7850-01

The horizontal and vertical flanges were semifinish-machined from pot forgings for critical assembly diameters and faces prior to brazing.

The hot- and cold-air tube elbows were formed from sheet metal as die-formed halves. The tube halves were precision-trimmed, then welded together with the TIG (tungsten inert gas) process while fixtured with end plugs to retain the internal backup argon gas. The tube ends were rough-trimmed and assembled. The air separator seal was manufactured by spinning to obtain the desired form, except that the expansion embossments were individually die-formed. A fuel control temperature sensing probe support boss was added to one of the hot-air return-tube elbows. The boss consists of a sheet metal tube which is welded to a machined support flange brazed onto the curved portion of the hot-air-tube elbow.

All details were tack-welded to the assembly in order to establish the necessary braze gaps and the proper alignment. Fuel drain valve holes were jig-bored. The unit was mounted on a flat-cast chromax spider to retain dimensional stability, then vacuum-furnace-brazed. Several rebraze cycles were required before a satisfactory (leak tight) braze was achieved throughout the whole assembly. After brazing, the unit was pressure-tested at 110 psi. The assembly was then installed in a deep-freeze chamber for subzero cooling (-100°F and below) to obtain a martinsitic structure. The assembly was tempered at 1000°F. Prior to final machining, the air separator seal area was potted with Cerro Bend to provide a solid support area for clamping. The assembly was jig-bored, tapped, deburred, and dimensionally and zyglo inspected.

8.2.2 Cold-Tube Assembly - EXP 7840-01

The cold-tube cylinders were rolled and TIG-welded. The units were trimmed so that the end faces were parallel to each other and square to the tube centerline to assure proper assembly alignment. The end flanges were machined from bare stock and vacuum-furnace-brazed to the cylinder with high-temperature, high-strength, nickel braze. The flanges were machined parallel to each other and square to the tube centerline within 0.005 inch full indicator reading; then the holes were jig-bored and deburred. Dimensional and zyglo inspection followed.

8.2.3 Toroidal Shell Assembly - EXP 7830-01

The toroidal shell assembly (Figures 79 and 80) consumed the longest manufacturing time. The basic shell was spin-formed, since it was too large for hydroforming. Ten spin passes were required on the male and female spin chucks. Each spin pass required a special cleaning cycle prior to vacuum annealing. The basic shell was potted with wax to make it more rigid; then undersize tube holes were jig-bored at the tube entrance angles. Die-formed rims were drawn from these tube holes in the shell. After each forming operation, an immediate degrease and 600°F oven bake was performed to prevent creep fractures. For assembly all detail flanges were semifinish-machined from pot forgings. The inner seal flange support and retainer were spun, then seam-welded together into a subassembly. While fixture-retaining the tubes to the extruded shell rims, the tubes were tack-welded and gapped in preparation for brazing. Prior to vacuum-furnace-brazing, the tack-welded assembly was cleaned. After each brazing operation, a pressure test per blueprint specification was performed; several braze cycles and pressure checks were required. The assembly was subzero-cooled in the toroidal shell assembly and brazing fixture (Figure 92) to maintain critical flange and tube dimensional location tion. The unit was tempered at 1000°F. In preparation for shell flange final-machining, the assembly was mounted in the machining fixture (Figure 93), the tube channels were closed with teflon plugs, and the shell was potted with Cerro Bend to support the sheet metal and provide clamping surfaces.

To finish-machine the cold-air-tube flanges and finish-lap the hot-air-tube flanges, the entire assembly was potted into a solid ring of wax. All holes were jig-bored and the unit was deburred. Finally, the assembly was subjected to X-ray, zyglo, and dimensional inspections.

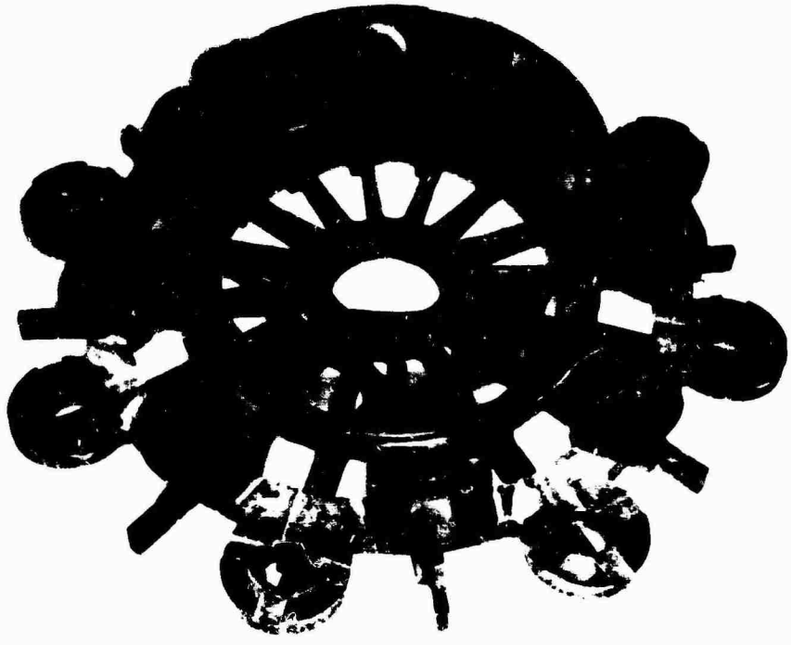

Figure 92. Toroidal Shell Assembly and Brazing Fixture.

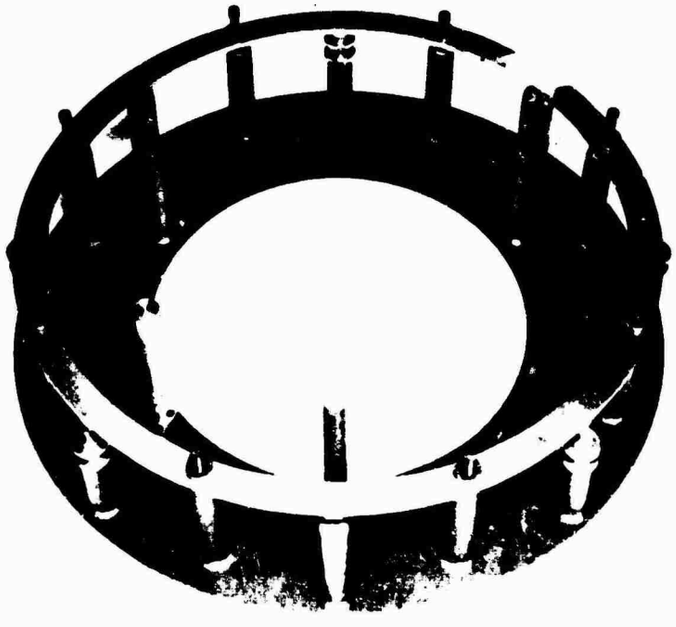

Figure 93. Toroidal Shell Machining Fixture.

8.2.4 Exhaust Duct Assembly - EXP 7845-01

The cylinder detail for the exhaust duct (Figure 82) was spun, annealed, respun, and heat treated to an equalized condition. The forward and aft flanges were semifinish-machined from pot forgings. The flange details were then resistance-seam-welded to the prefitted cylinder detail. The unit was inspected by X-ray and zyglo methods, cleaned, heat treated in a vacuum furnace, deep frozen, tempered, recleaned, and potted with Cerro Bend for additional support during final machining. Holes were drilled and tapped; the aft flange was mill-scalloped, deburred, and dimensionally and zyglo inspected.

8.2.5 Seal Support - EXP 7841-01

The seal support (Figure 82) was semifinish-machined from a pot forging, heat treated, deep frozen, tempered, cleaned, machined, deburred, and dimensionally and zyglo inspected.

8.2.6 Aft Combustor Housing Assembly - EXP 7855-01

The hydroformed aft casing end is a T53-L-11 production item. The deflector cylinder was rolled and butt-welded as a detail and seam-welded to the aft outer semifinish-machined flange. The inner support flange, a production item, was seam-welded to the hydroformed end casing. The semifinish-machined vaporizer support bosses were vacuum-brazed to the hydroformed end casing with a high-temperature gold braze (Lycoming Specification M3860). The final assembly was inspected by X ray and zyglo, deep frozen, tempered, cleaned, final machined, drilled, deburred and dimensionally and zyglo inspected.

8.2.7 Bypass Cover Assembly - PSK 8636-01

The bypass cover assembly (Figure 94) is used to replace the regenerator during testing of the basic engine and combustor interface hardware. The cover shell was spin-formed from 321 stainless steel material; the inner and outer mounting flanges were semifinish-machined from AM 355 forgings and seam-welded to the shell. The assembly was subzero-cooled, tempered at 1000°F, cleaned, final machined, jig bored, deburred, and inspected by X-ray, dimensional, and zyglo methods.

Figure 94. Bypass Cover Assembly.

8.3 ENGINE HARDWARE MODIFICATIONS

8.3.1 Power Turbine Nozzle - EXP 7899-01

The power turbine nozzle was fabricated from present production nozzle details except for a revision in the effective flow area, which was increased from 25.50 ±0.25 square inches to 26.77 ±0.25 square inches by changing the inner and outer punch angles by 1.9 degrees.

8.3.2 Gas Producer Nozzle - EXP 7896-01

The gas producer nozzle was fabricated from present production nozzle details except for a revision in the effective flow area, which has been increased from 9.85 ±0.10 square inches to 10.34 ±0.10 square inches by changing the inner and outer punch angles by 1.0 degree.

8.3.3 Combustor Liner Assembly - EXP 7870-01

A standard production-type liner assembly (P/N 1-130-410-01) was reworked to the EXP 7870-01 configuration by adding two additional starting fuel nozzle provisions. This modification involved changes to the sheet metal detail holes and the final subassembly hole sealing.

8.3.4 Segment, Seal - EXP 7832-01

The seal segments used in the toroidal shell divider assembly were machined from a single ring forging of AM 355 material, and sectioned into sixteen equal segments (Figure 81).

8.3.5 Adapter, Drain Valve - EXP 7863-01

Two drain valve adapters were machined from AM 5645 bar stock.

8.3.6 Fireshield Assembly - EXP 7860-01

The engine fireshield assembly (P/N 1-150-030-06) was reworked to the EXP 7860-01 configuration to provide holes for the two additional starting fuel nozzles.

8.3.7 Vaporizer Assembly - PSK 9344-01

Standard production-type vaporizers (P/N 1-130-580-01) were reworked to the PSK 9344 configuration by shortening the vaporizer inlet leg and exit legs to reduce vaporizer surface area while maintaining the same vaporizer exit tip location with respect to the liner end. The vaporizers

were then recoated with ceramic, baked, and flow-checked with the fuel dividers installed.

8.3.8 Hose Assemblies

Two new hose assemblies and four reworked hose assemblies were provided by using Government-approved available hoses and connectors. Each hose assembly was pressure-checked for leakage.

8.4 VENDOR-SUBCONTRACTED PARTS

The principal vendor-subcontracted item was the AiResearch tube-type regenerator (P/N 180530). In addition, the following subcontracted vendor parts were purchased to support the system hardware requirements:

VENDOR	PART NUMBER	NAME
Arrowhead Products Division, California	PSK 8581-01	Hot-Air Tubes
Precision Piston Rings, Inc., Indiana	EXP 7842-01	Ring, Sealing Lock
Aeroquip Corporation, California	MVT61107-1537-M	Clamp, Quick Disconnect
Tube Processing Corp., Indiana	EXP 7905-01	Starter, Fuel Manifold Assembly Upper
Aeroquip Corporation, California	4369C-335M	Clamp, Quick Disconnect
Wallace-Barnes Division, Connecticut	EXP 7833-01	Spring, Seal
Johns-Manville Corporation, New Jersey	EXP 7831-01	Seal
Delavan Mfg. Co., Iowa	1-300-192-01	Nozzle, Starting Fuel

VENDOR	PART NUMBER	NAME
United Engineering Mfg. Corp., Connecticut	PSK 8762-01	Bolt, Probe Support
Triangle Machine, Connecticut	EXP 7916-01, -02	Bolt

SECTION NINE. INSTRUMENTATION FOR TUBE-TYPE REGENERATOR TEST

9.1 OBJECTIVES

Adaption of a regenerator to a standard T53 engine necessitated the addition of special instrumentation to the basic engine in order to evaluate, fully and adequately, the engine-regenerator performance characteristics. Principal instrumentation requirements were based on regenerator effectiveness, system pressure losses, and engine overall performance.

The following section defines in detail the instrumentation and the instrumentation nomenclature.

9.2 ENGINE STATION INSTRUMENTATION DETAILS

Figure 95 schematically identifies the principal regenerator instrumentation station locations.

9.2.1 Engine Inlet

Engine inlet conditions and air weight flow rate will be determined by standard calibrated bellmouth and allied instrumentation.

9.2.2 Station 3.0 - Discharge Plane of the Engine Compressor

Four outer-wall static pressure probes, four stagnation pressure probes, and four stagnation temperature probes have been incorporated. The instrument location and individual probe identification are given in Figure 96. All probes are positioned circumferentially midway between adjacent diffuser axial vanes, and the stagnation probes are located at midchannel height.

9.2.3 Station 3.1 - Entrance Plane to the Eight Air Ducts Carrying Compressor Discharge Air to the Regenerator Core

Four outer-wall static pressure probes are used to determine static pressures in the compressor exit plenum. It is expected that the static pressure readings will yield a close approximation to the tube inlet stagnation pressure values since local Mach number should be quite low. Each of the four static pressure probes is located circumferentially midway between the adjacent air duct entrance ports. Figure 97 shows the probe circumferential location, identification, and installation method for this station.

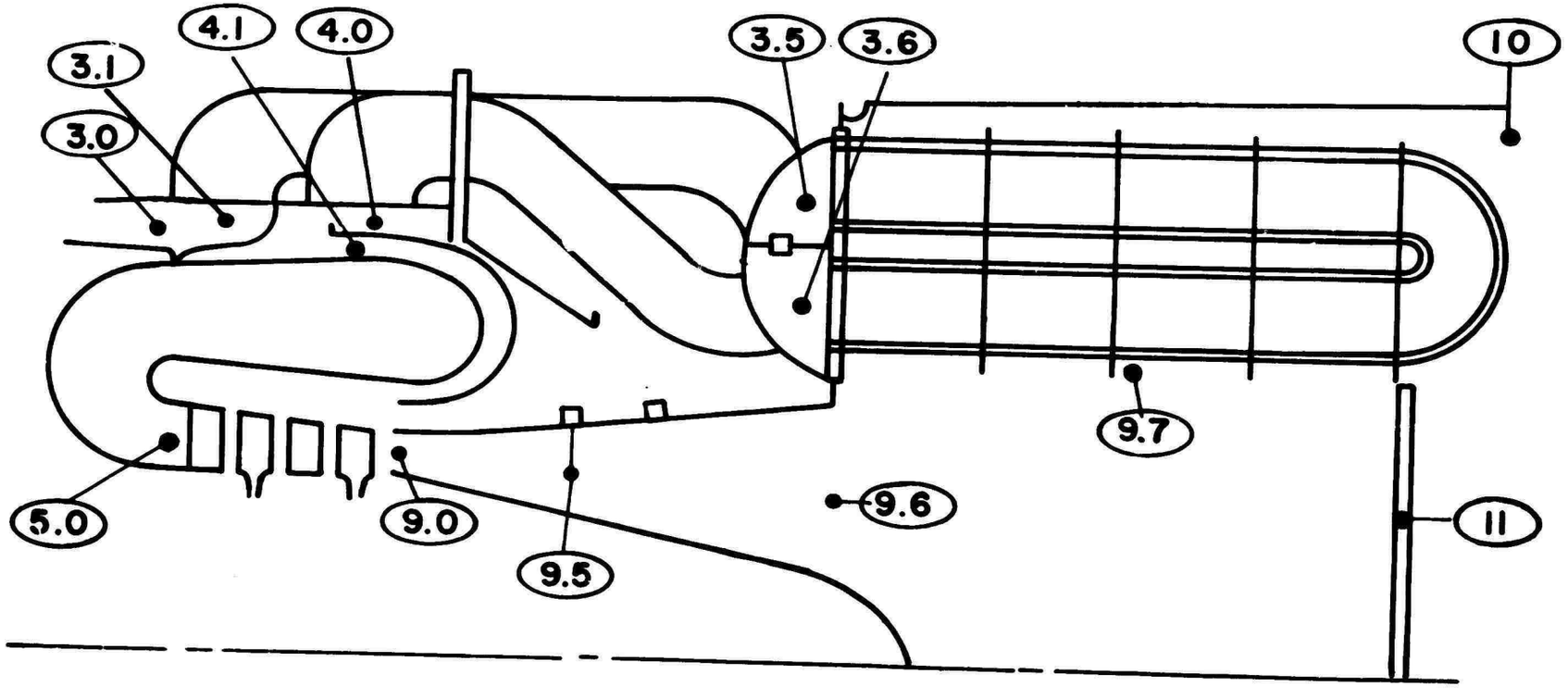

Figure 95. Regenerator Station Identification.

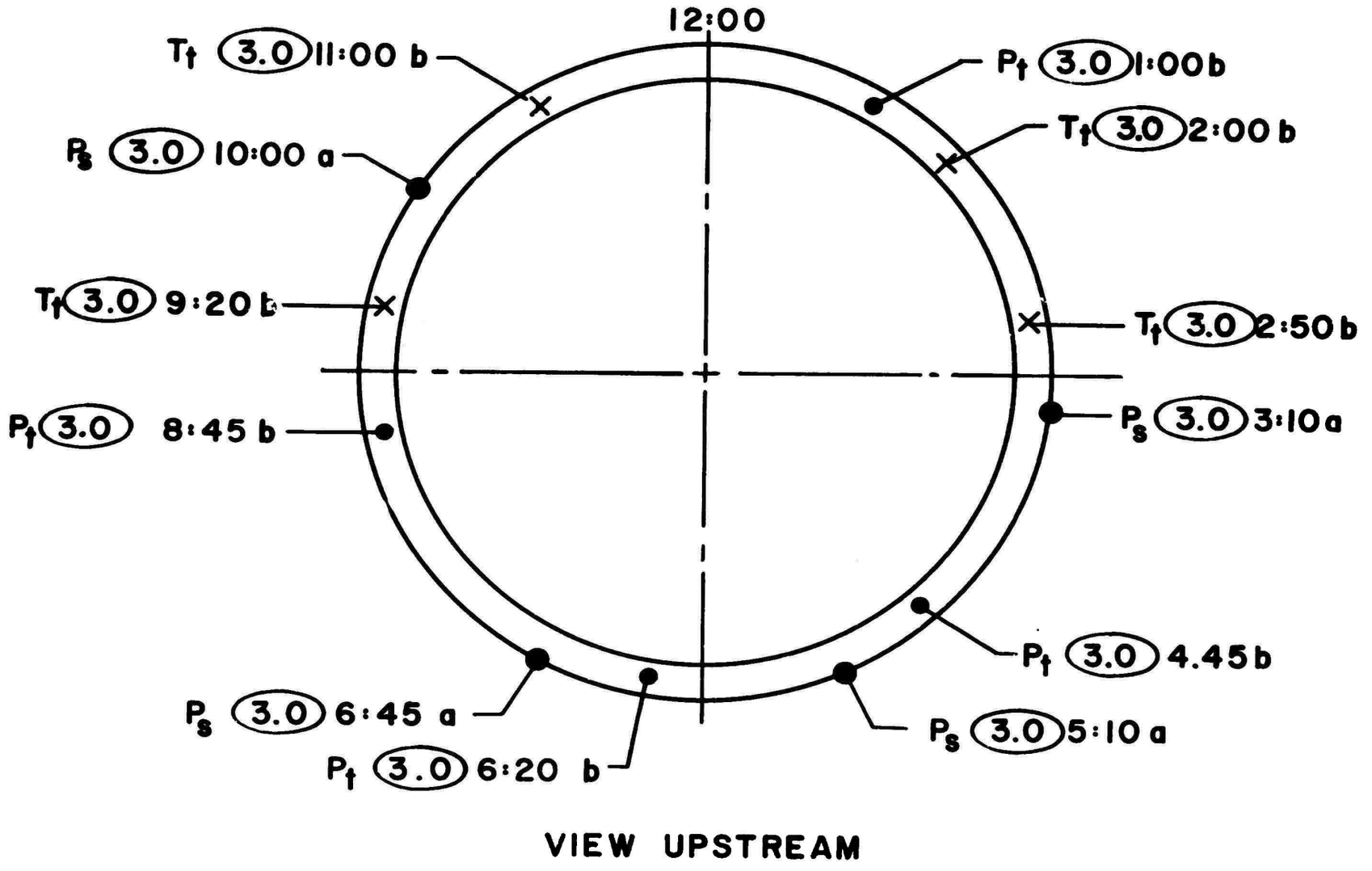

Figu 96. Station 3.0 Instrumentation: Radial Diffuser Discharge.

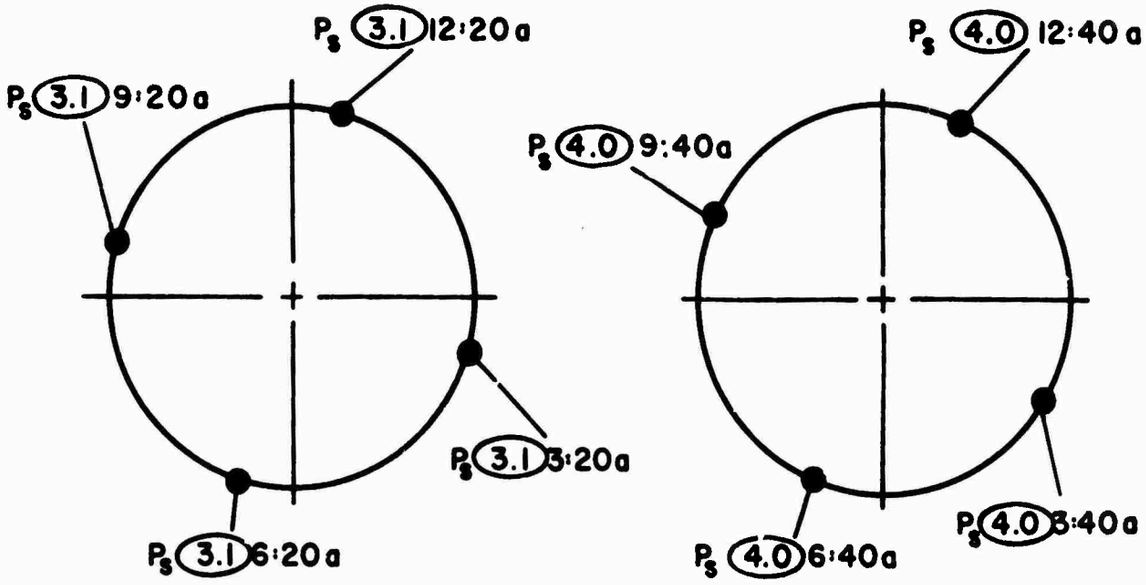

STATION 3.1
AIR DUCT ENTRANCE
DIFFUSER EXIT

STATION 4.0
AIR DUCT EXIT
COMBUSTION ENTRANCE

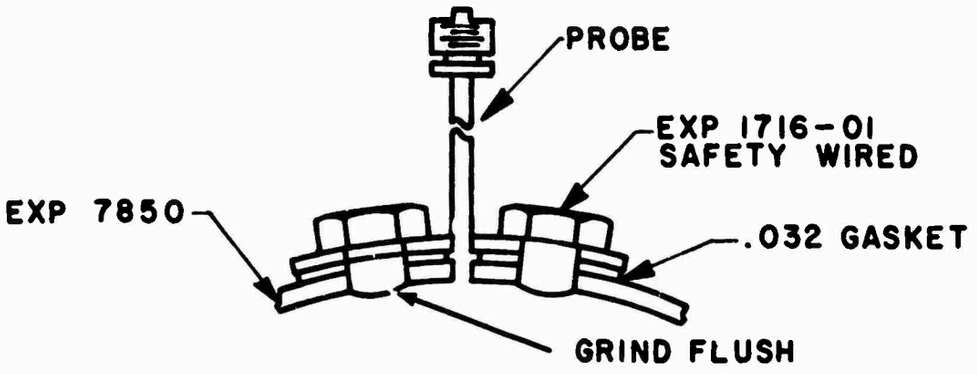

PROBE PSK 8671-01 STATION 3.1
PROBE PSK 8671-04 STATION 4.0

Figure 97. Station 3.1 and 4.0 Instrumentation.

9.2.4 Station 3.5 - Regenerator Inlet Air-Side Plane

The instrumentation installed in this plane consists of:

1) Four static pressure probes (PSK 8671-02).
2) Eight Kiel stagnation pressure probes mounted two each in four radial locations (Figure 98).
3) Twelve stagnation temperature bare wire probes mounted three each in four radial locations (Figure 98).

Figure 99 shows the probe circumferential and radial location, identification, and installation method for this station. The flanges of the toroidal shell assembly (EXP 7830) are constructed extra thick in order to provide sufficient material for the probe installation.

9.2.5 Station 3.6 - Regenerator Exit Air-Side Plane

This plane will have instrumentation similar to that in Station 3.5. Figure 100 shows the probe circumferential and radial location, identification, and installation method for this station.

The installation of the probes at this station (see Figure 101) warrants a detailed explanation. The engine exhaust duct assembly is scalloped to allow the duct to be assembled to the toroidal shell assembly. This instrumentation is secured by special slotted bolts. Slotting was necessary because installation of the bolts was initiated from inside the toroidal shell by judicious bending of instrumentation lead lines and secured by three special bolts that are used to wed the exhaust duct and toroidal shell as one unit. The bolts are locked by means of safety wire.

9.2.6 Station 4.0 - Combustor Inlet Plenum

This station is located at the plenum entrance to the combustor, into which the eight air ducts from the regenerator empty. Instrumentation consists of four outer-wall static pressure probes similar to those in Station 3.1. Figure 97 shows the probe circumferential location, identification, and installation method.

9.2.7 Station 4.1 - Combustor Entrance Channel

This station is located in the entrance channel to the combustor beyond the point where the regenerator air turns 90 degrees from the combustor entrance plenum. The channel will have four static pressure probes, two stagnation temperature probes (PSK 8673), and two total pressure probes (PSK 8674) mounted in the combustor housing as shown in Figure 102.

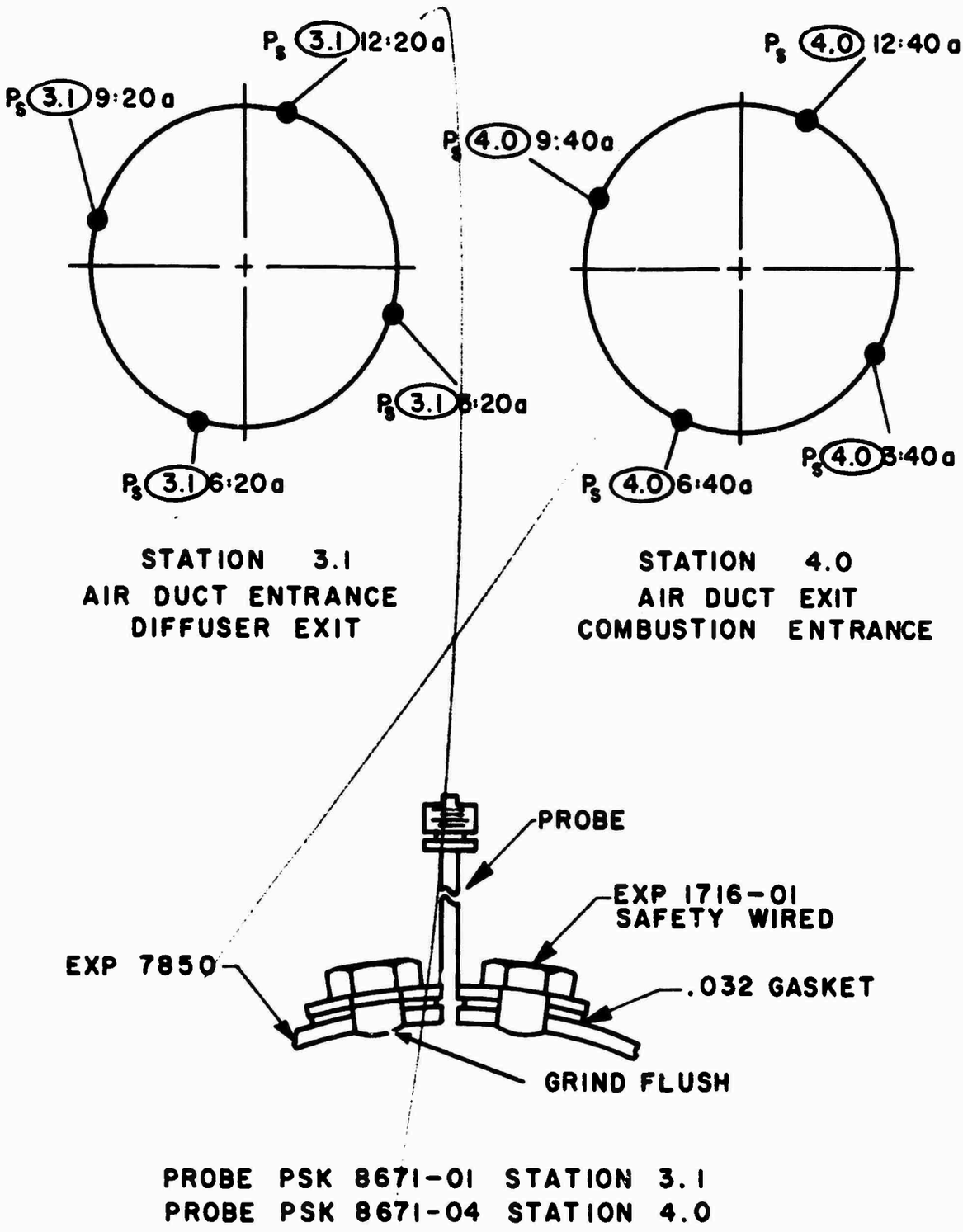

Figure 97. Station 3.1 and 4.0 Instrumentation.

9.2.4 Station 3.5 - Regenerator Inlet Air-Side Plane

The instrumentation installed in this plane consists of:

1) Four static pressure probes (PSK 8671-02).
2) Eight Kiel stagnation pressure probes mounted two each in four radial locations (Figure 98).
3) Twelve stagnation temperature bare wire probes mounted three each in four radial locations (Figure 98).

Figure 99 shows the probe circumferential and radial location, identification, and installation method for this station. The flanges of the toroidal shell assembly (EXP 7830) are constructed extra thick in order to provide sufficient material for the probe installation.

9.2.5 Station 3.6 - Regenerator Exit Air-Side Plane

This plane will have instrumentation similar to that in Station 3.5. Figure 100 shows the probe circumferential and radial location, identification, and installation method for this station.

The installation of the probes at this station (see Figure 101) warrants a detailed explanation. The engine exhaust duct assembly is scalloped to allow the duct to be assembled to the toroidal shell assembly. This instrumentation is secured by special slotted bolts. Slotting was necessary because installation of the bolts was initiated from inside the toroidal shell by judicious bending of instrumentation lead lines and secured by three special bolts that are used to wed the exhaust duct and toroidal shell as one unit. The bolts are locked by means of safety wire.

9.2.6 Station 4.0 - Combustor Inlet Plenum

This station is located at the plenum entrance to the combustor, into which the eight air ducts from the regenerator empty. Instrumentation consists of four outer-wall static pressure probes similar to those in Station 3.1. Figure 97 shows the probe circumferential location, identification, and installation method.

9.2.7 Station 4.1 - Combustor Entrance Channel

This station is located in the entrance channel to the combustor beyond the point where the regenerator air turns 90 degrees from the combustor entrance plenum. The channel will have four static pressure probes, two stagnation temperature probes (PSK 8673), and two total pressure probes (PSK 8674) mounted in the combustor housing as shown in Figure 102.

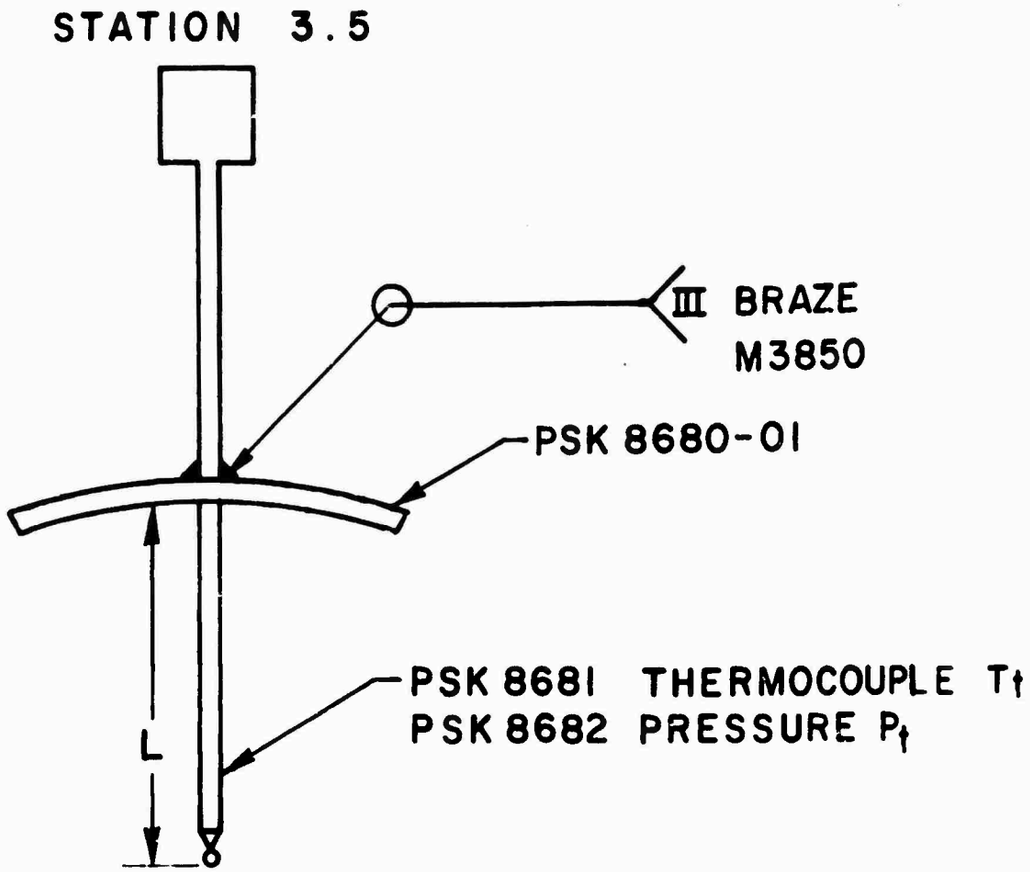

NOTE: USE STATIC PRESSURE PRO E PSK
USE STATIC PRESSURE PROBE PSK

PROBE				L DIMENSION	RADIUS
P_t OR T_t	(3.5)	a		.64	13.485
P_t OR T_t	(3.5)	b		1.08	13.045
P_t OR T_t	(3.5)	c		1.52	12.605
P_t OR T_t	(3.5)	d		1.96	12.165

Figure 98. Station 3.5 and 3.6 P

A

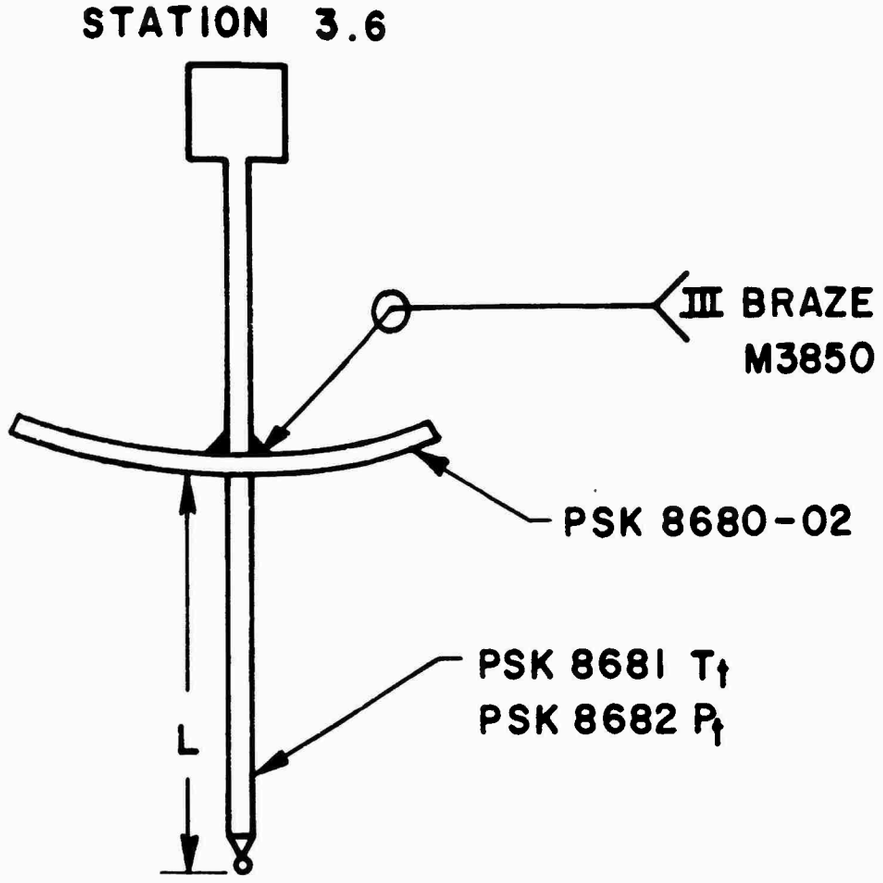

BRAZE
M3850
-01

MOCOUPLE T_t
SURE P_t

URE PROBE PSK 8671-02 AT STATION 3.5
URE PROBE PSK 8672 AT STATION 3.6

S	PROBE	L DIMENSION	RADIUS
5	P_t OR T_t (3.6) a	.780	8.965
5	P_t OR T_t (3.6) b	1.360	9.545
5	P_t OR T_t (3.6) c	1.940	10.125
5	P_t OR T_t (3.6) d	2.520	10.705

tation 3.5 and 3.6 Probe Construction.

B

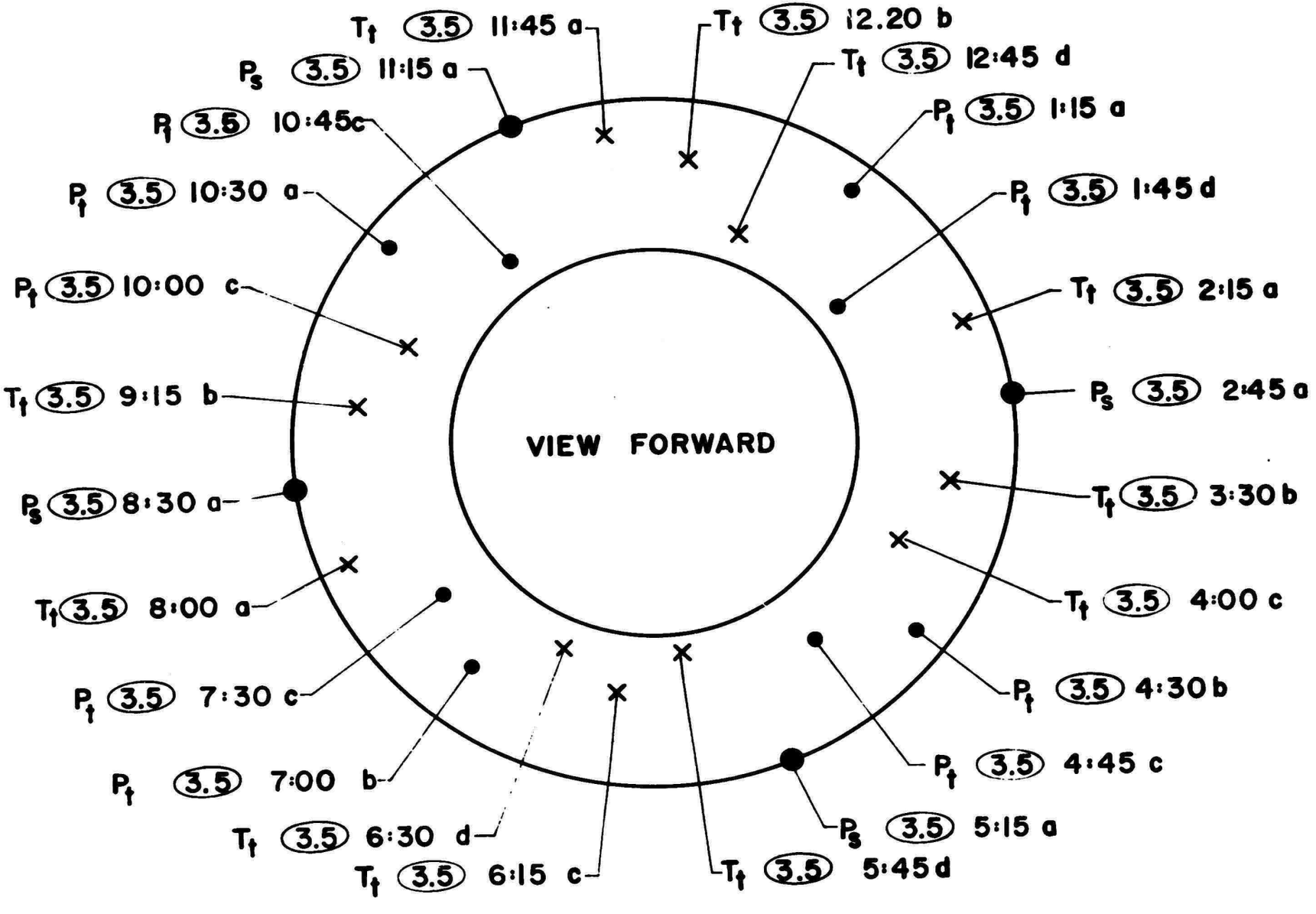
VIEW FORWARD
T_f 3.5 11:45 a
P_s 3.5 11:15 a
P_f 3.5 10:45c
P_f 3.5 10:30 a
P_f 3.5 10:00 c
T_f 3.5 9:15 b
P_s 3.5 8:30 a
T_f 3.5 8:00 a
P_f 3.5 7:30 c
P_f 3.5 7:00 b
T_f 3.5 6:30 d
T_f 3.5 6:15 c
T_f 3.5 12.20 b
T_f 3.5 12:45 d
P_f 3.5 1:15 a
P_f 3.5 1:45 d
T_f 3.5 2:15 a
P_s 3.5 2:45 a
T_f 3.5 3:30 b
T_f 3.5 4:00 c
P_f 3.5 4:30 b
P_f 3.5 4:45 c
P_s 3.5 5:15 a
T_f 3.5 5:45 d

A

T_t (3.5) 6:30 d

T_t (3.5) 6:15 c

P_s (3.5) 5:15 a

T_t (3.5) 5:45 d

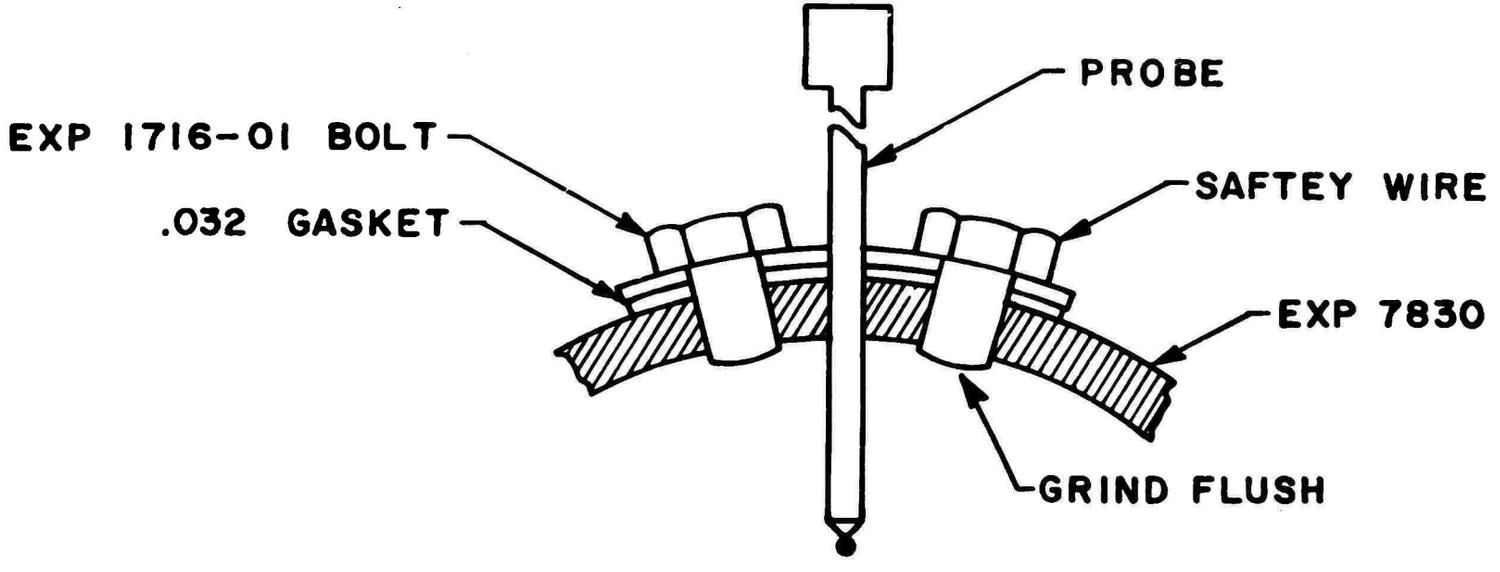

PROBE MOUNTING TECHNIQUE

PROBES

STATIC PRESSURE	PSK 8671-02
TOTAL PRESSURE	FIGURE 98
TOTAL TEMP.	FIGURE 98

Figure 99. Station 3.5 Instrumentation.

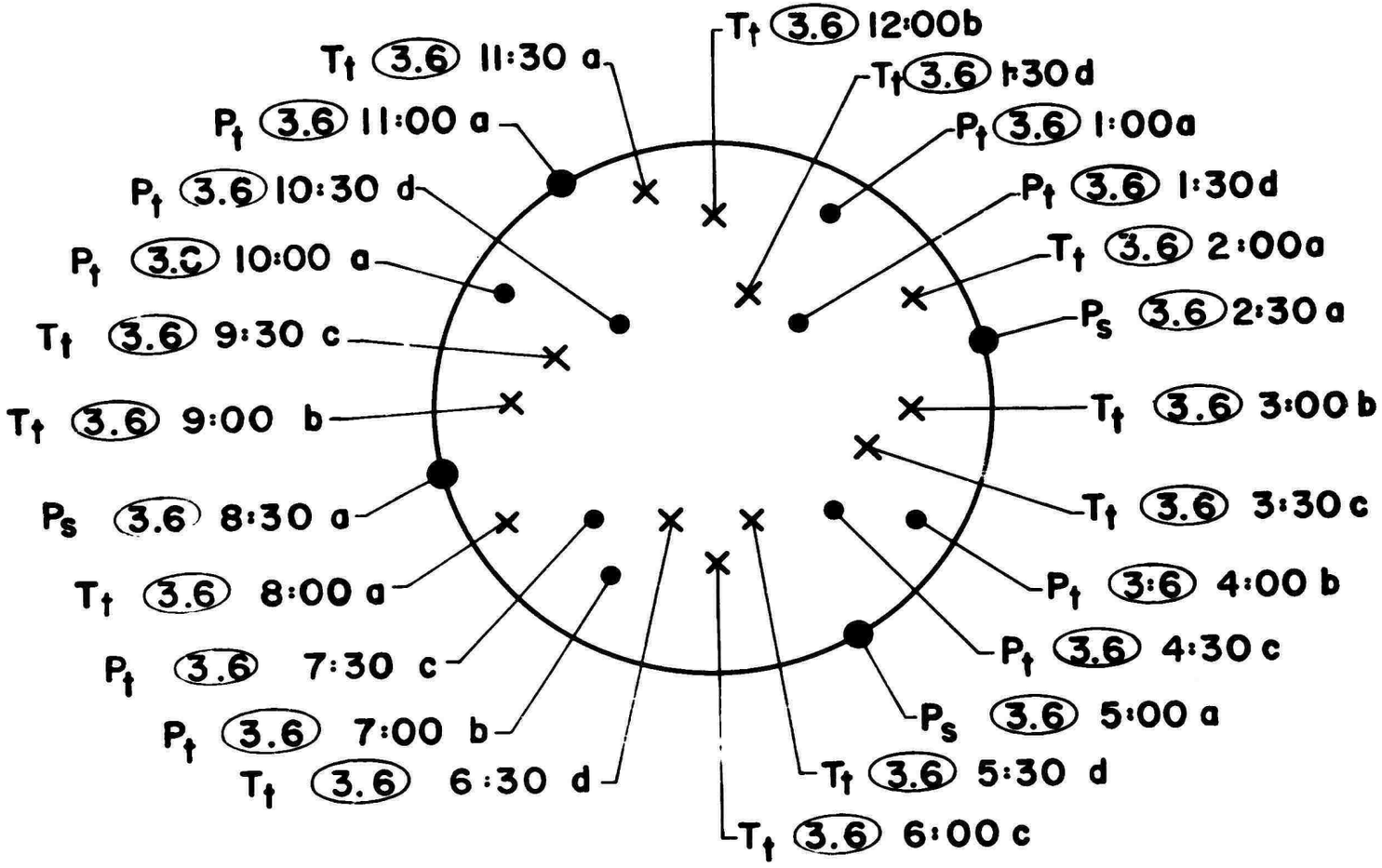
T_f 3.6 12:00b
T_f 3.6 11:30 a
T_f 3.6 1:30 d
P_f 3.6 11:00 a
P_f 3.6 1:00a
P_f 3.6 10:30 d
P_f 3.6 1:30d
P_f 3.C 10:00 a
T_f 3.6 2:00a
T_f 3.6 9:30 c
P_s 3.6 2:30 a
T_f 3.6 9:00 b
T_f 3.6 3:00 b
P_s 3.6 8:30 a
T_f 3.6 3:30 c
T_f 3.6 8:00 a
P_f 3:6 4:00 b
P_f 3.6 7:30 c
P_f 3.6 4:30 c
P_f 3.6 7:00 b
P_s 3.6 5:00 a
T_f 3.6 6:30 d
T_f 3.6 5:30 d
T_f 3.6 6:00 c

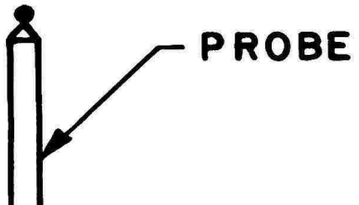
PROBE

EXP 1716-02

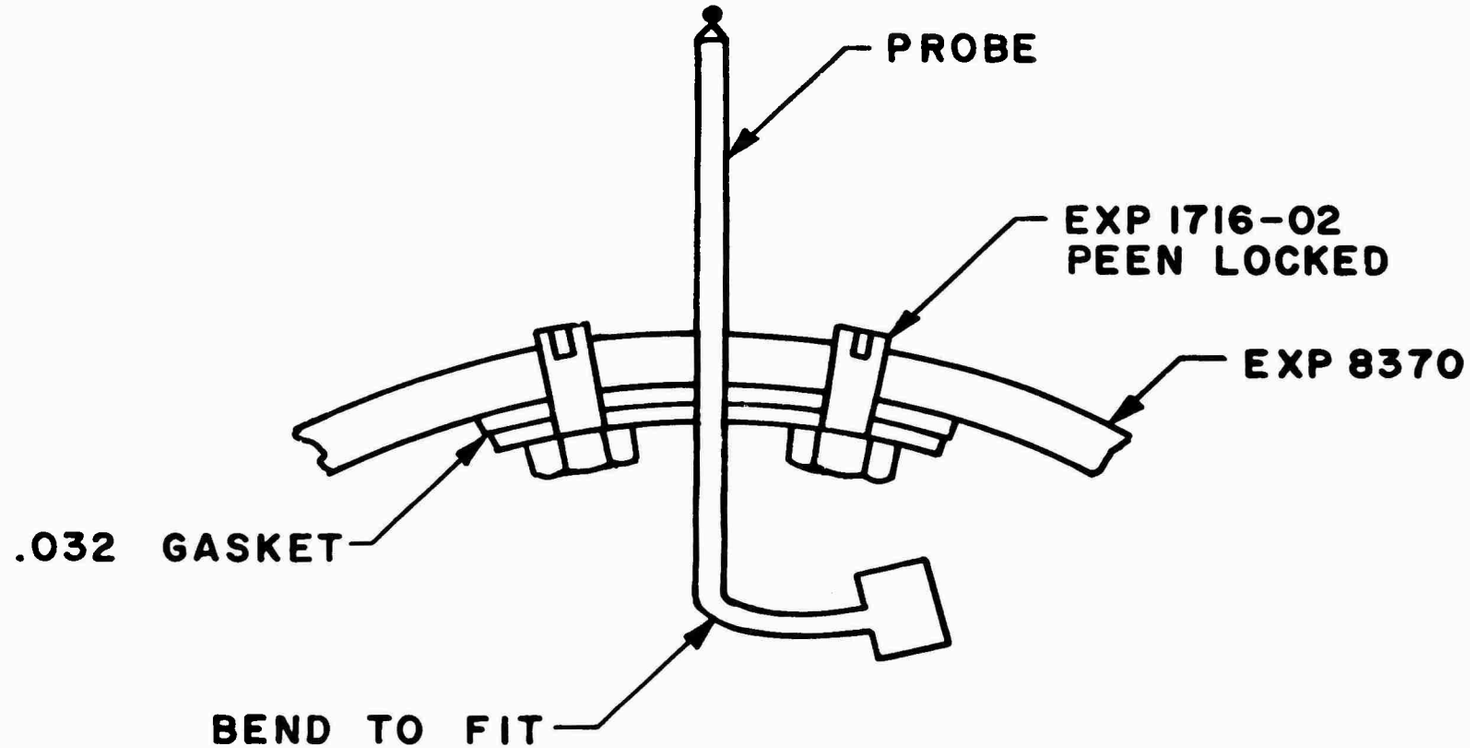

PROBE MOUNTING TECHNIQUE

PROBES

STATIC PRESSURE PSK 8672

TOTAL PRESSURE

TOTAL TEMP.

FIGURE 98

Figure 100. Station 3.6 Instrumentation.

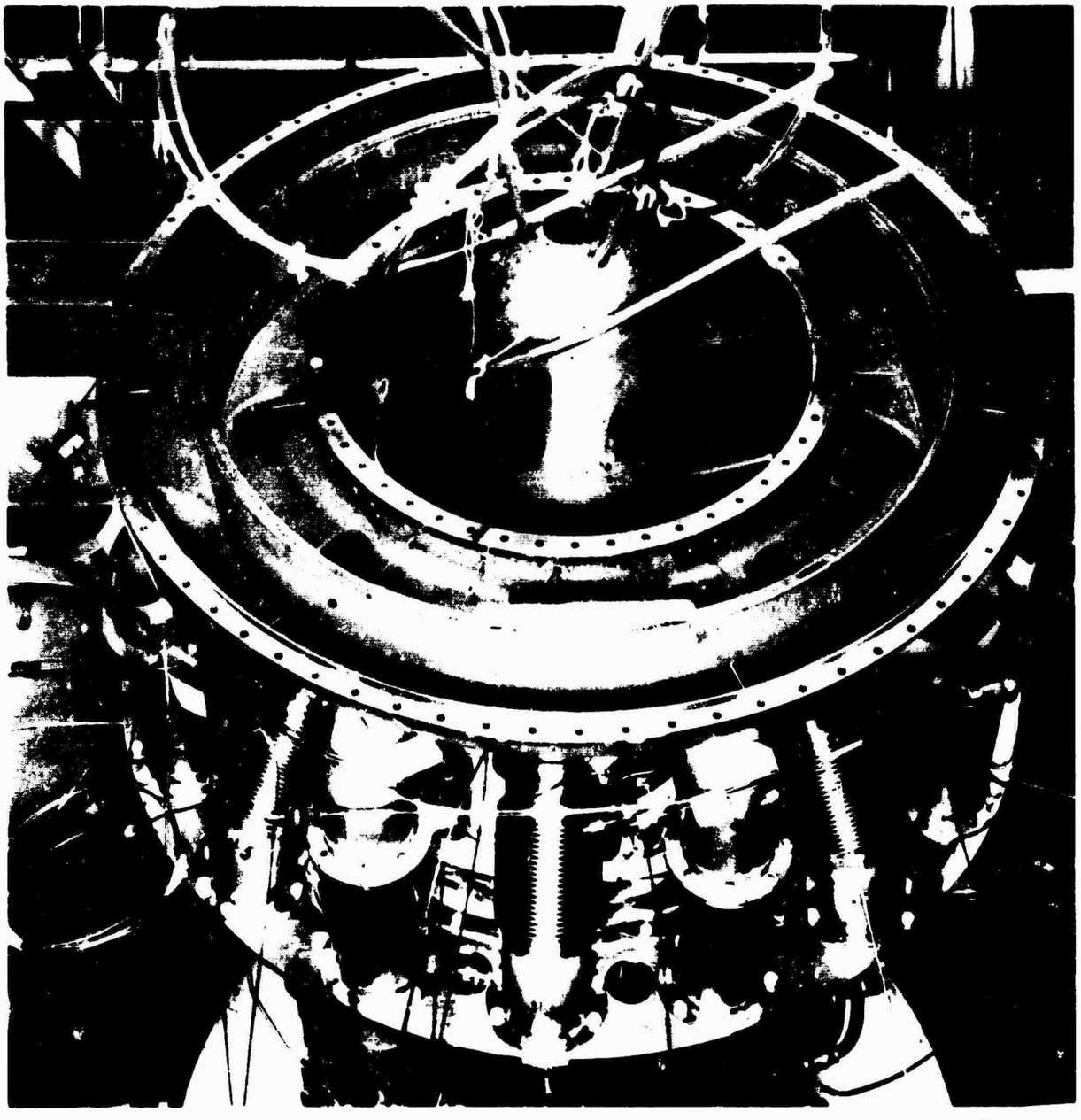

Figure 101. View of Instrumentation at Stations 3.5, 3.6, and 9.6.

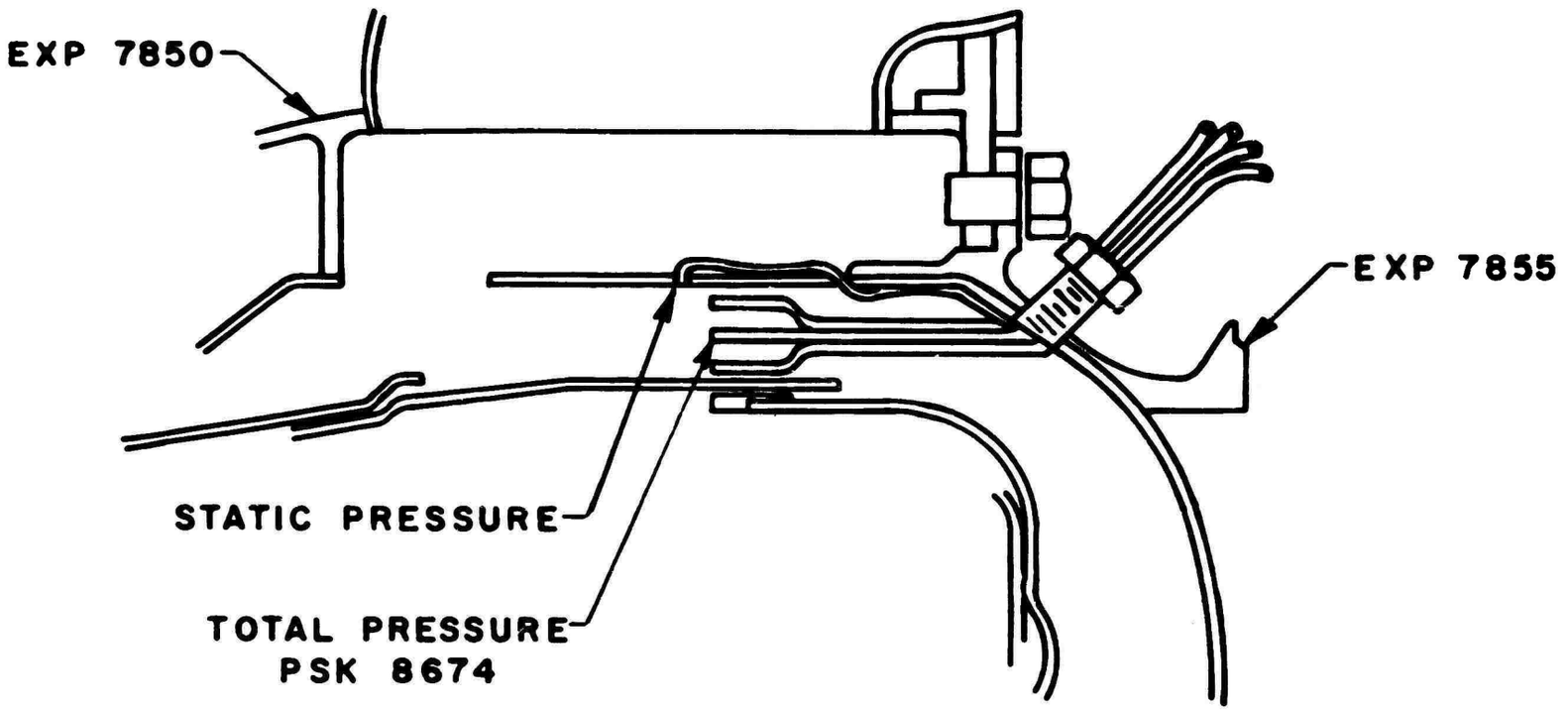
EXP 7850
EXP 7855
STATIC PRESSURE
TOTAL PRESSURE
PSK 8674

A

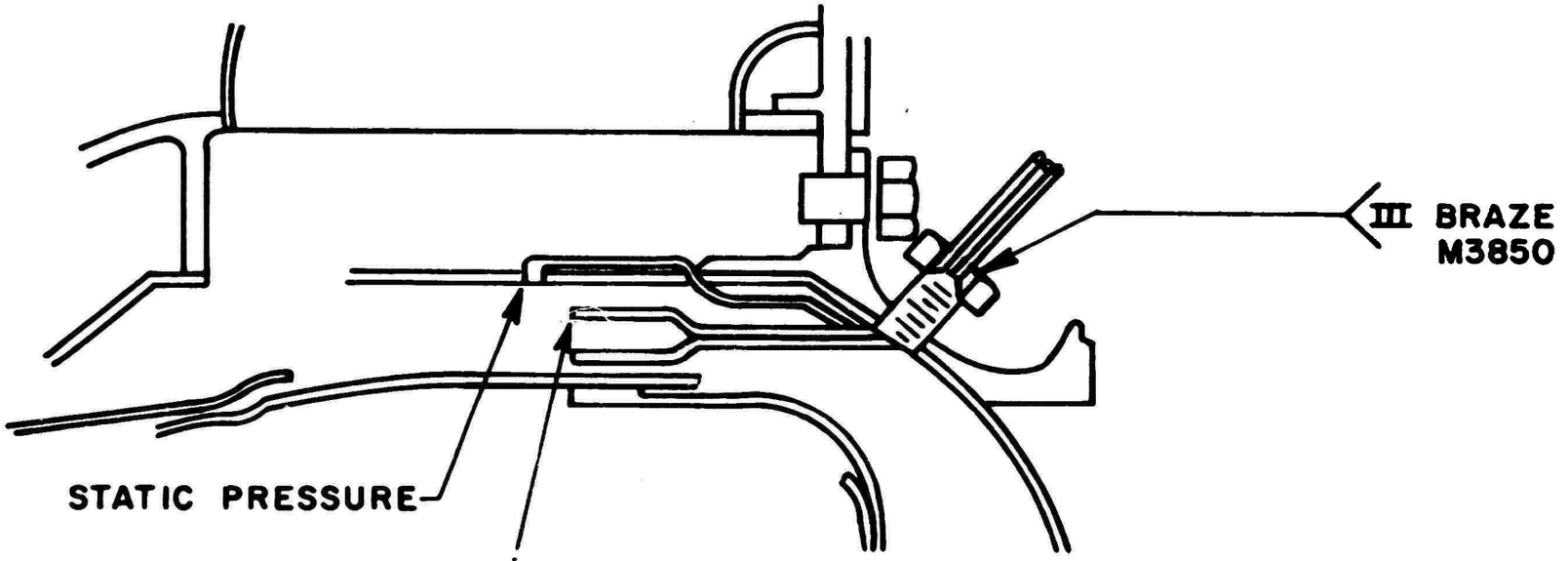
III BRAZE
M3850
STATIC PRESSURE

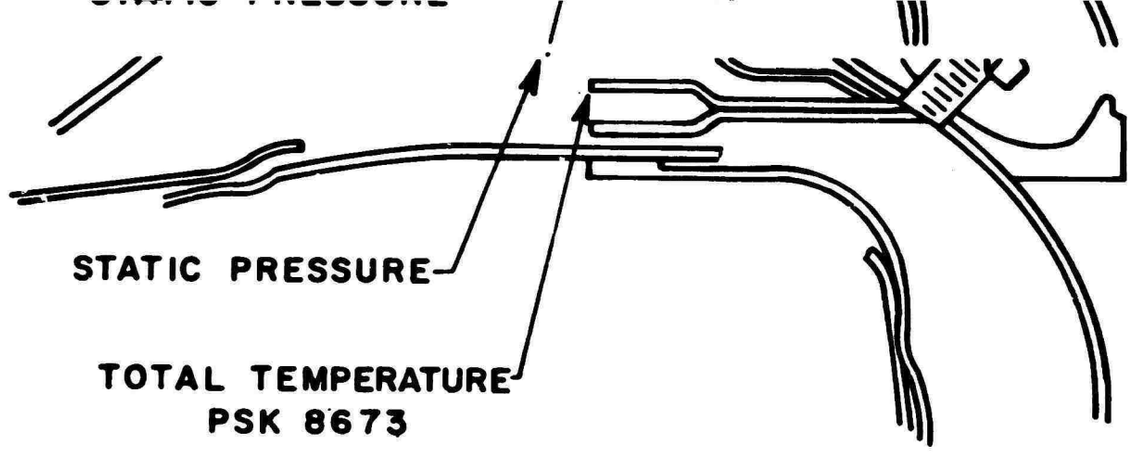

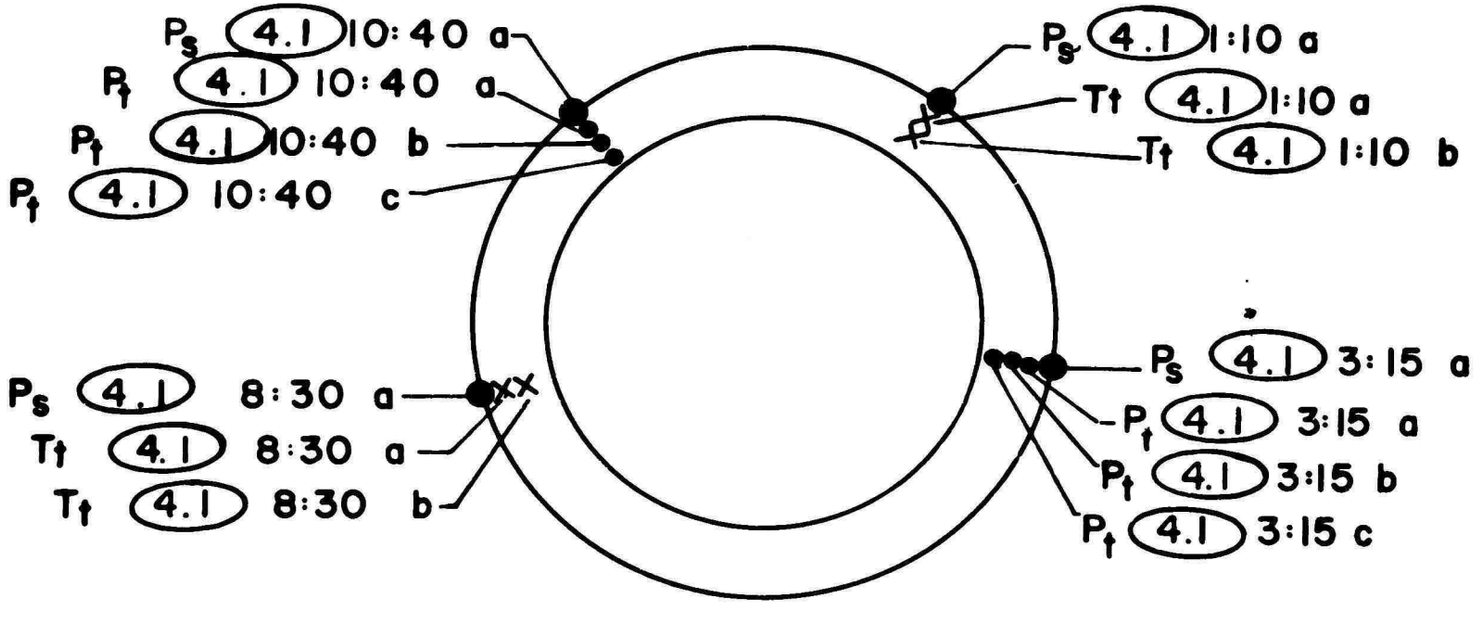

Figure 102. Station 4.1 Instrumentation.

The radial spacing of the instrumentation is given in Table 18.

TABLE 18
STATION 4.1 - INSTRUMENTATION RADIAL SPACING

Probe	Radius Change Measured from Outer Wall (in.)
T_t (4.1) 1:10 a	0.200
T_t (4.1) 1:10 b	0.375
T_t (4.1) 8:30 a	0.200
T_t (4.1) 8:30 b	0.375
P_t (4.1) 3:15 a	0.150
P_t (4.1) 3:15 b	0.300
P_t (4.1) 3:15 c	0.400
P_t (4.1) 10:40 a	0.125
P_t (4.1) 10:40 b	0.275
P_t (4.1) 10:40 c	0.400
Outer Wall Radius = 11.235 in.	
Combustor Wall Radius = 10.737 in.	
Channel Height = 0.498 in.	

9.2.8 Station 5.0 - Turbine Inlet Temperature (T_{t5})

This plane contains the standard six-probe T_{t5} harness (PN 19070) mounted in the combustion curl deflector.

9.2.9 Station 9.5 - Exhaust Gas Temperature (T_{t9})

This plane contains the T53-L-11 engine standard T_{t9} harness assembly (GE 5469087-G5).

9.2.10 Station 9.6 - Exit Exhaust Diffuser

The instrumentation for this station consists of three inner and four outer-wall static pressure probes and three pressure-temperature rakes (Figure 103). Each rake consists of eight stagnation pressure probes and four stagnation temperature probes mounted from the inner exhaust tailcone. The pressure and temperature leads are brought out through Conax fittings mounted in the modified end pan (PSK 8760).

9.2.11 Station 9.7 - Regenerator Entrance Gas Side

The regenerator core is divided axially into seven radial compartments. At the entrance of each compartment are three temperature probes and three total pressure probes. The instruments are located circumferentially by means of three rakes mounted from the modified end-pan and supported at the front end by three special core mounting bolts. Figure 104 shows the details for the assembly. Instrument nomenclature is given in Table 19.

Upon closure of the modified end-pan, a viewing port allows the small adjustments necessary to facilitate the probe installation (PSK 8764). The final operation involves the threading of Conax fittings over the instrumentation leads from the inner exhaust tailcone (PSK 8684). A special Conax lava sealant requires replacement during each installation.

9.2.12 Station 10 - Exit Plane of Regenerator

This exit plane of the regenerator contains six outer-wall static pressure probes. The exit total pressure is measured by three 9-fingered probes (TE 8754). Exit total temperature distribution is obtained by three 5-fingered probes (TE 8753). Outer- and inner-wall exhaust contours are formed by a cylindrical outer-wall duct (TE 8883) and an inner 12-degree cone extension (TE 8882).

Figure 105 describes the circumferential and radial location and the identification for the probes mounted in this plane.

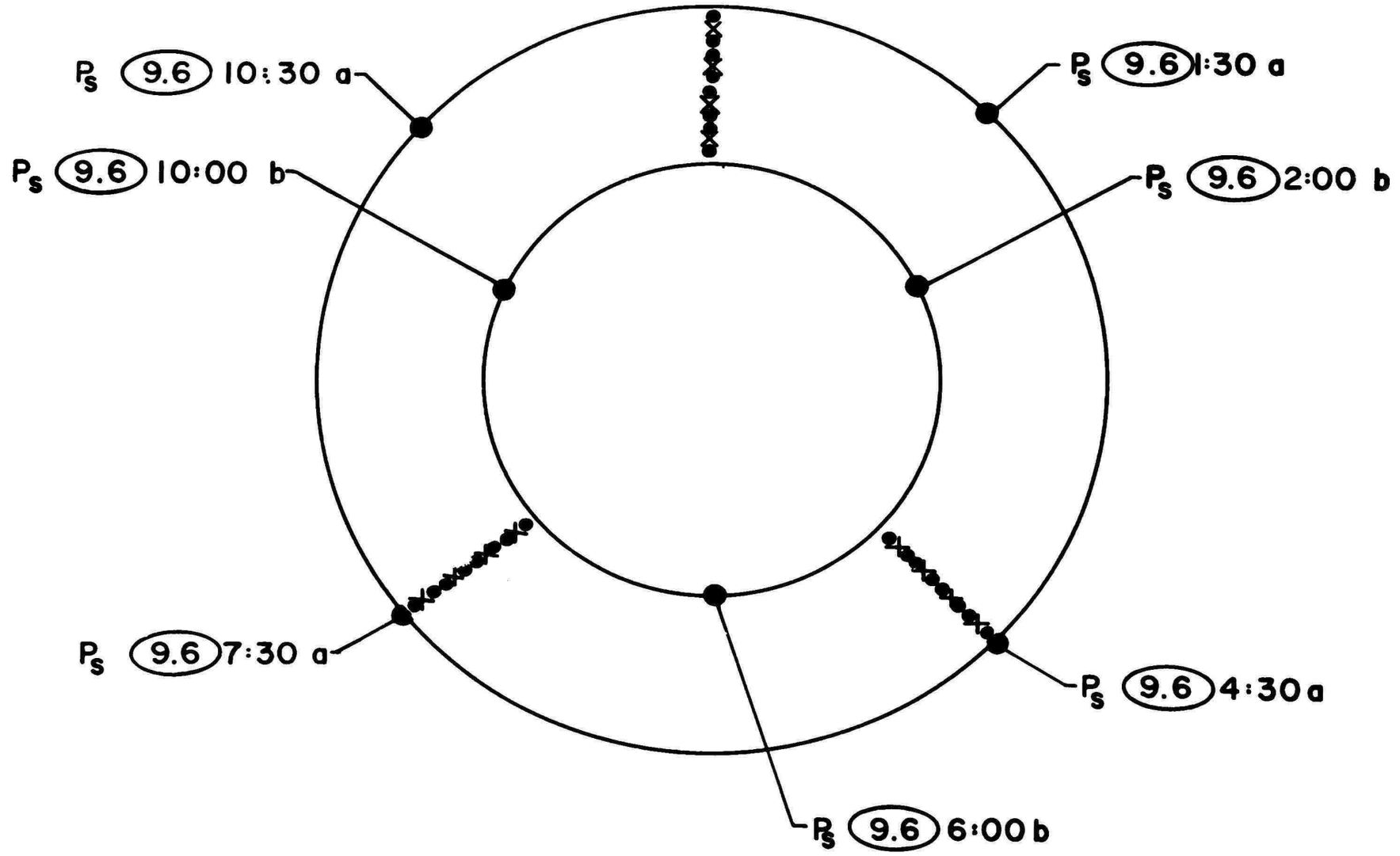

189

RADIUS											
	PROBES										
7.005	P_f	(9.6)	12:00	a	P_f	(9.6)	4:30	a	P_f	(9.6)	7·30 a
6.725	T_f	"	"	a	T_f	"	"	a	T_f	"	" a
6.530	P_f	"	"	b	P_f	"	"	b	P_f	"	" b

6.530	P_t	"	"	b	P_t	"	"	b	P_t	"	"	b					
6.055	P	"	"	c	P	"	"	c	P	"	"	c					

P_s (9.6) 6:00 b

RADIUS	PROBES											
7.005	P_t	(9.6)	12:00	a	P_t	(9.6)	4:30	a	P_t	(9.6)	7·30	a
6.725	T_t	"	"	a	T_t	"	"	a	T_t	"	"	a
6.530	P_t	"	"	b	P_t	"	"	b	P_t	"	"	b
6.055	P_t	"	"	c	P_t	"	"	c	P_t	"	"	c
5.785	T_t	"	"	b	T_t	"	"	b	T_t	"	"	b
5.580	P_t	"	"	d	P_t	"	"	d	P_t	"	"	d
5.005	P_t	"	"	e	P_t	"	"	e	P_t	"	"	e
4.895	T_t	"	"	c	T_t	"	"	c	T_t	"	"	c
4.630	P_t	"	"	f	P_t	"	"	f	P_t	"	"	f
4.155	P_t	"	"	g	P_t	"	"	g	P_t	"	"	g
3.965	T_t	"	"	d	T_t	"	"	d	T_t	"	"	d
3.680	P_t	"	"	h	P_t	"	"	h	P_t	"	"	h

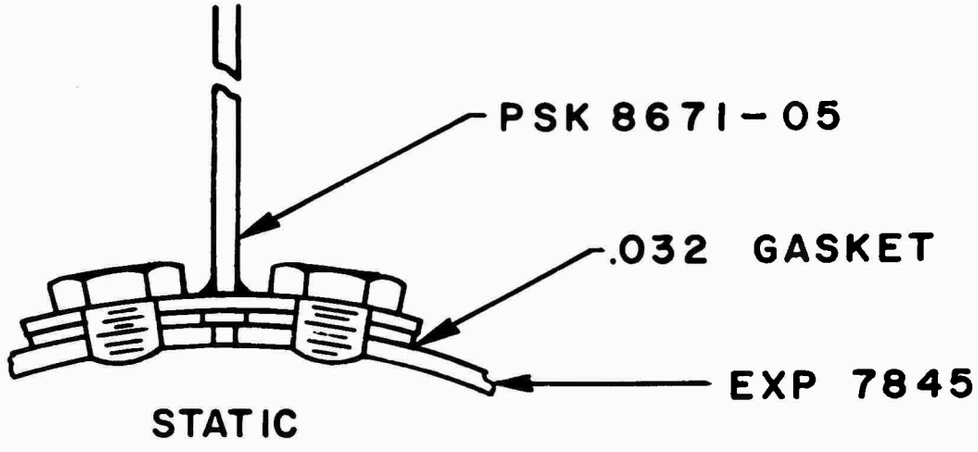

Figure 103. Station 9.6 Instrumentation.

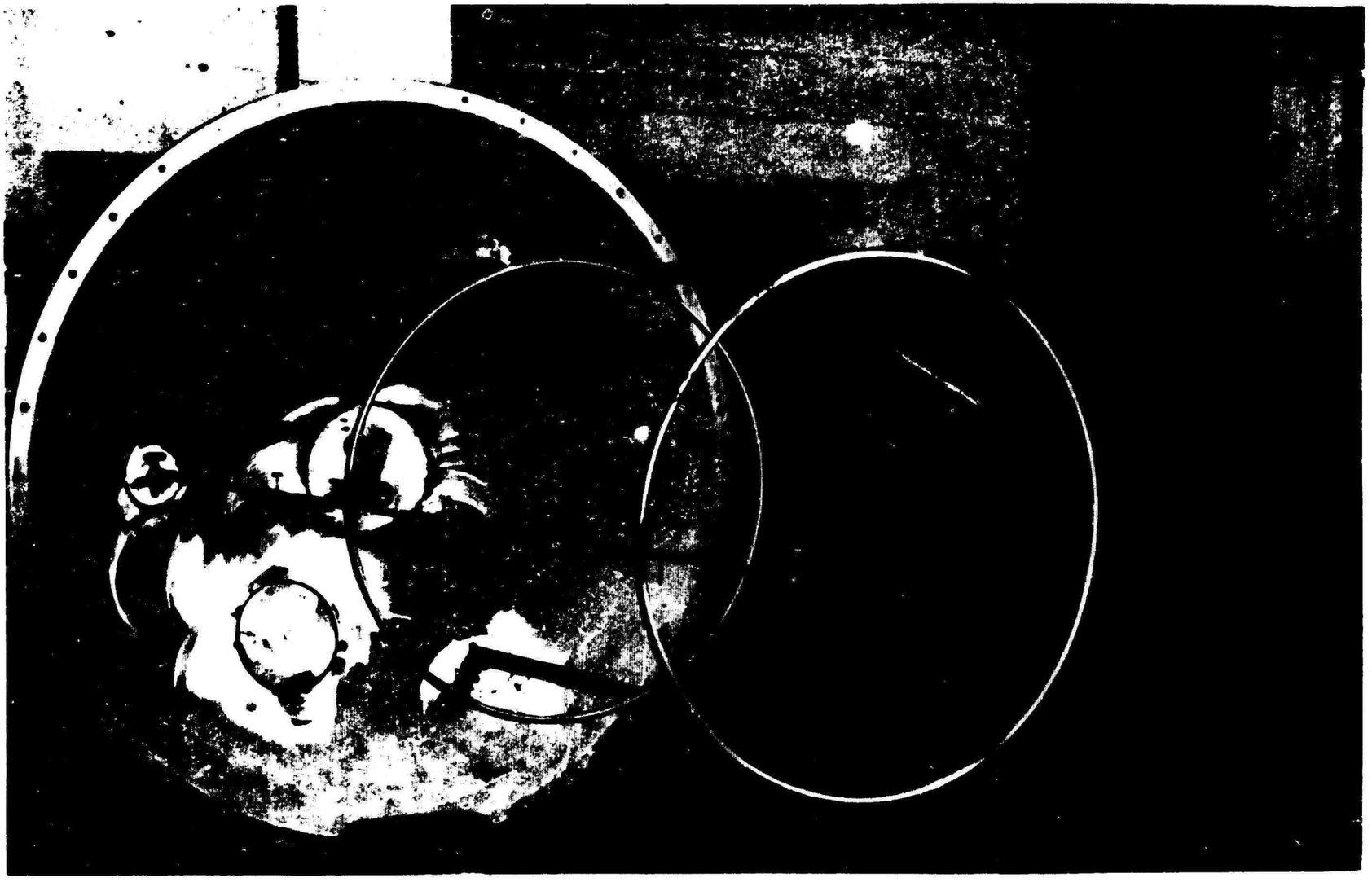

Figure 104. View of Instrument Probes at Station 9.7.

TABLE 19
STATION 9.7 - INSTRUMENT NOMENCLATURE

P_t	9.7	12:00	a	P_t	9.7	4:00	a	P_t	9.7	8:00	a
	9.7		b		9.7		b		9.7		b
	9.7		c		9.7		c		9.7		c
	9.7		d		9.7		d		9.7		d
	9.7		e		9.7		e		9.7		e
	9.7		f		9.7		f		9.7		f
	9.7		g		9.7		g		9.7		g
T_t	9.7	12:00	a	T_t	9.7	4:00	a	T_t	9.7	8:00	a
	9.7		b		9.7		b		9.7		b
	9.7		c		9.7		c		9.7		c
	9.7		d		9.7		d		9.7		d
	9.7		e		9.7		e		9.7		e
	9.7		f		9.7		f		9.7		f
	9.7		g		9.7		g		9.7		g

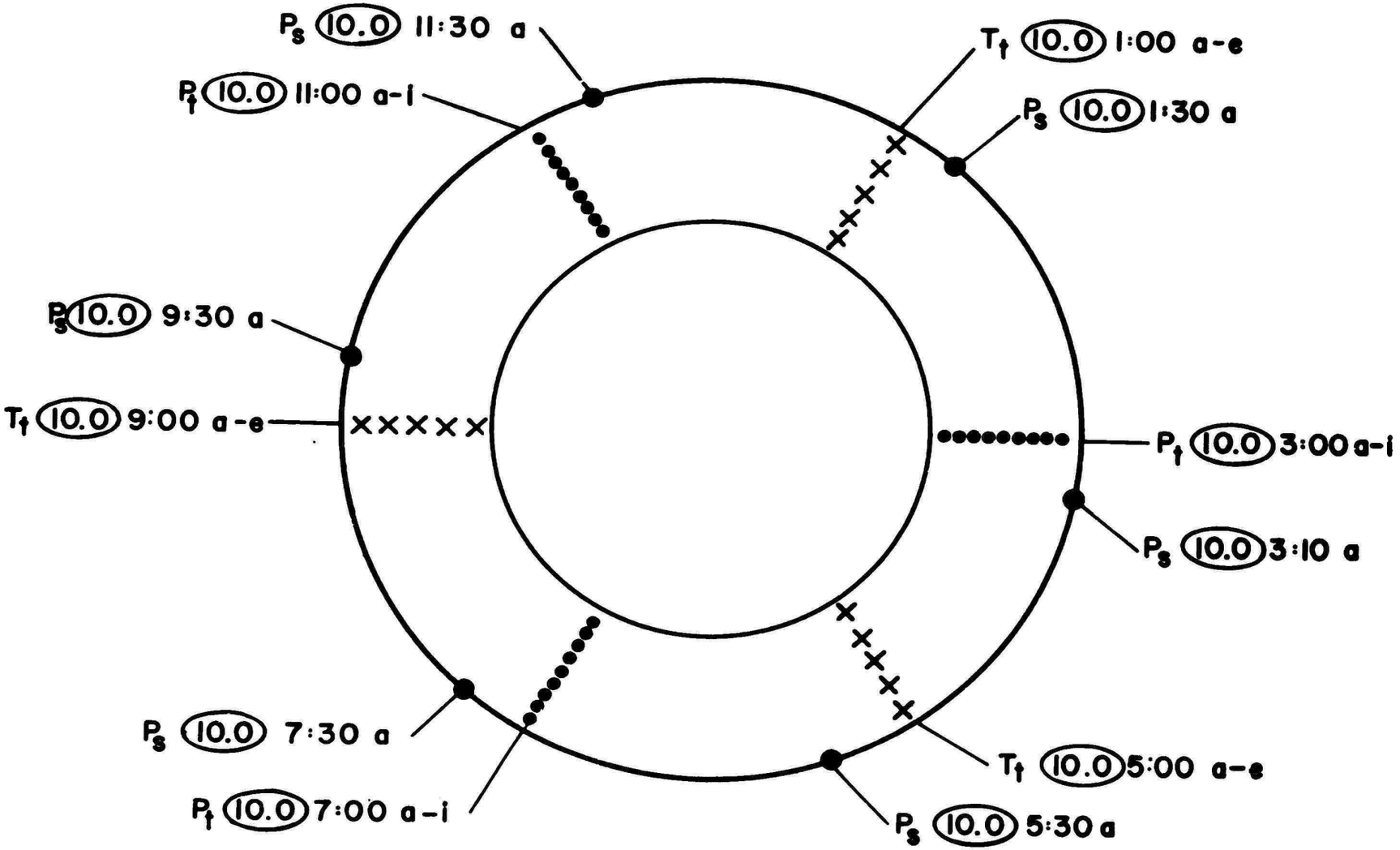

PRESSURE PROBE TE 8754
TEMPERATURE PROBE TE 8753

PROBE	RADIUS
P_t (10.0) 3:00 / 7:00 / 11:00 a	

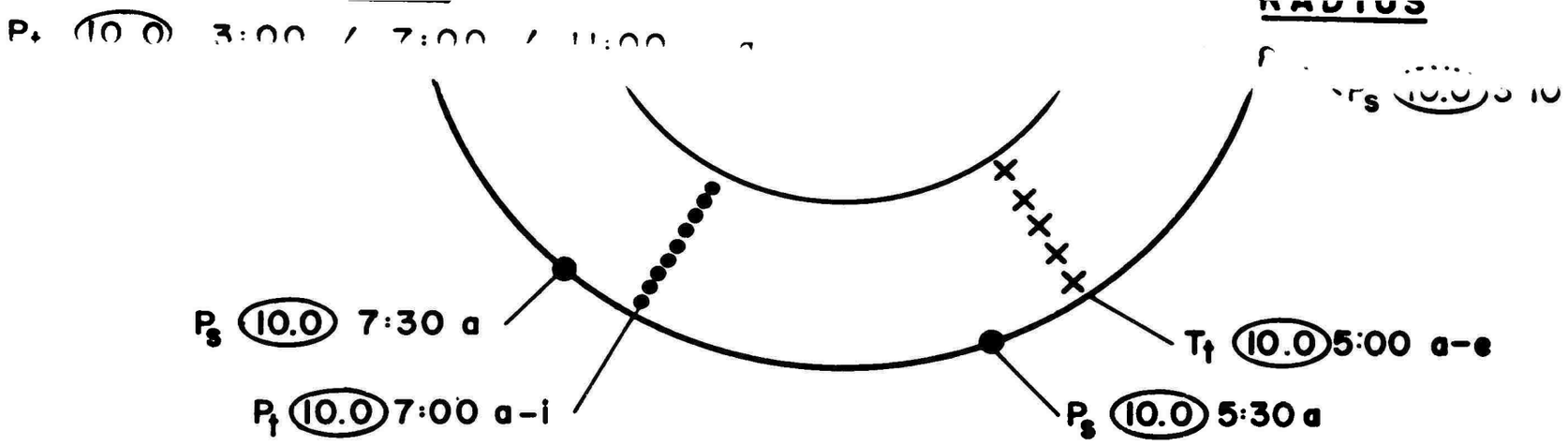

PRESSURE PROBE TE 8754
TEMPERATURE PROBE TE 8753

PROBE					RADIUS	
P_t (10.0)	3:00	/ 7:00	/ 11:00	a	15.830	INCHES
"	"	"	"	b	15.630	"
"	"	"	"	c	15.280	"
"	"	"	"	d	14.940	"
"	"	"	"	e	14.610	"
"	"	"	"	f	14.270	"
"	"	"	"	g	13.950	"
"	"	"	"	h	13.620	"
"	"	"	"	i	13.290	"
T_t (10.0)	1.00	/ 5:00	/ 9:00	a	15.750	INCHES
"	"	"	"	b	15.360	"
"	"	"	"	c	14.750	"
"	"	"	"	d	14.160	"
"	"	"	"	e	13.560	"

Figure 105. Station 10.0 Instrumentation.

SECTION TEN. VEHICLE ASSEMBLY FOR TUBE-TYPE REGENERATOR TEST

The basic engine buildup to the air diffuser was made according to normal T53 assembly procedures. The engine and the interface hardware were assembled with the engine positioned vertically (Figure 106). The regenerator was then assembled to the interface toroidal shell with the engine positioned horizontally (Figure 107). The special fuel and hose assemblies, fuel control temperature probe, and special instrumentation were installed to complete the assembly.

The regenerative engine assembly constitutes an integral structure which is mounted (Figure 108) at three points on the engine: at the two forward mounting pads by a ball and socket connection and a pin connection, respectively, and at the regenerator mountirg flange by a swivel joint connection. The standard engine without regenerator is normally mounted at 3 points on the inlet housing. For the regenerative engine installation, the added cantilevered weight required the deletion of the 12:00 o'clock inlet housing mount and the introduction of a mount at the regenerator mounting flange to preclude undue stress loading of the axial compressor casing.

Only three areas of concern were encountered during the assembly of the unit, all attributed to manufacturing and fabricating discrepancies:

1) The air separator seal assembly of the housing and tube assembly (EXP 7850) was found to be slightly out-of-round. This deviation would have resulted in unfavorable bypass of compressor discharge air into the combustion area. To remedy the problem the air separator seal assembly was reworked to provide the desired sealing capability.

2) The retainer and inner seal flange support of the toroidal shell assembly (EXP 7830) was found to be slightly eccentric. To resolve this condition, the AiResearch divider assembly (P/N 179899) was reworked.

3) Buckling of the regenerator outer shell became evident prior to installation of the unit. Twelve buckling waves ran the total length of the shell and were most pronounced between the two stiffener rings. Review of the problem disclosed that lack of proper shell stress relieving during manufacture resulted in this stress rippling of the outer shell. Performance of the regenerator assembly is not expected to be adversely affected.

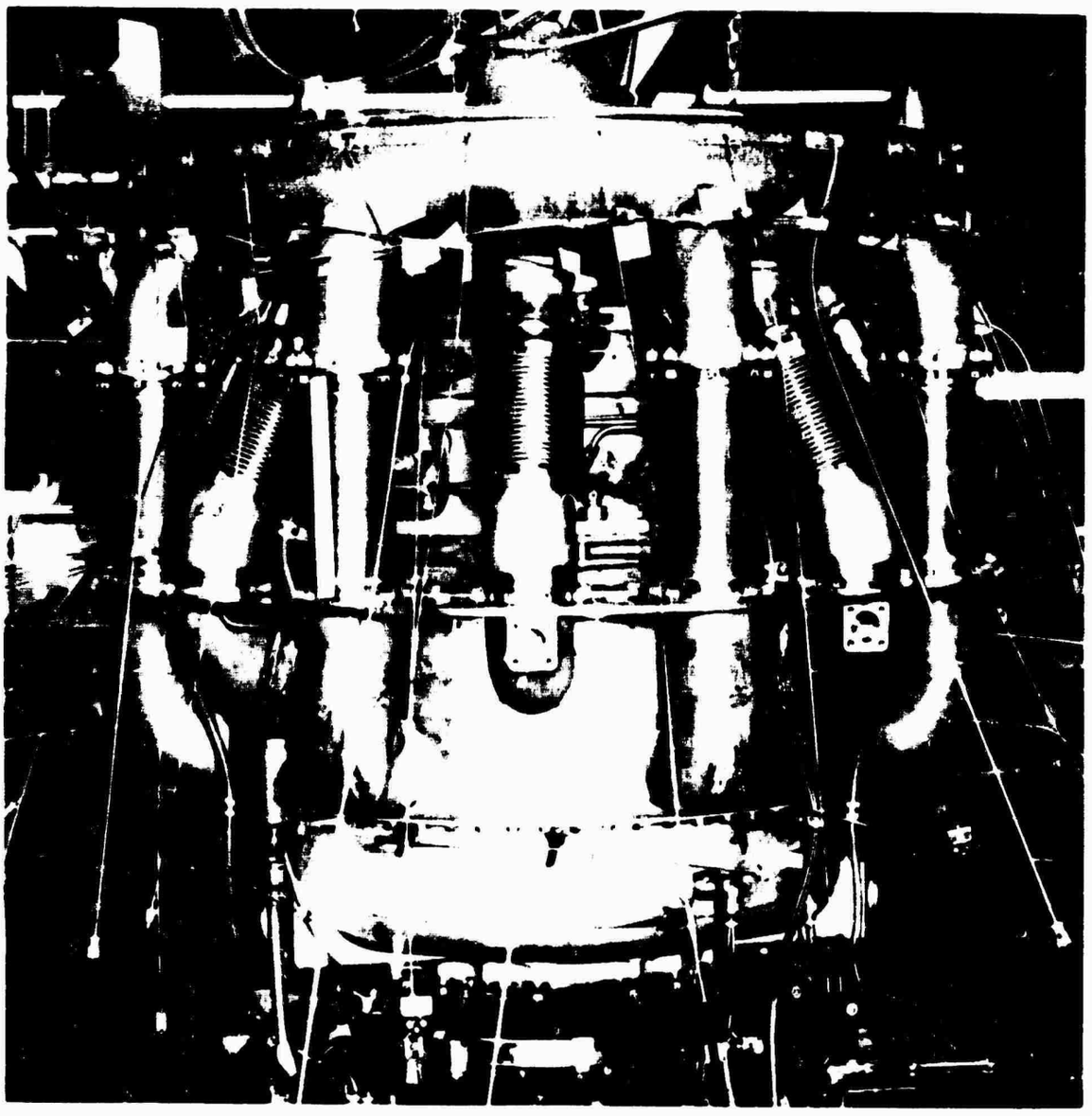

Figure 106. Engine Interface Hardware Assembly.

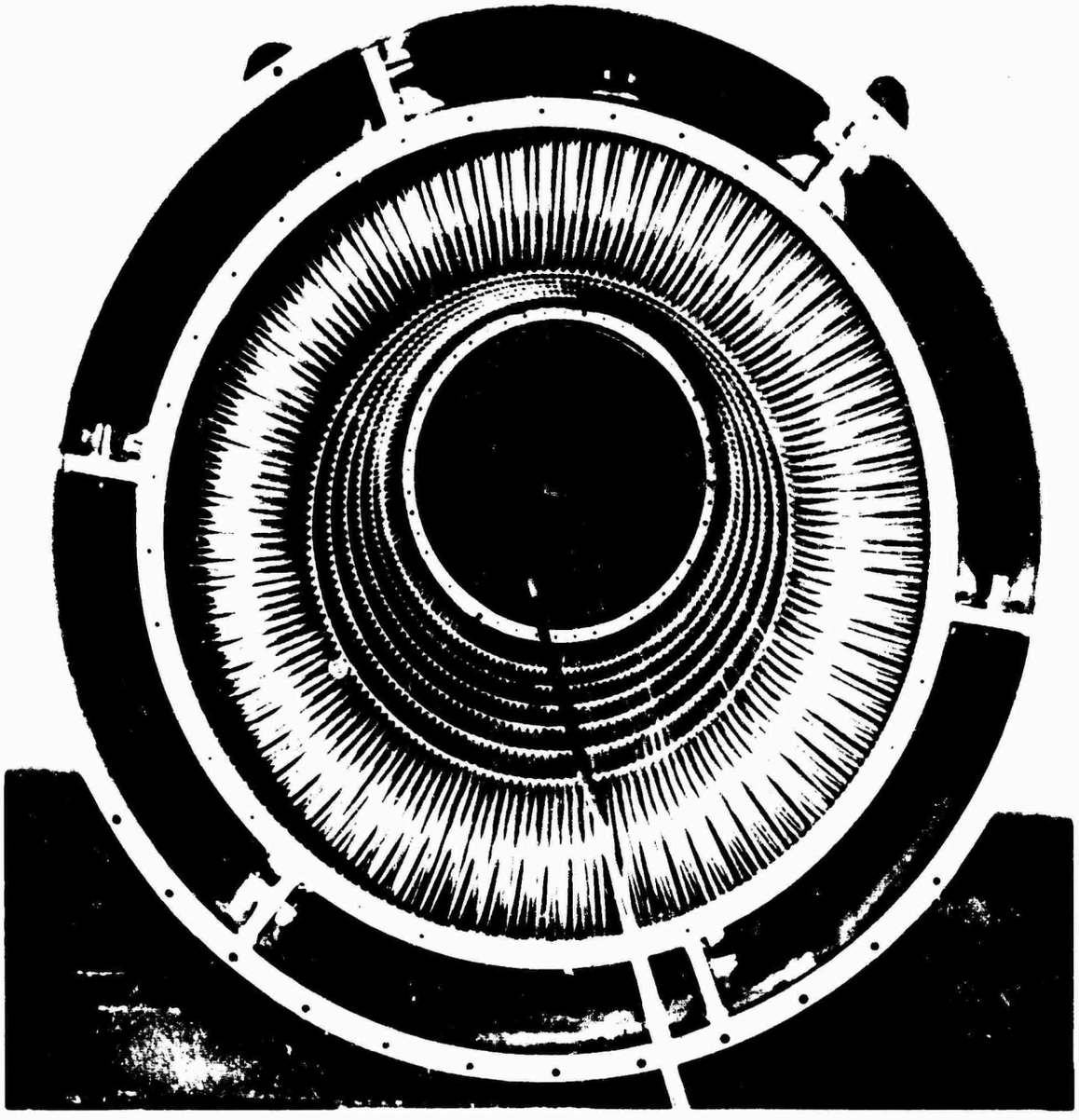

Figure 107. Regenerator Assembly; Aft View.

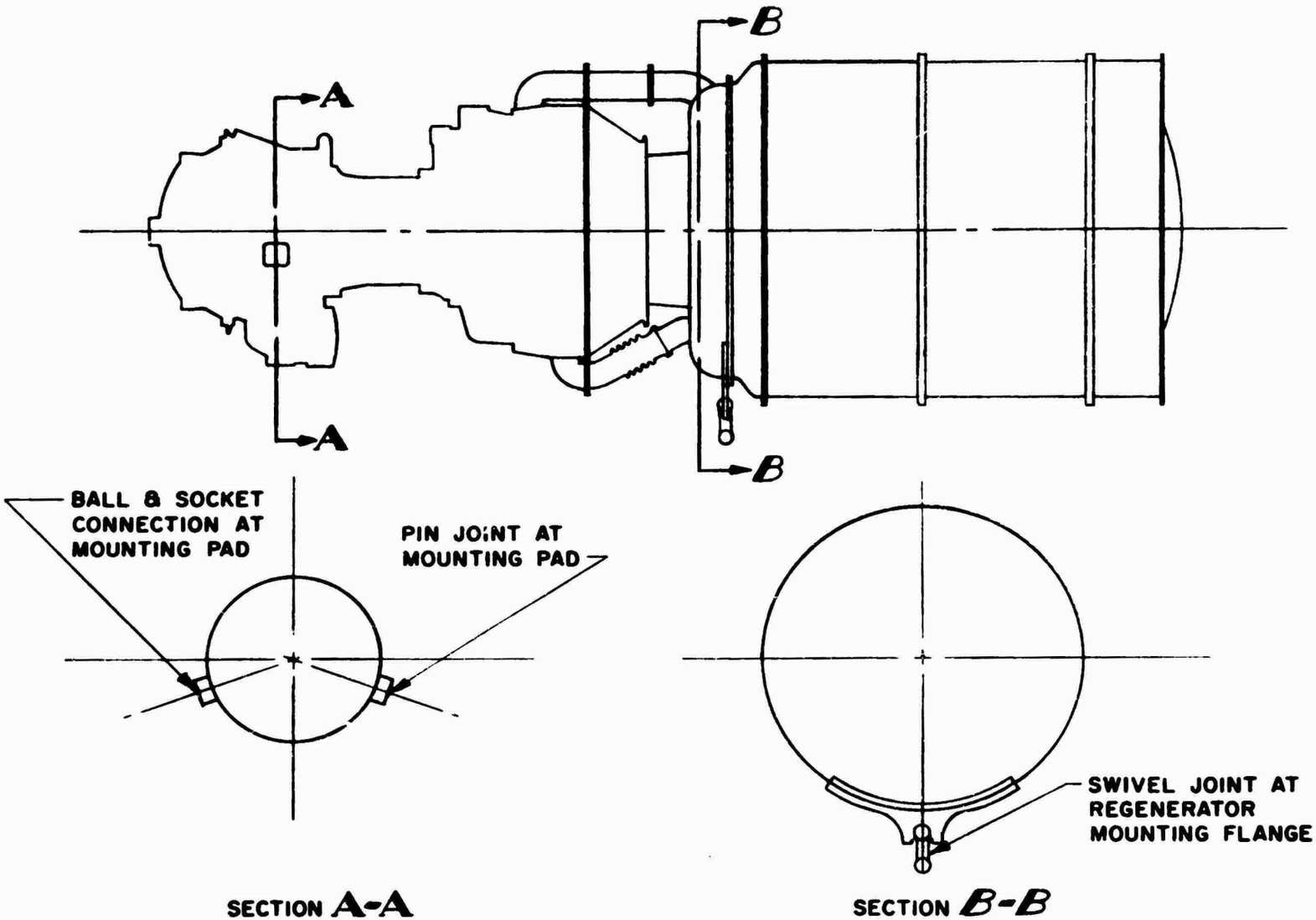

Figure 108. Regenerative Engine; Mounting Arrangement.

The entire engine-regenerator assembly (Figure 109) was weighed, and the weight was found to be distributed as follows:

	Weight (lb)
Basic T53-L-11 Engine	487
Instrumentation	38
Interface Hardware*	99
Regenerator	224
Total	848

It is estimated that a potential weight savings of 26 pounds may be realized by:

1) Eliminating the additional flange material on the toroidal shell assembly that was required for instrumentation attachment.

2) Reducing the 0.070-inch oversize dimension of the housing and tube assembly vertical flange thickness.

3) Rescinding the requirement for removal of the outer shell for core inspection and cleaning. The forward outer shell flange could then be eliminated with a resultant weight savings.

4) Using exotic materials.

5) Using smaller diameter tubing.

The potential weight of the uninstrumented regenerator-engine system would therefore be 784 pounds. The complete regenerative engine assembly is shown in Figure 110.

---

* Interface hardware is defined as modified engine hardware and additional engine hardware necessary to adapt and mount the regenerator. No standard engine hardware is included. All interface hardware is itemized in Appendix III.

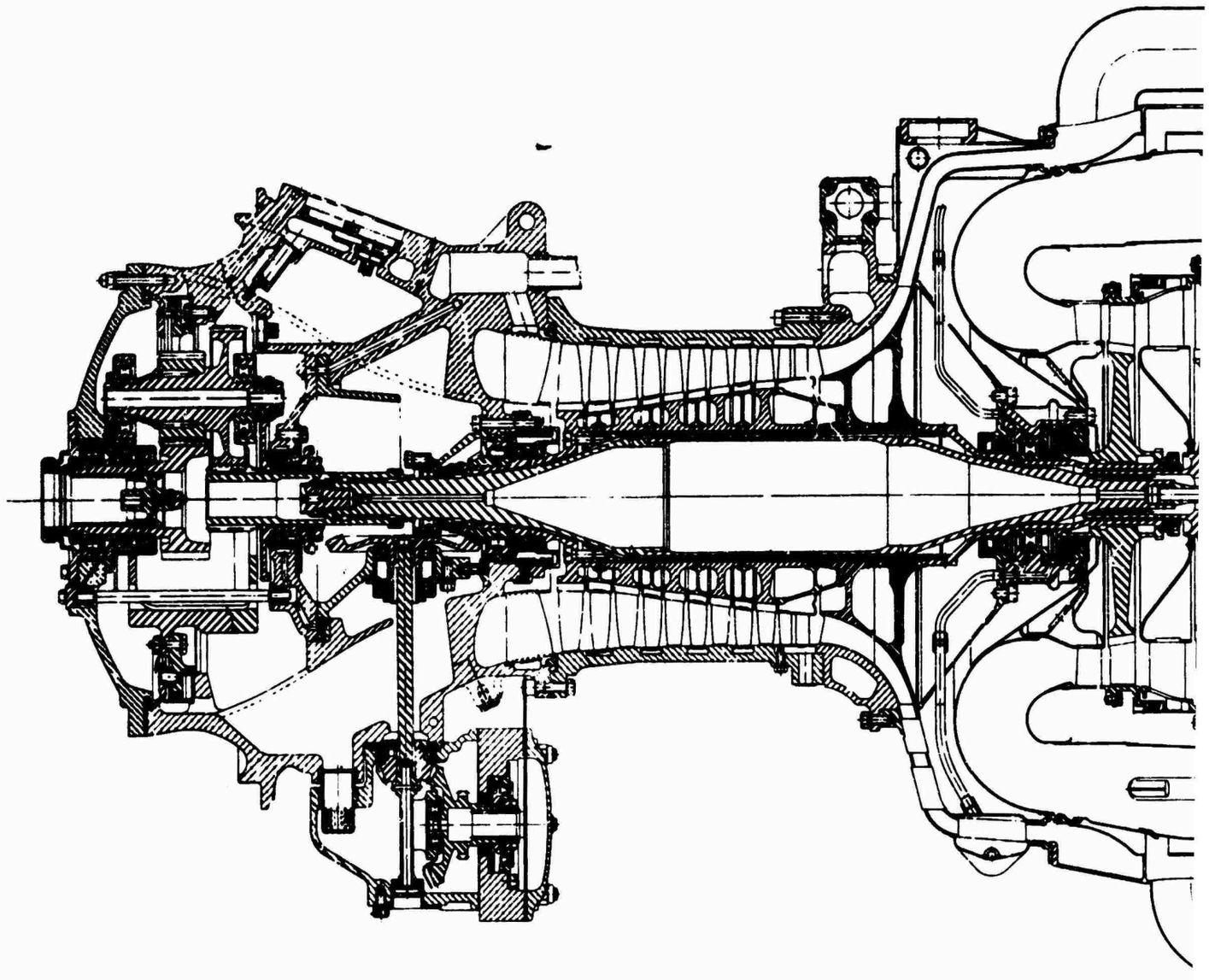

Fig

A

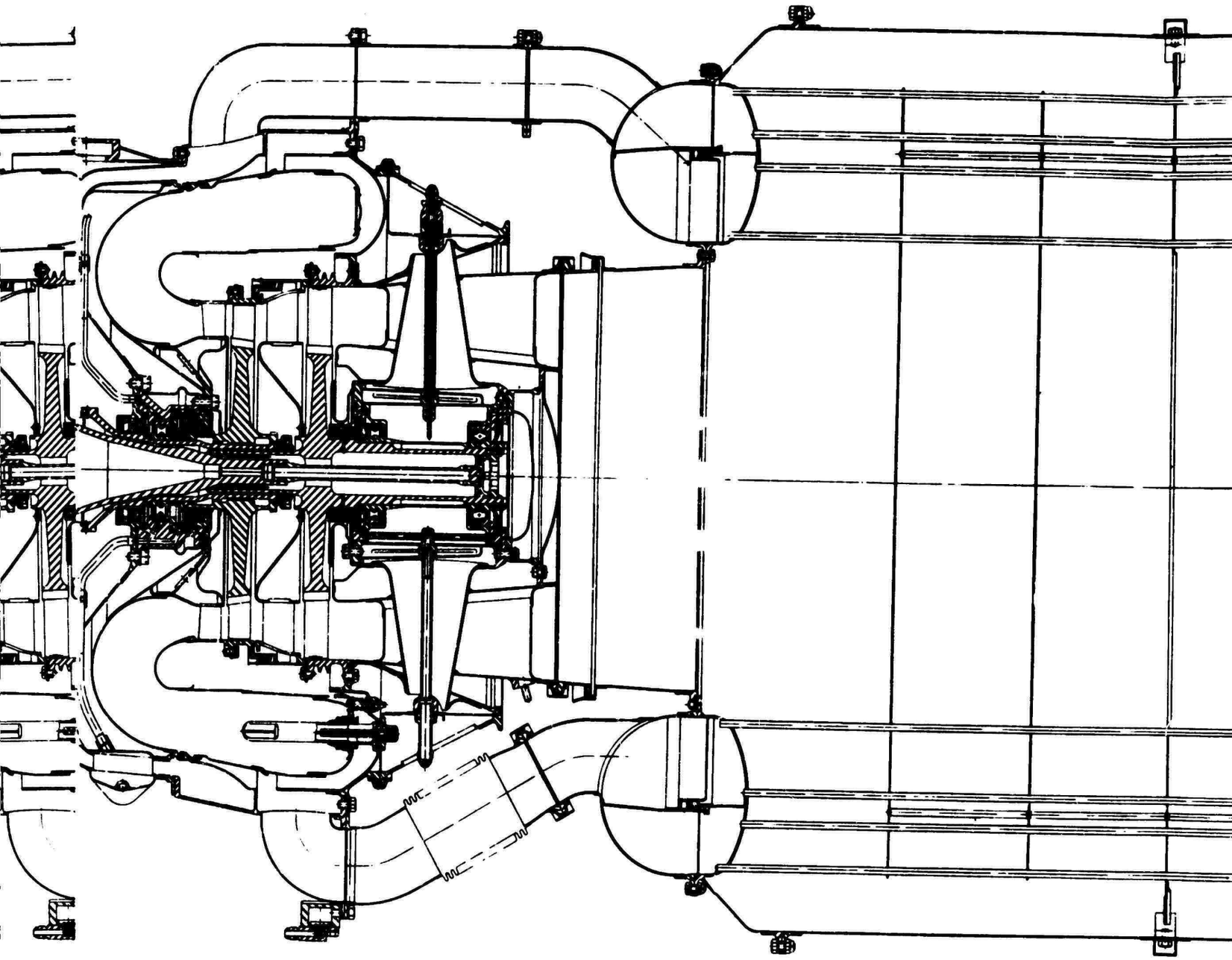

Figur

Figure 109. Regenerative Engine; Assembly Drawing.

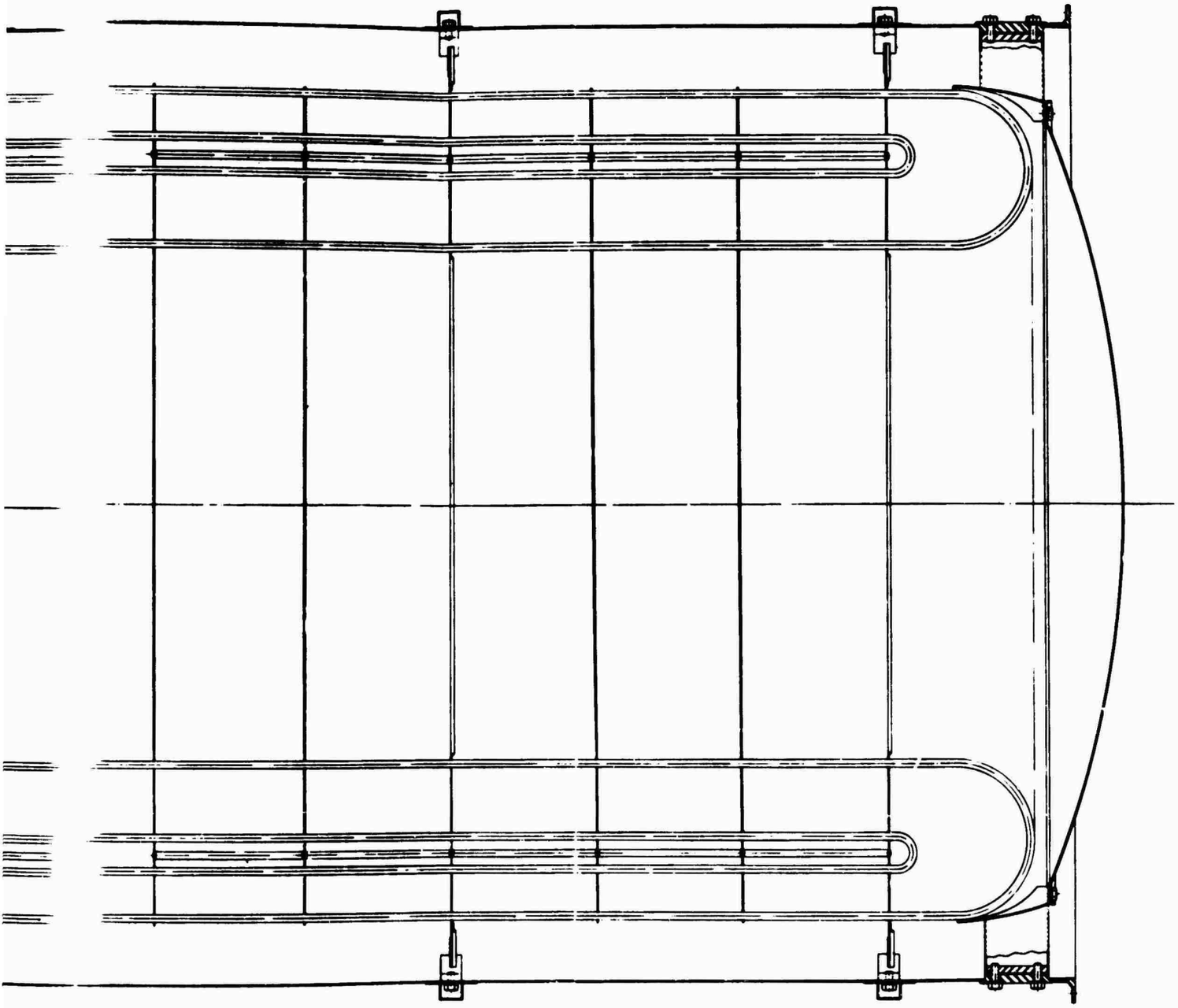

rawing.

C

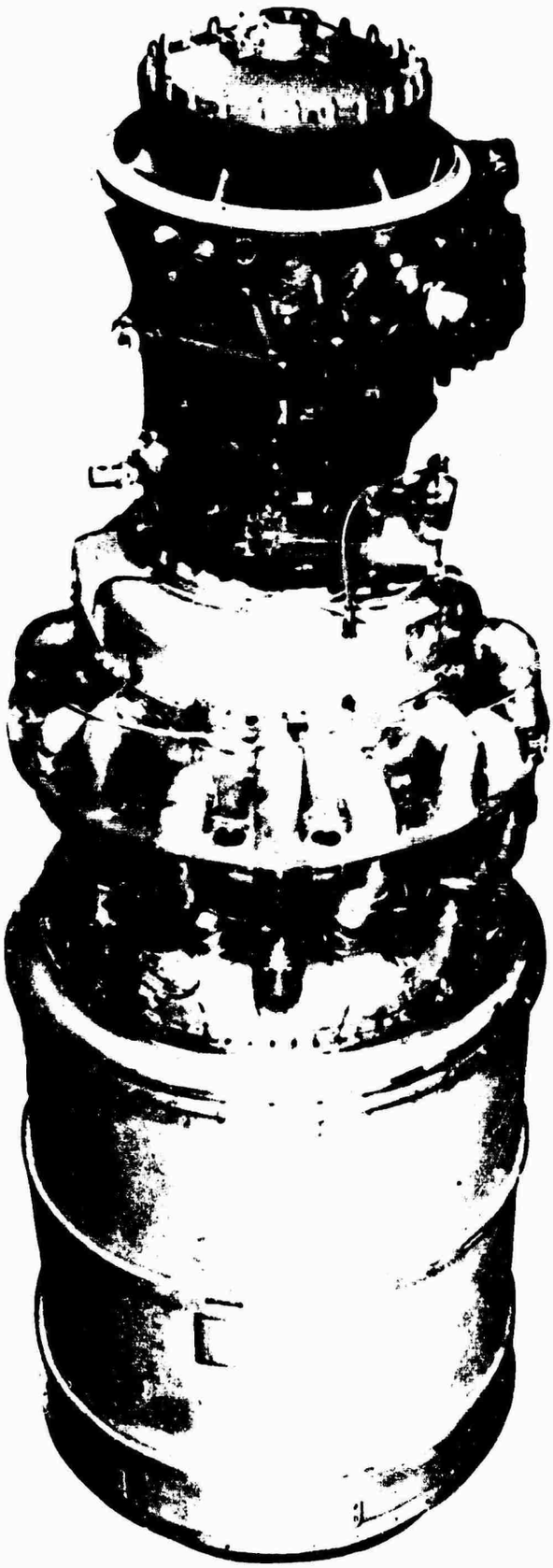

Figure 110. Regenerative Engine; External View.

BIBLIOGRAPHY

1) Eckert, E. R. G., Introduction to the Transfer of Heat and Mass, McGraw-Hill Book Co., New York, 1950

2) Giedt, W. H., Principles of Engineering Heat Transfer, D. Von Nostrand Co., Princeton, New Jersey, 1958

3) Kays, W. M. and London, A. L., Compact Heat Exchangers, The National Press, Palo Alto, California, 1958

4) Keenan, J. H., and Keys, F. G., Gas Tables, John Wiley and Sons, Inc., London, 1947

5) Kays, W. M., Loss Coefficients for Abrupt Changes in Flow Cross Section With Low Reynolds Number Flow in Single and Multiple-Type Systems, A. S. M. E. Paper No. 50-57, November 1949

6) Stevens, R. A., Fernandey, J., and Wolf, J. R., Mean Temperature Difference in One, Two, and Three-Pass Crossflow Heat Exchangers, Condensed from A. S. M. E. Papers Nos. 55-A89 and 55-A90, August 1955

7) Aero-Space Applied Thermodynamics Manual, Society of Automotive Engineers, Inc., Committee A-9, New York, January 1962.

8) Parametric Study Recuperator Designs Lycoming T53 Engine, AiResearch Engineering Discussion SRSJ 3499-0513, 15 May 1963

9) Engineering Discussion AiResearch Recuperator 178515-1-1, AiResearch Engineering Discussion SRSJ 3611-0621, 21 June 1963

DISTRIBUTION

US Army Materiel Command	1
US Army Mobility Command	1
US Army Aviation Materiel Command	6
US Army Aviation Materiel Laboratories	22
US Army Engineer R&D Laboratories	3
US Army Tank-Automotive Center	1
Air Force Systems Command, Wright-Patterson AFB	1
Bureau of Ships, D/N	1
Bureau of Naval Weapons	1
NASA Representative, Scientific and Technical Information Facility	2
National Aeronautics and Space Administration, RAP	1
Defense Documentation Center	20

APPENDIX I

SPECIFICATION 105.23.1 FOR GAS TURBINE REGENERATOR FOR LYCOMING T53 ENGINE

4 September 1962

1. SCOPE

This specification covers the detail requirements for the design and performance of a regenerator (integrated heat exchanger) for a turboshaft engine. The design objective for this unit is to produce a maximum saving in the engine fuel consumption with minimum penalty in weight.

2. APPLICABLE SPECIFICATIONS

2.1 The following military specification forms a part of this model specification, except as modified herein.

SPECIFICATION	
Military Specification -	
MIL-E-8593 3 September 1952	Engines, Aircraft Turboprop General Specification for

2.2 The following documents of the issue in effect on the date specified and the publications listed in the applicable sections of ANA Bulletin 343n dated 14 December 1960 entitled "Specifications and Standards Applicable to Aircraft Engines and Propellers, Use of" form a part of this specification.

DOCUMENT	TITLE
MIL-E-005272B 5 July 1957	Environmental Testing, Aeronautical and Associated Equipment, General Specification for
ANA 407	Engines, Turbojet, Design and Installation Criteria for

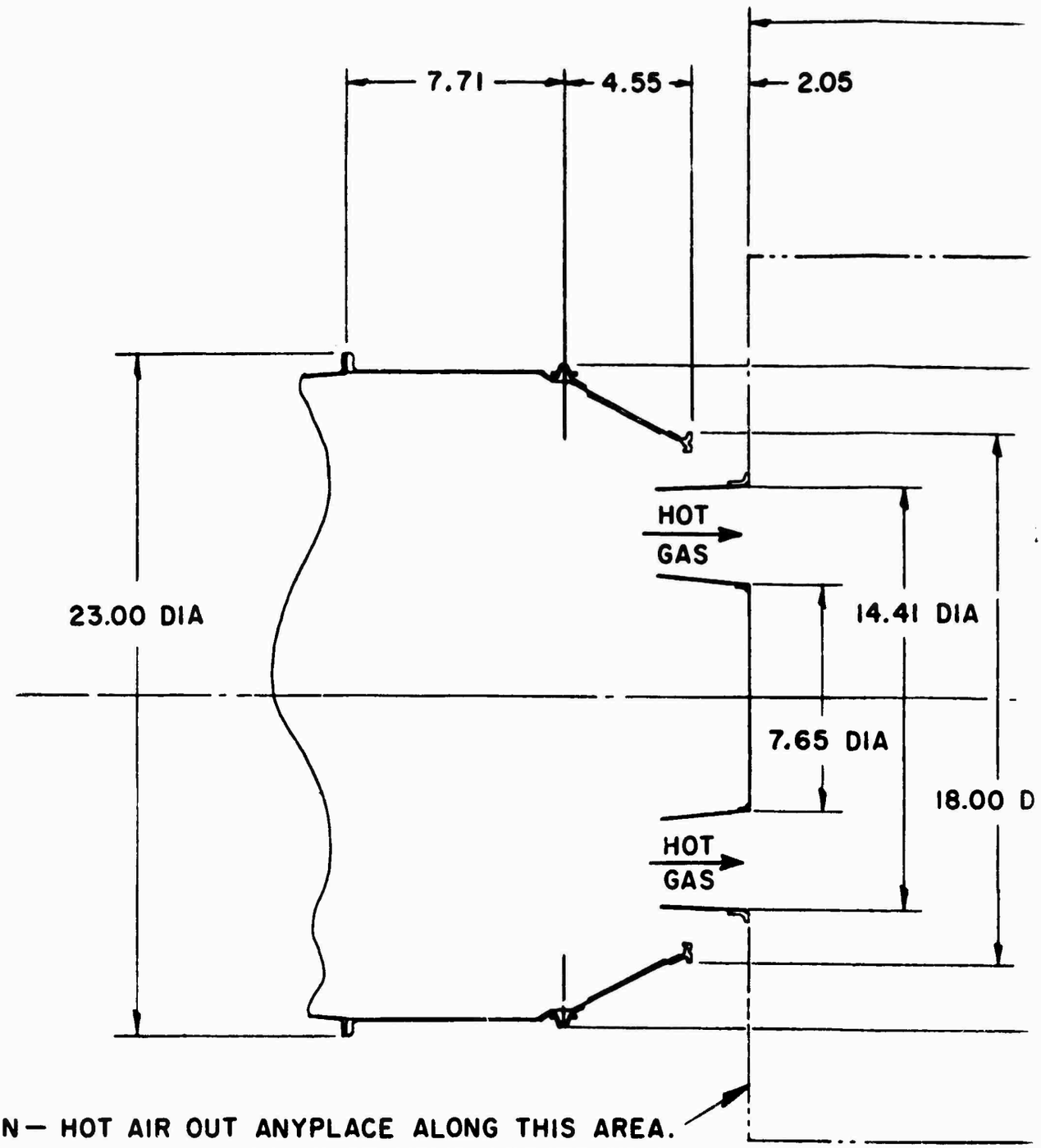

COLD AIR IN— HOT AIR OUT ANYPLACE ALONG THIS AREA. IF FULL ANNULAR DUCTS ARE TO BE USED, LOCATE THE COLD AIR DUCT EXTERNAL TO THE HOT AIR DUCT OR PIPES. DUCTING AND/OR PIPES MUST NOT EXTEND BEYOND THE 30-INCH DIAMETER.

Figure 111. Regenerator I

A

3. COMPONENTS

3.1 The regenerator shall be an integrated structure capable of being cantilevered from mount points located at the front of the unit. The detailed specification of the mount points will be subject to negotiation. The regenerator shall receive high pressure air in the plane of the outer annulus as specified in drawing LO-7140 (Figure 111) a minimum number of pipe connections (recommended number: 4 to 6).

3.2 The regenerator shall return high temperature, high pressure air to the engine at the inner annulus specified in drawing LO-7140 at a minimum number of pipe locations (recommended number: 4 to 6).

3.3 The regenerator shall receive high temperature turbine exhaust at the turbine exit plane specified in drawing LO-7140.

3.4 The exhaust gas leaving the regenerator shall be directed rearward.

3.5 The regenerator components shall be such as to satisfy the requirements specified in 3.2 to 3.5 and perform the heat exchange function specified in Section 4.

3.6 The basic heat exchange design shall be such as to permit the incorporation of a direct flow bypass of the turbine exhaust gases at high power ratings. The design of such a bypass is not considered as part of this specification.

4. RATINGS

4.1 Optimization

The heat exchanger shall be optimized at the 75% rated power condition of the basic design.

4.2 Inlet Conditions

The conditions for which the heat exchanger shall be optimized are listed in Table 20, Column 2: The 75% Power Point.

4.3 The optimization criteria shall be minimum weight for a given fuel saving. Fuel savings vs. effectiveness is presented in Figure 112.

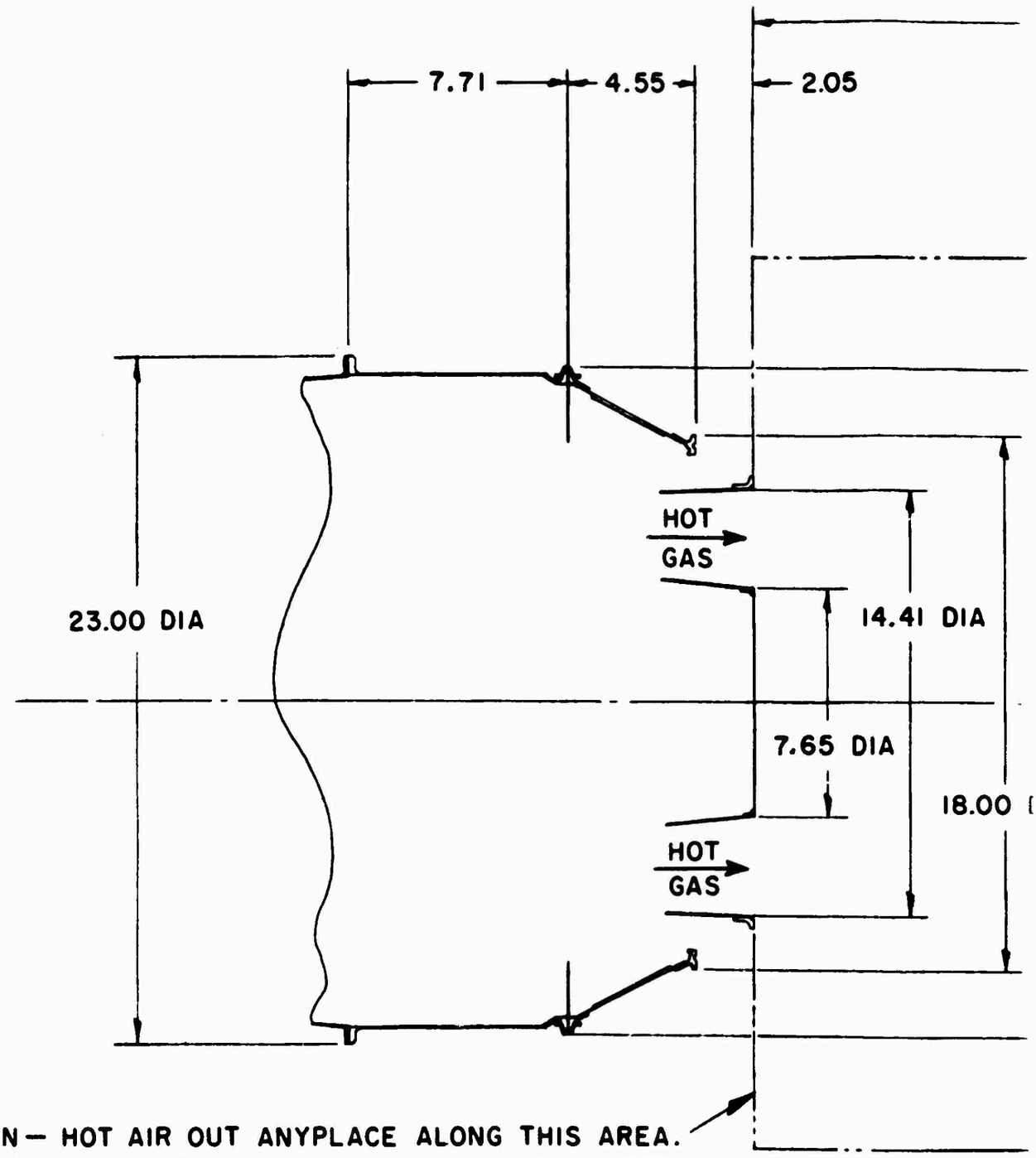

COLD AIR IN— HOT AIR OUT ANYPLACE ALONG THIS AREA. IF FULL ANNULAR DUCTS ARE TO BE USED, LOCATE THE COLD AIR DUCT EXTERNAL TO THE HOT AIR DUCT OR PIPES. DUCTING AND/OR PIPES MUST NOT EXTEND BEYOND THE 30-INCH DIAMETER.

Figure 111. Regenerator

A

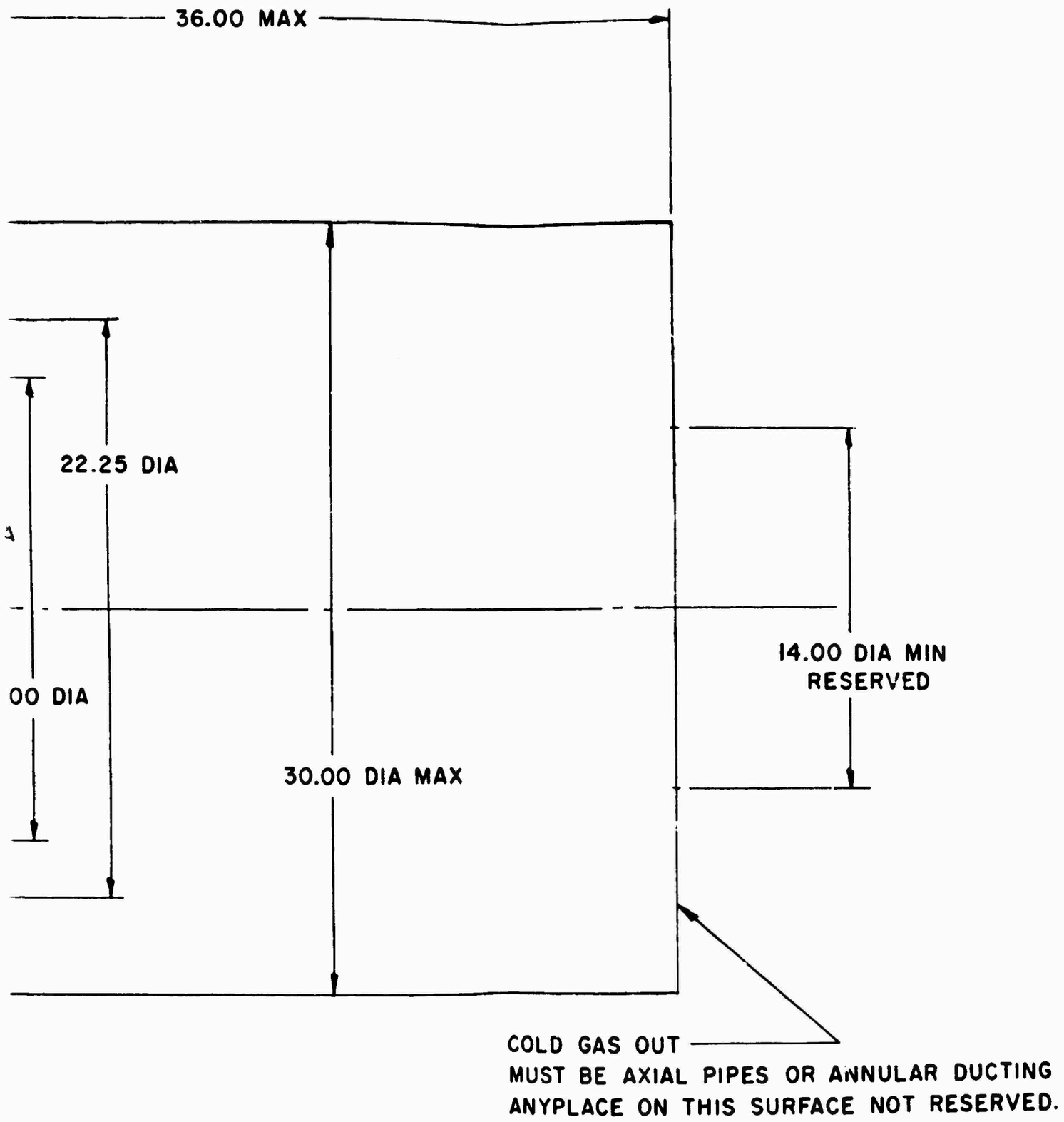

tor Envelope (Drawing LO-7140).

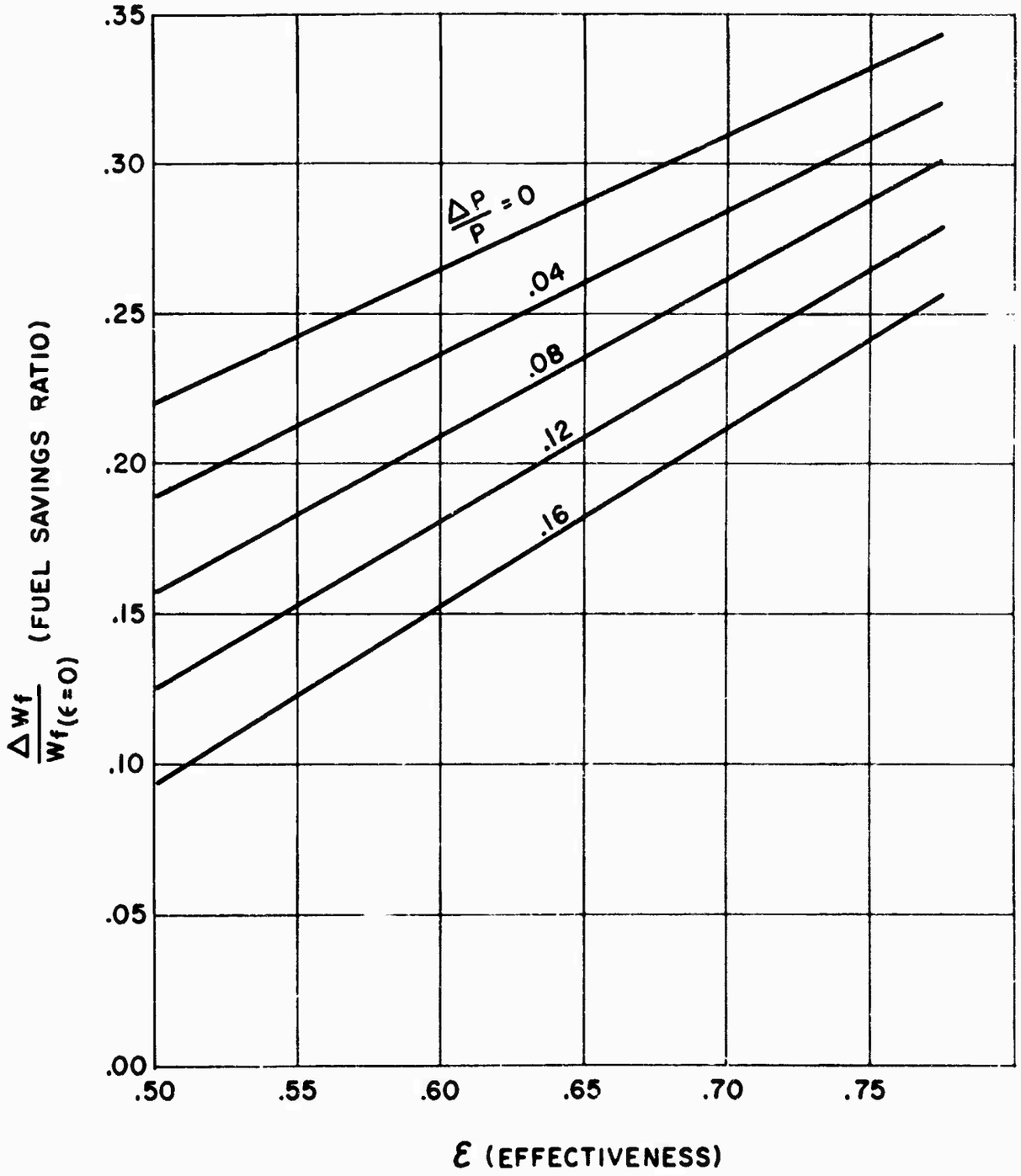

Figure 112. T53-L-5 Engine; Regenerator Economy Benefit at 75% Normal Rated Power.

4.4 Weight Fuel Saving Trade-Off

The trade-off between weight and fuel saving for the purpose of initial optimization is given in Figure 113. This curve should not be construed as specifying the weight goal for the heat exchanger.

4.5 The summation of the permissible total pressure loss for the conditions specified in Column 4 of Table 20 shall be 10% - 12% with a maximum of 30% of the summation permitted on the air side.

4.6 The definition of summation pressure loss in this specification is the percentage pressure loss on the air side, defined as the inlet total pressure at the regenerator flange connection minus the exit total pressure at the flange connection divided by the inlet total pressure, plus the percentage pressure loss on the gas side, defined as the inlet total pressure at the slip joint connection minus the exit static pressure (ambient) divided by the inlet total pressure.

The definition of effectiveness in this specification is the actual increase in enthalpy of the air passing through the heat exchanger divided by the increase in enthalpy which the air would incur if the temperature were increased to a value equal to the gas inlet temperature.

4.7 A table of guarantee values shall be submitted as part of the fulfillment of this specification.

5. DIMENSIONS AND ENVELOPE

5.1 Weight

The weight goal for this heat exchanger is the minimum possible weight at a given performance level within the state of the art.

5.2 Envelope

Drawing LO 7140 specifies a nominal envelope for a regenerator which Lycoming believes to be within the state of the art. It should not be construed as the ultimate which would be desirable in this design.

5.3 Maximum Envelope

The maximum allowable dimensions for this regenerator are 36-inch diameter and 42-inch length. This envelope is considered highly undesirable, and its use must be justified on the basis of significant other advantages as compared to the nominal envelope.

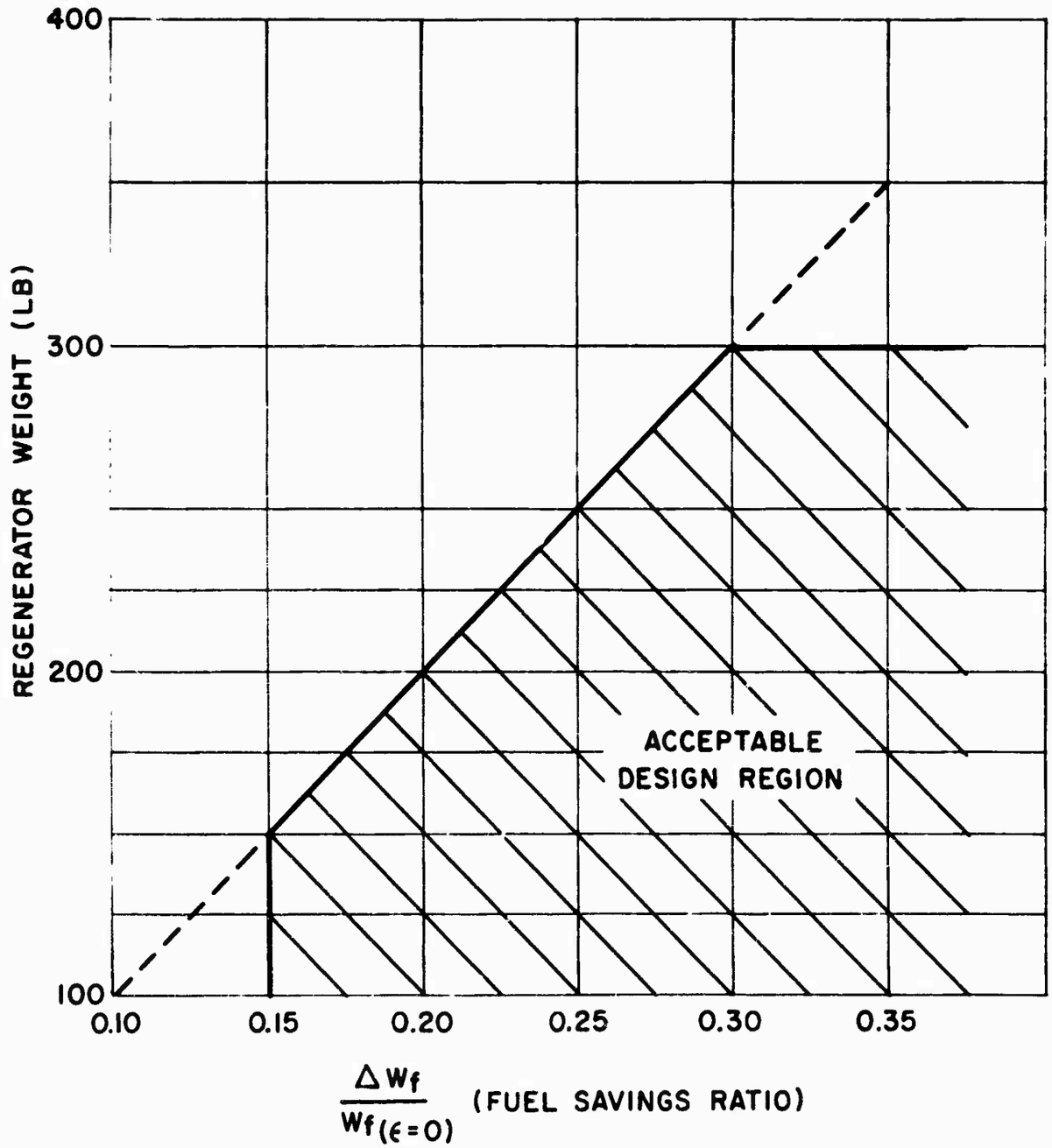

Figure 113. T53-L-5 Engine; Regenerator Weight Vs. Fuel Savings.

6. STRUCTURAL REQUIREMENTS

6.1 The regenerator shall be designed based on the conditions specified in Section 7 of this specification.

6.2 Stress Criteria

The regenerator shall be designed on the basis of the most conservative of the following allowable stresses at conditions specified in Section 7.

6.2.1 Allowable stress based on 0.2% offset yield point stress divided by 1.2.

6.2.2 Ultimate strength divided by 1.8.

6.2.3 Thousand hour creep rupture strength.

6.3 The regenerator shall be designed to withstand pressure differentials of 120% of those encountered in column 4 of Table 20 and at the operating temperatures corresponding to this condition.

6.4 The regenerator shall be capable of withstanding the maneuver loads as specified in MIL-E-8593, paragraph 3.14 (this note serves merely to point out one specific area and does not in any way relieve the responsibility of satisfying MIL-E-8593 and associated specifications in total).

6.5 Application

The application of the engine using this regenerator is not at present specified; therefore, details concerning mounting and interface provisions will be settled by direct negotiation between Lycoming and the regenerator manufacturer.

6.5.1 Preliminary design should be based on the assumption that flanges for quick disconnect connections will be provided for the high pressure intake and exhaust pipes.

6.5.2 Preliminary design shall be based on the assumption that a minimum leakage slip joint must be provided at the turbine exit.

6.6 Design Steady State Pressures and Temperatures

The regenerator shall be designed for 1000 hours endurance where the endurance will include the equivalent of two full qualification endurance tests (150 hours each) as specified in MIL-E-8595, plus 700 hours of

operation at the nominal design point specified in Section 4.2.

7. OPERATING CONDITIONS

7.1 Cold Soak

The regenerator shall be capable of reliable operation after cold soaking at -65°F for a period of 24 hours prior to start up.

7.2 Steady State Design

The regenerator shall be designed on the basis of the following series of pressures and temperatures.

TABLE 20
ENGINE OPERATING CONDITIONS

	1		2		3		4	
	Flight Idle		75% Power		Normal Rated		Military	
	Air	Gas	Air	Gas	Air	Gas	Air	Gas
Inlet Total Press. (atmos.)	2.60	-	5.15	-	5.70	-	6.25	-
Exit Static Press. (atmos.)	-	1.0	-	1.0	-	1.0	-	1.0
Inlet Total Temp. °F	272	730	440	900	480	992	513	1085
Mass Flow Rate lb/sec	5.5	-	9.6	-	10.3	-	10.9	-
Inlet Mach No.	.15	.13	.15	.24	.14	.27	.14	.30

7.3 Transient Operating Conditions

The regenerator shall be capable of undergoing the thermal cycling imposed by the conditions described in Figure 114.

7.3.1 The regenerator shall be capable of undergoing the thermal cycling as required by MIL-E-8595 during a qualification endurance test. The conditions for these transient conditions are presented in Figure 114

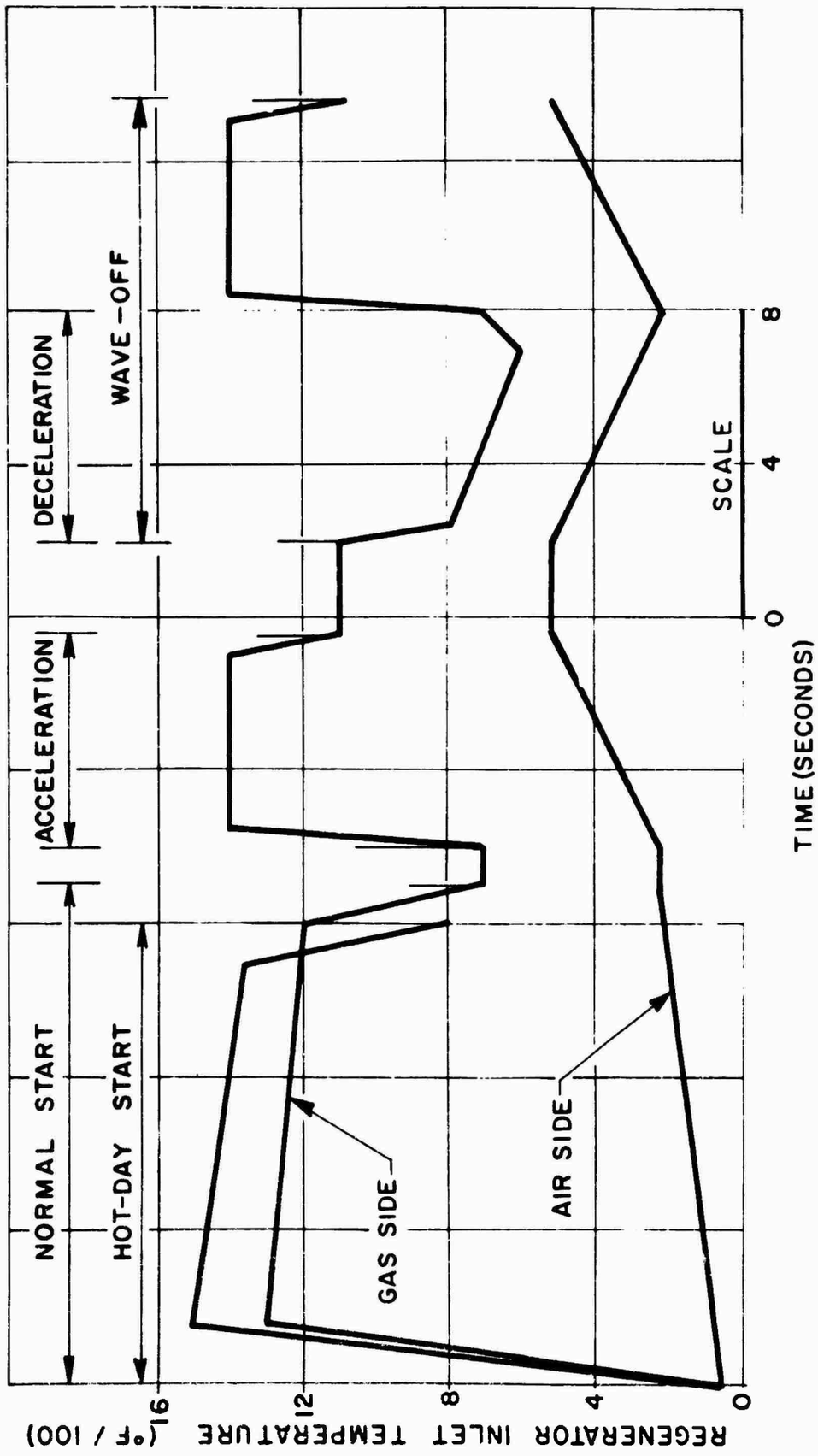

Figure 114. T53-L-5 Engine; Transient Operating Conditions.

and include normal starts, accelerations, and decelerations.

7.3.2 The regenerator shall be designed to withstand hot starts. Hot start conditions as shown in Figure 114 may be expected to occur on 10% of the starts.

7.3.3 The regenerator shall be designed for the same number of wave-offs as starts. Wave-off consists of a normal deceleration followed immediately by a normal acceleration.

7.4 Vibration

7.4.1 Mount Point Vibration

The regenerator shall be capable of withstanding vibrations at the attachment points as specified in Figure 115.

7.4.2 The regenerator shall be capable of withstanding fluctuations of air side pressure of 5% maximum continuous design pressure at a frequency of 50 cps to 300 cps.

7.4.3 Surge

The regenerator shall be capable of maintaining structural integrity when the engine is in surge for periods of 5 seconds. During surge, pressure fluctuations of 50% of the maximum design pressure may be expected at approximately 10 cps. The gas side will be directly exposed to flame during this period.

7.5 Fouling

During field operation, the regenerator system shall possess the following characteristics:

7.5.1 The regenerator will be subjected to the following contaminants:

Air Side:	
Oil: MIL-L-7808	0.1 lb/hr
Gas Side:	
Sulfur in the form of SO or SO_2	1.0 lb/hr
Oil: MIL-L-7808	0.4 lb/hr
JP-4 Fuel	1.0 lb/hr

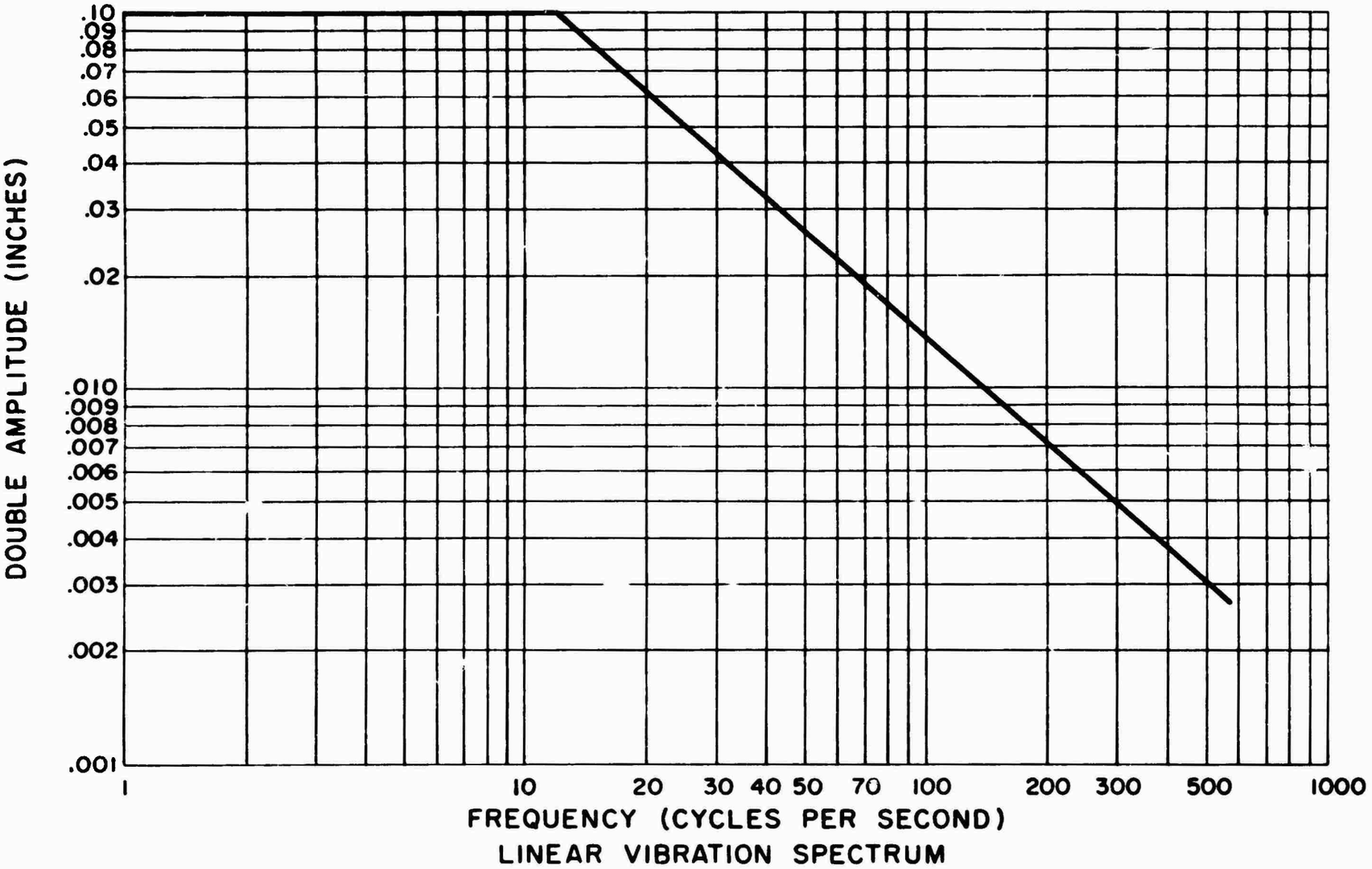

Figure 115. T53-L-5 Engine; Double Amplitude of Vertical Displacement of Engine Measured at Mount Pads.

7.5.2 The regenerator shall be capable of maintaining performance within 5% of optimum for periods of ten (10) hours without requiring cleaning.

7.5.3 The regenerator shall be capable of being cleaned in the installed condition and with no deleterious effects on the engine.

7.5.4 Any cleaning equipment shall be portable and self contained.

8. HANDLING PROVISIONS

8.1 The regenerator shall be capable of shipment as a unit from the vendor to Lycoming.

8.2 The regenerator when cantilevered from the front mount point shall be capable of withstanding handling loads of a half sinusodial shock pulse characterized by an amplitude of 60g's and rise time of 0.005 sec. This is equivalent to a 5-inch drop to a concrete floor.

9. FUEL DRAIN PROVISIONS

9.1 A drain port shall be provided to purge the regenerator of fuel trapped under such conditions as aborted starts, flame-outs, etc.

10. LEAKAGE

10.1 Maximum

The regenerator shall have a maximum leakage of 0.25% of nominal flow under the most adverse conditions.

10.2 Performance

Any leakage shall be charged against the regenerator performance at a rate of 1% leakage equal to 2% pressure loss. This value must be included in performance estimates.

APPENDIX II

SPECIFICATION XCS3R.1.1 FOR A PROTOTYPE REGENERATOR FOR A LYCOMING T53 GAS TURBINE ENGINE

25 February 1964

1. SCOPE

This document covers the detail requirements for the design and performance of a regenerator (integrated heat exchanger) for a T53 turboshaft engine. The design objective for this unit is to produce a maximum saving in the engine fuel consumption with minimum penalty in the weight. The regenerator manufacturer shall assert his best efforts to meet the objectives described in the following sections.

2. APPLICABLE SPECIFICATIONS

2.1 The following Military Specification forms a part of this requirement except as modified herein:

SPECIFICATION	
MIL-E-8593 3 September 1952	Engines, Aircraft Turboprop, General Specification for

2.2 The following documents of the issue in effect on the date specified and the publications listed in the applicable sections of ANA Bulletin 343n dated 14 December 1960 entitled "Specifications and Standards Applicable to Aircraft Engines and Propellers, Use of" form a part of this requirement.

DOCUMENT	TITLE
MIL-E-005272B 5 July 1957	Environmental Testing, Aeronautical and Associated Equipment, General Specification for
ANA 407	Engines, Turbojet, Design and Installation Criteria for

3. COMPONENTS

3.1 The regenerator shall be an integrated structure capable of being cantilevered from mount points located at the front of the regenerator. The detailed configuration of the mount points will be subjected to negotiation. The regenerator shall receive high pressu re air in the plane of the outer annulus as specified in drawing LO-7602 (Figure 116).

PROVIDE THIS PORTION OF THE FLOW DIVIDER WITH A SMOOTH SPHERICAL SURFACE AT THE POINT OF CONTACT WITH THE SEAL

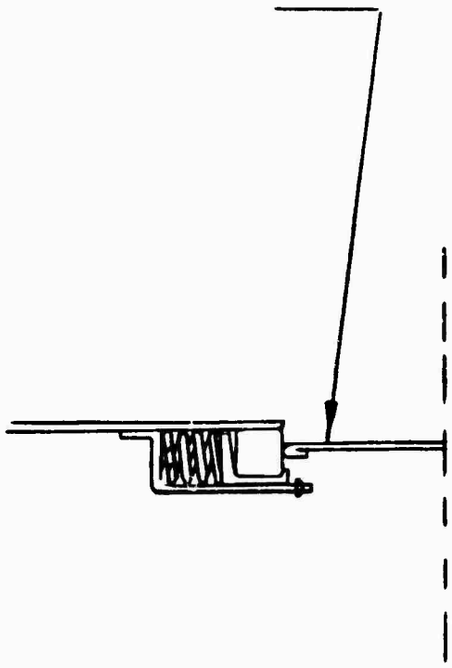

DETAIL "A"

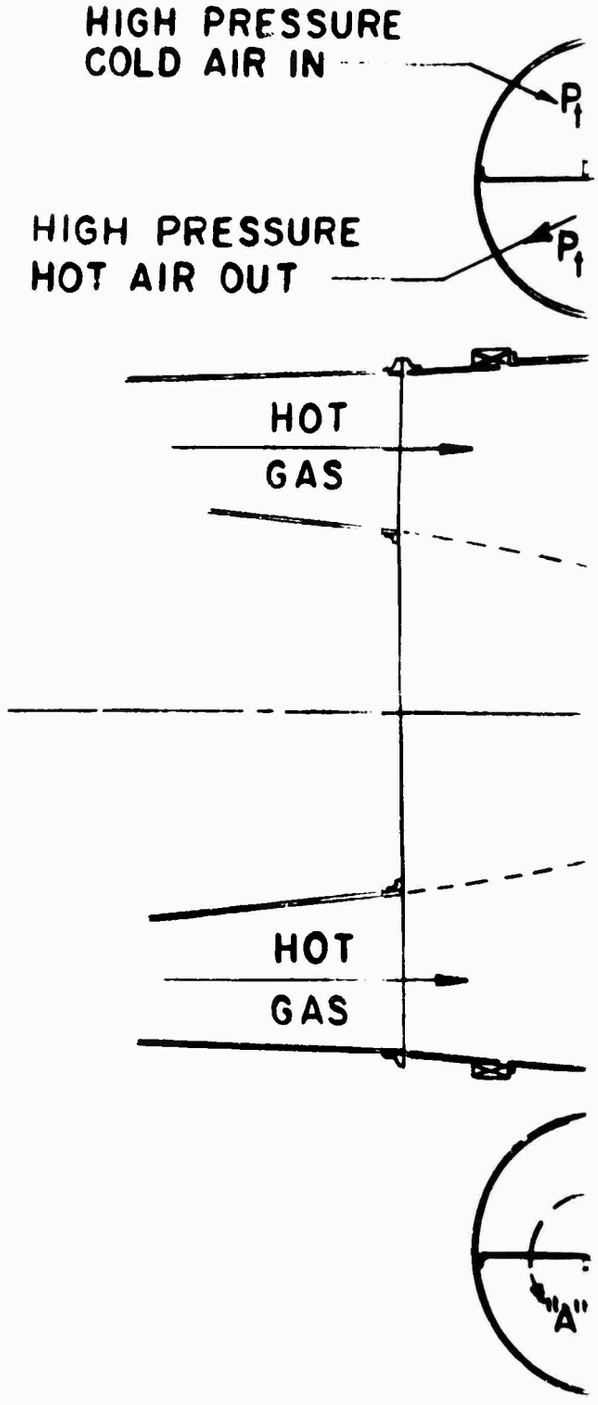

A

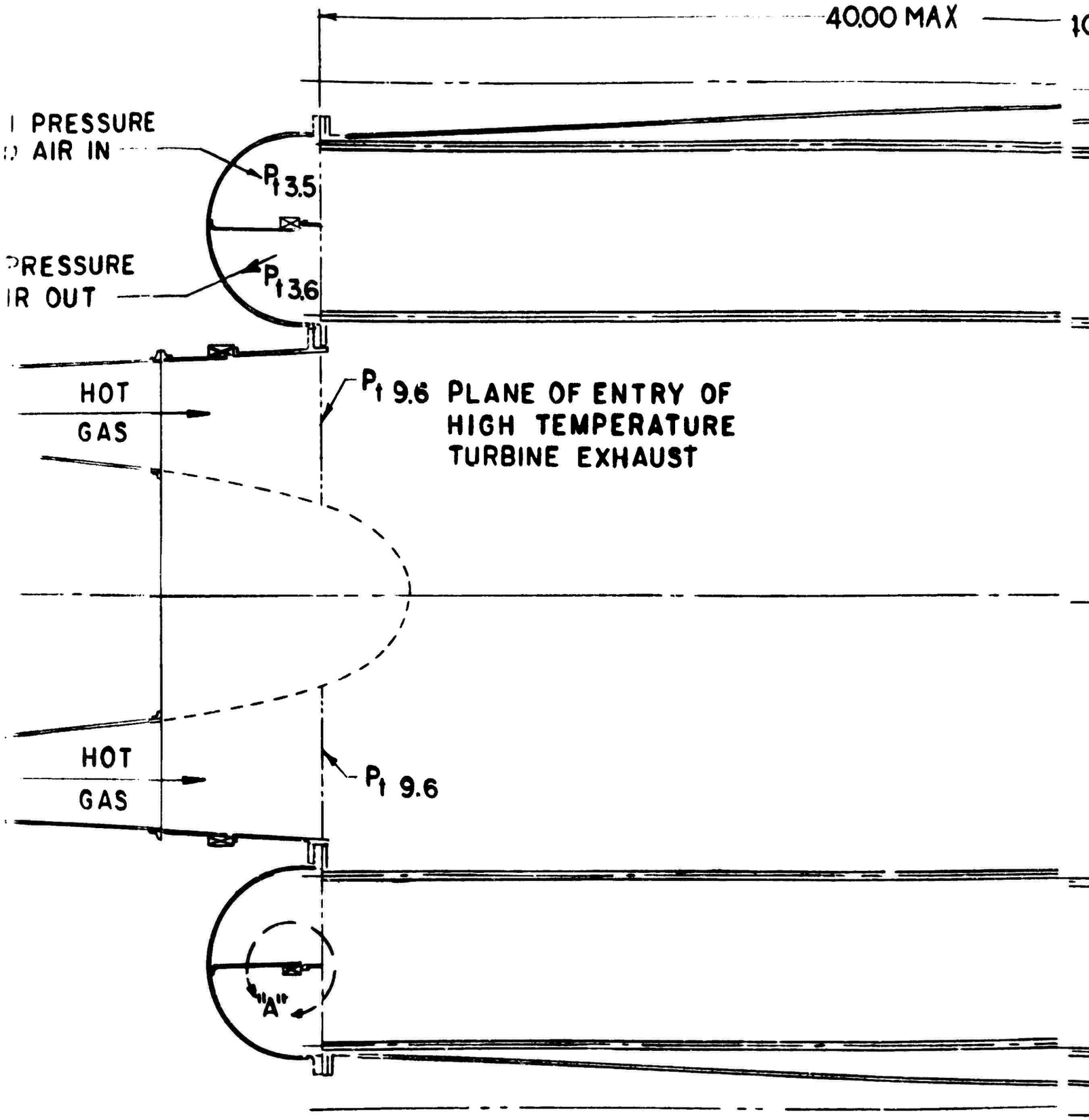

Figure 116. Regenerator Envelope (Drawing L0-7602).

B

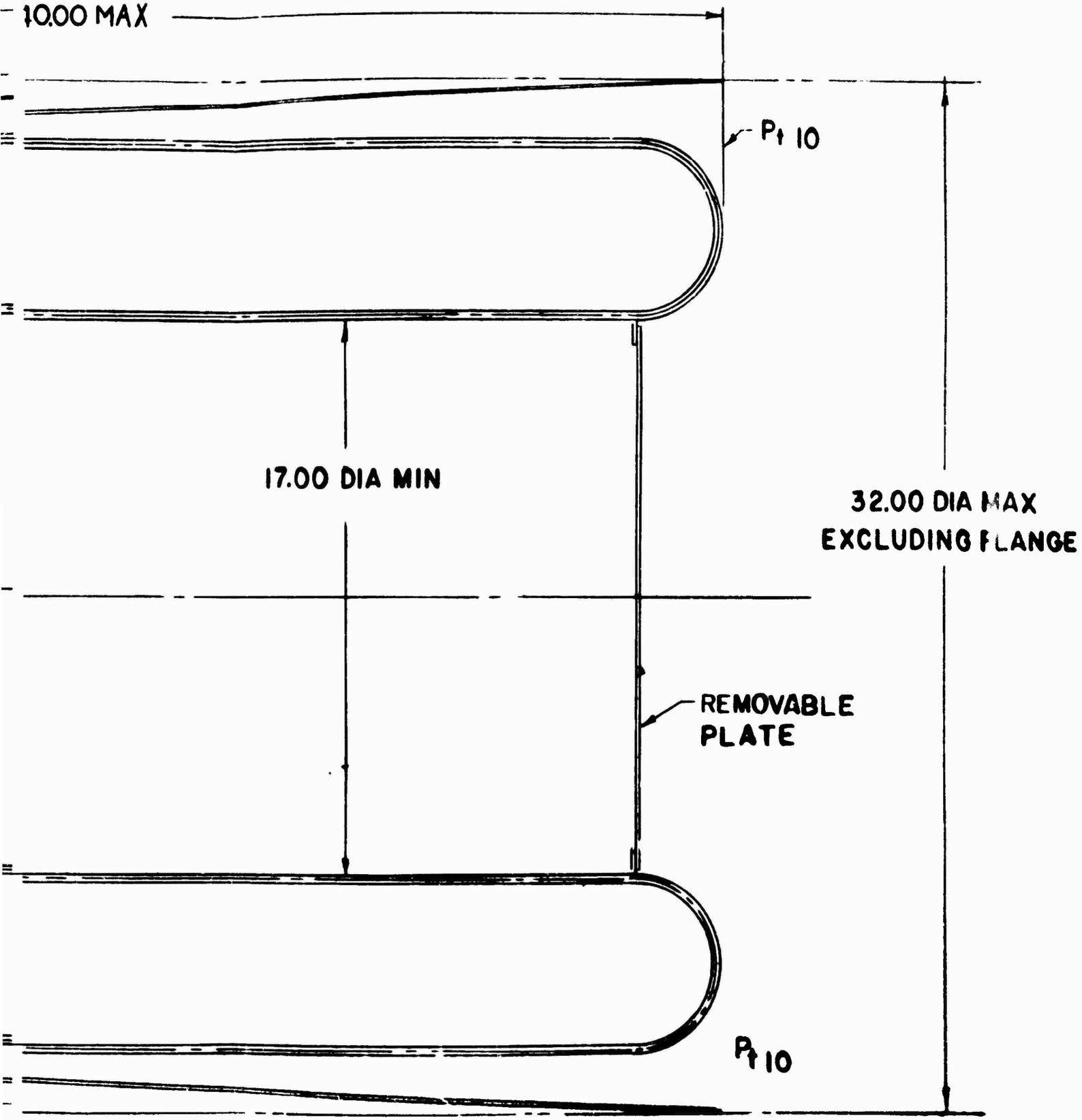
10.00 MAX
Pt 10
17.00 DIA MIN
32.00 DIA MAX
EXCLUDING FLANGE
REMOVABLE
PLATE
Pt 10

0-7602).

3.2 The regenerator shall return high temperature, high pressure air to the engine at the inner annulus specified in drawing LO-7602.

3.3 The sealing arrangement dividing the incoming and outgoing high pressure air shall be in accordance with the design specified in drawing LO-7602.

3.4 The regenerator shall receive high temperature turbine exhaust in the plane specified in drawing LO-7602.

3.5 The exhaust gas leaving the regenerator shall be directed rearward.

3.6 The basic heat exchanger design shall be such as to permit the incorporation of a direct flow bypass of the turbine exhaust gases at high power ratings. The design of a remote control bypass is not considered as part of this requirement. A removal blank-off plate must be provided at the rear center portion of the regenerator.

3.7 A flange suitable for mounting an instrumentation ring section shall be provided at the aft end of the regenerator outer shell.

4. DESIGN

4.1 Design Conditions

The conditions for which the heat exchanger shall be designed are listed in Table 21, Column 2: the 75% Engine Power Point.

4.2 The definition of summation pressure loss in this requirement is (a) the percentage pressure loss on the air side plus (b) the percentage loss on the gas side where (a) is defined as the inlet total pressure (P_t 3.5) at the regenerator flange connection minus the exit total pressure (P_t 3.6) at the flange connection divided by the inlet total pressure (P_t 3.5) and (b) defined as the inlet total pressure (P_t 9.6) in the plane of the forward regenerator flange minus the total pressure (P_t 10.0) leaving the regenerator divided by the inlet total pressure (P_t 9.6).

The definition of effectiveness in this requirement is the actual increase in enthalpy of the air passing through the heat exchanger divided by the air enthalpy increase which would occur if the air exit temperature were increased to a value equal to the gas inlet temperature.

4.3 The regenerator shall be a tube-type, two-pass, cross-counterflow design. The exhaust gas shall make a single pass over the tubes and the compressor air shall make two passes inside the tubes.

4.4 The performance of the regenerator at the design point shall be as follows:

Effectiveness	= 0.66 minimum
Summation of Total Pressure Loss	= 0.07 maximum
Core Total Pressure Loss	= 0.04
Core Total Pressure Drop Split - Air	= 45% ± 5
- Gas	= 55% ± 5
Maximum Gas Mach Number Leaving Regenerator	= 0.15 (discharging in this plane to ambient pressure)

4.5 A table of Design Point and Off-Design Performance values shall be submitted, for both bypass and non-bypass conditions.

5. DIMENSIONS AND ENVELOPE

5.1 Tube Size and Spacing

5.1.1 The tube diameter, wall thickness, and tube spacing shall be at the discretion of the designer. The envelope design shall be compact, light weight, and commensurate with advanced state-of-the-art airborne design practice.

5.2 Envelope

5.2.1 Core inside diameter shall not be less than 17.0 inches.

5.2.2 The outside diameter at the forward end of the regenerator shall be the minimum compatible with the outside diameter of the core and the desired flow conditions in this region.

5.2.3 The maximum diameter of the outer shell of the regenerator shall not exceed 32.0 inches.

5.2.4 The maximum length of the regenerator from the forward flange to the aft end of the tube bundle shall not exceed 40 inches.

5.3 Weight

The weight goal for this heat exchanger shall be the minimum possible at the given performance level within the state of the art. The maximum weight of the delivered regenerator shall not exceed 188 pounds.

6. STRUCTURAL REQUIREMENTS

6.1 The regenerator shall be designed based on the conditions specified in Section 7 of this requirement.

6.2 Stress Criteria

The regenerator shall be designed on the basis of the most conservative of the following allowable stresses at conditions specified in Section 7.

6.2.1 The design steady stress shall not exceed 80% of the material 0.2% offset yield strength.

6.2.2 The design steady stress shall not exceed 50% of the material ultimate strength.

6.2.3 The design steady stress shall not exceed the 1000-hour creep rupture strength of the material.

6.3 The regenerator shall be designed to withstand pressure differentials of 120% of those encountered in Column 4 of Table 21 and at the operating temperatures corresponding to this condition.

7. OPERATING CONDITIONS

7.1 Steady State Design

The regenerator shall be designed on the basis of the pressures and temperatures shown in Table 21.

7.2 Transient Operating Conditions

The regenerator shall be designed to be capable of undergoing the thermal cycling imposed by the conditions described in Figure 117.

7.2.1 The regenerator shall be designed to be capable of undergoing the thermal cycling as required by MIL-E-8595 during a qualification endurance test. The conditions for these transient conditions are presented in Figure 117 and include normal starts, hot day starts, accelerations,

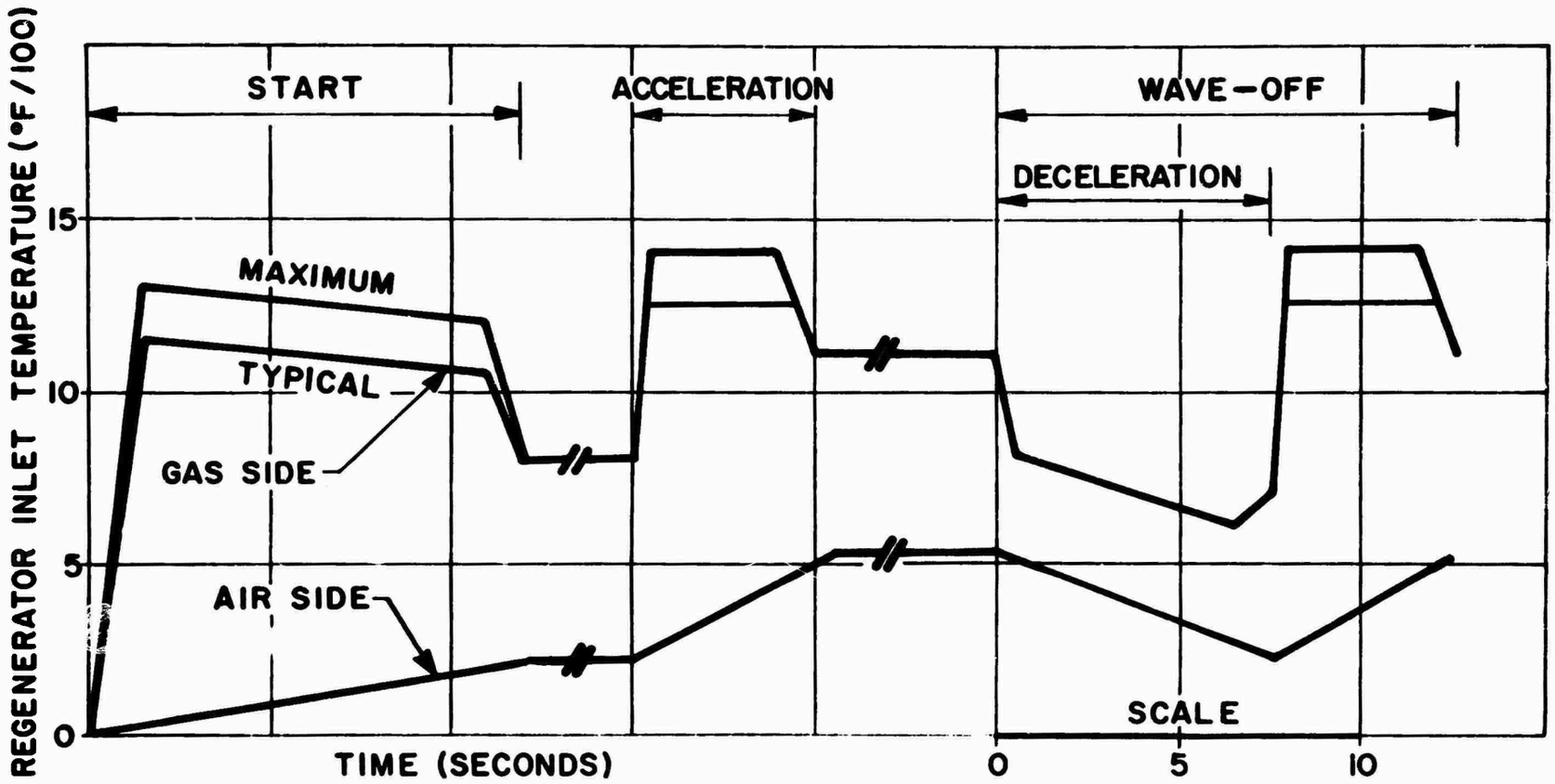

Figure 117. T53 Engine Transient Operating Conditions.

and decelerations.

TABLE 21
ENGINE OPERATING CONDITIONS

	1		2		3		4	
	Flight Idle		75% Power		Normal Rated		Military	
	Air	Gas	Air	Gas	Air	Gas	Air	Gas
Inlet Total Press. (atmos.)	2.60	-	5.07	-	5.73	-	6.27	-
Exit Static Press. (atmos.)	-	1.0	-	1.0	-	1.0	-	1.0
Inlet Total Temp. (^{o}F)	275	730	440	900	480	995	513	1085
Mass Flow Rate (lb/sec)	5.5	5.65	9.45	9.71	10.1	10.4	10.73	11.06
Inlet Mach No.	.05	.10	.05	.19	.05	.21	.05	.24

7.3 Vibration

7.3.1 Mount Point Vibration

The regenerator shall be designed to be capable of withstanding vibrations as specified in Figure 118 at the attachment points.

7.3.2 The regenerator shall be designed to be capable of withstanding fluctuations of air side pressure of ‡ 2 1/2 psi at a frequency of 50 cps to 300 cps.

7.3.3 Surge

The regenerator shall be designed to be capable of maintaining structural integrity when the engine is in surge for periods up to 5 seconds. During surge, pressure fluctuations of plus 20 to minus 50% of the maximum design pressure may be expected at approximately 10 cps. The gas side may be directly exposed to flame during this period.

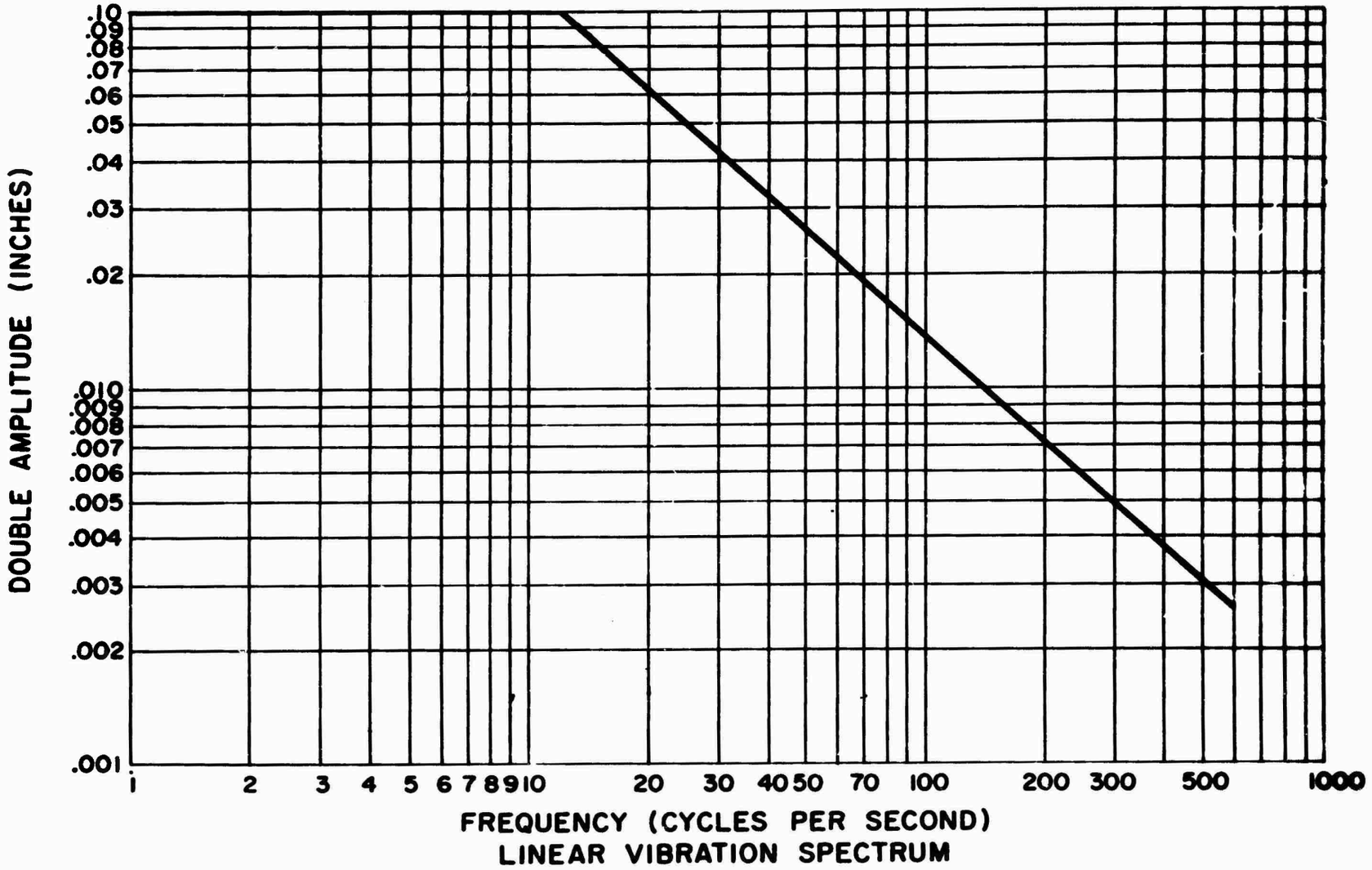

Figure 118. T53 Engine Maximum Vibration at Unsupported Regenerator Mount Flange.

7.4 Fouling

During field operation, the regenerator system shall be designed to possess the following characteristics:

7.4.1 The regenerator will be subjected to the following contaminants:

Air Side:

Oil: MIL-L-7808	0.1 lb/hr

Gas Side:

Sulfur in the form of SO or SO_2	1.0 lb/hr
Oil: MIL-L-7808	0.4 lb/hr
JP-4 Fuel	1.0 lb/hr

7.4.2 The regenerator shall be designed to be capable of maintaining performance within 5% of design pressure loss and effectiveness for periods of ten (10) hours without requiring cleaning.

7.4.3 The regenerator shall be capable of being cleaned in the installed condition and with no deleterious effects on the engine. It is desirable that the outer shell of the regenerator be removable.

7.4.4 Any cleaning equipment shall be portable and self-contained.

8. HANDLING PROVISIONS

8.1 The regenerator shall be capable of shipment as a unit from the vendor to Lycoming.

9. FUEL DRAIN PROVISIONS

Fuel will drain into the exhaust system and hence through the gas side of the regenerator on abort starts, etc. The regenerator shell design must be free from corners and crevices which would collect and pool fuel.

10. LEAKAGE

10.1 Maximum

The regenerator shall have a maximum leakage of 0.10% of nominal flow

under the most adverse conditions.

10.2 Performance

Any leakage shall be charged against the regenerator performance at a rate of 1% leakage equal to 2% pressure loss. This value must be included in performance estimates.

APPENDIX III

LIST OF DRAWINGS

MULTIWAVE PLATE REGENERATOR

Part No.	Title
EXP-7337	Wave Plate, Regenerator, Outside Ends
EXP-7338	Wave Plate, Regenerator, Inside Ends
EXP-7339	Wave Plate, Regenerator, Inside Ends (Dimpled)
EXP-7340	Wave Plate, Regenerator, Outside Ends (Dimpled)
EXP-7341	Flange, Regenerator, Core Test Section, Pressurized Air
EXP-7342	Flange, Regenerator, Core Test Section, Exhaust Gas
EXP-7343	Strip, End Plate Reinforcing, Regenerator Core Test Section
EXP-7344	End Plate, Regenerator Core Test Section
EXP-7345	Side Plate, Regenerator Core Test Section
EXP-7346	Regenerator Core Test Section Assembly
EXP-7347	Regenerator Core Test Section Assembly (Dimpled Wave Plates)
EXP-7373	Channel, End Plate Reinforcing, Regenerator Core Test Section
EXP-7374	Flange, Regenerator Core Test Section, Exhaust Gas
EXP-7375	Side Plate, Regenerator Core Test Section
EXP-7376	Regenerator Core Test Section Assembly
EXP-7378	End Plate, Regenerator Core Test Section
EXP-7394	Wave Plate, Regenerator Inside Ends (Dimpled)

Part No.	Title
EXP-7395	Wave Plate, Regenerator Outside Ends (Dimpled)
EXP-7396	Regenerator Core Test Section Assembly (Dimpled) Wave Plates)
EXP-7433	Wave Plate - Plate A (Dimpled)
EXP-7434	Wave Plate - Plate B (Dimpled)
EXP-7438	Module Brazing Assembly
EXP-7439	Wave Plate - Plate A (Dimpled)
EXP-7440	Wave Plate - Plate B (Dimpled)
EXP-7515	End Plate, Regenerator Core Module
EXP-7516	Positioning Plate, End Plate Flange, Regenerator Core Module
EXP-7517	Flange, End Plate, Regenerator Core Module
EXP-7518	Channel, End Plate, Reinforcing, Regenerator Core Module
EXP-7519	End Plate Assembly, Regenerator Core Module
EXP-7520	Regenerator Core Module Assembly (Brazing)
EXP-7521	Support Flange, Regenerator Core Module
EXP-7522	Stiffener Flange, Regenerator Core Module
EXP-7523	Louvered Brace, Regenerator Core Module
EXP-7524	Manifold Wall Assembly, Pressure Air, Regenerator Core Module
EXP-7525	Manifold Wall, Pressure Air, Regenerator Core Module
EXP-7526	Flange, Front, Manifold Wall, Regenerator Core Module

Part No.	Title
EXP-7527	Flange, Rear, Manifold Wall, Regenerator Core Module
EXP-7528	End Plate, Manifold Wall, Regenerator Core Module
EXP-7529	Front Plate Assembly, 1 Module Regenerator Test Section
EXP-7530	Front Plate, 1 Module Regenerator Test Section
EXP-7531	Flange, Front Plate, 1 Module Regenerator Test Section
EXP-7532	Rear Plate, 1 Module Regenerator Test Section
EXP-7533	Left Side Plate, 1 Module Regenerator Test Section
EXP-7534	Right Side Plate, 1 Module Regenerator Test Section
EXP-7535	Outer Wall Assembly, Exhaust Gas, 1 Module Regenerator Test Section
EXP-7536	Outer Wall, Exhaust Gas, 1 Module Regenerator Test Section
EXP-7537	Flange, Exhaust Gas Outer Wall, 1 Module Regenerator Test Section
EXP-7538	Support Assembly, Pressure Air Manifold, Regenerator Core Module
EXP-7539	Strip, Side Pressure Air Manifold, Support
EXP-7540	Strip, End Pressure Air Manifold, Support
EXP-7541	Strip, Middle, Pressure Air Manifold, Support
EXP-7542	Tubular Rib, Pressure Air Manifold, Support
EXP-7543	Adapter, Pressure Air, Regenerator Core Module
EXP-7544	Regenerator Core Module, Test Section Assembly

Part No.	Title
EXP-7560	Left Inner Wall Assembly, Exhaust Gas, 1 Module Regenerator Test Section
EXP-7561	Left Inner Wall, Exhaust Gas, 1 Module Regenerator Test Section
EXP-7562	Right Inner Wall Assembly, Exhaust Gas, 1 Module Regenerator Test Section
EXP-7563	Right Inner Wall, Exhaust Gas, 1 Module Regenerator Test Section
EXP-7564	Flange, Exhaust Gas Inner Wall, 1 Module Regenerator Test Section
EXP-7565	Boss, Exhaust Gas Inner Wall, 1 Module Regenerator Test Section
EXP-7566	Spacer, Curved Pressure Air Adapter, Regenerator Core Module
EXP-7567	Spacer, Straight, Pressure Air Adapter, Regenerator Core Module
EXP-7572	Strip, Sealing, Regenerator Core Module
EXP-7575	Wave Plate, Regenerator, Plate A
EXP-7576	Wave Plate, Regenerator, Plate B
EXP-7577	Spacer, Sealing Pressure Air Passage, Regenerator Core Module
EXP-7578	Spacer, Sealing, Exhaust Gas Passage, Regenerator Core Module
EXP-7579	Regenerator Core Test Section Assembly
EXP-7580	Flanges and Matrix Assembly (Brazing), Regenerator Core Module
EXP-7581	Flange, Matrix Supporting, Regenerator Core Module

Part No.	Title
EXP-7607	Regenerator Core Test Module Assembly (Brazing)
EXP-7608	Spacer, End Sealing, Regenerator Core Module
EXP-7609	Flange, End Sealing, Regenerator Core Module
EXP-7613	Regenerator Core Test Module Assembly (Brazing)
EXP-7614	Spacer, Sealing Pressure Air Passage, Regenerator Core Module
EXP-7615	Spacer, Sealing Exhaust Gas Passage, Regenerator Core Module
EXP-7616	Spacer, End Sealing, Regenerator Core Module
EXP-7617	Wave Plate, Regenerator, Plate A
EXP-7618	Wave Plate, Regenerator, Plate B
EXP-7638	Regenerator Core Test Section
PSK-7870	Installation Drawing, T53-L-5 Regenerator
PSK-8104	Rework, Regenerator Wave Plate, Plate A
PSK-8105	Rework, Regenerator Wave Plate, Plate B

TUBE-TYPE REGENERATOR

180530	Regenerator

T53 ENGINE MODIFICATION, TUBE-TYPE REGENERATOR

EXP-7857	Casing, End, Combustor Chamber Housing
EXP-7860	Shield, Fire, Assembly of
EXP-7865	Liner, End, Combustion Chamber
EXP-7866	Plate, End, Combustion Chamber
EXP-7867	Plate, End, Combustion Chamber, Assembly of

Part No.	Title
EXP-7868	Plate and End Liner, Assembly of
EXP-7869	Liner Assembly, Combustion Chamber
EXP-7874	Flange, Fire Shield
EXP-7894	Shroud, Inner, Turbine Nozzle, First Stage
EXP-7895	Shroud, Outer, Turbine Nozzle, First Stage
EXP-7896	Nozzle, Turbine, First Stage, Assembly of
EXP-7897	Shroud, Outer, Power Turbine Nozzle, Second Stage
EXP-7898	Shroud, Turbine, Second Stage, Inner
EXP-7899	Nozzle, Turbine, Second Stage
EXP-8055	Hose Assembly, Nonmetallic, Fuel Control to Filter Bypass
EXP-8057	Flexible Hose Assembly, Starting Fuel, Solenoid Valve to Starting Manifold
EXP-8058	Hose Assembly, Nonmetallic, Fuel Bypass Filter to Main Fuel Manifold
EXP-8059	Hose Assembly, Nonmetallic, Low Pressure
PSK-9342	Vaporizer, Fuel, Stamped, Assembly of (Rework)
PSK-9344	Vaporizer Assembly, Fuel, Shrouded
1-140-225-01	Lockwire, Preformed, Cylinder, Turbine
1-150-059-02	Bolt, Machine
1-160-220-02	Valve Assembly, Drain, Combustion Chamber

INTERFACE HARDWARE, TUBE-TYPE REGENERATOR

EXP-7900	Engine Assembly, Regenerator

Part No.	Title
EXP-7801	Ring Forging, Regenerator
EXP-7803	Ring Forging, Regenerator
EXP-7825	Shell, Toroidal, Regenerator
EXP-7826	Flange, Inner, Toroidal Shell, Regenerator
EXP-7827	Flange, Outer, Toroidal Shell, Regenerator
EXP-7828	Support, Seal, Regenerator
EXP-7829	Retainer, Regenerator
EXP-7830	Toroidal Shell Assembly, Regenerator
EXP-7831	Seal, Regenerator
EXP-7832	Segment, Regenerator Seal
EXP-7833	Spring, Seal, Regenerator
EXP-7834	Flange, Tubing, Hot-Air Duct, Regenerator
EXP-7835	Tube Assembly, Hot Air, Regenerator
EXP-7836	Tubing, Hot Air, Regenerator
EXP-7837	Tubing, Cool Air, Regenerator
EXP-7838	Flange, Tubing, Regenerator
EXP-7839	Tube, Cold Air, Regenerator
EXP-7840	Tube Assembly, Cold Air, Regenerator
EXP-7841	Support, Seal
EXP-7842	Ring, Sealing, Lock Joint, Regenerator
EXP-7843	Seal Flange, Exhaust Duct, Regenerator
EXP-7844	Cylinder, Exhaust Duct , Regenerator

Part No.	Title
EXP-7845	Exhaust Duct, Assembly of, Regenerator
EXP-7846	Flange, Exhaust Duct, Regenerator
EXP-7847	Flange, Temperature Probe, Regenerator
EXP-7848	Casing, Combustor, Regenerator
EXP-7849	Flange, Combustor Casing, Regenerator
EXP-7850	Housing and Tube Assembly
EXP-7851	Tube, Cold Air, Forward, Regenerator
EXP-7852	Tube, Hot Air, Forward, Regenerator
EXP-7853	Separater, Air, Combustion Changer
EXP-7854	Flange, Combustion Chamber, Housing
EXP-7855	Housing, Combustion Chamber, Assembly of
EXP-7856	Deflector, Combustor, Regenerator
EXP-7858	Ring Forging, Regenerator
EXP-7859	Ring Forging, Regenerator
EXP-7861	Tube, Drain, Regenerator
EXP-7862	Tube, Drain, Regenerator
EXP-7863	Adapter, Drain Valve, Regenerator
EXP-7864	Pad, Mounting, Nozzle
EXP-7871	Ring, Ignition Sealing
EXP-7872	Plate, Seal, R.H.
EXP-7873	Plate, Seal, L.H.
EXP-7877	Ring Forging, Regenerator

Part No.	Title
EXP-7878	Ring Forging, Regenerator
EXP-7879	Housing, Stator, Overspeed Governor Generator, Casting of
EXP-7902	Tube, Starting Fuel Manifold, Upper Inlet
EXP-7903	Tube, Starting Fuel Manifold, Upper
EXP-7904	Tube, Starting Fuel Manifold, Upper Supply, R.H. and L.H.
EXP-7905	Manifold Assembly, Starting Fuel, Upper
EXP-7908	Bracket, Upper, High Temperature Probe
EXP-7909	Bracket, Lower, High Temperature Probe
EXP-7911	Guide, High Temperature Probe
EXP-7912	Web, Probe Guide
EXP-7913	Support, Guide, High Temperature Probe
EXP-7914	Guide Assembly, High Temperature Probe
EXP-7915	Piping and Accessories
EXP-7916	Bolt, Special, 1900-32 NF-3A
EXP-8054	Hose Assembly, Nonmetallic, Fuel Temperature Probe to Fuel Control Inboard Line
EXP-8056	Hose Assembly, Nonmetallic, Fuel Temperature Probe to Fuel Control Outboard Line
PSK-8581	Hot Air Duct, Regenerator
PSK-8636	Bypass Cover Assembly, Test, Regenerator

INSTRUMENTATION, TUBE-TYPE REGENERATOR TEST

PSK-8671-01	Pressure Probe, Static, Station 3.1

Part No.	Title
PSK 8671-02	Pressure Probe, Static, Station 3.5
PSK 8671-04	Pressure Probe, Static, Station 4.0
PSK 8671-05	Pressure Probe, Static, Station 9.6
PSK-8672-01	Pressure Probe, Static, Station 3.6
PSK 8673-01	Thermocouple Rake, Station 4.1
PSK 8674-01	Pressure Rake, Station 4.1
PSK 8680-01	Plate, Probe Mounting, Station 3.5
PSK 8680-02	Plate, Probe Mounting, Station 3.6
PSK 8681-01	Thermocouple Probe
PSK 8682-01	Pressure Probe, Kiel
PSK 8684-01	Assembly, Tailcone Instrumentation
PSK 8705-01	Assembly, Probe, Station 9.7
PSK 8730-01	Air Diffuser Rework, Station 3.0
PSK 8762-01	Bolt, Special, Probe Holder
PSK 8763-01	Ring Support, Probe, Station 9.7
PSK 8764-01	Assembly, Probe, Station 9.7
TE 8753-01	Temperature Probe, Station 10.0
TE 8754-01	Pressure Probe, Station 10/0
TE 8882-01	Exhaust Duct, Inner, Station 10.0
TE 187	Probe Assembly, Kiel, Station 3.0
EXP-1928-01	Thermocouple Assembly, Station 3.0

Unclassified
Security Classification

DOCUMENT CONTROL DATA - R&D

(Security classification of title, body of abstract and indexing annotation must be entered when the overall report is classified)

1. ORIGINATING ACTIVITY (Corporate author) Lycoming Division AVCO Corporation Stratford, Connecticut	2a. REPORT SECURITY CLASSIFICATION Unclassified 2b GROUP

3. REPORT TITLE

HEAT REGENERATIVE SYSTEM FOR T53 SHAFT TURBINE ENGINES

4. DESCRIPTIVE NOTES (Type of report and inclusive dates)

Final Report, July 1962 to June 1963 (Phase I) and February to October 1964(Phase II)

5. AUTHOR(S) (Last name, first name, initial)

6. REPORT DATE July 1965	7a. TOTAL NO. OF PAGES 240	7b. NO. OF REFS 9
8a. CONTRACT OR GRANT NO. DA 44-177-TC-824 b. PROJECT NO. c. Task 1M121401D14409 d.	9a. ORIGINATOR'S REPORT NUMBER(S) USAAVLABS Technical Report 65-37 9b. OTHER REPORT NO(S) (Any other numbers that may be assigned this report) 2012.3	

10. AVAILABILITY/LIMITATION NOTICES

Qualified requesters may obtain copies of this report from DDC.
This report has been furnished to the Department of Commerce for sale to the public.

11. SUPPLEMENTARY NOTES	12. SPONSORING MILITARY ACTIVITY U. S. Army Aviation Materiel Laboratories Fort Eustis, Virginia

13. ABSTRACT

A heat regenerator has been designed to demonstrate the feasibility of regeneration for the T53 shaft turbine engine. Parameters of the initial design, a multiwave plate type, were optimized to provide a 27-percent fuel savings at 75-percent normal rated power. Test core modules leaked beyond the 0.25-percent flow-rate limit. Consequently, effort was directed toward a conventional tube-type regenerator, which was designed to provide a 24-percent fuel savings at 75-percent normal rated power. The tube-type regenerator and the interface hardware have been fabricated and integrated with the engine, and the system is ready for testing. (U)

DD FORM 1 JAN 64 1473

Unclassified
Security Classification

Unclassified
Security Classification

14. KEY WORDS	LINK A		LINK B		LINK C	
	ROLE	WT	ROLE	WT	ROLE	WT
AiResearch Heat Regenerator **Heat Regenerator** **Lycoming T53 Engine Heat Regenerator** **Multiwave Plate-Type Heat Regenerator** **Recuperator** **Regenerator** **T53 Engine Heat Regenerative System** **Tube-Type Heat Regenerator**						

INSTRUCTIONS

1. ORIGINATING ACTIVITY: Enter the name and address of the contractor, subcontractor, grantee, Department of Defense activity or other organization *(corporate author)* issuing the report.

2a. REPORT SECURITY CLASSIFICATION: Enter the overall security classification of the report. Indicate whether "Restricted Data" is included. Marking is to be in accordance with appropriate security regulations.

2b. GROUP: Automatic downgrading is specified in DoD Directive 5200.10 and Armed Forces Industrial Manual. Enter the group number. Also, when applicable, show that optional markings have been used for Group 3 and Group 4 as authorized.

3. REPORT TITLE: Enter the complete report title in all capital letters. Titles in all cases should be unclassified. If a meaningful title cannot be selected without classification, show title classification in all capitals in parenthesis immediately following the title.

4. DESCRIPTIVE NOTES: If appropriate, enter the type of report, e.g., interim, progress, summary, annual, or final. Give the inclusive dates when a specific reporting period is covered.

5. AUTHOR(S): Enter the name(s) of author(s) as shown on or in the report. Enter last name, first name, middle initial. If military, show rank and branch of service. The name of the principal author is an absolute minimum requirement.

6. REPORT DATE: Enter the date of the report as day, month, year, or month, year. If more than one date appears on the report, use date of publication.

7a. TOTAL NUMBER OF PAGES: The total page count should follow normal pagination procedures, i.e., enter the number of pages containing information.

7b. NUMBER OF REFERENCES: Enter the total number of references cited in the report.

8a. CONTRACT OR GRANT NUMBER: If appropriate, enter the applicable number of the contract or grant under which the report was written.

8b, 8c, & 8d. PROJECT NUMBER: Enter the appropriate military department identification, such as project number, subproject number, system numbers, task number, etc.

9a. ORIGINATOR'S REPORT NUMBER(S): Enter the official report number by which the document will be identified and controlled by the originating activity. This number must be unique to this report.

9b. OTHER REPORT NUMBER(S): If the report has been assigned any other report numbers *(either by the originator or by the sponsor)*, also enter this number(s).

10. AVAILABILITY/LIMITATION NOTICES: Enter any limitations on further dissemination of the report, other than those imposed by security classification, using standard statements such as:

(1) "Qualified requesters may obtain copies of this report from DDC."

(2) "Foreign announcement and dissemination of this report by DDC is not authorized."

(3) "U. S. Government agencies may obtain copies of this report directly from DDC. Other qualified DDC users shall request through _____."

(4) "U. S. military agencies may obtain copies of this report directly from DDC. Other qualified users shall request through _____."

(5) "All distribution of this report is controlled. Qualified DDC users shall request through _____."

If the report has been furnished to the Office of Technical Services, Department of Commerce, for sale to the public, indicate this fact and enter the price, if known.

11. SUPPLEMENTARY NOTES: Use for additional explanatory notes.

12. SPONSORING MILITARY ACTIVITY: Enter the name of the departmental project office or laboratory sponsoring *(paying for)* the research and development. Include address.

13. ABSTRACT: Enter an abstract giving a brief and factual summary of the document indicative of the report, even though it may also appear elsewhere in the body of the technical report. If additional space is required, a continuation sheet shall be attached.

It is highly desirable that the abstract of classified reports be unclassified. Each paragraph of the abstract shall end with an indication of the military security classification of the information in the paragraph, represented as *(TS)*, *(S)*, *(C)*, or *(U)*.

There is no limitation on the length of the abstract. However, the suggested length is from 150 to 225 words.

14. KEY WORDS: Key words are technically meaningful terms or short phrases that characterize a report and may be used as index entries for cataloging the report. Key words must be selected so that no security classification is required. Identifiers, such as equipment model designation, trade name, military project code name, geographic location, may be used as key words but will be followed by an indication of technical context. The assignment of links, rules, and weights is optional.

Unclassified
Security Classification